ZooKeys 1082: 1–26 (2022)
doi: 10.3897/zookeys.1082.74323
https://zookeys.pensoft.net

RESEARCH ARTICLE

A peer-reviewed open-access journal
ZooKeys
Launched to accelerate biodiversity research

Two new species of the genus *Smaragdina* Chevrolat, 1836 (Coleoptera, Chrysomelidae, Cryptocephalinae) from China

Wen-Yuan Duan[1,2], Feng-Yan Wang[1,2], Hong-Zhang Zhou[1,2]

1 *Key Laboratory of Zoological Systematics and Evolution, Institute of Zoology, Chinese Academy of Sciences, 1 Beichen West Rd, Chaoyang District, Beijing 100101, China* **2** *University of the Chinese Academy of Sciences, 19A Yuquan Rd, Shijingshan District, Beijing 100049, China*

Corresponding author: Hong-Zhang Zhou (zhouhz@ioz.ac.cn)

Academic editor: C.S. Chaboo | Received 12 September 2021 | Accepted 23 December 2021 | Published 18 January 2022

http://zoobank.org/9969EEA9-F980-47D1-A559-C5E41E029FF3

Citation: Duan W-Y, Wang F-Y, Zhou H-Z (2022) Two new species of the genus *Smaragdina* Chevrolat, 1836 (Coleoptera, Chrysomelidae, Cryptocephalinae) from China. ZooKeys 1082: 1–26. https://doi.org/10.3897/zookeys.1082.74323

Abstract

Two new species of the genus *Smaragdina* Chevrolat from China are reported: *S. hejingensis* Duan, Wang & Zhou **sp. nov.** from Xinjiang, and *S. magnipunctata* Duan, Wang and Zhou **sp. nov.** from Yunnan. Six species, *S. divisa* (Jacoby), *S. insulana* Medvedev, *S. kimotoi* Lopatin, *S. laboissierei* (Pic), *S. laosensis* Kimoto & Gressitt, and *S. oculata* Medvedev are new country records for China. Color illustrations and line drawings of general habitus and morphological details are given. All types of two new species are deposited in the collection of Institute of Zoology, Chinese Academy of Sciences (IZ-CAS).

Keywords

Clytrini, distributional records, leaf beetles, taxonomy

Introduction

The genus *Smaragdina* Chevrolat, 1836 has 350 recognized species (Warchałowski 2012; Wang and Zhou 2013), making it the most species-rich genus of the tribe Clytrini. The genus is distributed in the Palearctic, Oriental, and Afrotropical regions, with 64 species found in China (Clavareau 1913; Gressitt and Kimoto 1961; Tan et al. 1980; Kimoto and Gressitt 1981; Tan 1988; Lopatin 2004; Medvedev 2010; Regalin

and Medvedev 2010; Warchałowski 2010, 2012; Wang and Zhou 2013). This genus is similar to *Aetheomorpha* Lacordaire, 1848 but can be distinguished by the slight epipleural lobe of elytra and the pygidium covered by the elytra (Warchałowski 2012). This distinction must be carefully used and examined, otherwise misidentification may occur for the beginner when facing some intermediate forms.

The Chinese species of *Smaragdina* have been studied by many specialists (e.g., Gressitt and Kimoto 1961; Tan et al. 1980; Kimoto and Gressitt 1981; Lopatin and Konstantinov 2009; Regalin and Medvedev 2010), but most of these studies were comprehensive and included all or most of the family Chrysomelidae, and *Smaragdina* was treated as only a part in those broader studies. Some recent studies on *Smaragdina* have included excellent keys to the species from the Oriental and Palearctic regions and, thus, are very important in identifying the Chinese species (Medvedev 2010; Warchałowski 2010). The most recent study on *Smaragdina* was by Wang and Zhou (2013), which is part of the series of publications concentrated on the Chinese leaf beetle fauna (Wang and Zhou 2011, 2012, 2013, 2020; Su and Zhou 2017; Duan and Zhou 2021; Duan et al. 2021a, 2021b).

There were few studies strictly concentrated on the biology of *Smaragdina*, i.e. life cycles, development, host plants, etc. Gao et al. (2019) studied the life cycle of *Smaragdina nigrifrons* (Hope, 1843) as vineyard pest, but this species is now moved out of the genus *Smaragdina*. Erber (1968, 1969, 1988) comprehensively reviewed Clytrinae and other related subfamilies, Agrain et al. (2015) reviewed the ant-nest related leaf beetles, and Chaboo et al. (2016) catalogued all known immature stages of camptosomate leaf beetles. Tan et al. (1980) provided some valuable records for host plants.

This paper, as a continuation of our leaf beetle studies (see above), describes two new species from China and reports six species as new country records for China. We increase the number of the Chinese species of *Smaragdina* to 72. We provide color illustrations and line drawings of general habitus and other structures for each species included. All types of the new species are deposited in the collection of Institute of Zoology, Chinese Academy of Sciences (IZ-CAS).

Material and methods

Dissection of specimens

Dried specimens were relaxed in hot distilled water at 80 °C for about 2 h to soften the body and ease dissection. The abdomen was separated with insect pins from the rest of the body and soaked in 10% KOH solution, and then in a hot water bath for 15 min to advance the process. After this procedure, the specimens were transferred to distilled water to rinse the residual KOH solution off and stop the bleaching process. The aedeagus, spermatheca, and rectal sclerites were dissected out from abdomen and placed in glycerin on a microslide.

Photography and drawings

The dissected parts were placed into glycerin for observation and measured with an apochromatic stereomicroscope Zeiss SteREO V12. Color photographs of the adults and genitalia were captured with an Axio Zoom V16 fluorescence stereo zoom microscope and photomontage was performed in Zen 2012 (blue edition) imaging software. Adobe Photoshop CS6 was used in digital post-processing of the color images, and Adobe Illustrator 2020 was used to make the line drawings.

Morphological terminology and measurement

The term "rectal sclerites" (ventral rectal sclerites, dorsal rectal sclerites) is used throughout the paper according to Schöller et al. 2008, and "fossa" is used throughout the paper to indicate the round and deep structure on the last abdominal segment in female; it is widely used term in many publications in Cryptocephalinae (Gressitt and Kimoto 1961; Tan et al. 1980; Kimoto and Gressitt 1981; Tan 1988). Body length was measured to cover the whole length from the apex of pronotum to the apex of elytra in dorsal view.

Specimens studied

Specimens used in this study are from the Institute of Zoology, Chinese Academy of Sciences, Beijing, China (**IZ-CAS**).

Measurements are average values calculated from the values of at least 10 specimens, or all if fewer specimens were available. The following abbreviations were used to identify the institutions of holotype deposition.

BPBM Bernice P. Bishop Museum, Honolulu, Hawaii, USA;
LM Lev N. Medvedev Collection, Moscow, Russia;
MNHN National Museum of Natural History, Paris, France.

Host plants for Chinese *Smaragdina* species (from Tan et al. 1980)

Smaragdina mandzhura: Gramineae, *Miscanthus*
Smaragdina semiaurantiaca: Rosaceae, *Prunus*, *Malus*
Smaragdina aurita hammarstroemi: Salicaceae, *Salix*, *Populus*
Smaragdina mandzhura: Ulmaceae, *Ulmus*
Smaragdina semiaurantiaca: Ulmaceae, *Ulmus*
Smaragdina mandzhura: Rhamnaceae, *Ziziphus jujuba*
S*maragdina aurita hammarstroemi*: Betulaceae, *Betula*; Melastomataceae, *Styrax japonica*

Results

Taxonomy

Diagnosis. Body shape elongate and subcylindrical, usually smaller than 6 mm. Head small, very short; mandibles short; eyes round or elongate; antennae slender, 2nd and 3rd antennomeres short and equal, following antennomeres serrate. Pronotum transverse, posterior angles rounded; scutellum large. Elytra without distinct epipleural lobes. Legs short, fore legs sometimes slightly longer than others; tarsi of females usually long and narrow, 1st tarsomere longer than 2nd; legs of males usually stouter than female's, tarsi broader and shorter. Pygidium not exposed.

***Smaragdina hejingensis* Duan, Wang & Zhou, sp. nov.**

http://zoobank.org/24F5ED4A-681C-4D20-A8C4-CD404D4F8D40

Figures 1, 2

Diagnosis. This new species is the nearest to *S. flavilabris* (Briet, 1917) but can be distinguished by the shape of pronotal marking: *S. flavilabris* has the metallic blue marking rhombic, whereas in the new species this marking is not. Additionally, the anterior margin of the clypeus in the new species is yellowish brown but black in *S. flavilabris*.

Etymology. The specific is named after the type locality, Hejing.

Type locality. China: Xinjiang: Hejing.

Material examined (*n* = 6). ***Holotype*:** male, **China: Xinjiang**: Hejing, 30.VII.1958, coll. Changqing Li (IZ-CAS). ***Paratypes*: China: Xinjiang**: 3 males, 2 females, Hejing, 31.VII.1958, coll. Changqing Li (IZ-CAS).

Measurements (*n* = 6). Body length males: 5.2–5.9 mm, females: 5.1–5.6 mm.

Description. Body (Figs 1A, B, 2A) oblong, largely metallic blue. Mandibles yellowish brown, apex tinged with brown; labrum darkish brown; ventral side of mouthpart yellowish brown; four basal antennomeres yellow, others brown. Pronotum largely metallic blue, lateral sides with yellowish brown marking. Scutellum black. Ventral side of body largely metallic blue, prosternum yellowish brown, femora of hind legs tinged with black, last segments of tarsi and claws brown.

Head small, with dense and coarse punctures. Mandibles (Fig. 2B) short, labrum slightly incised at anterior margin, length ratio of maxillary palpomeres 0.5:2.4:1.5:2.4; while that of labial palpomeres 0.5:1.8:2.8; mentum rectangular emarginated at anterior margin. Clypeus lateral sides slightly depressed, anterior margin feebly incised; frons covered with shallow wrinkles; inner sides of eyes with short pubescence; vertex not convex, with fine wrinkles. Antennae short, extending to base of prothorax, pubescent, 1st antennomere oblong, 2nd rounded, 3rd slender, slightly longer than 2nd, 4th triangular, a little longer than 3rd, serrated from 5th segment onwards.

Pronotum transverse, about 2× as wide as long, moderately convex; anterior margin slightly convex, lateral margins rounded, posterior margin sinuated, all margins

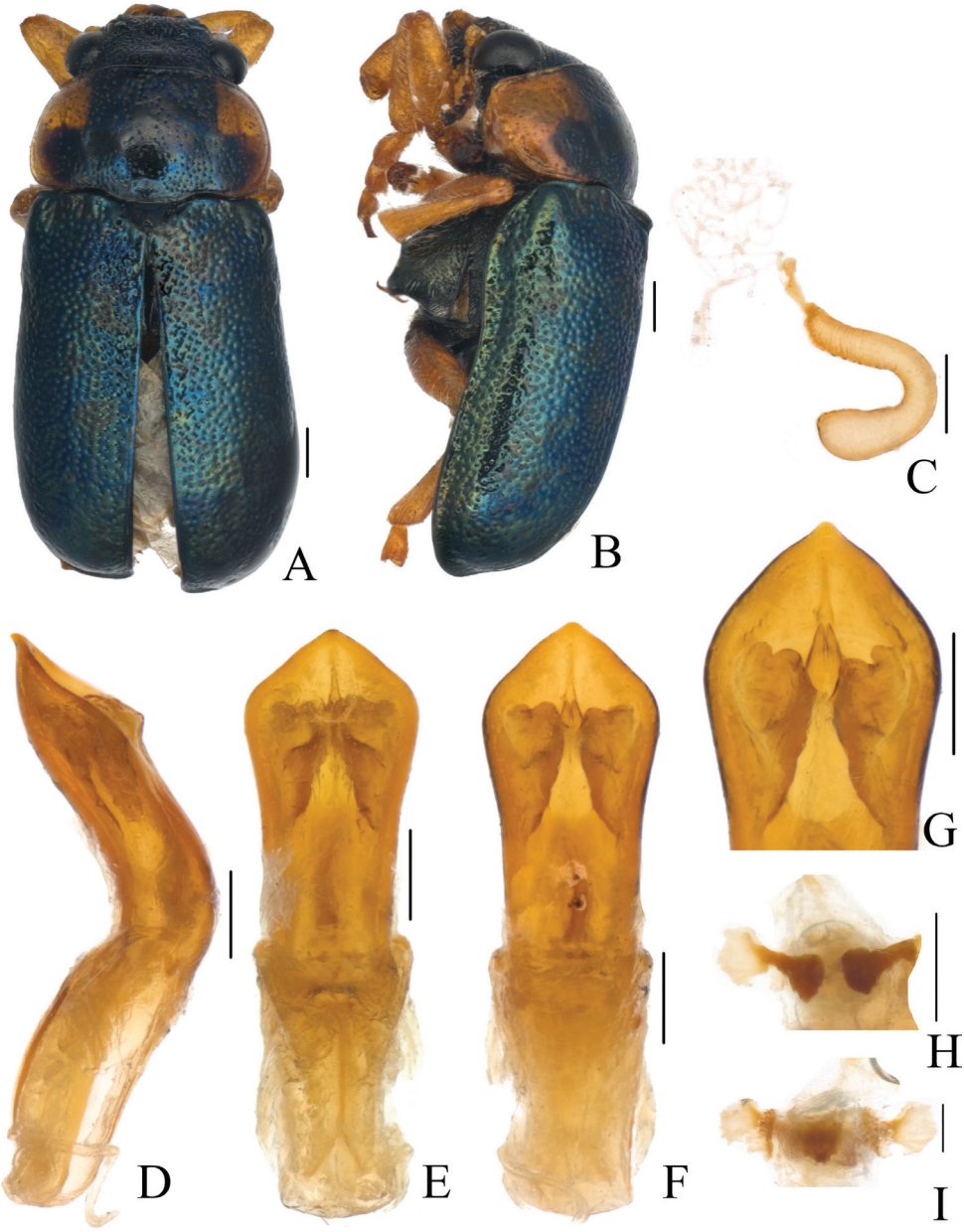

Figure 1. *Smaragdina hejingensis* Duan, Wang & Zhou, sp. nov. **A** habitus **B** lateral view of habitus **C** spermatheca **D** lateral view of aedeagus **E** ventral view of aedeagus **F** dorsal view of aedeagus **G** apex of aedeagus **H** ventral rectal sclerites **I** dorsal rectal sclerites. Scale bars: 0.5 mm (**A, B**), 0.2 mm (**C–I**).

(especially lateral ones) bordered; surface with coarse punctures, denser on median basal area. Scutellum widely triangular, with extremely fine punctures; apex slightly elevated over elytral surface.

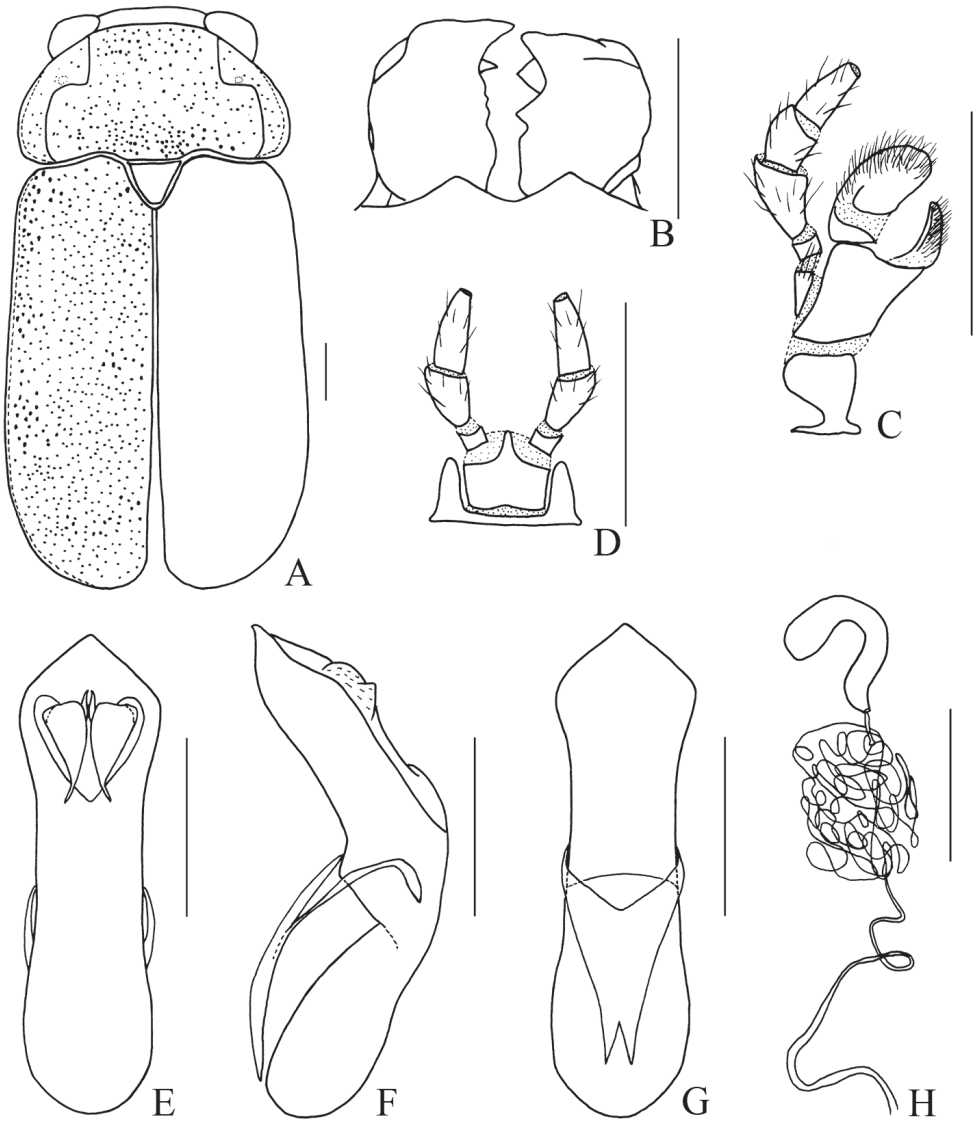

Figure 2. *Smaragdina hejingensis* Duan, Wang & Zhou, sp. nov. **A** habitus **B** mandibles **C** maxilla **D** labium **E** dorsal view of aedeagus **F** lateral view of aedeagus **G** ventral view of aedeagus **H** spermatheca. Scale bars: 0.5 mm.

Elytra 1.7 times as long as wide at humeri, covered with confused and dense punctures, interstices shorter than a puncture diameter, punctures becoming sparse posteriorly, and nearly disappearing at elytral apices.

Underside and legs thickly clothed with silvery pubescence; apex of pygidium arcuate. Tarsi slender, length ratio of protarsomeres 1.6:1.0:0.3:2.0. Tibiae of females slightly curved, legs robust, tarsi broad.

Aedeagus (Figs 1D–G, 2E–G) sword-shaped, about 3.4× as long as wide; apex triangular; bent ventrally; without pubescence.

Female. Coloration of body darker than male, base of hind tibiae black; legs slender, tarsi narrow. Last segment of abdomen with a fossa. Spermatheca (Figs 1C, 2H) hook-shaped, apex swollen and blunt, duct base thickened, not coiled. Rectal sclerites moderately sclerotized, ventral rectal sclerites (Fig. 1H) large, clubbed; dorsal rectal sclerites (Fig. 1I) protruding medially; lateral sclerites large.

Distribution. China (Xinjiang).

Smaragdina magnipunctata Duan, Wang & Zhou, sp. nov.

http://zoobank.org/DB4FD31E-D2CF-45DF-91C6-2A7CE6B84FA5
Figures 3, 4

Diagnosis. This new species is well distinguished from all its congeners by the presence of unique black markings on the elytra and strong punctures arranged in regular rows with their interspaces impunctate.

Etymology. The specific epithet is from the Latin words "*magni-*" and "*punctata*" in reference to the big punctures of the elytra.

Type locality. China: Yunnan Province: Xishuangbanna, Xiaomengyang.

Material examined (*n* = 4). *Holotype*: male, **China: Yunnan Province:** Xishuangbanna, Xiaomengyang, 7.VII.1957, coll. Shuyong Wang (IZ-CAS). ***Paratypes*: China: Yunnan Province:** 1 female, Xishuangbanna, Xiaomengyang, 10.X.1957, coll. Shuyong Wang (IZ-CAS); 1 female, Xishuangbanna, Xiaomengyang, 21.X.1957, coll. Shuyong Wang (IZ-CAS); 1 female, Xishuangbanna, Xiaomengyang, 22.X.1957, coll. Lingchao Zang (IZ-CAS).

Measurements (*n* = 4). Body length males: 3.7 mm, females: 3.9–4.3 mm.

Description. Body (Figs 3A, B, 4A) oblong, largely khaki. Head yellowish brown, Mandibles with black apex; two basal antennomeres yellow, others brown; sometimes vertex black. Pronotum yellowish brown. Scutellum black. Elytra khaki, margins black, disc with two black round markings. Ventral side of body largely yellowish brown, ventral side of mesothorax and metathorax black; legs yellowish, tibiae outer side and tarsi somewhat brown.

Head small, glabrous. Mandibles short; labrum slightly incised at anterior margin; length ratio of maxillary palpomeres 0.5:2.2:2.0:2.5; length ratio of labial palpomeres 0.4:1.8:3.0. Clypeus glabrous, anterior margin slightly incised; frons with 3 grooves arranged in triangular pattern; inner sides of eyes with short pubescence; vertex slightly convex, glabrous. Antennae short, extending to base of prothorax, pubescent, 1st antennomere oblong and thick, 2nd rounded, 3rd slender, similar in length with 2nd, 4th triangular, a little longer than 3rd, serrated from 5th segment onwards, while last segment ovate, apex sharp.

Pronotum transverse, about 2× as wide as long, strongly convex; anterior and lateral margins rounded, posterior margin weakly sinuated and bordered; surface without any punctures. Scutellum triangular, impunctate, apex slightly elevated over elytral surface.

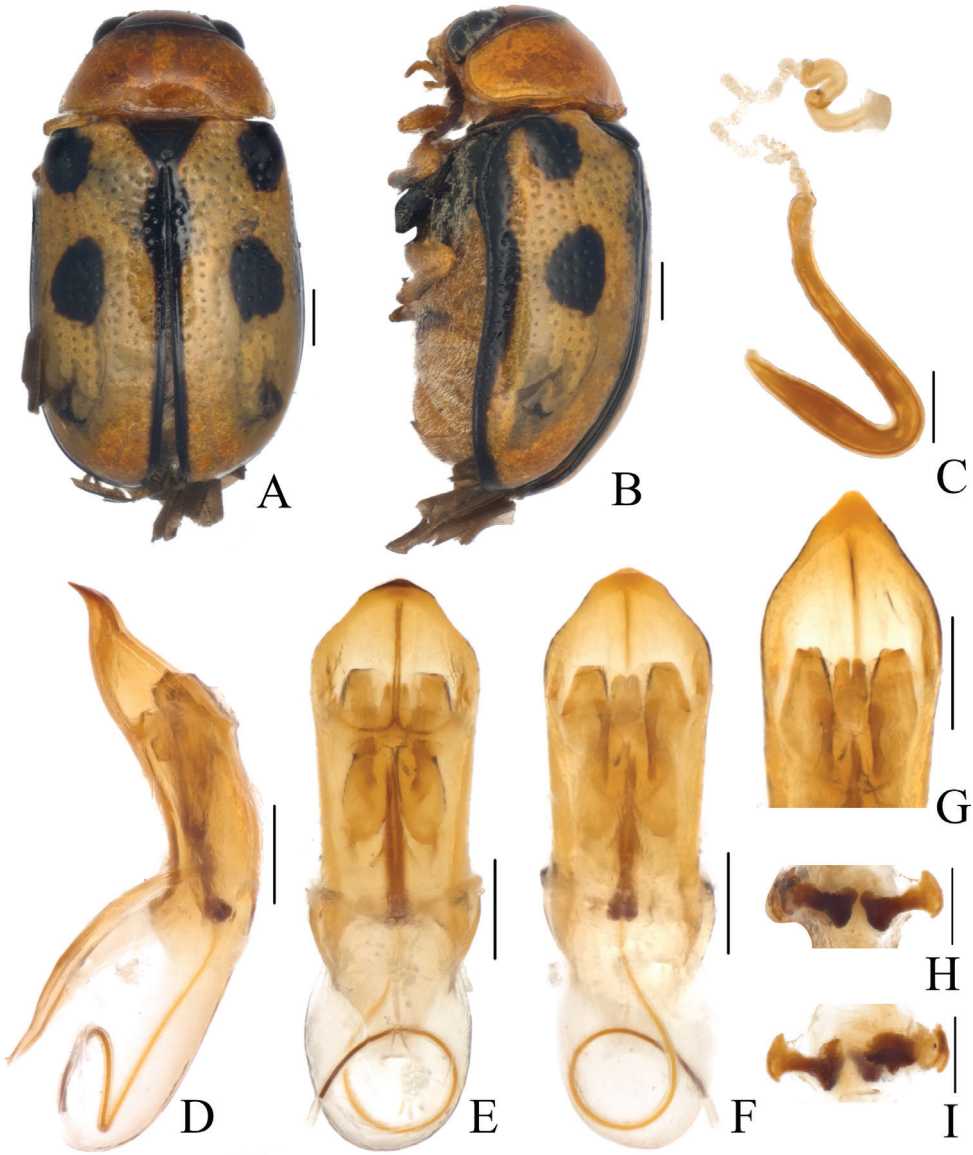

Figure 3. *Smaragdina magnipunctata* Duan, Wang & Zhou, sp. nov. **A** habitus **B** lateral view of habitus **C** spermatheca **D** lateral view of aedeagus **E** ventral view of aedeagus **F** dorsal view of aedeagus **G** apex of aedeagus **H** ventral rectal sclerites **I** dorsal rectal sclerites. Scale bars: 0.5 mm (**A, B**), 0.2 mm (**C–I**).

Elytra glabrous, 1.5× as long as wide at humeri; 2/3 basal part with coarse, sparse punctures, forming regular rows, with interspaces impunctate; 1/3 apical part with sparse, fine punctures, almost obsolete.

Underside and legs thickly clothed with silvery pubescence; apex of pygidium slightly concave. Tarsi slender, length ratio of protarsomeres 1.0:0.7:0.2:1.2.

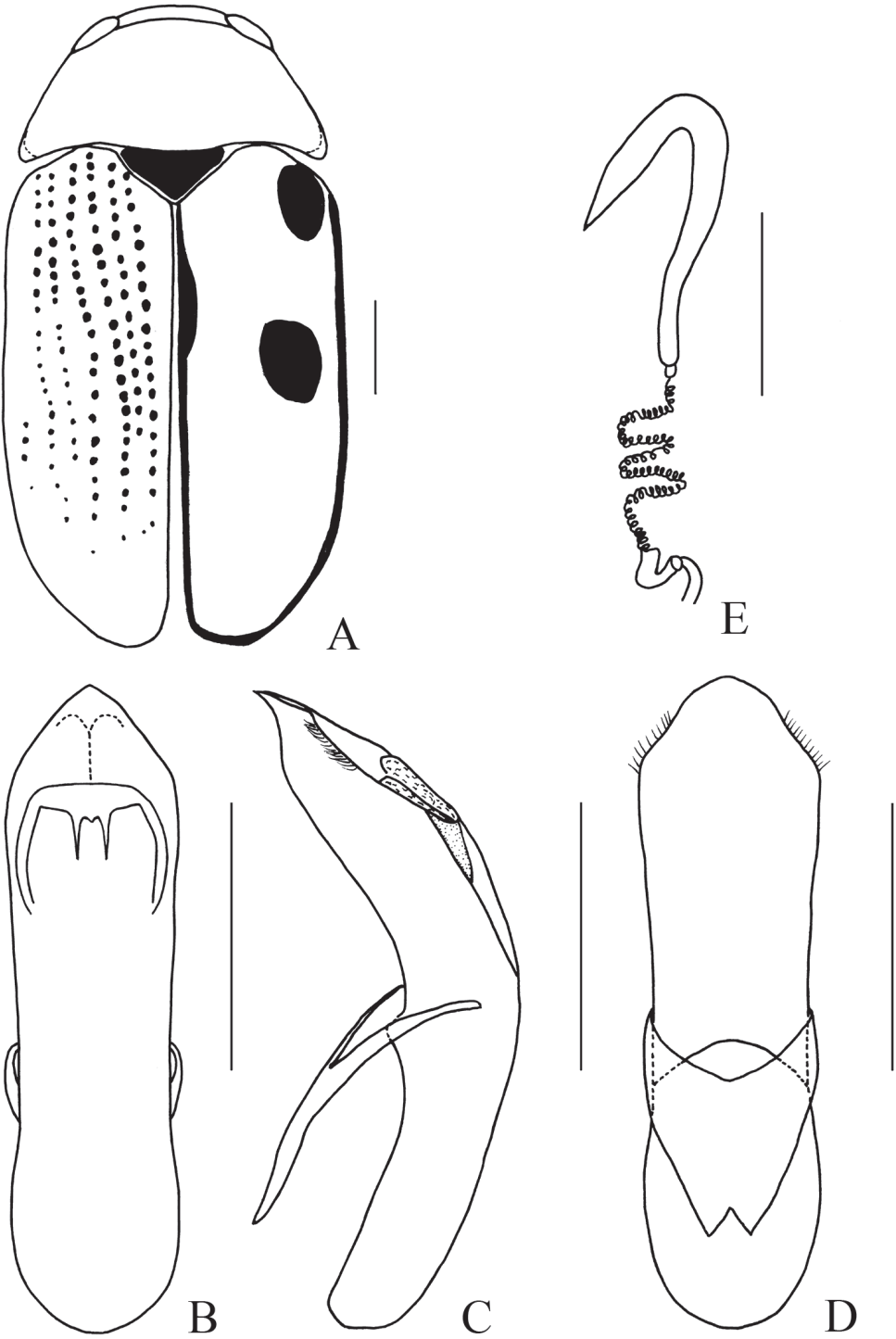

Figure 4. *Smaragdina magnipunctata* Duan, Wang & Zhou, sp. nov. **A** habitus **B** dorsal view of aedeagus **C** lateral view of aedeagus **D** ventral view of aedeagus **E** spermatheca. Scale bars: 0.5 mm.

Aedeagus (Figs 3D–G, 4B–D) oblong, about 3.6× as long as wide, apex triangular, bent ventrally; without pubescence.

Female. Punctures of elytra more obvious than male, last segment of abdomen with a fossa, apex of pygidium truncate. Spermatheca (Figs 3C, 4E) hooked, slender; duct strongly sclerotized, base thickened, coiled up about 20–30×. Rectal sclerites strongly sclerotized, ventral rectal sclerites (Fig. 3H) large, dumbbell-like; dorsal central sclerite (Fig. 3I) rectangular; lateral sclerites slightly small.

Distribution. China (Yunnan).

Smaragdina divisa (Jacoby, 1889), new country record for China

Figures 5, 6

Smaragdina divisa Jacoby, 1889: 156 (orig.: *Gynandrophthalma divisa*); 1908: 117, fig. 29; Clavareau 1913: 60; Medvedev 1988a: 31 (redescription); Medvedev 2010:265; Regalin and Medvedev 2010: 576 (catalogue).

Gynandrophthalma indica Jacoby, 1895: 263; Jacoby 1908: 117 (as synonym of *Gynandrophthalma divisa*). Syn.

Material examined (*n* = 17). China: Hainan province: 6 males, 4 females, Jianfeng, 20.IV.1980, coll. Fuji Pu (IZ-CAS); 2 males, Jianfenglin, 20.IV.1980, coll. unknown (IZ-CAS); 1 male, Lehui, 4.V.1954, coll. Keren Huang (IZ-CAS); 1 female, Nada, 25.IV.1954, coll. Keren Huang (IZ-CAS); 1 female, Baoting, 16.V.1960, coll. Zhenfu Li (IZ-CAS); 1 female, Ledong, 10.VI.1960, coll. Xuezhong Zhang (IZ-CAS); 1 female, Tongshi, 8.V.1960, coll. Zhenfu Li (IZ-CAS).

Measurements (*n* = 10). Body length males: 3.4–3.8 mm, females: 5.1–5.3 mm.

Distribution. China (Hainan); Vietnam; Burma; Nepal; Sri Lanka; Malaysia.

Remark. This species is recognized by having the apical half of the elytra distinctly paler than the basal half, and the apex of aedeagus narrowly truncate. It has not previously been recorded from the territory of China.

Smaragdina insulana Medvedev, 1992, new country record for China

Figures 7, 8

Smaragdina insulana Medvedev, 1992a: 73 (type locality: Vietnam, Prov. Quang Nam-Da Nang); Medvedev 2010: 266.

Material examined (*n* = 3). China: Guangxi province: 1 female, Longzhou, Daqingshan, 20.IV.1963, coll. Shuyong Wang (IZ-CAS); 1 male, Longzhou, Daqingshan, 26.IV.1963, coll. Shuyong Wang (IZ-CAS); 1 male, Longzhou, Daqingshan, 27.IV.1963, coll. Shuyong Wang (IZ-CAS).

Measurements (*n* = 3). Body length males: 4.8–4.9 mm, females: 5.0 mm.

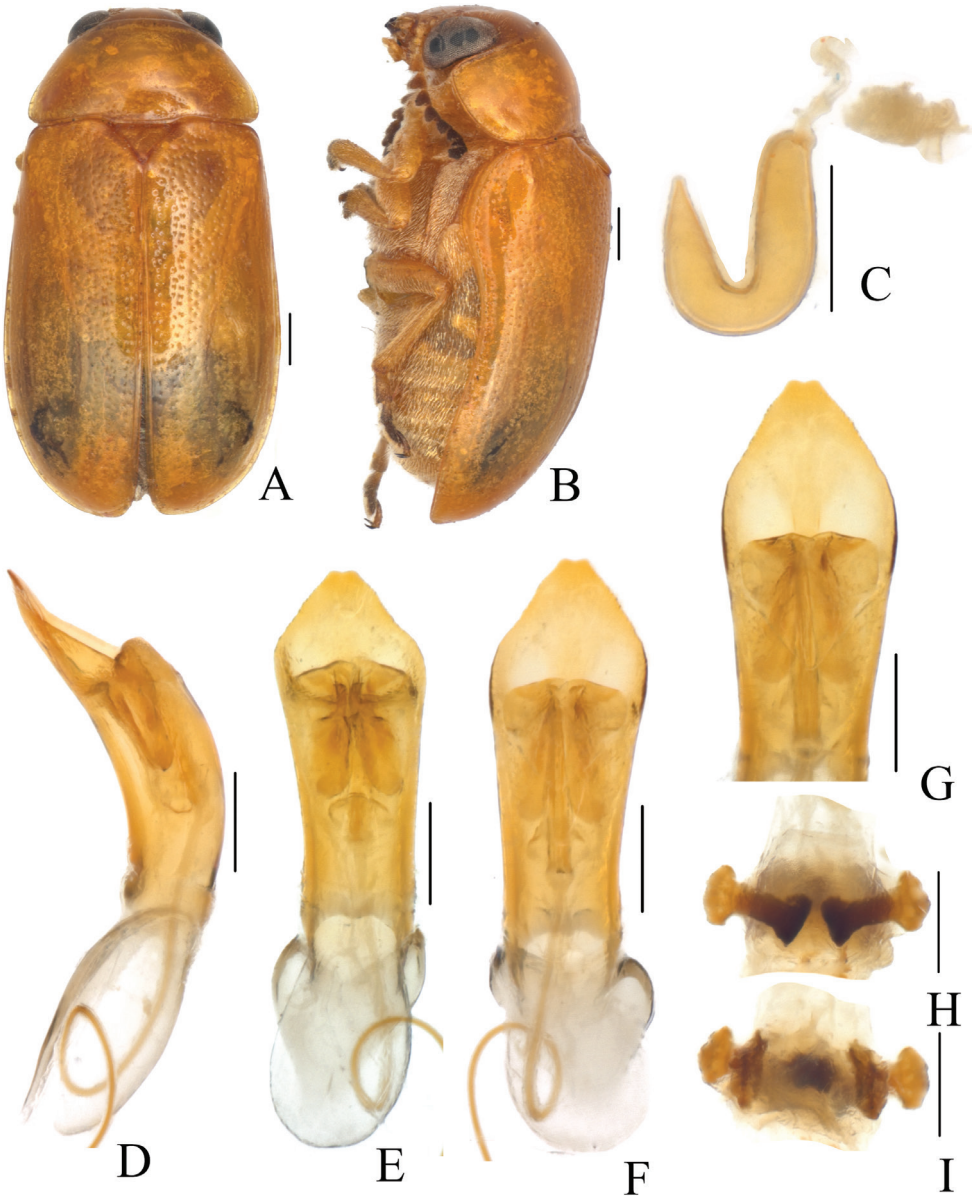

Figure 5. *Smaragdina divisa* (Jacoby, 1889) **A** habitus **B** lateral view of habitus **C** spermatheca **D** lateral view of aedeagus **E** ventral view of aedeagus **F** dorsal view of aedeagus **G** apex of aedeagus **H** ventral rectal sclerites **I** dorsal rectal sclerites. Scale bars: 0.5 mm (**A, B**), 0.2 mm (**C–I**).

Distribution. China (Guangxi); Vietnam.

Remark. This species is recognized by the fulvous body color, pale flavous spots on the elytra, and the sharp apex of the aedeagus. Originally found in Vietnam, we can confirm this species occurs in China.

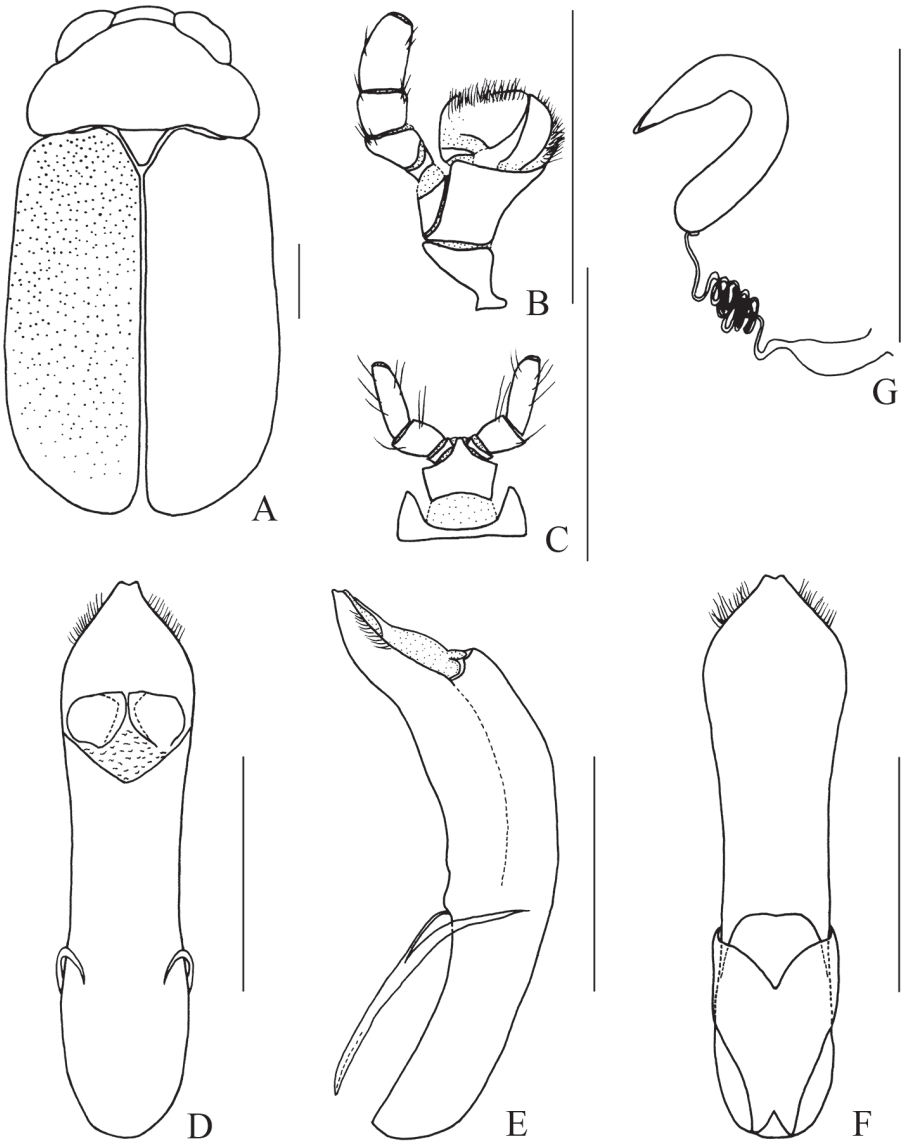

Figure 6. *Smaragdina divisa* (Jacoby, 1889) **A** habitus **B** maxilla **C** labium **D** dorsal view of aedeagus **E** lateral view of aedeagus **F** ventral view of aedeagus **G** spermatheca. Scale bars: 0.5 mm.

Smaragdina kimotoi Lopatin, 2003, new country record for China

Figures 9, 10

Smaragdina kimotoi Lopatin, 2003: 301 (type locality: South Vietnam, northeast of Ho Chi Minh); Medvedev 2010: 284.

Material examined (*n* = 13). China: Hainan province: 1 male, 3 females, Jianfeng, 20.IV.1980, coll. Fuji Pu (IZ-CAS); 2 males, Jianfenglin, 29.IV.1983, coll. Maobin

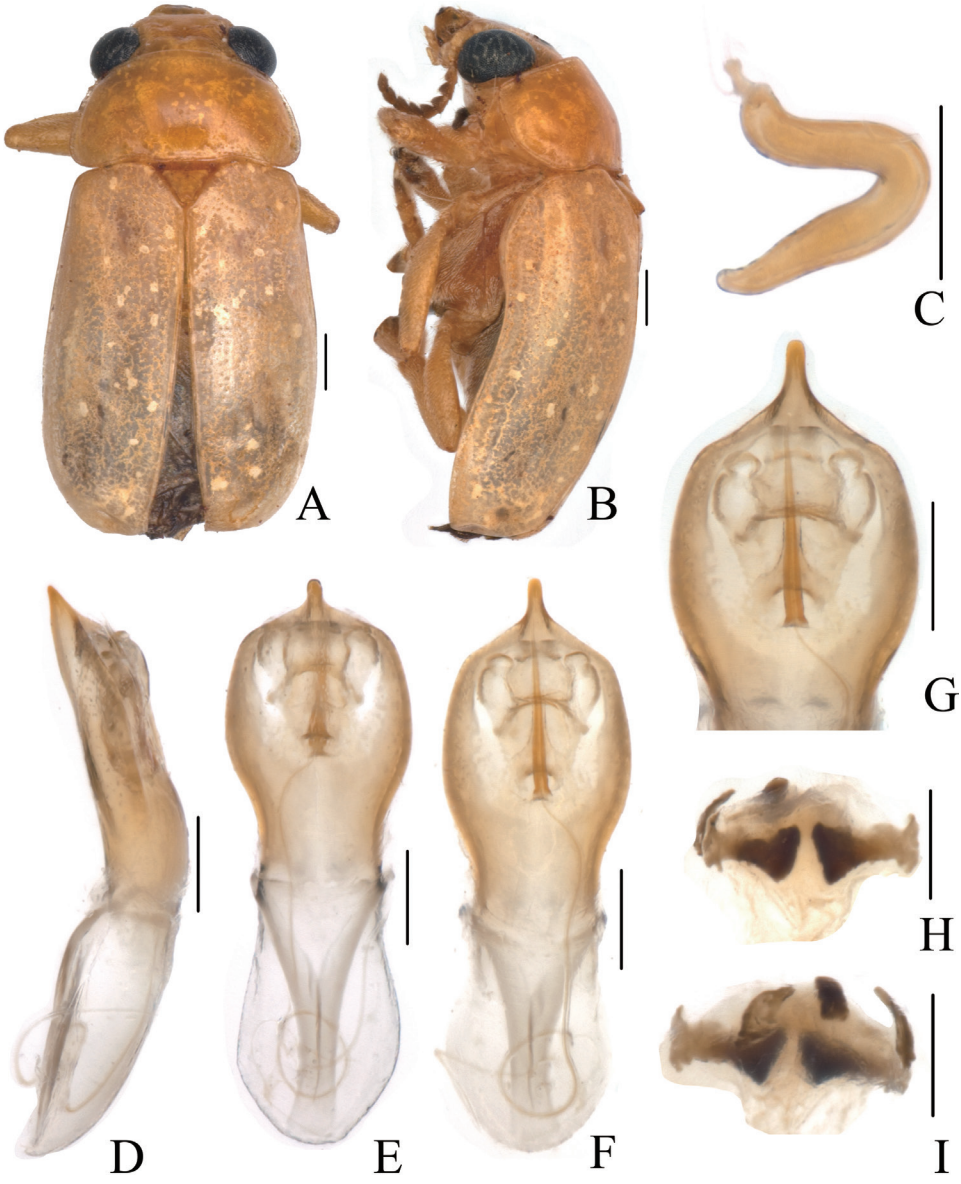

Figure 7. *Smaragdina insulana* Medvedev, 1992 **A** habitus **B** lateral view of habitus **C** spermatheca **D** lateral view of aedeagus **E** ventral view of aedeagus **F** dorsal view of aedeagus **G** apex of aedeagus **H** ventral rectal sclerites **I** dorsal rectal sclerites. Scale bars: 0.5 mm (**A, B**), 0.2 mm (**C–I**).

Gu (IZ-CAS); 1 female, Jianfenglin, 19.IV.1984, coll. Chunling Wang (IZ-CAS); 1 female, Wuzhishan, 4.IV.1980, coll. Shuyong Wang (IZ-CAS); 1 female, Nada, 25.IV.1954, coll. Keren Huang (IZ-CAS); 2 females, Nada, 30.IV.1954, coll. Keren Huang (IZ-CAS); 1 male, Nada, 30.V.1954, coll. Keren Huang (IZ-CAS); 1 female, Tongshi, 27.III.1960, coll. Changqing Li (IZ-CAS); 1 female, Tongshi, 23.IV.1960, coll. Zhenfu Li (IZ-CAS).

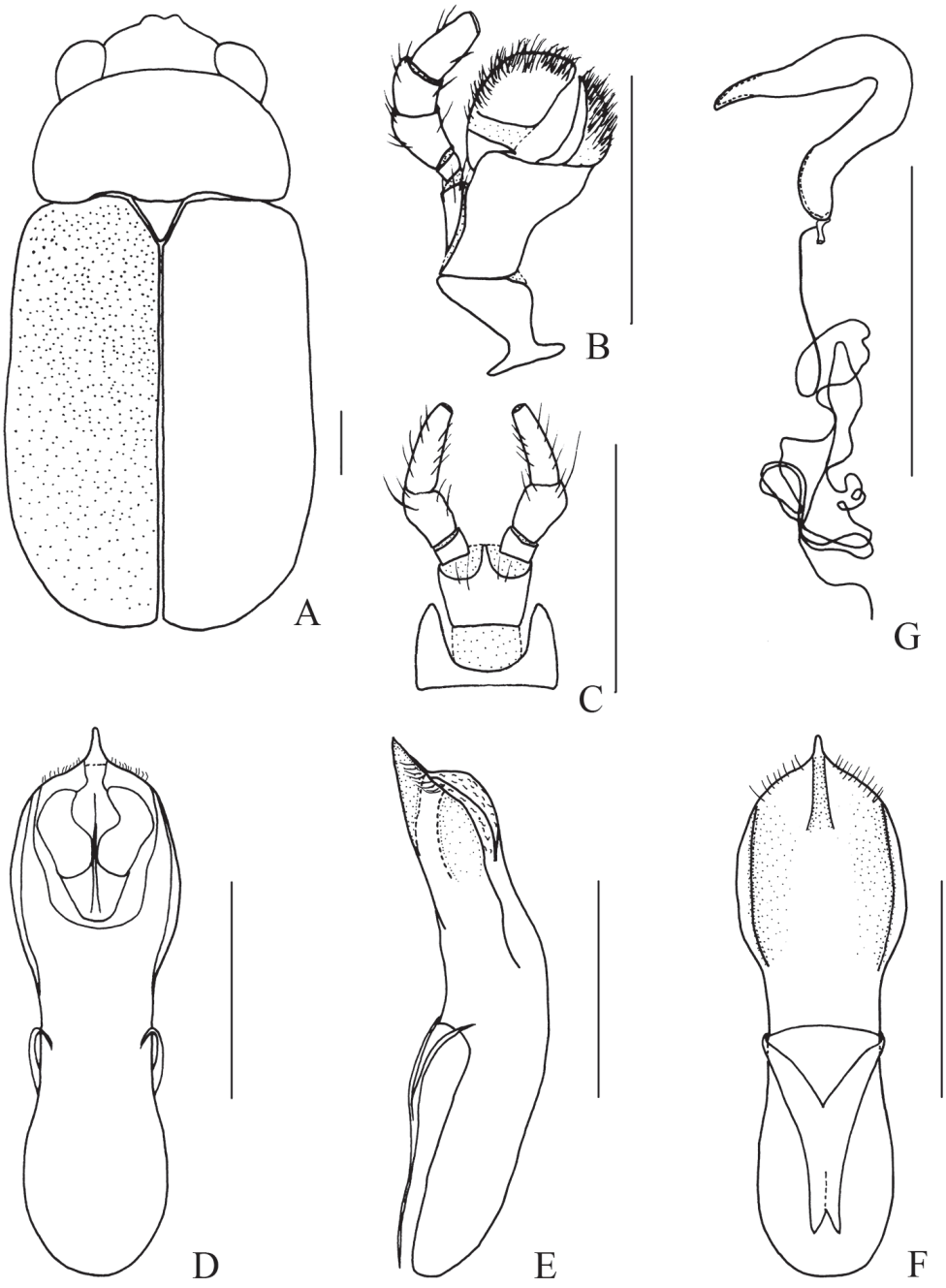

Figure 8. *Smaragdina insulana* Medvedev, 1992 **A** habitus **B** maxilla **C** labium **D** dorsal view of aedeagus **E** lateral view of aedeagus **F** ventral view of aedeagus **G** spermatheca. Scale bars: 0.5 mm.

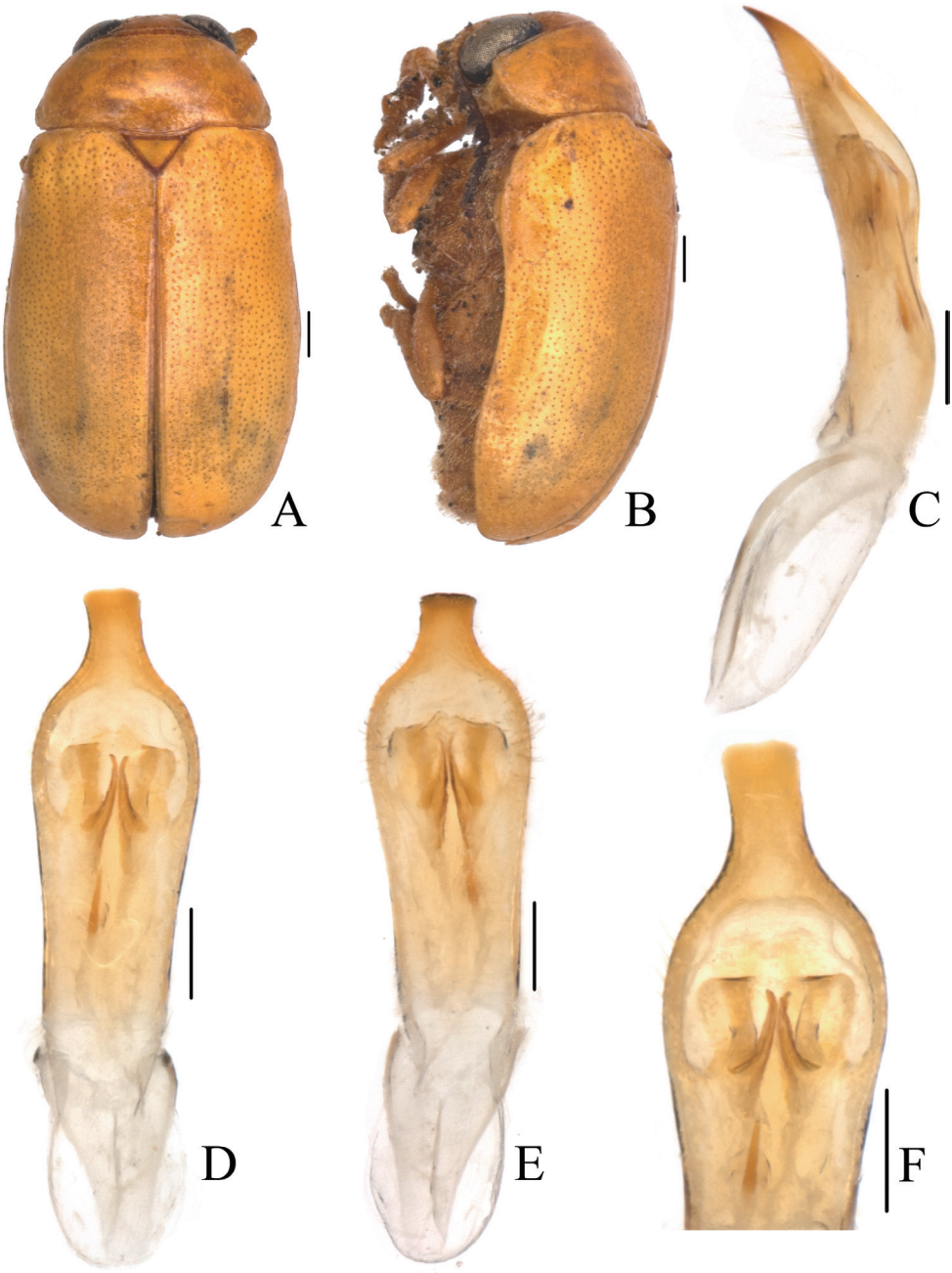

Figure 9. *Smaragdina kimotoi* Lopatin, 2003 **A** habitus **B** lateral view of habitus **C** lateral view of aedeagus **D** ventral view of aedeagus **E** dorsal view of aedeagus **F** apex of aedeagus. Scale bars: 0.5 mm (**A, B**), 0.2 mm (**C–F**).

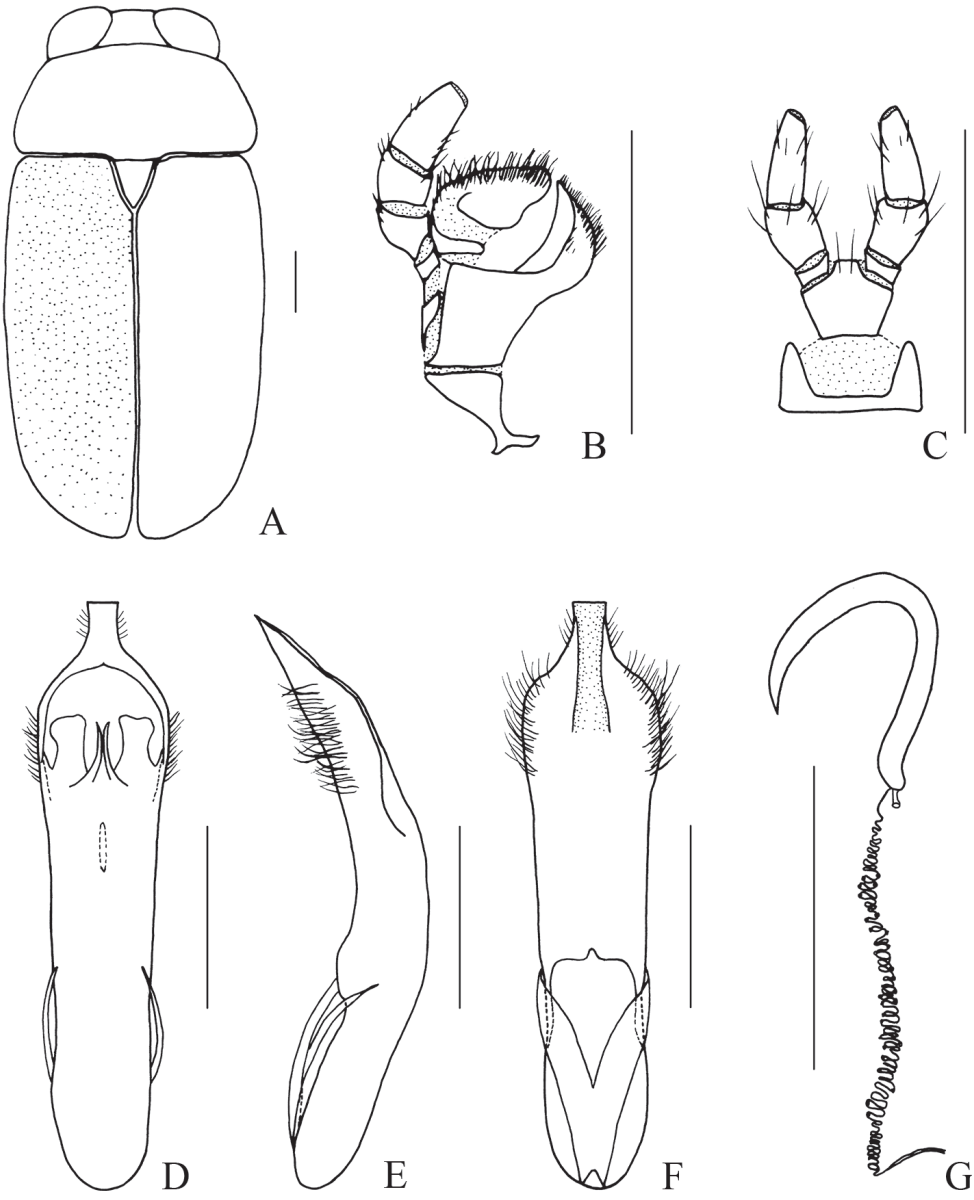

Figure 10. *Smaragdina kimotoi* Lopatin, 2003 **A** habitus **B** maxilla **C** labium **D** dorsal view of aedeagus **E** lateral view of aedeagus **F** ventral view of aedeagus **G** spermatheca. Scale bars: 0.5 mm.

Measurements (*n* = 10). Body length males: 4.4–4.9 mm, females: 4.9–5.9 mm.

Distribution. China (Hainan); Vietnam.

Remark. The fulvous dorsal body and the aedeagus with a broad and parallel-sided apical process, distinguish this species from *S. divisa*. Originally from Vietnam, we confirm that *S. kimotoi* occurs in China.

***Smaragdina laboissierei* (Pic, 1928), new country record for China**
Figures 11, 12

Smaragdina laboissierei Pic, 1928: 34 (orig.: *Cyaniris laboissierei*; type locality: Tonkin; type deposited: MNHN); Kimoto and Gressitt 1981: 320 (*Smaragdina laboissierei*); Medvedev 1992b: 23 (figure); Medvedev 2010: 264.

Material examined (*n* = 2). China: Guangxi province: 1 female, Longzhou, Daqingshan, 19. IV. 1963, coll. Shuyong Wang (IZ-CAS); 1 male, Longzhou, Daqingshan, 27. IV. 1963, coll. Shuyong Wang (IZ-CAS).

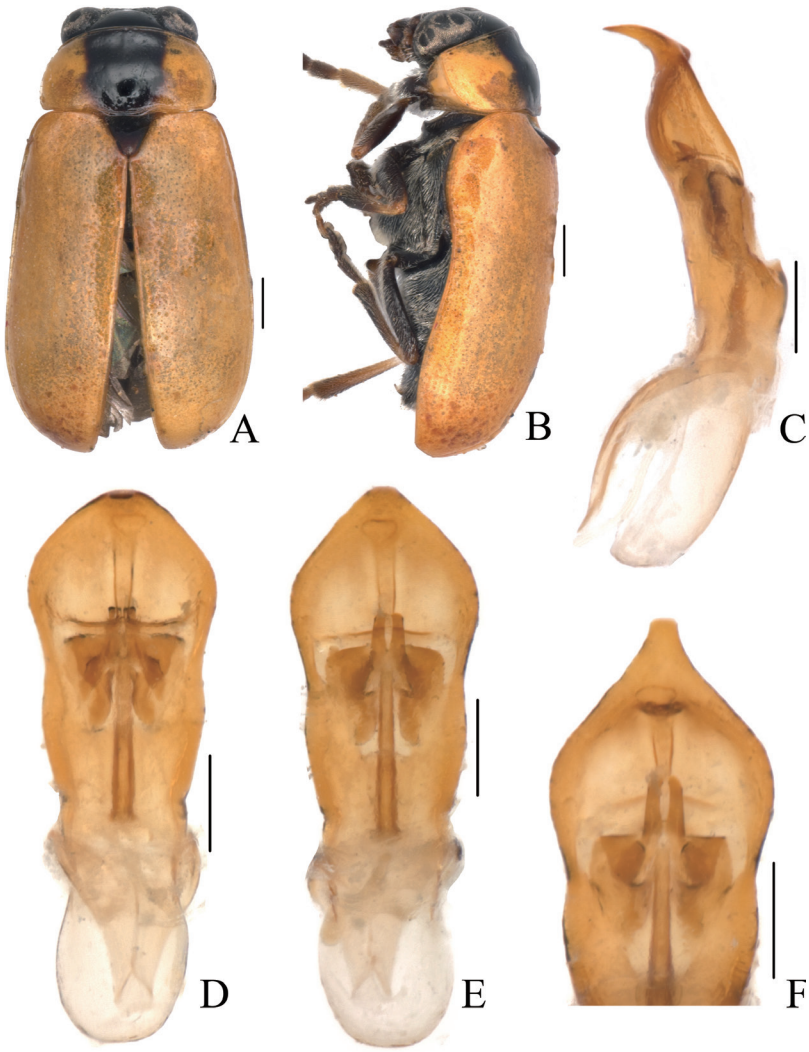

Figure 11. *Smaragdina laboissierei* (Pic, 1928) **A** habitus **B** lateral view of habitus **C** lateral view of aedeagus **D** ventral view of aedeagus **E** dorsal view of aedeagus **F** apex of aedeagus. Scale bars: 0.5 mm (**A, B**), 0.2 mm (**C–F**).

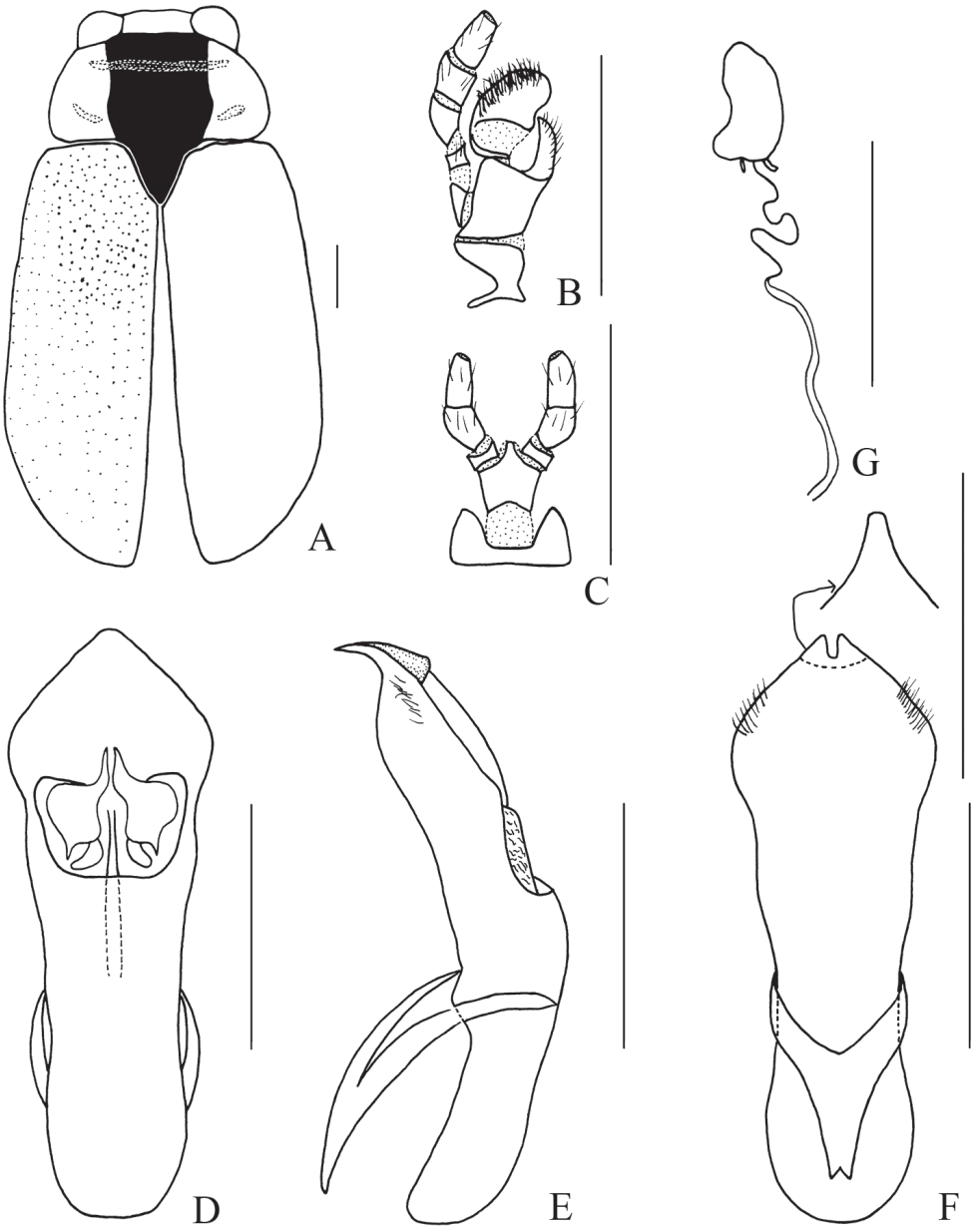

Figure 12. *Smaragdina laboissierei* (Pic, 1928) **A** habitus **B** maxilla **C** labium **D** dorsal view of aedeagus **E** lateral view of aedeagus **F** ventral view of aedeagus **G** spermatheca. Scale bars: 0.5 mm.

Measurements (*n* = 2). Body length males: 4.4–4.7 mm, females: 5.2–5.5 mm.

Distribution. China (Guangxi); Vietnam.

Remark. The Chinese specimens were identified as this species by the yellowish-brown pronotum with a black stripe and the apical process of aedeagus triangular, which is acute and strongly curved downwards. This species was previously only known from Vietnam.

***Smaragdina laosensis* Kimoto & Gressitt, 1981, new country record for China**
Figures 13, 14

Smaragdina laosensis Kimoto & Gressitt, 1981: 320 (type locality: Laos; type deposited: BPBM); Medvedev 2010: 269.

Material examined (*n* = 5). China: Yunnan province: 1 female, Cheli, 8.III.1957, coll. Fuji Pu (IZ-CAS); 1 male, Cheli, 11.III.1957, coll. Fuji Pu (IZ-CAS); 2 males,

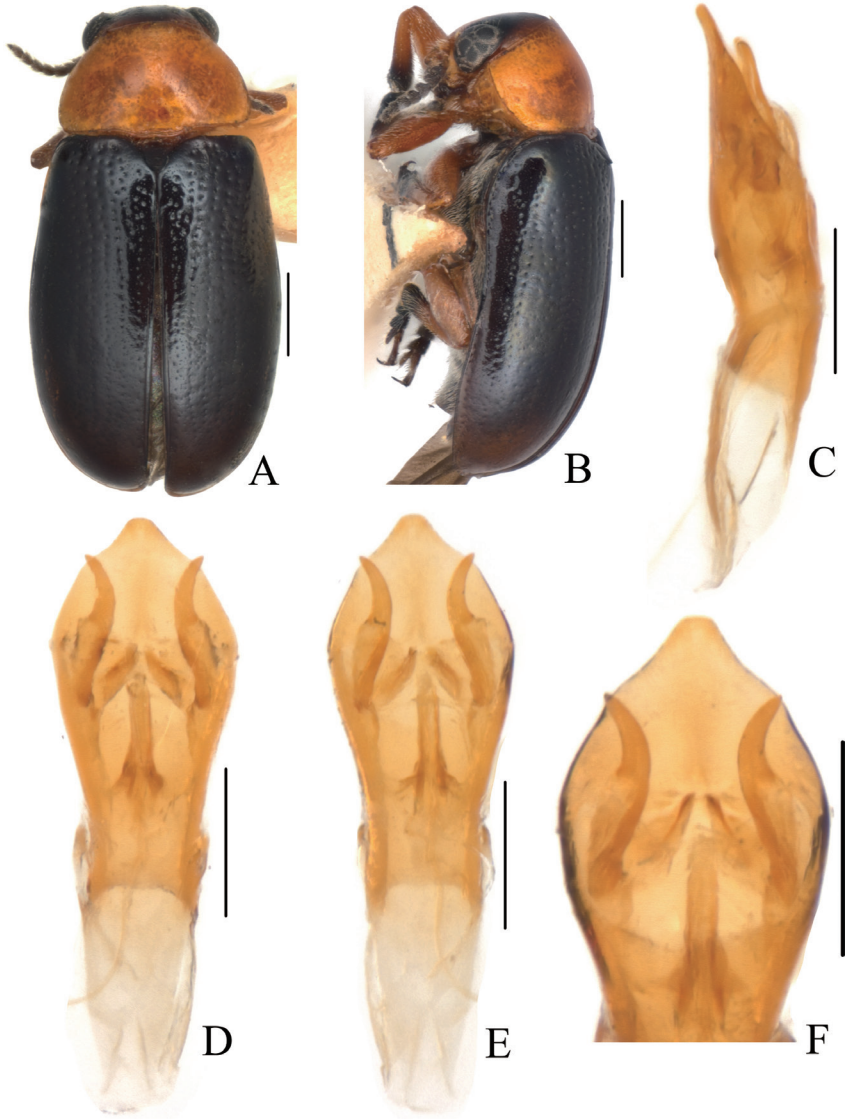

Figure 13. *Smaragdina laosensis* Kimoto & Gressitt, 1981 **A** habitus **B** lateral view of habitus **C** lateral view of aedeagus **D** ventral view of aedeagus **E** dorsal view of aedeagus **F** apex of aedeagus. Scale bars: 0.5 mm (**A, B**), 0.2 mm (**C–F**).

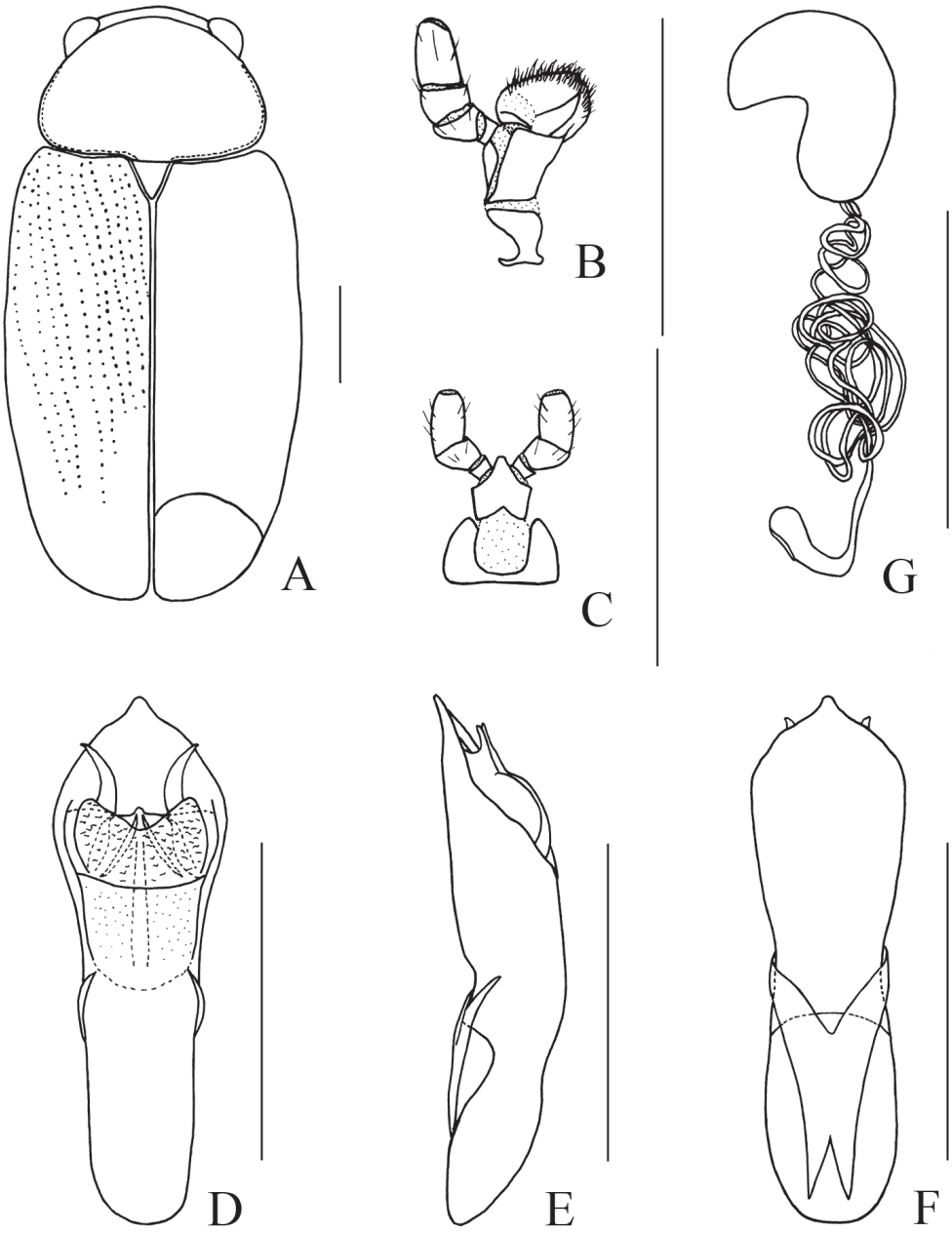

Figure 14. *Smaragdina laosensis* Kimoto & Gressitt, 1981 **A** habitus **B** maxilla **C** labium **D** dorsal view of aedeagus **E** lateral view of aedeagus **F** ventral view of aedeagus **G** spermatheca. Scale bars: 0.5 mm.

Xishuangbanna, Yunjinghong, 3.IV.1958, coll. unknown (IZ-CAS); 1 female, Xishuangbanna, Yunjinghong, 7.VIII.1958, coll. Xuwu Meng (IZ-CAS).

Measurements (*n* = 5). Body length males: 2.9–3.2 mm, females: 3.3–3.5 mm.

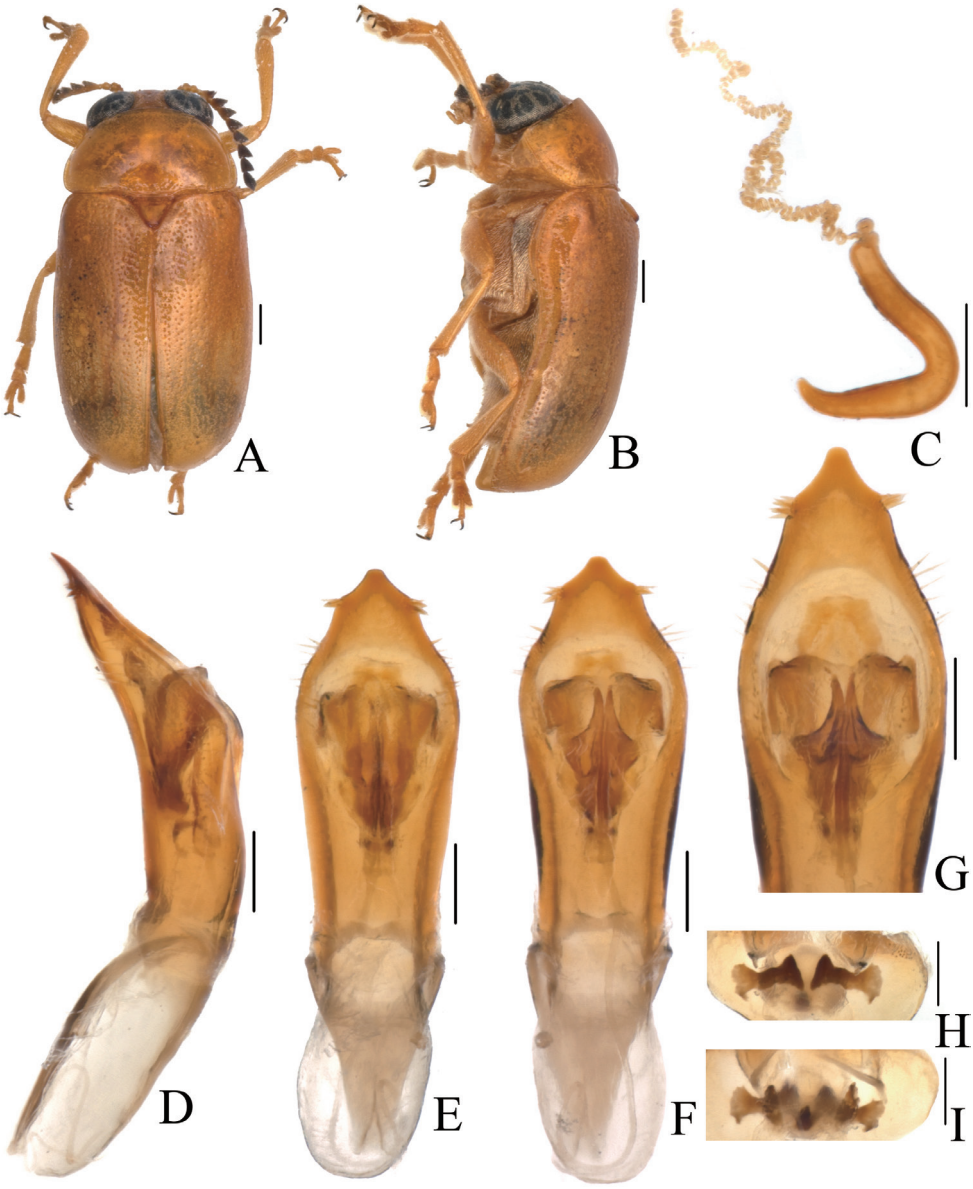

Figure 15. *Smaragdina oculata* Medvedev, 1988 **A** habitus **B** lateral view of habitus **C** spermatheca **D** lateral view of aedeagus **E** ventral view of aedeagus **F** dorsal view of aedeagus **G** apex of aedeagus **H** ventral rectal sclerites **I** dorsal rectal sclerites. Scale bars: 0.5 mm (**A, B**), 0.2 mm (**C–I**).

Distribution. China (Yunnan); Laos.

Remark. Following the description of Kimoto and Gressitt (1981, especially figs 21b, 23a), we determined the Chinese specimens as *S. laosensis*. This species was originally recorded in Laos.

Smaragdina oculata Medvedev, 1988, new country record for China

Figures 15, 16

Smaragdina oculata Medvedev, 1988b: 471 (type locality: Assam, Kaziranga; type deposited: LM); Medvedev 2010: 268.

Material examined (*n* = 4). China: Yunnan province: 1 male, 1 female, Mangshi, 15.V.1955, coll. B. Popov (IZ-CAS); 1 male, Mangshi, 17.V.1955, coll. Xingchi Yang (IZ-CAS); 1 male, Mangshi, 17.V.1955, coll. Krejanovsky (IZ-CAS).

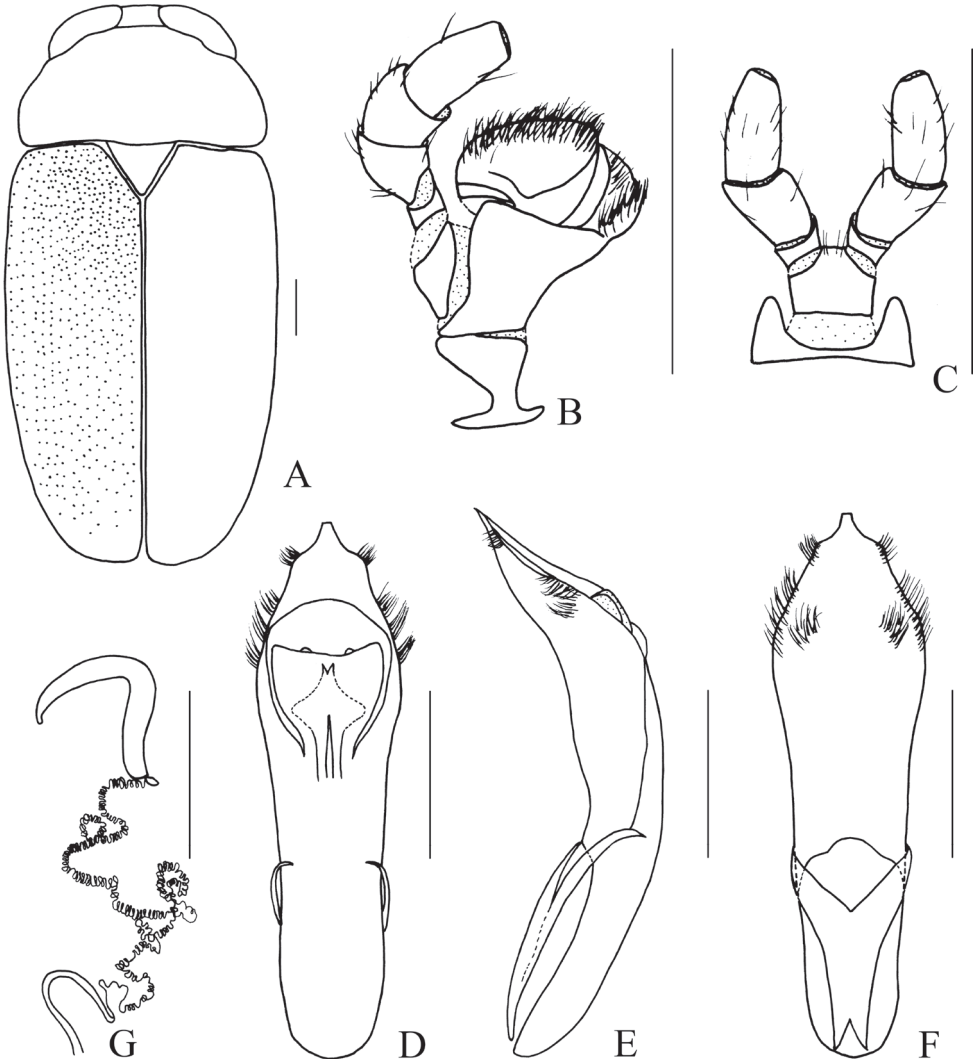

Figure 16. *Smaragdina oculata* Medvedev, 1988 **A** habitus **B** maxilla **C** labium **D** dorsal view of aedeagus **E** lateral view of aedeagus **F** ventral view of aedeagus **G** spermatheca. Scale bars: 0.5 mm.

Measurements (*n* = 4). Body length males: 4.8–5.0 mm, females: 5.5 mm.

Distribution. China (Yunnan); India.

Remark. According to the aedeagus with triangular apex and specific pubescence, the Chinese specimens are certainly *S. oculata* (Medvedev 2010: fig. 82), which has only been recorded from India.

Discussion

This study contributes new faunistic discoveries and increases the number of Chinese species of *Smaragdina* from 64 to 72. This is a very important advance in the taxonomy of this large genus in the tribe Clytrini. The Chinese *Smaragdina* have not been studied in last 30 years or longer (Gressitt and Kimoto 1961; Tan et al. 1980; Kimoto and Gressitt 1981; Tan 1988), except for one study originating from our laboratory (Wang and Zhou 2013). This is our second contribution, and it is of considerable value, as it adds to the data published by Medvedev (1988a: a systematic revision of Indo-China *Smaragdina*; 2010: a key to oriental species).

In the early studies on the leaf beetles, including *Smaragdina*, species were reported by older conventions without specimen dissections; thus, few morphological details of aedeagus, spermatheca, rectal sclerites, etc. were provided (Gressitt and Kimoto 1961; Tan et al. 1980; Kimoto and Gressitt 1981). All our papers on leaf beetles, including this and the previous on the Chinese *Smaragdina*, include morphological dissections and provide the detailed color figures of the new and other species (Wang and Zhou 2011, 2012, 2013, 2020; Su and Zhou 2017; Duan and Zhou 2021; Duan et al. 2021a, 2021b). This improvement in methodology dramatically decreases mistakes in species identifications and robustly grounds our discoveries. This, together with our other studies on leaf beetles, are of great significance in filling gaps in the Chinese faunistic composition and promoting the taxonomic progress in the subfamily Cryptocephalinae.

Acknowledgements

We thank the subject editor and the anonymous reviewers for their valuable suggestions in the reviewing process of this manuscript. This study was supported in part by the Ministry of Ecology and Environment, China (no. 2019HJ2096001006) and by the Ministry of Science and Technology of China (2015FY210300). Insect Diversity Observation Network of Sino BON (CAS, China) offered help for the field investigations.

References

Agrain FA, Buffington ML, Chaboo CS, Chamorro ML, Schöller M (2015) Leaf beetles are ant-nest beetles: the curious life of the juvenile stages of case-bearers (Coleoptera,

Chrysomelidae, Cryptocephalinae). In: Jolivet P, Santiago-Blay J, Schmitt M (Eds) Research on Chrysomelidae 5. ZooKeys 547: 133–164. https://doi.org/10.3897/zookeys.547.6098

Chaboo CS, Chamorro LM, Schöller M (2016) Catalogue of known immature stages of Camptosomate leaf beetles (Coleoptera, Chrysomelidae, Cryptocephalinae and Lamprosomatinae). Proceedings of the Entomological Society of Washington 118(2): 150–217. https://doi.org/10.4289/0013-8797.118.1.150

Chevrolat LAA (1836) In: Dejean PE, Catalogue des coléoptères de la collection de M. le comte Dejean. Édition 2, Fascicule 5, Mégrignon-Marvis Père et Fils, Paris, 361–443.

Clavareau H (1913) *Coleopterorum Catalogus.* Auspiciis et auxilio W. Junk editus a S. Schenkling. Pars 53: Chrysomelidae: 5. Megascelinae, 6. Magalopodinae, 7. Clytrinae, 8. Cryptocephalinae, 9. Chlamydinae, 10. Lamprosominae. Berlin, 278 pp.

Duan WY, Zhou HZ (2021) Revision of the subgenus *Burlinius* Lopatin (Coleoptera, Chrysomelidae, Cryptocephalinae) from China and description of four new wpecies. Diversity 13(11): e523. https://doi.org/10.3390/d13110523

Duan WY, Wang FY, Zhou HZ (2021a) Taxonomy of the *Cryptocephalus heraldicus* Group (Coleoptera: Chrysomelidae, Cryptocephalinae) from China. Diversity 13(9): e451. https://doi.org/10.3390/d13090451

Duan WY, Wang FY, Zhou HZ (2021b) Two new species of the genus *Melixanthus* Suffrian (Coleoptera, Chrysomelidae, Cryptocephalinae) from China. ZooKeys 1060: 111–123. https://doi.org/10.3897/zookeys.1060.70203

Erber D (1968) Bau, Funktion, und Bildung der Kotpresse mitteleuropaischer Clytrinen und Crptocephalinen (Coleoptera, Chrysomelidae). Zeitschrift für Morphologie der Tiere 62: 245–306. https://doi.org/10.1007/BF00401486

Erber D (1969) Beitrag zur Entwicklungs-Biologie mittleeuropäischer Clytrinae und Cryptocephalinen (Coleoptera, Chrysomelidae). Zoologische Jahrbücher Abteilung für Systematik, Ökologie, und Geographie der Tiere 96: 453–477.

Erber D (1988) Biology of Camptosomate Clytrinae – Cryptocephalinae – Chlamisinae – Lamprosomatinae. In: Jolivet P, Petitpierre E, Hsiao TH (Eds) Biology of the Chrysomelidae. Kluwer Academic Publisher, Dordrecht, 513–552. https://doi.org/10.1007/978-94-009-3105-3_30

Gao SH, Lu CK, Jia YX, Zhao CM, Cao X (2019) A new pest in vineyard under grass management model: study on the biological characteristics and control of *Smaragdina nigrifrons.* Journal of Fruit Science 36(9): 1185–1193. https://doi.org/10.13925/j.cnki.gsxb.20190098

Gressitt JL, Kimoto S (1961) The Chrysomelidae (Coleopt.) of China and Korea, part 1. Pacific Insects Monograph 1A, 299 pp.

Jacoby M (1889) Viaggio di Leonardo Fea in Birmania e regioni vicine. – List of the phytophagous Coleoptera obtained by Signor L. Fea at Burmah and Tenasserim, with descriptions of the new species. Annali del Museo Civico di Storia Naturale di Genova 27: 147–237.

Jacoby M (1895) Descriptions of new species of phytophagous Coleoptera obtained by Mr. Andrews in India. Annales de la Société Entomologique de Belgique 39: 252–288.

Jacoby M (1908) Fauna of British India, including Ceylon and Burma. Coleoptera, Chrysomelidae. Vol. 1. Taylor and Francis, London, 534 pp.

Kimoto S, Gressitt JL (1981) Chrysomelidae (Coleoptera) of Thailand, Cambodia, Laos and Vietnam. 2. Clytrinae, Cryptocephalinae and Chlamisinae, Lamprosomatinae and Chrysomelinae. Pacific Insects 23: 286–391.

Lacordaire JT (1848) Monographie des coléoptères subpentamères de la famille des phytophages. Tome second. Mémoires de la Société Royale des Sciences de Liége 5: 1–890.

Lopatin IK (2003) New species of leaf-beetles South-East Asia (Coleoptera, Chrysomelidae). Euroasian Entomological Journal 2(4): 301–304.

Lopatin IK (2004) Three new species of the genus *Smaragdina* from China (Coleoptera: Chrysomelidae). Zoosystematica Rossica 13(1): 29–31. https://doi.org/10.31610/zsr/2004.13.1.29

Lopatin IK, Konstantinov AS (2009) New genera and species of leaf beetles (Coleoptera: Chrysomelidae) from China and South Korea. Zootaxa 2083: 1–18. https://doi.org/10.11646/zootaxa.2083.1.1

Medvedev LN (1988a) Leaf beetles of the subfamily Clytrinae (Coleoptera, Chrysomelidae) in Vietnam. In: Medvedev LN (Ed.) Fauna and Ecology of Vietnamese Insects. Nauka, Moscow, 21–45.

Medvedev LN (1988b) Clytrinae (Coleoptera, Chrysomelidae) of the Himalayas from Basel Museum of Natural History. Entomologica Basiliensia 12: 469–480.

Medvedev LN (1992a) New and little known chrysomelid species (Coleoptera, Chrysomelidae) fromVietnamese coastal islands. In: Systematization [sic] and ecology of insects of Vietnam. Moscow, Nauka, 71–77.

Medvedev LN (1992b) Type specimens of the subfamily Clytrinae (Coleoptera: Chrysomelidae) from the Maurice Pic collection of the Museum national d'Histoire naturelle, Paris. Annales de la Société Entomologique de France 28(1): 15–25.

Medvedev LN (2010) A key to Oriental continental species of *Smaragdina* Chevrolat, 1836 (Chrysomelidae: Clytrinae). Entomologica Basiliensia et Collectionis Frey 32: 259–287.

Pic M (1928) Notes et descriptions. Mélanges Exotico-Entomologiques 51: 1–36.

Regalin R, Medvedev LN (2010) Chrysomelidae: Cryptocephalinae: Clytrini. In: Löbl I, Smetana A (Eds) Catalogue of Palaearctic Coleoptera, Vol. 6. Chrysomeloidea. Apollo Books, Stenstrup, 564–580.

Schöller M (2008) Comparative morphology of sclerites used by Camptosomatan leaf beetles for formation of the extrachorion (Chrysomelidae: Cryptocephalinae, Lamprosomatinae). In: Jolivet P, Santiago-Blay J, Schmitt M (Eds) (2008) Research on Chrysomelidae, Vol. 1. Brill, Leiden, 432 pp.

Su L, Zhou HZ (2017) Taxonomy of the genus *Chlamisus* Rafinesque (Coleoptera: Chrysomelidae) from China with description of three new species. Zootaxa 4233: 1–138. https://doi.org/10.11646/zootaxa.4233.1.1

Tan JJ (1988) Coleoptera: Eumolpidae. In: Huang FS, Wang PY, Yin WY, Yu PY, Lee TS, Yang CK, Wang XJ (Eds) Insects of Mt. Namjagbarwa Region of Xizang. Science Press, Beijing, 309–334.

Tan JJ, Yu PY, Li HX, Wang SY, Jiang SQ (1980) Economic Insect Fauna of China, Fasc. 18 Coleoptera: Chrysomeloidea (I). Science Press, Beijing, [xiii +] 213 pp.

Wang FY, Zhou HZ (2011) A synopsis on the Chinese species of *Clytra* Laicharting, with description of two new species (Coleoptera: Chrysomelidae: Cryptocephalinae: Clytrini). Zootaxa 3067: 1–25. https://doi.org/10.11646/zootaxa.3067.1.1

Wang FY, Zhou HZ (2012) Taxonomy of the genus *Aetheomorpha* Lacordaire (Coleoptera: Chrysomelidae: Cryptocephalinae: Clytrini) from China, with description of five new species. Journal of Natural History 46: 1407–1440. https://doi.org/10.1080/00222933.2012.673642

Wang FY, Zhou HZ (2013). Four new species of the genus *Smaragdina* Chevrolat, 1836 from China (Coleoptera: Chrysomelidae: Cryptocephalinae: Clytrini). Zootaxa 3737(3): 251–260. https://doi.org/10.11646/zootaxa.3737.3.4

Wang FY, Zhou HZ (2020) Taxonomy of the leaf beetle genus *Exomis* Weise (Coleoptera: Chrysomelidae: Clytrini) with description of six new species from China. Zootaxa 4748(2): 351–364. https://doi.org/10.11646/zootaxa.4748.2.7

Warchałowski A (2010) The Palaearctic Chrysomelidae: Identification Keys (Vol. 1). Natura Optima Dux Foundation, Warszawa, 629 pp. https://doi.org/10.1649/072.065.0210

Warchałowski A (2012) An attempt on an introductory review of *Smaragdina* Chevrolat, 1836 species from continental part of Southeastern Asia (Coleoptera: Chrysomelidae: Clytrinae). Genus 23(1): 39–97.

ZooKeys 1082: 27–50 (2022)
doi: 10.3897/zookeys.1082.77637
https://zookeys.pensoft.net

RESEARCH ARTICLE

A peer-reviewed open-access journal
ZooKeys
Launched to accelerate biodiversity research

New species and new records of *Scolytoplatypus* Schaufuss (Curculionidae, Scolytinae) from China, and resurrection of *Scolytoplatypus sinensis* (Tsai & Huang, 1965) as a distinct species

Song Liao[1*], Shengchang Lai[2*], Roger A. Beaver[3], Heiko Gebhardt[4], Jianguo Wang[1]

1 *Laboratory of Invasion Biology, Jiangxi Agricultural University, Nanchang, Jiangxi 340045, China* **2** *College of Forestry, Nanjing Forestry University, Nanjing, Jiangsu 210037, China* **3** *161/2 Mu 5, Soi Wat Pranon, T. Donkaew, A. Maerim, Chiangmai 50180, Thailand* **4** *Maienfeldstraße 23/1, D-72074 Tübingen, Germany*

Corresponding author: Jianguo Wang (jgwang@jxau.edu.cn)

Academic editor: M. Alonso-Zarazaga | Received 4 November 2021 | Accepted 22 December 2021 | Published 18 January 2022

http://zoobank.org/EF5B03E7-A0DB-4F3A-BBDA-47D41C78E2D9

Citation: Liao S, Lai S, Beaver RA, Gebhardt H, Wang J (2022) New species and new records of *Scolytoplatypus* Schaufuss (Curculionidae, Scolytinae) from China, and resurrection of *Scolytoplatypus sinensis* (Tsai & Huang, 1965) as a distinct species. ZooKeys 1082: 27–50. https://doi.org/10.3897/zookeys.1082.77637

Abstract

This study describes two new species, *Scolytoplatypus wugongshanensis* Liao, Lai & Beaver, **sp. nov.** and *S. skyliuae* Liao, Lai & Beaver, **sp. nov.**, reinstates *S. sinensis* (Tsai & Huang, 1965) from synonymy with *S. mikado* (Blandford, 1893), and records five species for the first time from China, *S. brahma* Blandford, 1898, *S. curviciliosus* Gebhardt, 2006, *S. minimus* Hagedorn, 1904, *S. ruficauda* Eggers, 1939, *S. samsinghensis* Maiti & Saha, 2009, and three from mainland China, *S. blandfordi* Gebhardt, 2006, *S. calvus* Beaver & Liu, 2007, *S. pubescens* Hagedorn, 1904. A key to the males of *Scolytoplatypus* species in China is given. Genetic data from four genes indicate a rather isolated position for both new species, although their genetic relationship to each other was close.

Keywords

Ambrosia beetles, Fujian, Jiangxi, molecular phylogeny, Scolytoplatypodini, taxonomy

* These authors have contributed equally to this work.

Introduction

The genus *Scolytoplatypus* was erected for a single species, *S. permirus* Schaufuss, from Madagascar (Schaufuss 1891). To date, there are approximately 50 species reported in the world, most of which are distributed in the Afrotropical and Oriental regions, and a few in the temperate areas of Japan to India (Wood and Bright 1992; Bright and Skidmore 1997, 2002; Beaver and Liu 2007; Maiti and Saha 2009; Jordal 2013, 2018). Approximately 16 species are known from the Afrotropical region, including 12 or 13 species on the African continent and three species in Madagascar (Jordal 2018). Beaver and Gebhardt (2006) reviewed the genus in the Oriental region and recognised 28 species, six of which are known from China. Beaver and Liu (2007) described a new species *S. calvus* Beaver & Liu, from Taiwan. Knížek (2008) described a new species, *S. zahradniki* Knížek, from Shaanxi, China, and *S. darjeelingi* Stebbing was listed for Hunan, Sichuan, and Yunnan in Knížek (2011). The following nine species are currently recognised to occur in China: *S. blandfordi* Gebhardt, 2006; *S. calvus* Beaver & Liu, 2007; *S. darjeelingi* Stebbing, 1914; *S. mikado* (Blandford, 1893); *S. pubescens* Hagedorn, 1904; *S. raja* Blandford, 1893; *S. tycon* Blandford, 1893; *S. superciliosus* Tsai & Huang, 1965 and *S. zahradniki* Knížek, 2008. *S. blandfordi*, *S. calvus* and *S. pubescens* were found only in Taiwan, China.

All known species of *Scolytoplatypus* are ambrosia beetles (Beaver and Gebhardt 2006) which cultivate fungi in a gallery system as the only food source for larvae and adults. The females of most species have a unique mycangial structure for carrying fungal spores, located on the pronotum. However, this is absent in some species (Beaver and Gebhardt 2006), and the mechanism of ambrosial fungal transport is not known in these species (Mayers et al. 2020). In addition to the structural differences of the pronotum, the two sexes also show differences in the morphology of the frons, prosternum, protibia, and elytral declivity. The beetles are monogamous. The gallery system is started by the female. It consists of an entrance gallery leading to one or more circumferential branches in one transverse plane. The male joins the female soon after the beginning of maternal gallery construction, and mating occurs at the gallery entrance. The male remains in the entrance hole to prevent the entry of predators and helps with removal of the faecal material (Browne 1961). The eggs are laid in individual niches above and below the gallery. The larvae develop in individual barrel-shaped cells, feeding on the ambrosial fungus growing on the walls, and enlarging the cell as they grow. The fully grown larva pupates in the cell, and the new adult emerges into the gallery and leaves by the original entrance hole (Beeson 1961; Browne 1961; Beaver et al. 2014)

In recent years, we have made extensive collections of beetles in China. In this paper, we describe two new species of *Scolytoplatypus* from these collections and provide a DNA-based phylogenetic analysis of several Chinese and other *Scolytoplatypus* species. We also record eight species from mainland China for the first time and provide a key to the males of the Chinese species.

Materials and methods

Abbreviations used for collections

HGT Private collection of Heiko Gebhardt, Tübingen, Germany;
JXAU College of Agricultural Sciences, Jiangxi Agricultural University, Nanchang, China;
LLY Private collection of Liu, Lan-Yu, Yilan, Taiwan, China;
NACRC National Animal Collection Resource Center, Beijing, China;
RAB Private collection of Roger A. Beaver, Chiang Mai, Thailand;
SYU Museum of Biology, Sun Yat-sen University, Guangzhou, China;
USNM National Museum of Natural History, Washington D.C., USA.

Collections were made in Jiangxi, Yunnan, Sichuan, Zhejiang, Fujian, and Chongqing in China. The samples were immediately preserved in tubes containing 99.9% ethyl alcohol, which were stored at – 20 °C for DNA extraction and examination. We used a stereoscopic microscope (Cnoptec SZ680) to examine the beetles. Photographs were taken with Keens Ultra-Depth of Field 3D Microscope (VHX-600). All photographs were further adjusted and assembled with Adobe Photoshop CS6. All measurements were made on ten specimens of both sexes chosen to show the entire variability range. The body length was measured from the anterior pronotal margin to the elytral apex. Finally, we also provide references to published illustrations of several species, which can be found on the Internet or in publications.

DNA was extracted from the adult head. The total genomic DNA was extracted from each individual using the Ezup Column Animal Genomic DNA Purification Kit (Sangon Biotech Co. Ltd). Amplification of four gene fragments (COI, EF-1α, CAD, 28S) was made by PCR, using primers and cycling conditions previously described (Jordal et al. 2011). The PCR products containing target bands were sent to Sangon Biotech Co. Ltd (Shanghai, China) for purification and sequencing, and the sequences were analysed using the software DNAstar. Additional information on the *Scolytoplatypus* material was collected by the authors in China or downloaded from **NCBI** (The National Center for Biotechnology Information) (Table 1). Concatenated DNA sequence data from Jordal (2013) were analysed in MrBayes v. 3.2.6, Partitions and models were estimated by PartitionFinder 2 and ModelFinder respectively in PhyloSuite, GTR+G were selected for each partition. 10 million generations were run, with 25% of the generations as burn-in, PSRF close to 1.0 and standard deviation of split frequencies below 0.01 were accepted (Lai et al. 2021). Maximum likelihood (ML) analyses were conducted with IQ-TREE. The optimal model of molecular evolution found by ModelFinder each partition based on the Bayesian information criterion (BIC) scores. Each partition was as follows: 28S = GTR+I+G, CAD = TVMEF+I+G, COI= GTR+I+G, EF-1α = TRN+I+G. Clade support was assessed by 5000 bootstrap pseudoreplicates of the combined data set.

Table 1. Material used for phylogenetic analyses, including their GenBank accession numbers.

No.	Taxon	Country	COI	CAD	EF-1α	28S	Reference
1	*Remansus mutabilis*	Madagascar	KF758328	KF758316	KF758341	KF758300	Jordal 2013
2	*R. pygmaeus*	Madagascar	–	KF758310	KF758338	KF758294	Jordal 2013
3	*R. sahondrae*	Madagascar	KF758331	KF758319	KF758347	KF758303	Jordal 2013
4	*Scolytoplatypus africanus*	Uganda	EU191866	HQ883822	EU191898	AF308391	Jordal 2013
5	*S. brahma*	China: Yunnan	LC657958	LC657966	LC657974	LC657950	This study
6	*S. calvus*	China: Yunnan	LC657960	LC657968	LC657976	LC657952	This study
7	*S. congonus*	Tanzania	KF758322	KF758306	KF758334	KF758290	Jordal 2013
8	*S. entomoides*	Papua New Guinea	HQ883679	HQ883823	HQ883748	–	Jordal 2013
9	*S. fasciatus*	South Africa	KF758324	KF758309	KF758337	KF758293	Jordal 2013
10	*S. hova*	Madagascar	KF758326	KF758314	KF758340	KF758298	Jordal 2013
11	*S. javanus*	Malaysia	KF758333	–	KF758349	KF758305	Jordal 2013
12	*S. minimus*	China: Sichuan	LC657959	LC657967	LC657975	LC657951	This study
13	*S. neglectus*	Cameroon	KF758332	KF758320	KF758348	KF758304	Jordal 2013
14	*S. permirus*	Madagascar	KF758325	KF758311	KF758339	KF758295	Jordal 2013
15	*S. pubescens*	China: Yunnan	LC657956	LC657964	LC657972	LC657948	This study
16	*S. raja*	China: Yunnan	LC657954	LC657962	LC657970	LC657946	This study
17	*S. rugosus*	Madagascar	KF758330	KF758317	KF758345	KF758301	Jordal 2013
18	*S. sinensis*	China: Jiangxi	LC657957	LC657965	LC657973	LC657949	This study
19	*S. truncatus*	Cameroon	KF758323	KF758308	KF758336	KF758292	Jordal 2013
20	*S. tycon*	Japan	JF894375	–	JF713688	JX263764	Jordal 2013
21	*S. unipilus*	Gabon	MG979488	MG979490	MG979489	–	Jordal 2013
22	*S. wugongshanensis* sp. nov.	China: Jiangxi	LC657953	LC657961	LC657969	LC657945	This study
23	*S. skyliuae* sp. nov.	China: Jiangxi	LC657955	LC657963	LC657971	LC657947	This study

Taxonomic account

***Scolytoplatypus wugongshanensis* Liao, Lai & Beaver, sp. nov.**
http://zoobank.org/5D6F7CDD-65BE-4EDF-B594-E61DFC226527
Figure 1

Type material. ***Holotype.*** Male, China: Jiangxi Province, Pingxiang City, Luxi County, Wanlongshan Town, Wugong Mountain, Yangshimu, 27°34'47"N, 114°13'57"E, 27.IX.2017, log dissection, host Fagaceae sp, Shengchang Lai leg. (deposited in NACRC).

Allotype. Female, the same data as the holotype (deposited in NACRC).

Paratypes. 10 males, 10 females, the same data as the holotype (8 males, 8 females JXAU; 2 males, 2 females NACRC); 3 males, China: Jiangxi Province, Ji'an City, Jinggangshan national nature reserve of Jiangxi, Luofu reservoir, 26°38'27"N, 114°8'45"E, 21.V.2017, log dissection, host unclear, Shengchang Lai leg. (deposited in JXAU); 4 males, 3 females, China: Jiangxi Province, Ganzhou City, Xunwu County, Xiangshan Town, Congkeng Village, 24°55'51"N, 115°51'14"E, 20.V.2018, log dissection, host unclear, Shengchang Lai leg. (1 male, 1 female RAB; 3 males, 2 females JXAU); 17 males, 17 females, China: Fujian Province, Nanping City, Jianyang District, Huilong Town, 27°28'31"N, 118°24'35'E, 152.7m, 15.VIII.2020, log dissection, host unclear, Ling Zhang, Yufeng Cao leg. (2 males, 2 females USNM; 2 males, 2 female LLY; 2 males, 2 females NACRC; 2 males, 2 females RAB; 2 male, 2 females SYU; 7 males, 7 females JXAU).

Diagnosis. The morphology of the species, especially the male prosternum, indicates that it is more closely related to *S. blandfordi* Gebhardt. Both species have the

Figure 1. *Scolytoplatypus wugongshanensis* (**A–F** male **G, H** female) **A** dorsal view **B** head anterior view **C** ventral view **D** lateral view **E** prosternum **F** elytral declivity **G** dorsal view **H** lateral view.

Table 2. Diagnostic characters separating *Scolytoplatypus wugongshanensis*, *Scolytoplatypus blandfordi* and *Scolytoplatypus skyliuae*.

	S. wugongshanensis	***S. blandfordi***	***S. skyliuae***
Body size	Male 3.8–4.2 mm long; female 4.0–4.6 mm long.	Male 3.1–3.3 mm long; female 3.1–3.3 mm long.	Male 4.0–4.3 mm long; female 4.4–4.8 mm long.
Frons	Male frons with two distinct brushes of long hairs on the margins.	Male frons with a sparse fringe of long hairs.	Male frontal margin with a fringe of hairs dorsally extending to vertex.
Anterior processes of male prosternum	Processes short, bluntly rounded at tip, lying parallel to anterior margin.	Processes longer, falcate, sharply tipped, curving anteriorly.	Processes inserted just behind anterior margin, broadly triangular, diverging at an angle of ~ 90°
Elytral disc	Angularly separated from declivity	Evenly curving into declivity	Evenly curving into declivity
Elytral declivity	Male declivity with small spines present on interstriae 1–7.	Male declivity with spines present only on interstriae 1, 3, 5–7.	Male declivity with granules present on interstriae 2–5, 8.
	Female declivity with long, dense pubescence.	Female declivity with fine, dense, yellowish setae.	Female declivity with long, dense pubescence.

male prosternum raised in a triangle with the apex anterior, and on the anterior margin, two small, flattened processes set close together on each side of the midline (compare Fig. 1E with Beaver and Gebhardt 2006: fig. 2B). Males of *S. wugongshanensis* and *S. blandfordi* can be distinguished using the characters given in Table 2.

Description. Male. ***Body.*** Length 3.8–4.2 mm (3.8 mm in holotype), 2.00–2.21× as long as wide (2.00 in holotype); dark brown to black in mature specimens, shiny, elytra slightly darker. Whole body covered with fine, yellowish hairlike setae.

Frons. Shallowly concave, slightly flattened above epistoma, with short and shallow depressions on its sides and a fine median impressed line on upper half, lower flattened part without punctures and setae, upper part with minute punctures bearing fine, erect, yellowish setae, margin with two brushes of long golden hairlike setae above the eye, widely separated dorsally, curved towards centre of frons and extending nearly to epistoma; a few long setae on frontal margin at level of antennal insertions.

Antennal club. 2.1–2.2× as long as wide, elongate and triangular, widest near the base, acuminate, densely covered with short appressed setae, anteroventral margin in basal half with a row of seven long, erect setae, thickened and curved at tips, apex with a few long, erect setae.

Pronotum. 0.81–0.87× as long as wide (0.81 in holotype), widest in the middle of its length, anterior margin with distinct median emargination, posterior margin bisinuate, slightly produced in the middle, posterolateral corners approximately rectangular, dorsal surface shining, minutely, moderately densely, rather irregularly punctured except for small, median, impunctate area just anterior to middle of pronotum, corresponding to site of mycangium in female, vestiture of very fine and short hairlike setae. Anteroventral angles with a deep, oval fovea, extending to anterior but not ventral margin of pronotum.

Prosternum. Median part raised in a triangle, its apex anterior not reaching the anterior margin, anterior quarter shining, smooth, the extreme tip sharply pointed, posterior three-quarters of triangle more coarsely granulate. Each granule with a moderately long, backwardly directed seta; anterior margin of prosternum with two symmetrical, divergent, triangular, translucent processes.

Procoxa. Slightly flattened anteriorly, rugose, a group of longer setae near the anterior margin; posteriorly with a small, raised, granulate process bearing a loose brush of long, medially curved, coarse, yellow setae.

Elytra. 1.10–1.21× as long as wide (1.15 in holotype), 1.62–1.76× as long as pronotum (1.69 in holotype), clearly wider than pronotum, sides almost parallel, widest in posterior part, then strongly converging to rounded apex, disc of elytra shining, finely, densely, confusedly punctured, with short, fine, semi-erect, posterior pubescence, declivity angularly separated from disc, striae and interstriae more clearly distinct on declivity, striae broadly but weakly impressed, interstriae very densely, shallowly punctured, interstriae 1–7 each with a row of minute, backwardly directed spines, vestiture longer and denser than elytral disc.

Abdomen. Ventrites shallowly, densely punctured, each puncture with a fine, backwardly directed seta, setae variable in length; last visible ventrite with a band of long golden setae directed posteriorly.

Female. (Fig.1G, H). Length 4.0–4.6 mm (4.0 mm in allotype), 2.11–2.42× as long as wide (2.11 in allotype). Similar to male, slightly larger. Frons triangularly impressed above epistoma, otherwise convex, matt, moderately densely, finely punctured, reticulate between punctures which bear fine, white, erect, hairlike setae, median cranial suture prominent, extending as a fine line to apex of frontal impression. Antennal scape shorter and antennal club oval, shorter and wider than male, rounded at apex, without a row of erect setae antero-ventrally. Pronotum generally as male, but with oval mycangial pit surrounded by erect yellow setae in midline anterior to middle; anteroventral fovea absent. Prosternum a flattened plate lacking specific characters. Procoxae flattened without a process or brush of hairs posteriorly. Elytra generally as in male, but interstrial spines on declivity smaller.

Host. Fagaceae sp.

Distribution. China: Fujian (Nanping) and Jiangxi (Ganzhou, Pingxiang).

Biology. Specimens were collected from small branches (2.0–2.3 mm diameter) of broadleaved trees, including an unidentified species of Fagaceae. The maternal gallery penetrates almost through the whole diameter of the twig, and pupal chambers lie perpendicular to the maternal gallery.

Etymology. The specific name refers to the type locality, Wugongshan Mountain.

Scolytoplatypus skyliuae **Liao, Lai & Beaver, sp. nov.**
http://zoobank.org/2DCE3543-8434-49A8-8CCC-DD6B0D07BB40
Figure 2

Type material. ***Holotype.*** Male, China: Jiangxi Province, Shangrao City, Yanshan County, Wuyishan national nature reserve of Jiangxi, Huanggang Mountain, 27°52'56"N, 117°46'37"E, 17.VII.2017, log dissection, host unclear, Shang Tian, Shengchang Lai, Lifang Xiao & Peishan He leg. (deposited in NACRC).

Allotype. Female, the same data as the holotype (deposited in NACRC).

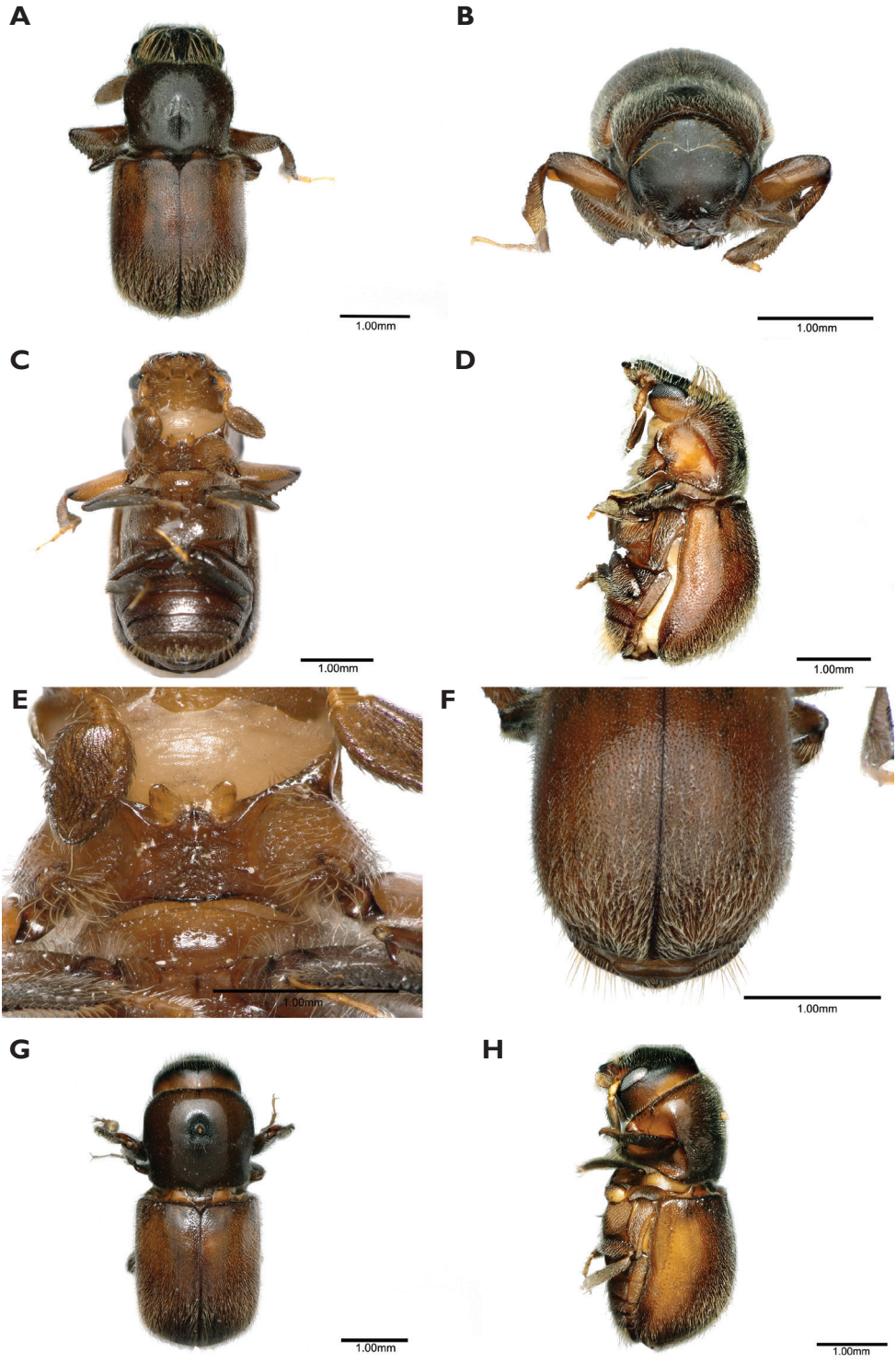

Figure 2. *Scolytoplatypus skyliuae* (**A–F** male **G, H** female) **A** dorsal view **B** head anterior view **C** ventral view **D** lateral view **E** prosternum **F** elytral declivity **G** dorsal view **H** lateral view.

Paratypes. 8 males, 8 females, the same data as the holotype (6 males, 6 females JXAU; 2 males, 2 females NACRC); 25 males, 19 females, China: Fujian province, Wuyishan city, Wuyishan national nature reserve of Fujian, Guadun Village, 27°44'34"N, 117°38'2"E, 9.VII.2018, 1347.1m, log dissection, host *Castanopsis fargesii* Franch., Shengchang Lai, Kaiping Hu, Jia Lv & Ling Zhang leg. (2 males, 2 females USNM ; 2 males, 2 females LLY; 2 males, 2 females NACRC; 2 males, 2 females RAB; 2 males, 2 females SYU; 15 males, 9 females JXAU).

Diagnosis. Like *S. wugongshanensis*, this species is similar to *S. blandfordi* in its general form and in the structure of the prosternum. The males of those can be distinguished using the characters given in Table 2.

Description. Male. ***Body.*** Length 4.0–4.3 mm (4.0 mm in holotype), 2.11–2.26× as long as wide (2.11 in holotype); dark brown to black in mature specimens, whole body covered with fine, yellowish hairlike setae.

Frons. Strongly concave, slightly flattened above epistoma, with small, shallow depressions at sides, surface minutely reticulate, finely, sparsely punctured, punctures with erect, fine hairs, median line extending ~ 1/4 of frontal height, margins with a row of longer setae below eyes, above eyes a fringe of long, golden setae, extending to vertex, and inwardly curved to middle of frons.

Antennal club. Ovate, ~ 1.7× longer than wide, widest ~ 1/4 length from base, apex narrowly rounded, densely covered with short, appressed setae, anteroventral margin with a row of five or six long erect setae with thickened and incurved tips.

Pronotum. 0.94–1.00× as long as wide (0.94 in holotype), widest at middle, narrowed posteriorly, anterior margin with distinct median emargination, posterior margin bisinuate, slightly produced in the middle, posterolateral corners approximately rectangular, surface smooth, shining, with fine, shallow, irregularly spaced punctures, more densely placed towards posterior margin, bearing fine setae. Anteroventral angles with a deep, oval fovea, not extending to anterior or ventral margins of pronotum.

Prosternum. Median part raised in a triangle, its apex anterior, sharply pointed, not reaching the anterior margin, anterior tip shining, impunctate, posterior part rugose, shallowly punctured, the punctures with appressed, backwardly directed setae. Two symmetrical, triangular, translucent processes diverging at an angle of ~ 90°, inserted just behind anterior margin.

Procoxae. Anterior part flattened, rugose, coarsely, shallowly punctured; posteriorly with a raised, granulate process bearing long, coarse setae, not forming a distinct brush.

Elytra. 1.10–1.16× as long as wide (1.16 in holotype), 1.31–1.47× as long as pronotum (1.37 in holotype), clearly wider than pronotum, sides almost parallel, widest in posterior part, then strongly converging to rounded apex; disc of elytra shining with confused, fine punctures, more closely placed towards declivity, pubescence fine and short, semi-erect, posterior; disc evenly rounded into declivity; declivity convex, densely, finely punctured, sutural interstriae weakly raised in mid-declivity bearing a row of small pointed granules, striae 1 and 2 and interstriae 2 slightly impressed, interstriae 2 without granules except for one or two at top of declivity, interstriae 3 slightly raised with a row of pointed granules, interstriae 4 and 5 with a few scattered granules, interstriae 8 finely carinate posteriorly, the carina extending to the elytral

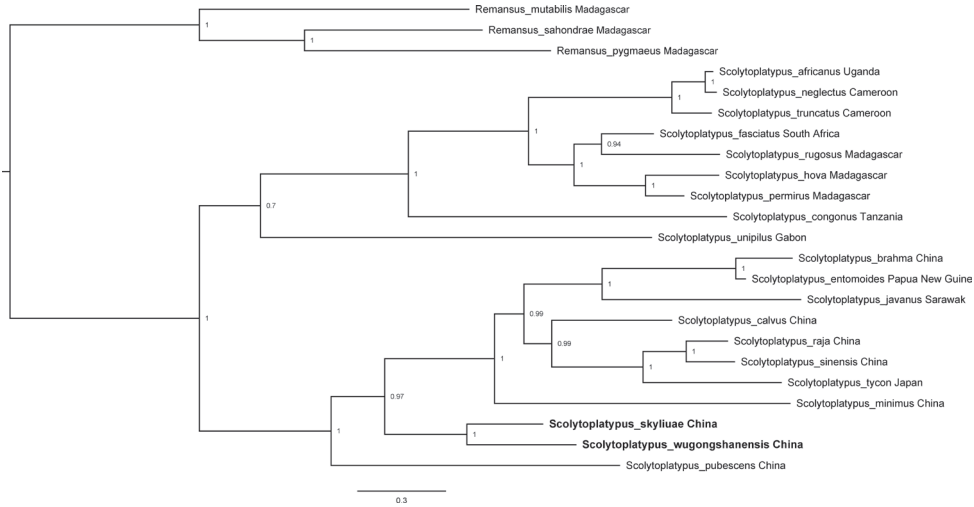

Figure 3. Tree topology resulting from Bayesian and ML analyses of four gene fragments.

apex, with a row of minute sharply pointed granules posterolaterally; pubescence denser and longer on the declivity then elytral disc .

Abdomen. Ventrites shallowly, densely punctured, each puncture with a fine, backwardly directed seta, setae variable in length; last visible ventrite with a band of long golden setae directed posteriorly.

Female. (Fig. 2G, H). Length 4.4–4.8 mm (4.6 mm in allotype), 2.32–2.53× as long as wide (2.42 in allotype). Similar to male, but slightly larger. Frons convex, a weak, triangular impression above epistoma, surface finely reticulate, sparsely, finely punctured, punctures bearing short, fine, erect setae, median cranial suture extending as a median line to apex of triangular impression. Antennal scape shorter than in male, antennal club oval, shorter and wider than male, without a row of erect setae antero-ventrally. Pronotum generally as male, but with a median oval mycangial pit surrounded by erect yellow setae anterior to middle; anteroventral fovea absent. Prosternum a flattened plate lacking specific characters. Procoxae flattened without a posterior process. Elytral declivity generally as in male, but sutural interstriae very slightly raised, and impression lateral to it obsolescent, interstrial granules minute.

Host. *Castanopsis fargesii* Franch. (Fagaceae).

Distribution. Fujian (Wuyishan) and Jiangxi (Shangrao).

Etymology. The species is named for Dr. Sky Liu Lan-Yu for her contributions to the systematics and biology of wood-boring beetles.

Molecular data. The tree topology resulting from the Bayesian and ML analyses of the combined molecular data were near identical and all nodes except one received high support (Fig. 3). Additionally, *S. wugongshanensis* and *S. skyliuae* formed a sister clade to the Asian species of *Scolytoplatypus*. Phylogenetic analysis indicates a rather isolated position for both new species, although their genetic relationship was close.

New records and notes on species

Scolytoplatypus sinensis Tsai & Huang, 1965, revised status

Figure 4

Scolytoplatypus sinensis Tsai & Huang, 1965: 121.

Taxonomy. This species has been considered to be a synonym of *S. mikado* Blandford (Wood 1989; Beaver and Gebhardt 2006). Having now examined a larger number of specimens from various provinces of China (including Taiwan), we believe it to be a distinct species. Park (2016) in an unpublished thesis came to the same conclusion based on morphology and DNA differences, but has not officially published his results. Therefore, we resurrect the species here. The species was previously recorded from China (Fujian, Sichuan), Korea and Taiwan (Tsai and Huang 1965; Park 2016). Park (2016) also includes Japan, but we have seen no specimens from that country, nor any published records.

Material examined. China: Jiangxi, Ganzhou, Longnan, Jiulanshan Mtn Nat. Res., 24.622N, 114.564E, 440 m, 17.v.2018, Lai, S-C. (1m, 1f RAB); 5 males 5 females (JXAU) as previous except: Chongyi County, Yangmingshan Forest Park, 25°33'56"N, 114°20'18"E, 10.VII.2021, log dissection, *Cinnamomum cassia* Presl, Ye Xu leg.; China: Yunnan, Honghe, Hani Yi Auton, Pref., Jinping Co., 22.78N, 103.23E, 30.vii.2019, A-Hong-chang, Duan-bo (1m, 1f RAB); China: Zhejiang, Gutianshan Nat. N. Res., 29°8'18"–29°17'29"N, 118°2'14"–118°11'12"E. CSP 21–SE5, 2009, [no collector] (1f RAB); as previous except: 29°25'N, 118°12'E, 402 m, CSP 13–SE4, 2010 (1m RAB); 7 males, 7 females (JXAU) China: Fujian Province, Zhangzhou City, Yunxiao County, Wushan, 23°55'20"N, 117°11'31"E, ca 740 m, 15.VII.2019, log dissection, *Cinnamomum camphora* (L.) Presl, Song Liao, Ling Zhang & Shengchang Lai leg.; 14 males, 20 females (JXAU) China: Chongqing, Wushan County, Luoping Town, 31°12'23"N, 110°05'18"E, 21.VIII.2016, log dissection, host unclear, Shang Tian leg.; 43 males, 27 females (JXAU) China: Sichuan Province, Xichang City, Leibo County, Mahu Township, 28°24'54"N, 103°46'16"E, ca 1088 m, 5.VIII.2021, log dissection, *C. camphora*, Song Liao leg.

Distribution. China (Chongqing, Fujian, Jiangxi, Sichuan, Yunnan, Zhejiang)

Remarks. The characters given by Tsai and Huang (1965) to distinguish the species from *S. mikado* are not entirely reliable, showing some degree of intraspecific variation, and their figures can be misleading. The male of *S. sinensis* can be distinguished from *S. mikado* by the following characters (*S. sinensis* given first): Prosternum strongly humped anteriorly when viewed from below vs. anterior part of prosternum almost flat or weakly raised, never strongly humped; anterior processes of prosternum directed forwards, diverging by up to 60° vs. anterior processes directed more laterally, diverging at an angle of 60–120°; procoxae with a dense brush of 15–20 long, erect setae anteriorly near the inner margin vs. procoxae with only a few (4–7) long, erect setae anteriorly; smaller size, male 3.0–3.2 mm long vs. male 3.3–3.6 mm long. It has not been possible to find characters which will reliably separate the females of the two species if they are not collected in association with males. The suggestion of Tsai

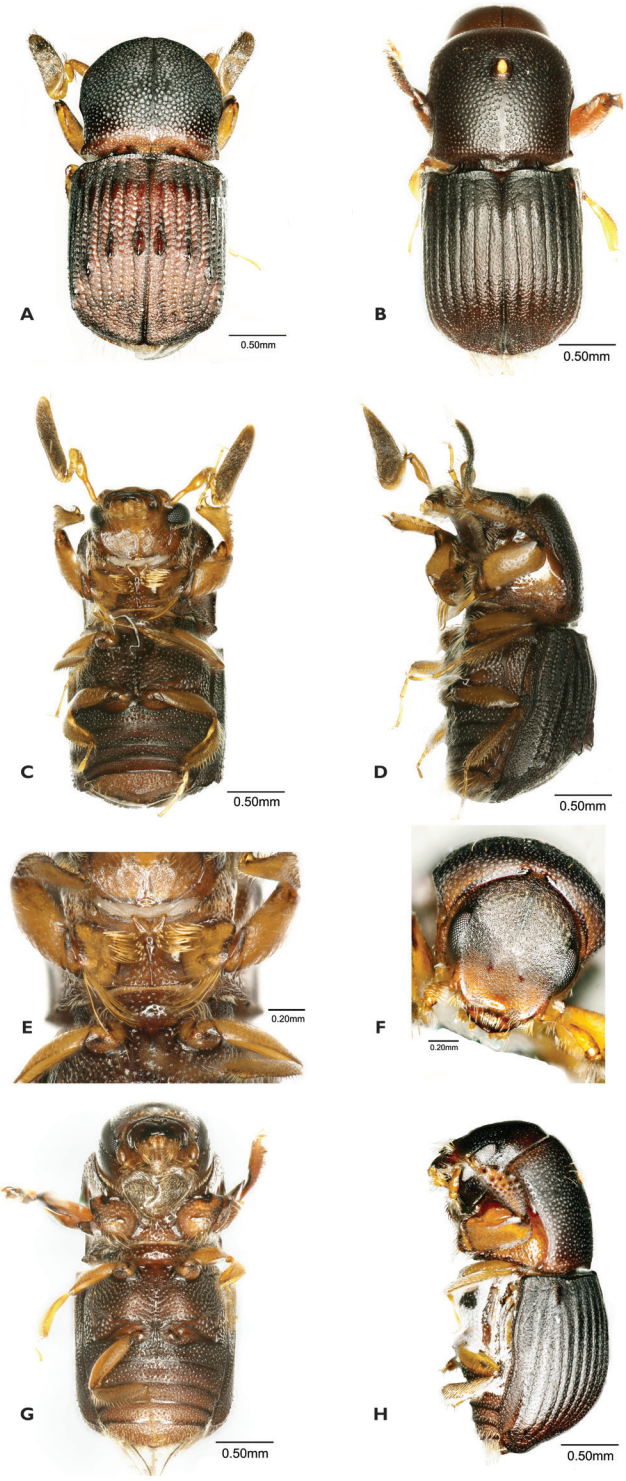

Figure 4. *Scolytoplatypus sinensis* (**A, C–F** male **B, G, H** female) **A** dorsal view **B** dorsal view **C** ventral view **D** lateral view **E** prosternum **F** head anterior view **G** ventral view **H** lateral view.

and Huang (1965) that there is a difference in the position of the mycangial pore on the dorsal surface of the pronotum is not borne out by the examination of numerous specimens of both species.

Hosts. *Alnus cremastogyne* Burk. (Betulaceae), *Amygdalus davidiana* (Carr.) C. de Vos (Rosaceae), *Phoebe zhennan* S.K. Lee & F.N.Wei (Lauraceae), Theaceae (Tsai and Huang 1965). *Cinnamomum camphora* and *C. cassia* (Lauraceae) are newly recorded hosts.

***Scolytoplatypus blandfordi* Gebhardt**

Scolytoplatypus blandfordi Gebhardt, 2006: 162, fig. 2B.

Material examined. China: Yunnan, Honghe, Maguanm Gulingqin, 22.731N, 103.993E, 592 m, FIT, 24.iv.2018, DJS17, L.Z. Meng (1m RAB); as previous except: Lijiang, 24.143N, 100.227E, 3221 m, 28.v.2018, LJ3200–4FI (2m RAB); as previous except: Puer, Jingdong, Ailoshan, 24.532N, 101.015E, 2499 m, 8.v.2018, ALS(S)2400–3FI (2m RAB); as previous except: 24.517N, 101.012E, 9.vi.2018, FIT, ALS2200–2FI (1f RAB).

Distribution. China (Taiwan). New to Chinese mainland (Yunnan).

Diagnosis. The species is related to *S. wugongshanensis* and *S. skyliuae*. The males can be distinguished by the characters given in Table 2 and the key.

Host. Recorded from *Cyclobalanopsis morii* (Hayata) Schottky (Fagaceae) (Beaver and Gebhardt 2006).

***Scolytoplatypus brahma* Blandford**

Figure 5

Scolytoplatypus brahma Blandford, 1898: 425.
Scolytoplatypus hamatus Hagedorn, 1904: 260. Synonymy: Schedl 1952: 159.
Scolytoplatypus hirsutus Blackman, 1943: 124. Synonymy: Schedl 1952: 159.
Scolytoplatypus paucegranulatus Eggers, 1935: 242. Synonymy: Beaver and Gebhardt 2006: 167.

Material examined. 4 males, 1 female (JXAU) China: Yunnan Province, Honghe Hani and Yi Autonomous Prefecture, Jinping County, 22°46'48"N, 103°13'48"E, 21.IV.2017, ethanol trap, Bo Duan, Hongchang A leg.; 1 female (JXAU) as previous except: Hekou County, Mahuangbao, 22°34'49"N, 103°58'30"E, 10.VIII.2018, ethanol trap, Bo Duan, Hongchang A leg.; 1 male (JXAU) as previous except: Xishuangbanna Dai Autonomous Prefecture, Mengpeng Farm, 21°24'45"N, 101°20'21"E, 26.VII2018, ethanol trap, Bo Duan, Hongchang A leg.; 1 male (JXAU) as previous except: Mengman Farm, 21°23'34"N, 101°18'51"E,

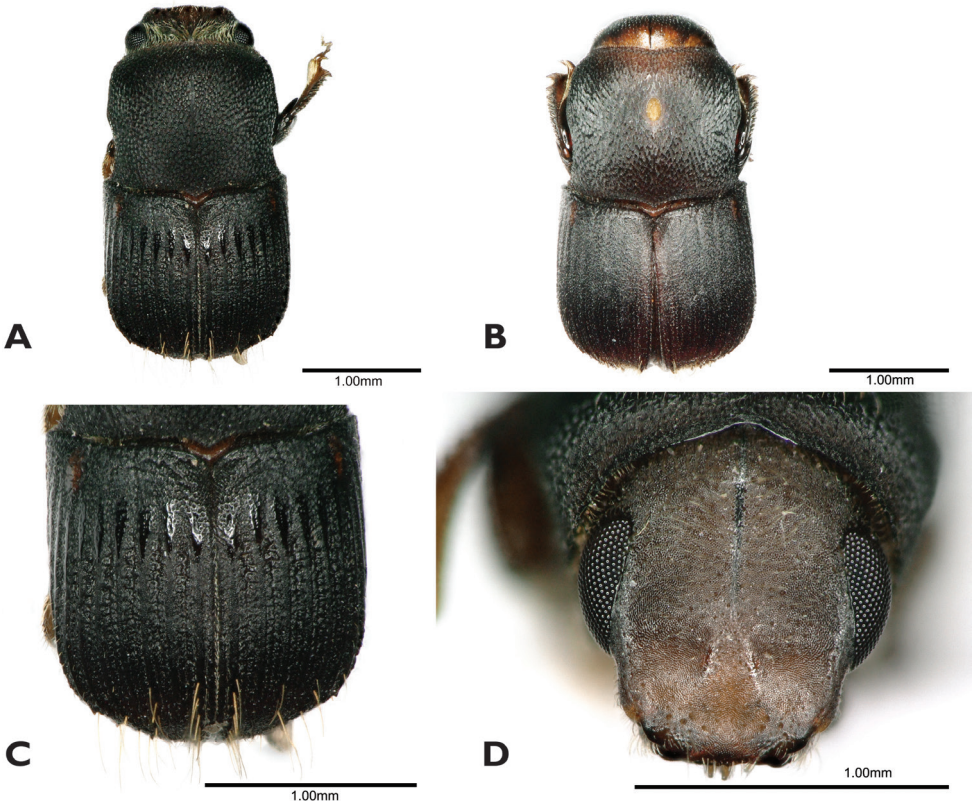

Figure 5. *Scolytoplatypus brahma* (**A, C, D** male **B** female) **A** dorsal view **B** dorsal view **C** elytral declivity **D** head anterior view.

26.VII.2018, ethanol trap, Bo Duan, Hongchang A leg.; 1 male (JXAU) as previous except: Mengpeng Farm, 21°24'45"N, 101°20'21"E, 17.XI2019, ethanol trap, Bo Duan, Hongchang A leg.

Distribution. Bangladesh, Borneo, India, Indonesia (Sumatra, Java) Malaysia, Thailand (Sabah) (Beaver and Gebhardt 2006; Beaver et al. 2014). New to China (Yunnan)

Diagnosis. The species is most closely related to *S. bombycinus*, but is considerably smaller. The male of *S. brahma* is characterised by its characteristic prosternal plate, which is structurally similar to that of *S. bombycinus*, and by a small elongate swelling in the midline on the upper part of the frons (Blackman 1943: fig. 12).

Host. This species is polyphagous attacking a wide range of host trees in many families, including: *Cryptocarya wightiana* Thwaites (Lauraceae), *Ilex dipyrena* Wall. (Aquifoliaceae), *Swietenia mahagoni* (L.) Jacq. (Meliaceae) (Wood 1992), *Erythrina subumbrans* (Hassk.) Merr. (Leguminosae), *Hevea brasiliensis* (Willd. ex A. Juss.) Muell. Arg. (Euphorbiaceae), *Theobroma cacao* L. (Sterculiaceae), *Vernonia arborea* Buch.-Ham. (Compositae) (Kalshoven 1959).

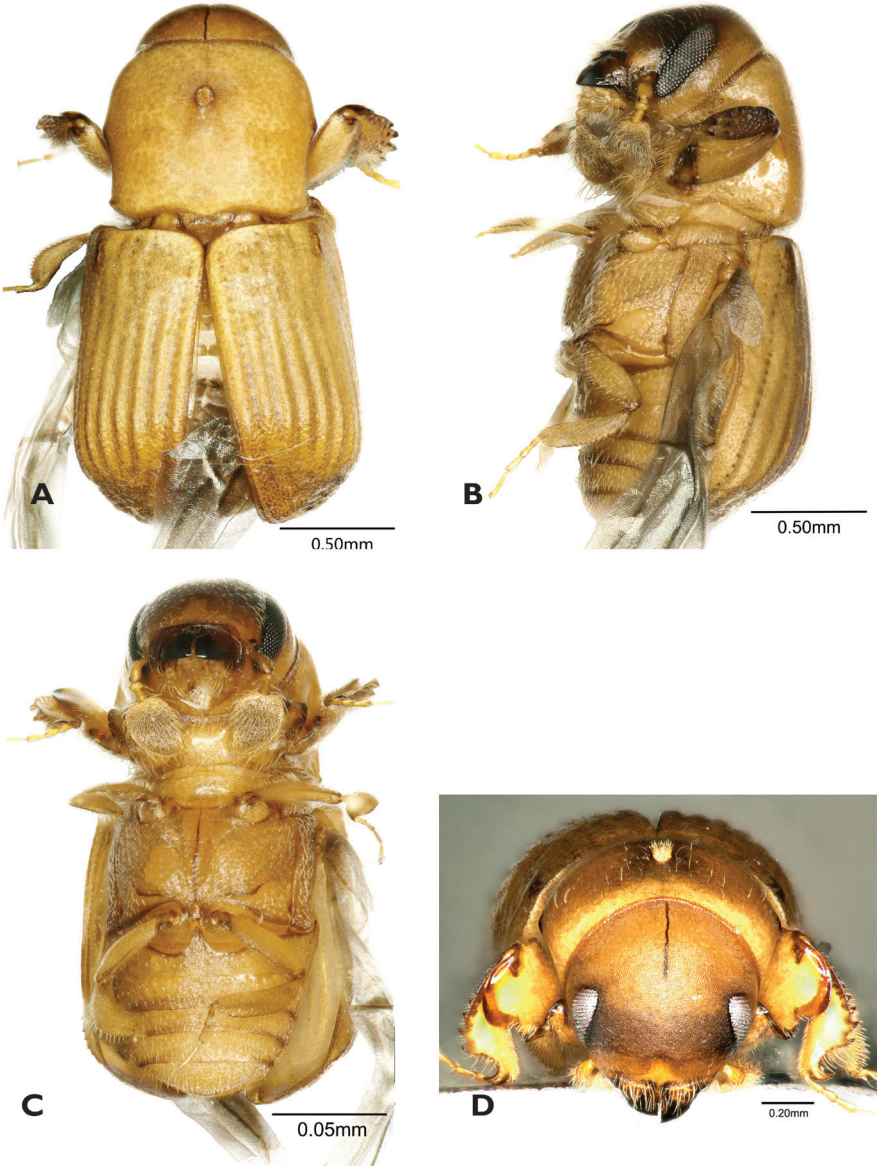

Figure 6. *Scolytoplatypus calvus* (**A–D** female) **A** dorsal view **B** lateral view **C** ventral view **D** head anterior view.

***Scolytoplatypus calvus* Beaver & Liu**
Figure 6

Scolytoplatypus calvus Beaver & Liu, 2007: 227.

Material examined. China: Sichuan Prov., Moxi env., Hailuogou valleu, Gonghe vill., 29°37'27"N, 102°06'28"E, 1715 m, 17–21.vi.2014, at light, J. Hájek, J. Růžička, M.

Thoč (1m RAB); China: W Fujian, Emei Feng, 27°01'N, 117°04'E, 1200–1500 m, 3.-4.vi.2008, Jaroslav Turna (1 female HGT); 2 females (JXAU) China: Yunnan Province, Chuxiong City, Zixi Mountain, 25°0'15"N, 101°24'39"E, ca. 2354 m, 12.VIII. 2021, ethanol trap, Song Liao, Guangyu Yu leg.

Distribution. China (Taiwan). New to Chinese mainland (Fujian, Sichuan, Yunnan).

Diagnosis. *S. calvus* is most closely related to *S. mikado* and *S. raja*, but is smaller than either, and may be distinguished by the characters given in the key.

Host. Not known.

Scolytoplatypus curviciliosus Gebhardt

Scolytoplatypus curviciliosus Gebhardt, 2006: 165, fig. 2K.

Material examined. China: Yunnan, Xishuangbanna, 28 km NW Jinghong, vic. An Ma Xi Zhan (NNNR), 22°12'E, 100°38'E, 700 m, forest, EKL, 8.vii.2008, A. Weigel (1m, 6f RAB); as previous except: Mengla, Bubeng, 21.610N, 101.582E, 709 m, 6.iii.2019, BB(S)600–4FI, L.Z. Meng (4m, 4f RAB); as previous except: Menglun, 21.929N, 101.254E, 600 m, 2.iv.2018, XTBG600–1FI (2m, 1f RAB).

Distribution. Philippines, Thailand. New to China (Yunnan).

Diagnosis. The species most closely resembles *S. parvus* and *S. reticulatus*. The male can be distinguished from *S. parvus* by the absence of granules and conspicuous white hairs on the lower part of the elytral declivity, and from *S. reticulatus* by the lack of teeth on the interstriae at the summit of the elytral declivity, and the impressed elytral striae. The females of all three species lack a mycangial pore on the pronotum. The female of *S. curviciliosus* can most easily be distinguished from *S. parvus* by its slightly larger size (2.0–2.1 mm vs. 1.8–1.9 mm in *S. parvus*), and the more strongly angulate posterior angles of the pronotum, and from *S. reticulatus* by the non-impressed elytral striae, obsolescent on the declivity, and flat, not convex, interstriae (Beaver and Gebhardt 2006).

Host. Unclear.

Scolytoplatypus minimus Hagedorn
Figure 7

Scolytoplatypus minimus Hagedorn, 1904: 125.

Material examined. 1 female (JXAU) China: Yunnan Province, Baoshan City, Gaoligong Mountain Nature Reserve, Baihualing, 25°18'22"N, 98°47'45"E, ca. 1600 m, 28.VII.2019, ethanol trap, Song Liao, Shengchang Lai leg.; CHINA: Yunnan, Yulongshan mts., Ganhaizi pass, 3500 m, 18–23.vii.1990, V. Kubáň (1m RAB); as previous except: Xishuangbanna, 28 km NW Jinghong, vic. An Ma Xi Zhan (NNNR), 22°12'E,

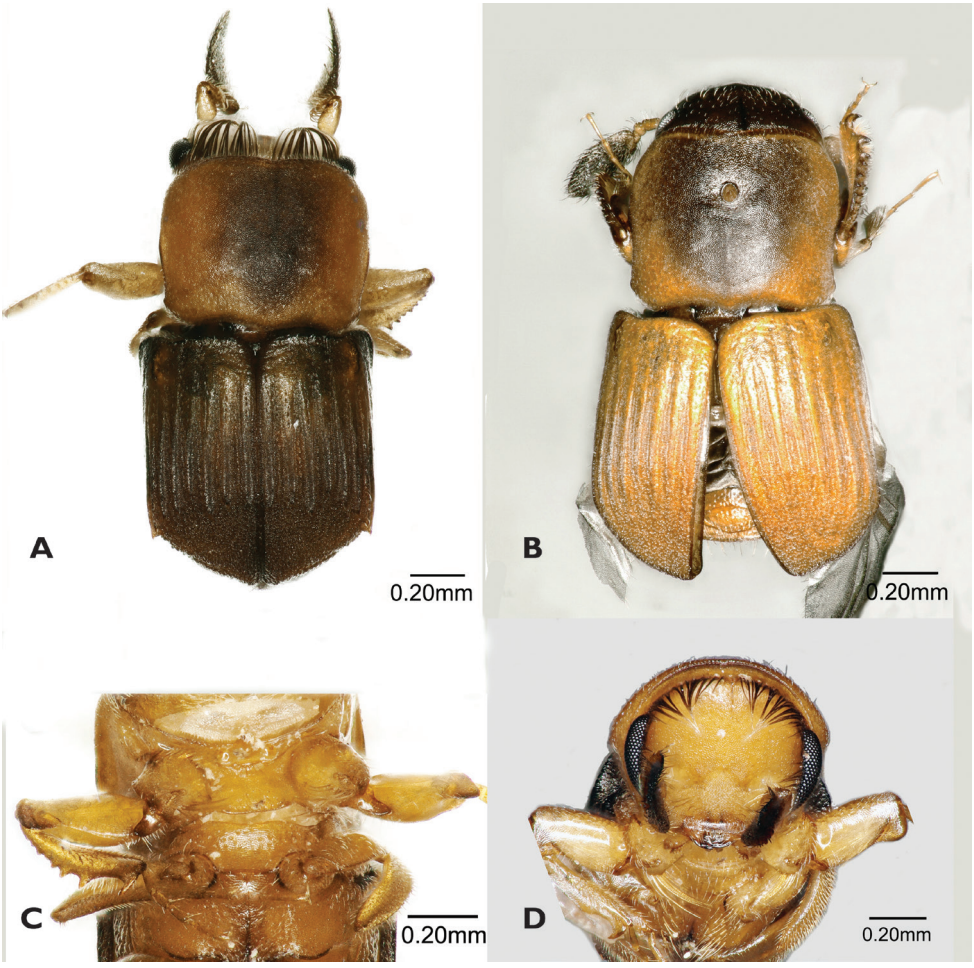

Figure 7. *Scolytoplatypus minimus* (**A, C, D** male **B** female) **A** dorsal view **B** dorsal view **C** prosternum **D** head anterior view.

100°38'E, 700 m, EKL, 16.iii.2009, L. Meng (1f RAB); as previous except: Mengla, Bubeng, 21.610N, 101.582E, 717 m, 16.iii.2019, BB(X)600–3FI, L.Z. Meng (2f RAB); 17 males, 3 females (JXAU) China: Sichuan Province, Xichang City, Leibo County, Mahu Township, 28°24'54"N, 103°46'16"E, ca. 1088 m, 5.VIII.2021, log dissection, host *Cinnamomum camphora*, Song Liao leg.; CHINA: Sichuan, Mt. Emei, 600–1050 m, 5–19.v.1989, L. Bocák (4f RAB); as previous except 1000 m, 4–20.v.1979, V. Kubáň (4f RAB); as previous except: [no altitude], viii.2016, Tian-Shang (1m, 1f RAB).

Distribution. India (Uttar Pradesh, West Bengal); Thailand (Chiang Mai, Nakhon Sri Thammarat) (Beaver and Gebhardt 2006). New to China (Sichuan, Yunnan).

Diagnosis. The male appears to be related to *S. reticulatus* which has a similar prosternum (compare figures 1K and 1L in Beaver and Gebhardt 2006). The females are also very similar, but the female of *S. reticulatus* lacks the typical mycangial pore on the pronotum.

Host. Recorded from species of *Alnus* (Betulaceae), *Cornus* (Cornaceae), and *Prunus* (Rosaceae) (Beeson 1961), *Cinnamomum* (Lauraceae) (Beaver and Browne 1975), and *Acrocarpus* (Leguminosae) (Saha and Maiti 1996). Evidently polyphagous. In Thailand, the species was found in smaller branches (1–2 cm diameter) of *Cinnamomum iners* Reinw. ex Bl. than those attacked by *S. raja* and *S. pubescens* (Beaver and Browne 1975).

Scolytoplatypus pubescens Hagedorn

Figure 8

Scolytoplatypus pubescens Hagedorn, 1904: 123.
Scolytoplatypus pubescens kabakovi Axentjev, 1992: 192.

Material examined. China: Sichuan, Mt. Emei, 600–1050 m, 5–19.v.1989, L. Bocák (4m, 2f RAB); as previous except 1000 m, 4–20.v.1979, V. Kubáň (4m, 3f RAB); Yunnan, Baoshan, Gaoligong Nat. Res., Bai-Hua-Ling, 25.306N, 98.796E, ca.1600 m, 8.vii.2019, Lai, S-C. & Liao, S. (1m, 1f RAB); 28 males, 19 females (JXAU) as previous except: 25°17'59"N, 98°47'12"E, ca. 1970 m, 20.VIII.2021, host *Carya cathayensis*, Song Liao, Guangyu Yu leg.; Honghe, Hekou, Dajianshan, 22.909N, 103.697E, 2130 m, FIT, 12.v.2018, DJS4–3S, LZ Meng (1m,1f RAB); Wenshan, Maguan, Gulingqin, 22.732N, 103.994E, 594 m, FIT, 1.iv.2018, GLQ31, LZ Meng (1m RAB); Xishuangbanna, 23 km NW Jinghong, vic. Na Ban village (NNNR), 22°10'N, 100°39'E, 7–1000 m, L. Meng (3f RAB).

Distribution. India (Assam, Uttar Pradesh, West Bengal), Myanmar, Nepal, Thailand, Vietnam (Beaver et al. 2014), China (Taiwan). New to Chinese mainland (Sichuan, Yunnan)

Diagnosis. *S. pubescens* is most closely similar to *S. superciliosus* and *S. zahradniki*, but can be distinguished by the characters given in the key.

Host. The species is known to attack at least 12 different families of trees (Beaver and Gebhardt 2006). *Carya cathayensis* Sarg. (Juglandaceae) is recorded here as a new host.

Scolytoplatypus ruficauda Eggers

Scolytoplatypus ruficauda Eggers, 1939: 9: Beaver and Gebhardt 2006: fig.2A.

Material examined. CHINA: Yunnan, Puer, Jingdong, Ailoshan, 24.5411N, 101.030E, 2690 m, 8.v.2018, ALS(S)2600–5FI, L.Z. Meng (6m HGT).

Distribution. Myanmar, Nepal (Beaver and Gebhardt 2006). New to China (Yunnan).

Diagnosis. The species is most closely similar to *S. wugongshanensis*. but can be distinguished by the characters given in the key.

Host. Not known.

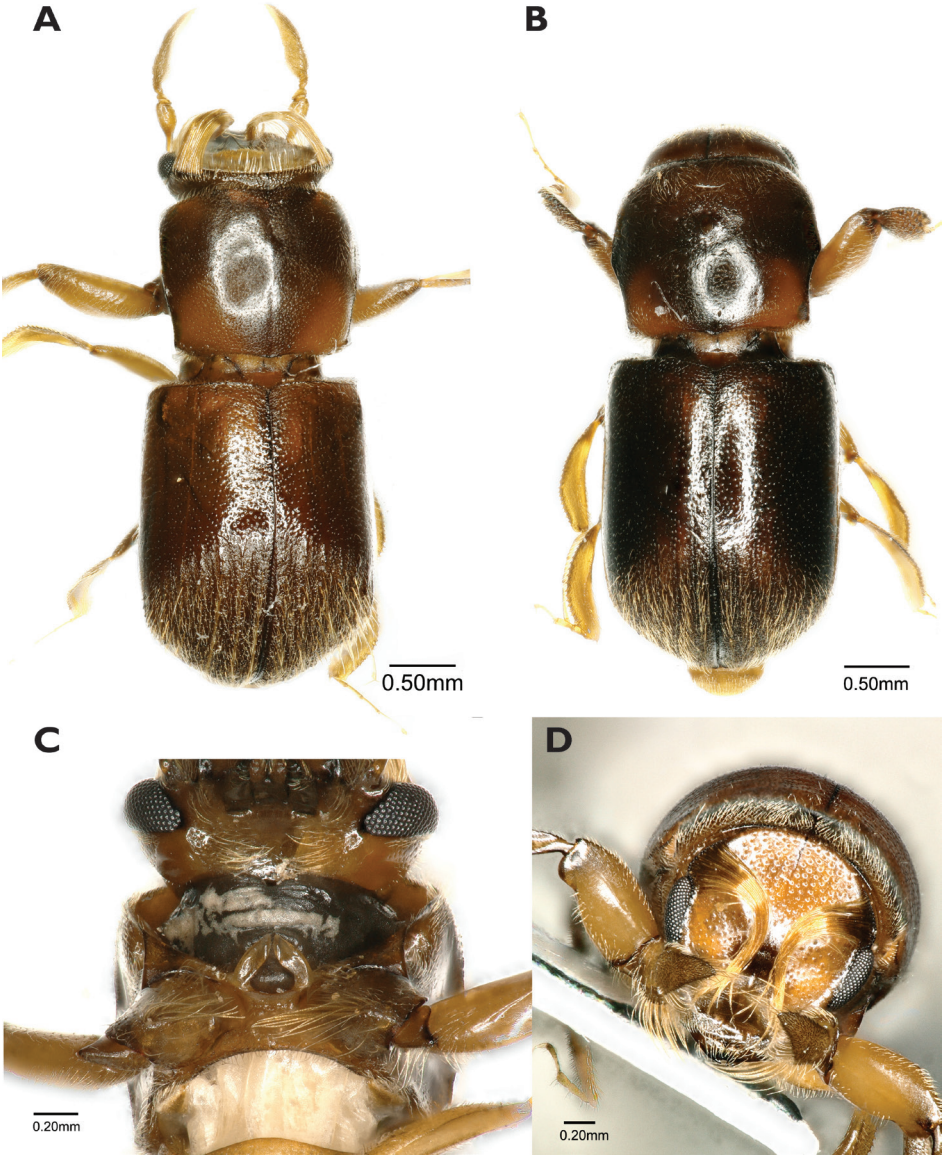

Figure 8. *Scolytoplatypus pubescens* (**A, C, D** male **B** female) **A** dorsal view **B** dorsal view **C** prosternum **D** head anterior view.

Scolytoplatypus samsinghensis Maiti & Saha

Scolytoplatypus samsinghensis Maiti & Saha, 2009: 101, fig. 20.

Material examined. China: Yunnan, Xishuangbanna, Mengle, Bubeng, 21.615N, 101.579E, 853 m, FIT, 5.v.2018, BB800–1FI, L.Z. Meng (3m RAB); as previous except: 21,611N, 101.581E, 712 m, 15.v.2018. BB600–2FI (3f RAB).

Distribution. India (West Bengal). New to China (Yunnan).

Diagnosis. The species is very close to *S. eutomoides* Blandford, but differs from it on the basis of the following characters of the males (*S. samsinghensis* given first): 1. striae 1 and 2 marked up to the lower half of declivity, little elevation at interstriae 1 and 3, on or near the elevation with fairly large granules vs. striae 1 and 2 marked up to upper half of declivity and lower half with smaller granules; 2. punctures on pronotum rather deep vs. punctures on pronotum, rather shallow; 3. strial groove marked by elongate and confluent punctures vs. strial groove devoid of any distinct punctures; 4. frontal hairs restricted only towards vertex vs. upper half of frons with hairs (Maiti and Saha 2009).

Host. Not known.

Key to males of Chinese *Scolytoplatypus* species

1 Front femur with a tooth above near apex **2**
– Front femur not toothed above **3**
2 Prosternum with median carina, extending from near the base and clearly separating the anterior, concave processes, its tip minutely granulate and setose, extending just beyond the anterior margin of the prosternum. Striae and interstrial carinae becoming obsolescent on declivity. Larger species, 3.7–3.8 mm long .... ***S. samsinghensis*** **Maiti & Saha**
– Prosternum almost flat, the concave, anterior processes almost contiguous in midline, very narrowly separated by a carinate process extending to anterior margin of pronotum, its tip smooth and glabrous. Impressed striae visible almost to apex of elytra. Smaller species, 2.6–3.1 mm long..... ***S. brahma*** **Blandford**
3 Small species, not more than 2 mm long..... **4**
– Larger species, more than 2 mm long..... **5**
4 Declivity beginning posterior to the middle of elytra. Elytra with distinct teeth on interstriae at summit of declivity, alternately longer and shorter. Frons with an even fringe of hairs around the upper half of the frontal impression. Prosternum with a small triangular median projection anteriorly, behind this a pair of widely separated, weakly shining, flattened areas. 1.4–1.6 mm long ..... ***S. minimus*** **Hagedorn**
– Declivity beginning anterior to the middle of elytra. Summit of elytral declivity without denticles. Frons with brushes of long, incurving hairlike setae both above and below eyes. Prosternum flat, smooth, with a small, flat, broadly rounded process anterior. 1.8–1.9 mm long ..... ***S. curviciliosus*** **Gebhardt**
5 Summit of elytral declivity marked by strongly developed spines on alternate interstriae, the spines projecting over a steep declivity. Basal angles of pronotum strongly produced, pointed apically..... **6**
– Summit of elytral declivity without spines or with small spines on all interstriae. Spines not projecting over a steep declivity, declivity in side view angular or gradually rounded. Basal angles of pronotum not produced..... **9**
6 Body length 2.4–2.5 mm. Frons without a dorsal fringe of longer setae. Pronotum minutely punctured. Prosternum with a transverse ridge anteriorly, some-

times bearing two tubercles, and anterior to this a pair of widely separated tapering processes ..... ***S. calvus*** **Beaver & Liu**

– Body length 3.0–3.6 mm. Frons with a dorsal fringe of setae. Pronotum coarsely, shallowly punctured. Prosternum with two tubercles anteriorly, and anterior to them a pair of narrowly separated tapering processes **7**

7 Elytral spines with a few short setae only, elytral declivity glabrous or almost so. 3.0–3.6 mm long **8**

– Elytral spines with tufts of long setae, elytral declivity covered with short interstrial hairs. 3.0–3.2 mm long ..... ***S. raja*** **Blandford**

8 Prosternum strongly humped anteriorly. Anterior prosternal processes directed forwards, diverging by up to 60°. Procoxae with a dense brush of 15–20 long, erect setae anteriorly near the inner margin. 3.0–3.2 mm long ..... ***S. sinensis*** **Tsai & Huang**

– Prosternum not strongly humped anteriorly, flat or weakly raised. Anterior prosternal processes directed more laterally, diverging at an angle of 60–120°. Procoxae with only a few (4–7) long, erect setae anteriorly. 3.3–3.6 mm long ..... ***S. mikado*** **Blandford**

9 Interstriae on posterior part of disc distinctly costate or carinate. Elytra with small interstrial teeth near summit of declivity **10**

– Interstriae on posterior part of disc not raised. Elytra without interstrial teeth at summit of declivity (except *pubescens* with minute teeth) **11**

10 Frons with brushes of hairlike setae above and below eyes. Anterior margin of prosternum projecting in two rounded lobes, slightly asymmetrical, and with a translucent process on the right side only. Pronotum without a deep fovea at the antero-ventral angle. 2.8–3.0 mm long ..... ***S. superciliosus*** **Tsai & Huang**

– Frons with a fringe of setae around upper part of frontal impression. Anterior margin of prosternum with two symmetrical, divergent, triangular processes. Pronotum with a deep fovea at the antero-ventral angle. 2.6–3.3 mm long ..... ***S. zahradniki*** **Knížek**

11 Middle of frons with an area with very dense, short setae. Elytra with minute interstrial teeth at summit of declivity. Prosternum anteriorly with two triangular processes inserted on anterior margin, widely separated at the base but converging towards the midline. 3.5–3.7 mm long ..... ***S. pubescens*** **Hagedorn**

– Middle of frons without an area with very dense, short setae. Elytra without teeth at summit of declivity. Prosternum not as above **12**

12 Prosternum raised in middle in a triangle, the apex anterior or posterior **13**

– Prosternum flat or weakly convex, not raised in a triangle **16**

13 Apex of prosternal triangle anterior, with a single pointed tubercle; anterior margin with two symmetrical, divergent, triangular, translucent processes **14**

– Apex of prosternal triangle posterior, anterior margin projecting in two rounded lobes, slightly asymmetrical, and with a translucent process on the right side only. 2.8–3.0 mm long ..... ***S. ruficauda*** **Eggers**

14 Elytral disc angularly separated from declivity. Anterior processes of prosternum inserted on anterior margin, small, short, bluntly rounded at tip, lying parallel to

anterior margin. 3.8–4.2 mm long.....
.....***S. wugongshanensis*** **Liao, Lai & Beaver, sp. nov.**

– Elytral disc evenly curving into declivity. Prosternal processes inserted just behind anterior margin, not as above.....**15**

15 Anterior processes of prosternum falcate, sharply tipped and curving anteriorly. Smaller species, 3.1–3.3 mm long.....***S. blandfordi*** **Gebhardt**

– Anterior processes of prosternum broadly triangular, diverging at an angle of ~ 90°. Larger species, 4.0–4.3 mm long...***S. skyliuae*** **Liao, Lai & Beaver, sp. nov.**

16 Upper half of frons clearly punctured, lower half impunctate, with a rather sparse fringe of hairs on each side curving inwardly, but not extending to lower half of frons. Prosternum without a pair of translucent processes anteriorly. Rows of punctures on elytral disc feebly but clearly impressed before declivity. Larger species, 3.5–4.5 mm long.....***S. tycon*** **Blandford**

– Frons impunctate throughout, the incurved brushes of hairs denser and longer, extending beyond middle of frons. Prosternum with a pair of widely separated, translucent, divergent processes anteriorly. Rows of punctures on elytral disc not impressed, usually indistinct. Smaller species, 2.9–3.2 mm long .....
.....***S. darjeelingi*** **Stebbing**

Conclusions

Although the biology of the two new species has not been systematically studied, it can be expected to be similar to that of other species of *Scolytoplatypus* (Beaver and Gebhardt 2006). *Scolytoplatypus* is a very characteristic genus of ambrosia beetles, and even the smallest of the known species are larger than the average wood boring beetle (Jordal 2018). The species of *Scolytoplatypus* show marked sexual dimorphism. Some morphological characteristics of Asian species, as opposed to African species, differ between the sexes, e.g., antenna, pronotum, male prosternum. The characters of the male prosternum are particularly useful at specific level in the Oriental species (Beaver and Gebhardt 2006).

The total number of species, host plants and distribution of *Scolytoplatypus* in China are still unclear and need further study. Many other species have been reported in neighbouring countries of China, which still have not been found in China. In addition, new species of *Scolytoplatypus* are being described one after another (Beaver and Gebhardt 2006; Browne 1971; Jordal 2013, 2018; Knížek 2008), indicating quite strongly that many more species remain to be discovered, especially on the mainland China.

Acknowledgements

We appreciate the help provided by Jia Lv, Ling Zhang, and others in our fieldwork. We are also most grateful to Mr. Hongbin Zhu (Nanjing Customs, District P. R. China) and Chengpeng Long (Zhejiang A&F University, District P. R. China) for the

photographic equipment. We are thankful to Max Barclay (Natural History Museum, London), Arnaud Faille (Naturkundemuseum Stuttgart), Matthias Hartmann (Naturkundemuseum Erfurt), and Harald Schillhammer (Naturhistorisches Museum, Vienna) for providing the loan of types and other specimens.

This research was funded by grant National Natural Science Foundation of China (no. 31160380, 31360457, 31760543),Thousand Talents Program of Jiangxi Province (no. jxsq2018102116), National Foreign Experts Project of Jiangxi Province (no. G20200222010, G2021022002), Science and Technology Project of Jiangxi Education Department (no. GJJ200443).

References

Blandford WFH (1898) On some Oriental Scolytidae of economic importance, with descriptions of five new species. Transactions of the Entomological Society of London, 423–430.

Beaver RA, Browne FG (1975) The Scolytidae and Platypodidae (Coleoptera) of Thailand: A checklist with biological and zoogeographical notes. Oriental Insects 9(3): 283–211. https://doi.org/10.1080/00305316.1975.10434499

Beaver RA, Gebhardt H (2006) A review of the oriental species of *Scolytoplatypus* Schaufuss (Coleoptera, Curculionidae, Scolytinae). Deutsche Entomologische Zeitschrift 53(2): 155–178. https://doi.org/10.1002/mmnd.200600014

Beaver RA, Liu LY (2007) A new species of *Scolytoplatypus* Schaufuss (Coleoptera: Curculionidae: Scolytinae) from Taiwan. Entomologist's Monthly Magazine 143: 1721–1723.

Beaver RA, Sittichaya W, Liu LY (2014) A synopsis of the Scolytine ambrosia beetles of Thailand (Coleoptera, Curculionidae, Scolytinae). Zootaxa 3875(1): 1–82. https://doi.org/10.11646/zootaxa.3875.1.1

Beeson CFC (1961) The ecology and control of the forest insects of India and the neighbouring countries. Government of India, New Delhi, 1007 pp.

Blackman MW (1943) New species of *Scolytoplatypus* Schaufuss from Malaysia (Coleoptera: Scolytoidea). Proceedings of the Entomological Society of Washington 45: 121–126.

Blandford WFH (1893) The Scolyto-platypini, a new subfamily of Scolytidae. Transactions of the Entomological Society of London, 425–442. https://doi.org/10.1111/j.1365-2311.1893.tb02075.x

Bright DE, Skidmore RE (1997) A Catalog of Scolytidae and Platypodidae (Coleoptera), Supplement 1 (1990–1994). NRC Research Press, Ottawa, [vii +] 368 pp.

Bright DE, Skidmore RE (2002) A Catalog of Scolytidae and Platypodidae (Coleoptera), Supplement 2 (1995–1999). NRC Research Press, Ottawa, [viii +] 523 pp.

Browne FG (1961) The biology of Malayan Scolytidae and Platypodidae. Malayan Forest Records 22: [xi +] 255 pp.

Browne FG (1971) The African species of *Scolytoplatypus* Schaufuss (Coleoptera, Scolytidae). Revue de Zoologie et de Botanique Africaines 84: 111–129.

Eggers H (1939) Entomological results from the Swedish expedition 1934 to Burma and British India. Coleoptera: Ipidae, gesammelt von René Malaise. Arkiv för Zoologi 31A(4): 1–14.

Hagedorn M (1904) Enumeratio Scolytidarum e Sikkim et Japan natarum Musei historico-naturalis Parisiorum, quas Dominus J.Harmand annis 1890 et 1901 collegit descriptionibus specierum novarum adjectis. Bulletin du Muséum d'Histoire Naturelle, Paris, 22–126.

Jordal BH (2013) Deep phylogenetic divergence between *Scolytoplatypus* and *Remansus*, a new genus of Scolytoplatypodini from Madagascar (Coleoptera, Curculionidae, Scolytinae). ZooKeys 352: 9–33. https://doi.org/10.3897/zookeys.352.6212

Jordal BH (2018) The smallest known species of Afrotropical *Scolytoplatypus* Schaufuss (Curculionidae, Scolytinae) – with unique features and an isolated phylogenetic position. ZooKeys 749: 125–130. https://doi.org/10.3897/zookeys.749.24199

Jordal BH, Sequeira AS, Cognato AI (2011) The age and phylogeny of wood boring weevils and the origin of subsociality. Molecular Phylogenetics and Evolution 59: 708–724. https://doi.org/10.1016/j.ympev.2011.03.016

Kalshoven LGE (1959) Studies on the biology of Indonesian Scolytoidea. 4. Data on the habits of Scolytidae. Second part. Tijdschrift voor Entomologie 102: 135–173.

Knížek M (2008) A new species of *Scolytoplatypus* (Coleoptera: Scolytidae) from China. Studies and reports of District Museum Prague-East, Taxonomical Series 4: 119–124.

Knížek M (2011) Scolytinae. In: Löbl I, Smetana A (Eds) Catalogue of Palaearctic Coleoptera Vol.7. Apollo Books, Stenstrup, 204–251.

Lai SC, Zhang L, Li Y, Wang JG (2021) A new species, a new combination, and a new record of *Crossotarsus* Chapuis, 1865 (Coleoptera: Curculionidae: Platypodinae) from China. ZooKeys 1028: e69. https://doi.org/10.3897/zookeys.1028.61018

Maiti PK, Saha N (2009) Fauna of India and the Adjacent Countries: Scolytidae: Coleoptera (Bark and Ambrosia Beetles), Vol. I (Part 2). Zoological Survey of India, Kolkata, 246 pp.

Mayers CG, Harrington TC, Masuya H, Jordal BH, McNew DL, Shih H-H, Roets F, Kietzka GJ (2020) Patterns of coevolution between ambrosia beetle mycangia and the Ceratocystidaceae, with five new fungal genera and seven new species. Persoonia 44(1): 41–66. https://doi.org/10.3767/persoonia.2020.44.02

Park S (2016) Taxonomic review of Scolytinae and Platypodinae (Coleoptera: Curculionidae) in Korea. Seoul National University, 335 pp. https//s-space.snu.ac.kr

Saha N, Maiti PK (1996) Insecta: Coleoptera: Scolytidae. In: Director, Zoological Survey of India (Eds) Fauna of West Bengal. Part 6B. (Insecta: Coleoptera). Zoological Survey of India, Calcutta, 775–866.

Schaufuss CFC (1891) Beitrag zur Käferfauna Madagascar's II. Tijdschrift voor Entomologie 34: 1–35.

Schedl KE (1952) Zur Synonymie der Borkenkäfer, I. Entomologische Blätter 47/48: 158–164.

Stebbing EP (1914) Indian forest insects of economic importance. Coleoptera. Eyre & Spottiswoode, London, 648 pp. https://doi.org/10.5962/bhl.title.23135

Tsai PH, Huang FS (1965) Two new species of *Scolytoplatypus* Schaufuss (Curculionidae, Scolytinae) from China (Study on Scolytidae (6)). Zoological Systematics 2: 35, 36, 39. https://doi.org/CNKI:SUN:DWFL.0.1965-02-005

Wood SL (1989) Nomenclatural changes and new species of Scolytidae (Coleoptera), part IV. Great Basin Naturalist 49: 167–185. https://doi.org/10.5962/bhl.part.22642

Wood SL, Bright DE (1992) A catalog of Scolytidae and Platypodidae (Coleoptera), Part 2: Taxonomic Index Volume A. Great Basin Naturalist Memoirs 13: 1–1553.

ZooKeys 1082: 51–62 (2022)
doi: 10.3897/zookeys.1082.73272
https://zookeys.pensoft.net

RESEARCH ARTICLE

A peer-reviewed open-access journal
ZooKeys
Launched to accelerate biodiversity research

Nanhuaphasma Chen, He & Li, 2002 is a junior synonym of *Dajaca* Brunner von Wattenwyl, 1893 (Phasmatodea, Aschiphasmatidae, Dajacini)

Chong-Xin Xie[1], Jun Wen[1], Yu-Han Qian[1]

1 *Key Laboratory for Forest Resources Conservation and Utilization in the Southwest Mountains of China, Ministry of Education, Southwest Forestry University, Kunming, Yunnan 650224, China*

Corresponding author: Yu-Han Qian (nerv6667@163.com)

Academic editor: M. Gottardo | Received 20 August 2021 | Accepted 3 January 2022 | Published 18 January 2022

http://zoobank.org/4D3B8C28-D9F6-48E8-AB25-650CF91327CF

Citation: Xie C-X, Wen J, Qian Y-H (2022) *Nanhuaphasma* Chen, He & Li, 2002 is a junior synonym of *Dajaca* Brunner von Wattenwyl, 1893 (Phasmatodea, Aschiphasmatidae, Dajacini). ZooKeys 1082: 51–62. https://doi.org/10.3897/zookeys.1082.73272

Abstract

The genus *Nanhuaphasma* Chen, He & Li, 2002 was established as a member of the family Pseudophasmatidae Rehn, 1904 (now belonging to Aschiphasmatidae Brunner von Wattenwyl, 1893) based on the male of *N. hamicercum* Chen & He, 2002. We review the status of *Nanhuaphasma* and *N. hamicercum* by examining the holotype and male and female non-types which were collected in same location as the holotype. We find that *Nanhuaphasma* is a junior synonym of *Dajaca* Brunner von Wattenwyl, 1893 and *N. hamicercum* is a junior synonym of *D. napolovi* Brock, 2000. Complementing egg morphology of *D. napolovi* and keys to eight species of *Dajaca* are provided.

Keywords

External morphology, new synonym, stick insects, taxonomy

Introduction

Nanhuaphasma was established by Chen, He & Li in 2002, as a genus of the subfamily Pseudophasmatinae Rehn, 1904 and the family Pseudophasmatidae Rehn, 1904. This genus only includes *Nanhuaphasma hamicercum* Chen & He, 2002, with its holotype collected on Jianfengling Mountain in Hainan Province of China, and the male paratype collected on Mount Daqing in Guangxi Province of China; its female

was unknown in the original description. From the original description, the genus has the following characteristics: body medium-sized, without spines or granules, and covered with dense, short, yellow villi. Antennae filiform, distinctly segmented, longer than apex of fore legs. Pronotum wider than length and anterior with a pair of elliptically cavities, median segment longer than metanotum. Fore femora short and slightly curved, without distinct carina, mid and hind tibiae without spines or denticles, undersides with triangular cavities apically, tarsi V segmented, ungues not pectinate. Based on the above characteristics, Hennemann et al. (2008) thought *Nanhuaphasma* might belong to Aschiphasmatini Brunner von Wattenwyl, 1893. Ho (2016) considered *Nanhuaphasma* to belong to Dajacini Bragg, 2001.

The Dajacini are similar to Aschiphasmatini, but they are distinguished only by the ungules which are not pectinate (Bragg 2001). *Dajaca* is the type genus of Dajacini and only eight species worldwide are known; they have have been described from Indonesia, Malaysia, Brunei, Vietnam, Myanmar, and China (Brock et al. 2021). Bragg (2001) revised *Dajaca* and provided an identification key. Zompro (2004) revised *Phaeophasma* as a junior synonym of *Dajaca*. Seow-Choen (1998, 2016, 2017, 2020) systematically worked through *Dajaca* based on specimens from Borneo and Sumatra.

We observe that *N. hamicercum* is similar to species of *Dajaca* based on diagnostic features of the holotype and new specimens which were collected at the same location as the holotype. Here, we resolve the status of *Nanhuaphasma* and conclude that it is a junior synonym of *Dajaca*. We also provide new keys to *Dajaca* based on external morphology. Considering the individual variability of *D. napolovi*, we redescribe the female and male. The egg of *D. napolovi* is described for the first time in this paper.

Materials and methods

The recently collected specimens include 2♂, 2♀, and 3 eggs of *Nanhuaphasma hamicercum* collected from Jianfengling National Forest Park in Hainan Province, China. These specimens are pinned and deposited in the Insect Collection of Southwest Forestry University (**SWFU**), Yunnan Province, China. The holotype and paratype of *N. hamicercum* deposited in the Institute of Zoology, Chinese Academy of Sciences (**IZCAS**), Beijing, China. Retrieved from Phasmida Species File (Brock et al. 2021), the holotype and paratype of *D. napolovi* deposited in Natural History Museum, London, England (**NHMUK**), were photographed by Paul Brock, and the images are under copyright to the Natural History Museum, London.

Morphological observations were made with a SOPTOP SZ stereomicroscope (Sunny Group Co., Ltd, China). Digital images were obtained using a Liyang Super Resolution System LY-WN-YH (Chengdu Liyang Precision Machinery Co., Ltd, China). Whole view images of the new specimens were taken with Canon 5ds digital camera and LAOWA 100 mm F2.8 2× macro lens (Anhui Changgeng Optics Technology Co., Ltd, China). Image Stacking was done using Zerene Stacker (Zerene Systems LLC, USA). Morphological terminology follows that of Bragg (1997, 2001) and Vallotto et al. (2016).

Taxonomic account

Genus *Dajaca* Brunner von Wattenwyl, 1893
Chinese name. 达蝻属

Dajaca Brunner von Wattenwyl, 1893: 99 (original description; type species: *Dajaca monilicornis* Redtenbacher, 1906; type locality: Tam Dao, 55 km NNW Hanoi, Vietnam).
Nanhuaphasma syn. nov. Chen, He & Li, 2002: 100 (original description; type species: *Nanhuaphasma hamicercum* Chen & He, 2002; type locality: Jianfengling National Forest Park, Hainan province, China); Chen and He 2008: 365 (redescription).

Remarks. Head flattened, antennae long. Median segment twice as long as metanotum. Ungues not pectinate. Male apterous or winged, females apterous. Legs short, femora laterally compressed, dorsal surface rounded; ventral carinae with only a few minute spines or unarmed. Fore femora more or less straight. Tibiae unarmed (Bragg 2001; Zompro 2004). After comparing the diagnostic features, *Nanhuaphasma* shows similar characters to the *Dajaca*, and we could not find significant morphological differences between the two and therefore consider *Nanhuaphasma* to be a junior synonym of *Dajaca*.

For the convenience of research, we hereby give the Chinese name. Latin *Dajaca* in Chinese, transliterated as "达伽卡", simplified as "达".

***Dajaca napolovi* Brock, 2000**
Chinese name. 纳氏达蝻
Figures 1–5

Dajaca napolovi Brock, 2000: 2 (original description; type locality: Tam Dao, 55 km NNW Hanoi, Vietnam); Vallotto et al. 2016: 376; (described both male and female).
Nanhuaphasma hamicercum syn. nov. Chen & He, 2002: 100 (original description; type locality: Jianfengling National Forest Park in Hainan province, China; described male); Chen and He 2008: 365, 458 (redescription).

Material examined. 2♂, 2♀ and 3 eggs of *D. napolovi*, Jianfengling National Forest Park in Hainan Province, China, 18°44'35"N, 108°50'17"E, 1134 m alt., 6.VIII.2020, leg. Yun-Hu Mo; No. HN-25.

Description. Male. Wingless, the general coloration of the body is yellowish brown, with a few dark brown or black markings and pale yellow pilosity (Figs 1A, 2A). ***Head.*** Smooth, approximately as long as pronotum; nearly square, length almost as long as broad, vertex humped. Antennae filiform, longer than forelegs, with yellow bands; scapus rectangular and flattened, longer than pedicellus, pedicellus cylindrical and slightly wider than the third segment. Eyes rounded, colored yellow with

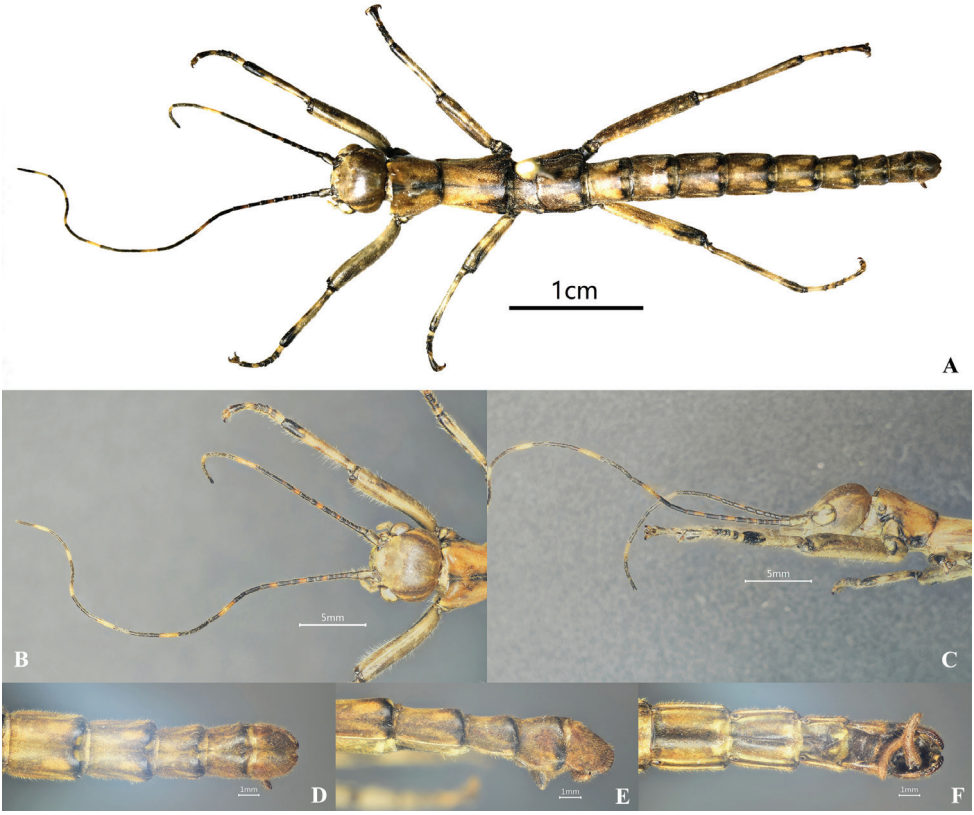

Figure 1. *Dajaca napolovi*, male, non-type (collected from Jianfengling National Forest Park in Hainan Province, China). **A** habitus, dorsal view **B** head, dorsal view **C** head, lateral view **D** terminalia, dorsal view **E** terminalia, lateral view **F** terminalia, ventral view.

a black median line, occupying 1/2 of gena (Figs 1B, C, 2C). ***Thorax.*** Smooth and unarmed. Pronotum rectangular, longer than wide, gradually narrowed posteriorly. Mesonotum slender and parallel-sided, ca 1.3× as long as pronotum. Metanotum wider than long. Median segment as long as wide, 2× length of metanotum (Figs 1A, 2A, C). ***Abdomen.*** Cylindrical, smooth, lacking armature. Terga II–IX gradually narrowed. Anal segment with small notch in middle of posterior margin. Poculum flat and short, nearly reaching posterior margin of tergum IX, apex rounded. Cerci cylindrical, moderately long, and slightly incurving, apices with tiny spines (Figs 1A, D–F, 2A, D–F). ***Legs.*** Brown with irregular black stripes; all femora laterally compressed, more or less triangular, lacking dorsal carinae, ventral carinae distinct. Ventroanterior carina of prefemur with some minute spines, remainder unarmed (Figs 1A, 2A).

Female. Larger than male, general coloration of body dark to light brown, with a few dark brown or black markings and pale yellow pilosity (Figs 3A, 4A, C). ***Head.*** Smooth, shorter than pronotum; rectangular, wider than long, vertex slightly

Figure 2. *Dajaca napolovi*, male, holotype (from Phasmida Species File 2021, photos by Paul Brock; published under CC BC -ShareAlike 4.0 International License). **A** habitus, dorsal view **B** data labels **C** head, lateral view **D** terminalia, dorsal view **E** terminalia, lateral view **F** terminalia, ventral view.

humped. Antennae filiform, longer than forelegs, with yellow bands; scapus rectangular and flattened, longer than pedicellus, pedicellus cylindrical and slightly wider than third segment. Eyes rounded, colored yellow with a black median line, occupying 1/2 of gena (Figs 3B, C, 4A, C). ***Thorax.*** Smooth and unarmed. Pronotum somewhat square, length almost as long as broad. Mesonotum anteriorly slightly narrowed and gradually broadening posteriorly, ca 1.5× as long as pronotum. Metanotum wider than long. Median segment slightly wider than long, 2× length of metanotum (Figs 3A, 4A, C). ***Abdomen.*** Cylindrical, smooth, and lacking armature. Terga II–VII

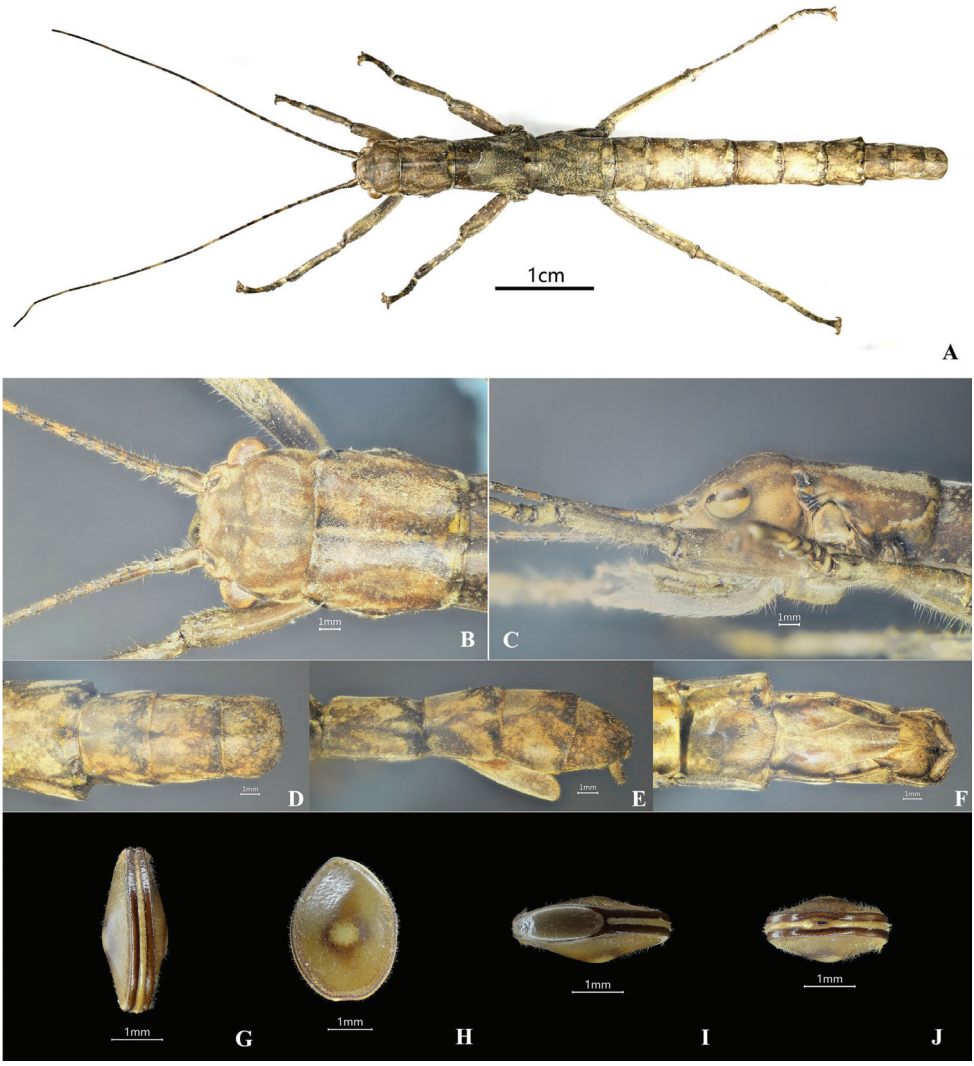

Figure 3. *Dajaca napolovi*, female & egg, non-type (collected from Jianfengling National Forest Park in Hainan Province, China). **A** female habitus, dorsal view **B** female head, dorsal view **C** female head, lateral view **D** female terminalia, dorsal view **E** female terminalia, lateral view **F** female terminalia, ventral view **G** egg, dorsal view **H** egg, lateral view **I** egg, opercular view **J** egg, polar view.

slightly broad, tergum VIII–IX distinctly narrowed. Anal segment as wide as tergum IX, posterior margin broadly rounded. Sternum VII lacking praeopercular organ. Lamina subgenitalis relatively long, without carinae, extending to posterior of tergum IX, anterior broad and posterior gradually narrowed, apex rounded and almost covering the ovipositor completely, paraprocts and epiproct not covered by lamina subgenitalis. Cerci cylindrical, moderately long, and slightly incurved, apices without tiny spines

Figure 4. *Dajaca napolovi*, female, paratype (from Phasmida Species File 2021, photos by Paul Brock, published under CC BC -ShareAlike 4.0 International License). **A** habitus, dorsal view **B** data labels **C** habitus, lateral view **D** terminalia, dorsal view **E** terminalia, lateral view **F** terminalia, ventral view.

(Fig. 3A, D–F, 4A, C, D–F). ***Legs.*** Brown with irregular black stripes, all femora laterally compressed, more or less triangular, lacking dorsal carinae, ventral carinae distinct (Figs 3A, 4A, C).

Eggs. Capsule a laterally flattened disk and slightly swollen in center; capsule longer than high, uniformly mid-brown, densely setose; rim of operculum and micropylar plate dark brown. Operculum elongate-oval, lacking capitulum. Micropylar plate a narrow band which extends around rim of egg, starting and ending at operculum. Micropyle situated at end of polar; micropylar plate slightly wider at this point (Fig. 3G–J).

Measurements (mm). Male. Body length 41–47; head length 5.0–5.5; pronotum length 3.5–4.0; mesonotum 5.3–5.5; metanotum 1.5–2.0; median segment 3.5–4.0;

Figure 5. *Dajaca napolovi*, female and male mating in the wild (from Jianfengling National Forest Park in Hainan Province, China, photograph by Mr Yun-Hu Mo)

profemora 7.0–8.0; mesofemora 6.0–7.0; metafemora 9.0–10.0; protibiae 5.5–6.0; mesotibiae 5.0–5.5; metatibiae 8.5–9.0. **Female.** Body length 58–61; head length 5.7–6.0; pronotum length 7.5–8.0; mesonotum 8.0–9.0; metanotum 2.6–3.0; median segment 4.5–5.0; profemora 7.5–9.0; mesofemora 7.0–8.0; metafemora 11.0–12.0; protibiae 6.5–7.0; mesotibiae 6.0–6.5; metatibiae 9.5–10.0. **Egg.** Width 1.2–1.3; height 2.4–2.6; length 3.0–3.3.

Remarks. Comparing the descriptions and illustrations in the original texts, the holotypes and the new specimens collected from the type locality, we find that *Nanhuaphasma hamicercum* shows similar characters to *Dajaca napolovi*, such as being wingless and having the body smooth and unarmed. Male anal segment with a small

notch in the middle of the posterior margin; poculum flat and short, nearly reaching to the posterior margin of tergum 9, apex rounded; cerci slightly incurving, apices with tiny spines. Female anal segment posterior margin broadly rounded; sternum 7 lacking preopercular organ; lamina subgenitalis relatively long, without carinae; anterior broadly and posterior gradually narrowed, apex rounded; almost covering the ovipositor completely, paraprocts and epiproct not covered by lamina subgenitalis. After the above comparison, we could not find significant differences between the two species and therefore consider *N. hamicercum* as a junior synonym of *D. napolovi*. Considering the geographical and intraspecific variability of *D. napolovi*, the colors of body are slightly different; due to contraction of the abdomen segments, the lamina subgenitalis sometimes extends slightly to the posterior of tergum IX, sometimes distinctly surpassing it to reach the posterior of tergum IX.

List of the species and distributions of *Dajaca*

D. alata (Redtenbacher, 1906) [Malaysia]
D. chani Seow-Choen, 1998 [Malaysia]
D. filiformis Bragg, 1992 [Malaysia]
D. monilicornis Redtenbacher, 1906 [Malaysia]
D. napolovi Brock, 2000 [China: Hainan, Hong Kong, Guangxi; Vietnam] = *Nanhuaphasma hamicercum* Chen & He, 2002, syn. nov.
D. nigrolineata Hennemann, Conle & Bruckner, 1996 [Myanmar]
D. swiae Seow-Choen, 2020 [Indonesia: Sumatra]
D. viridipennis Bragg, 2001 [Indonesia: Sarawak]

Key to males of *Dajaca* worldwide

1 Winged.....**2**
– Wingless.....**5**
2 Wings reaching to ca 1/2 way along 7th segment.....
.....***D. alata*** **(Redtenbacher, 1906)**
– Wings not reaching to 1/2 way along 7th segment.....**3**
3 Wings not reaching end of 5th segment...***D. monilicornis*** **Redtenbacher, 1906**
– Wings reaching to ca 1/2 way along 6th segment.....**4**
4 Body green, ventral surface of femora and tibiae black.....
.....***D. viridipennis*** **Bragg, 2001**
– Body and legs brown.....***D. filiformis*** **Bragg, 1992**
5 Body with a distinct black median line.....
.....***D. nigrolineata*** **Hennemann, Conle & Bruckner, 1996**
– Body without median line.....**6**
6 Body and legs green; antenna with yellow band.....
.....***D. chani*** **Seow-Choen, 1998**
– Body and legs brown and a few black stripes; antennal without yellow band.
.....***D. napolovi*** **Brock, 2000**

Key to females of *Dajaca* worldwide

1 Body with a distinct black median line ..... ***D. nigrolineata*** **Hennemann, Conle & Bruckner, 1996**
– Body without a median line **2**
2 Hind legs reaching or surpassing to 8th segment **3**
– Hind legs not surpassing to 8th segment **4**
3 Body and legs green; body length <45 mm ..... ***D. chani*** **Seow-Choen, 1998**
– Body and legs brown and with a few black stripes; body length >45 mm ..... ***D. napolovi*** **Brock, 2000**
4 Antennal segments 3–5 swollen; body and legs green ..... ***D.monilicornis*** **Redtenbacher, 1906**
– Antennal segments 3–5 slender; body and legs brown **5**
5 Ventro-anterior carina of metafemora with 4 small teeth ..... ***D. filiformis*** **Bragg, 1992**
– Ventro-anterior carina of metafemora with 5 teeth and ventro-anterior carina bearing 3 or 4 teeth ..... ***D. swiae*** **Seow-Choen, 2020**

Conclusions

Hainan Province is the largest tropical island in China, where the phasmids are a priority for biodiversity conservation. *Nanhuaphasma hamicercum* was collected in Jianfengling National Forest Park by Mr Yun-Hu Mo who photographed a mating pair of *N. hamicercum* (Fig. 5). Comparing the original description and the diagnostic features of the holotype, paratype and non-type specimens, we found that *Nanhuaphasma* should be a junior synonym of *Dajaca* and *N. hamicercum* should be a junior synonym of *D. napolovi*.

Acknowledgements

This study was supported by Yunnan Fundamental Research Projects (202001AT070142), Yunnan Provincial High-level Talent Training Support Program "Youth Top-notch Talent" Special Project (YNWR-QNBJ-2020-176), the Open Foundation of Key Laboratory for Forest Resources Conservation and Utilization in the Southwest Mountains of China of Ministry of Education of Southwest Forestry University (KLESWFU--201804) and National College Students Innovation and Entrepreneurship Project (no. 202010677126). We would like to thank subject editor Marco Gottardo, Dr Thies Büscher, and anonymous reviewers who put forward many valuable comments to this paper, and we also thank the following persons for their special help in this study: Mr Zi-Xu Yin (Ocean University of China, Qingdao), Mr Hao-Ran Gao (Yunnan Agricultural University, Kunming), Mr Francis Seow-Choen (Singapore), and Mr Hai-Tian Song (Fujian Academy of Forestry Sciences,

Fujian), who sent us some important literature on *Dajaca*. Mr Yun-Hu Mo (Hainan) provided the photographs of *Dajaca napolovi* mating in the wild. We also thank Mr Jin-Hong Xiang, Ms Xue Bai, Ms Gen-Ying Zhao, Ms Cui Li, and Ms Dan Shen who feed the stick insects in the insect Lab of Southwest Forestry University. Dr Paul D. Brock (The Natural History Museum, London), Dr David C. Eades (Illinois Natural History Survey), Dr Daniel Otte (Academy of Natural Sciences of Philadelphia), Dr Ed Baker (University of York, The Natural History Museum, London), Dr Thies Büscher (Christian-Albrechts-Universität, Kiel, Germany), and the cooperation of The Orthopterists' Society permitted us to use the information from the Phasmida Species File Online.

References

Bragg PE (1997) A glossary of terms used to describe phasmids. Phasmid Studies 6(1): 24–33.

Bragg PE (2001) Phasmids of Borneo. Natural History Publications, Kota Kinabalu, 49–63, 345–353.

Brock PD (2000) A new species of *Dajaca* Brunner (Phasmida: Pseudophasmatidae) from Vietnam. Journal of Orthoptera Research 9: 1–3. https://doi.org/10.2307/3503625

Brock PD, Büscher T, Baker E (2021) Phasmida Species File Online. Version 5.0/5.0. http://Phasmida.SpeciesFile.org [Accessed on 2021–8–19].

Brunner von Wattenwyl K (1893) Révision du système des orthoptères et description des espèces rapportées par M. Leon Fea de Birmanie. Annali des Museo Civico di Storia Naturale Giacomo Doria, Genova (2) 13(33): 1–230.

Chen SC, He YH (2008) Phasmatodea of China. China Forestry Publishing House, Beijing, 365 pp.

Chen SC, He YH, Li Yan (2002) Phasmatodea. In: Huang FS (Ed.) Forest insects of Hainan. Science Press, Beijing, 100–101.

Hennemann FH, Conle OV, Zhang WW (2008) Catalogue of the stick and leaf-insects (Phasmatodea) of China, with a faunistic analysis, review of recent ecological and biological studies and bibliography (Insecta: Orthoptera: Phasmatodea). Zootaxa 1735(1): 1–77. https://doi.org/10.11646/zootaxa.1735.1.1

Ho GW (2016) Contribution to the knowledge of Chinese Phasmatodea III: catalogue of the phasmids of Hainan Island, China, with descriptions of one new genus, one new species and two new subspecies and proposals of three new combinations. Zootaxa 4150(3): 314–340. https://doi.org/10.11646/zootaxa.4150.3.4

Redtenbachter J (1906) Die Insektenfamilie der Phasmiden. I. Phasmidae "Areolatae". W. Engelmann, Leipzig, 1–180.

Rehn JAG (1904) Studies in the Orthopterous family Phasidae. Proceedings of the Academy of Natural Sciences of Philadelphia 56: 38–107.

Seow-Choen F (1998) *Phobaeticus lambirica*, n. sp., and *Dajaca chani*, n. sp.: new species of Sick insects from east Malaysia (Phasmida: Phasmatidae). Serangga 3(1): 39–48.

Seow-Choen F (2016) A Taxonomic Guide to the Stick Insects of Borneo. Volume I. Natural History Publications, Kota Kinabalu, 365–369.

Seow-Choen F (2017) A Taxonomic Guide to the Stick Insects of Borneo. Volume II. Natural History Publications, Kota Kinabalu, 191–192.

Seow-Choen F (2020) A Taxonomic Guide to the Stick Insects of Sumatra. Volume II. Natural History Publications, Kota Kinabalu, 296–299.

Vallotto D, Bresseel J, Constant J, Gottardo M (2016) Morphology of the terminalia of the stick insect *Dajaca napolovi* from Vietnam (Insecta: Phasmatodea). Entomological Science 19(4): 376–380. https://doi.org/10.1111/ens.12209

Zompro O (2004) Revision of the genera of the Areolatae, including the status of *Timema* and *Agathemera* (Insecta, Phasmatodea). Abhandlungen des Naturwissenschaftlichen Vereins (NF) 37: 1–327.

ZooKeys 1082: 63–71 (2022)
doi: 10.3897/zookeys.1082.79011
https://zookeys.pensoft.net

RESEARCH ARTICLE

A peer-reviewed open-access journal
ZooKeys
Launched to accelerate biodiversity research

The second species of the genus *Ivoria* Kontschán, 2019: description of *Ivoria alourouai* sp. nov. from Ivory Coast (Acari, Mesostigmata, Urodinychidae)

Jenő Kontschán[1], Sergey G. Ermilov[2]

1 *Plant Protection Institute, Centre for Agricultural Research, ELKH, H-1525 Budapest, PO Box 102, Hungary* **2** *Institute of Environmental and Agricultural Biology (X-BIO), Tyumen State University, Semakova Str. 10, 625003 Tyumen, Russia*

Corresponding author: Jenő Kontschán (kontschan.jeno@atk.hu)

Academic editor: Farid Faraji | Received 7 December 2021 | Accepted 6 January 2022 | Published 18 January 2022

http://zoobank.org/FC96C395-605F-43C1-97CC-BBE166569371

Citation: Kontschán J, Ermilov SG (2022) The second species of the genus *Ivoria* Kontschán, 2019: description of *Ivoria alourouai* sp. nov. from Ivory Coast (Acari, Mesostigmata, Urodinychidae). ZooKeys 1082: 63–71. https://doi.org/10.3897/zookeys.1082.79011

Abstract

A new *Ivoria* species (*Ivoria alourouai* **sp. nov.**) is described from Ivory Coast based on five females. The new species differs from the previously described congener (*Ivoria taienesis* Kontschán, 2019) based on the shape of female genital shield, dorsal setae, centro-caudal part of the marginal shield and peritremes.

Keywords

New species, soil-inhabiting mite, taxonomy, Uropodina, West Africa

Introduction

Uropodina are a very diverse group of soil-inhabiting mites, especially in tropical rainforests (Lindquist et al. 2009). Despite this high diversity, these mites remain poorly investigated in many tropical countries, like Ivory Coast, from where only nine species

have been reported from the genera *Trichouropoda* Berlese, 1916 sensu lato, *Uroobovella* Berlese, 1903 sensu lato (Wiśniewski 1993) and *Rotundabaloghia* Hirschmann, 1975 (Kontschán 2009), *Ivoria* Kontschán, 2019, *Mahnertellina* Kontschán, 2020 and *Origmatrachis* Hirschmann, 1979 (Kontschán 2019, 2020a, b).

The genus *Ivoria* was described from Taï National Park in Ivory Coast (Kontschán 2019), which contains one of the largest primary rainforests in West Africa. In recent years, the first author spent numerous weeks in the Natural History Museum of Geneva to study the Uropodina mite diversity of the tropical soils. During the investigation of the West African soil samples, the second species of *Ivoria* was discovered from Taï National Park in a disturbed area close to the village Dropleu. This new species is described in this paper.

Materials and methods

Specimens were cleared in lactic acid for a week and investigated with a Leica 1000 scientific microscope with a drawing tube. The photos were taken with a Keyence 5000 digital microscope. Specimens examined were stored in 70% ethanol and deposited in the Natural History Museum, Geneva (NHMG). Measurements are given in micrometers (μm).

Abbreviations

Setae and pores: **st1 –5** sternal setae; **h1–h4** hypostomal setae; **p** pores.

Taxonomy

Suborder Uropodina Kramer, 1881
Family Urodinychidae Berlese, 1917

Genus *Ivoria* Kontschán, 2019

Ivoria Kontschán 2019: 1024.

Type species. *Ivoria taiensis* Kontschán, 2019

Diagnosis. Idiosoma subpentagonal, dorsally domed, marginal and dorsal shields fused anteriorly. All dorsal setae short, with pilose or serrate distal margins. Five pairs of sternal setae smooth or pilose. Genital shield of female subtriangular. Peritreme L-shaped or hook-shaped. Tritosternum with vase-like base, apically serrate, laciniae subdivided into two pairs of short lateral and one pair of long central branches. Hypostomal setae *h1* robust, basally with lateral teeth, *h2*, *h3*, and *h4* narrow and marginally serrate. Palptrochanter setae *v1* robust and serrate, *v2* situated on small protuberance and

divided into a short smooth and a long, basally serrate and apically pilose branches. Corniculi small and horn-like, situated at posterior level of *h2*. Internal malae long and smooth. Chelicerae large and robust with internal sclerotized nodes, movable digit shorter than fixed digit, both digits bearing a large central tooth in addition to smaller subapical teeth. Leg I without ambulacral claws; majority of leg setae marginally pilose.

Remarks. The robust and large chelicerae occur only in some genera within the Uropodina. The following genera *Baloghjkaszabia* Hirschmann, 1973, *Kaszabjbaloghia* Hirschmann, 1973, *Wernerhirschmannia* Hiramatsu, 1983, *Multidenturopoda* Wiśniewski & Hirschmann, 1991, *Bloszykiella* Kontschán, 2010, *Editella* Kontschán, 2011 and *Jedediella* Kontschán & Starý, 2012 have large and robust chelicerae; the most important differences among them are summarized in Kontschán (2019: table 1). Unfortunately, families of Uropodina are not well defined, and the classification system of Uropodina is confusing, so it is questionable which genera belong to the family Urodinychidae. The chelicerae of the other members (like species of the genus *Uroobovella* sensu lato) in the family Urodinychidae are small, narrow, and usually have a shorter or longer apical prolongation on the fixed digit.

***Ivoria alourouai* sp. nov.**

http://zoobank.org/B83D5B76-2A95-47D8-A1C1-A52AB3DA7964

Figures 1–4

Material examined. ***Holotype.*** Female. ”Afrique Occidentale, Côte d’Ivore, Dropleu, tamisage sans tronc mort” (Ivory Coast, Dropleu), 7°24'31"N, 8°19'14"W, 10 Oct. 1980, V. Mahnert and J.L. Peret leg. ***Paratypes.*** Four females, with same collection data as those for the holotype.

Diagnosis. Idiosoma subpentagonal, dorsally domed, marginal and dorsal shields fused anteriorly. All dorsal setae short, with pilose margins. Five pairs of sternal setae pilose. Genital shield of female triangular, anterior margin rounded and situated between coxae IV. Peritreme hook-shaped. Tritosternum with vase-like base, apically serrate, its laciniae subdivided into two pairs of short lateral branches and one pair of long central branches. Hypostomal setae *h1* robust, with a short lateral branch and with numerous lateral teeth, *h2*, *h3*, and *h4* narrow and marginally serrate. Palptrochanter setae *v1* robust and serrate, *v2* situated on small protuberance, basally serrate and apically pilose. Internal malae long and smooth with a short lateral branch.

Description. Female. Length of idiosoma 560–580, width at level of coxae IV 360–375 (*N* = 5), color reddish-brown. Shape of idiosoma pentagonal with vertex, dorsally domed.

Dorsal idiosoma (Figs 1, 4a, b). Anterior margin of vertex rounded and margins of vertex bearing marginally pilose setae, ca 32–36 long (Fig. 3a). Marginal and dorsal shields fused anteriorly, dorsal shield elevated on caudal region (Fig. 4b). Majority of dorsal shield covered by reticulate sculptured pattern. Long and robust marginally pilose setae (ca 32–36 long) situated on elevated central area of dorsal shield. 10–12 pairs

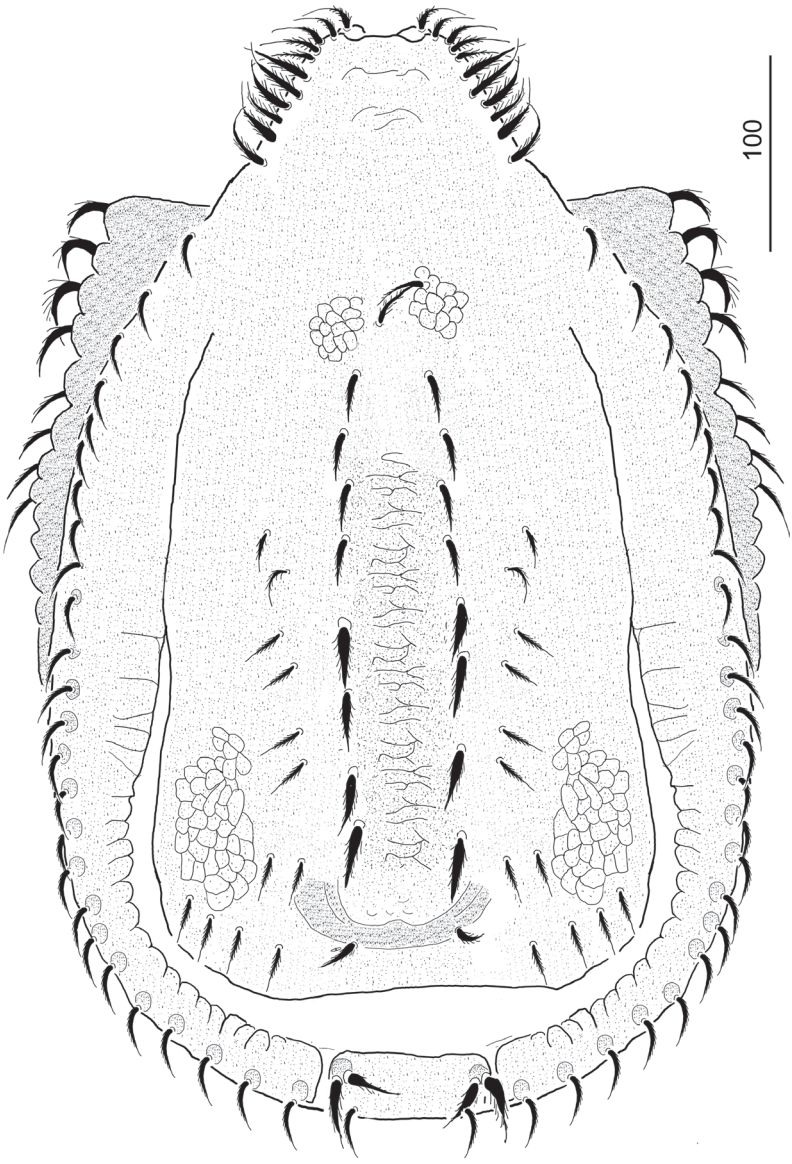

Figure 1. *Ivoria alourouai* sp. nov., female, holotype, dorsal view.

of short (ca 24–26) and narrow marginally pilose setae situated lateral to elevated area. One pair of poroid situated close to posterior margin of elevated area. Marginal shield without sculptural pattern, inner margins undulate on central and caudal area. All setae on marginal shield ca 23–26 long and marginally pilose. Centro-caudal part of marginal shield separated and forming a quadrangular shield (ca 280–290 wide and ca 30–34 long). This shield bears long and robust marginally pilose setae (ca 32–36) placed on small protuberances.

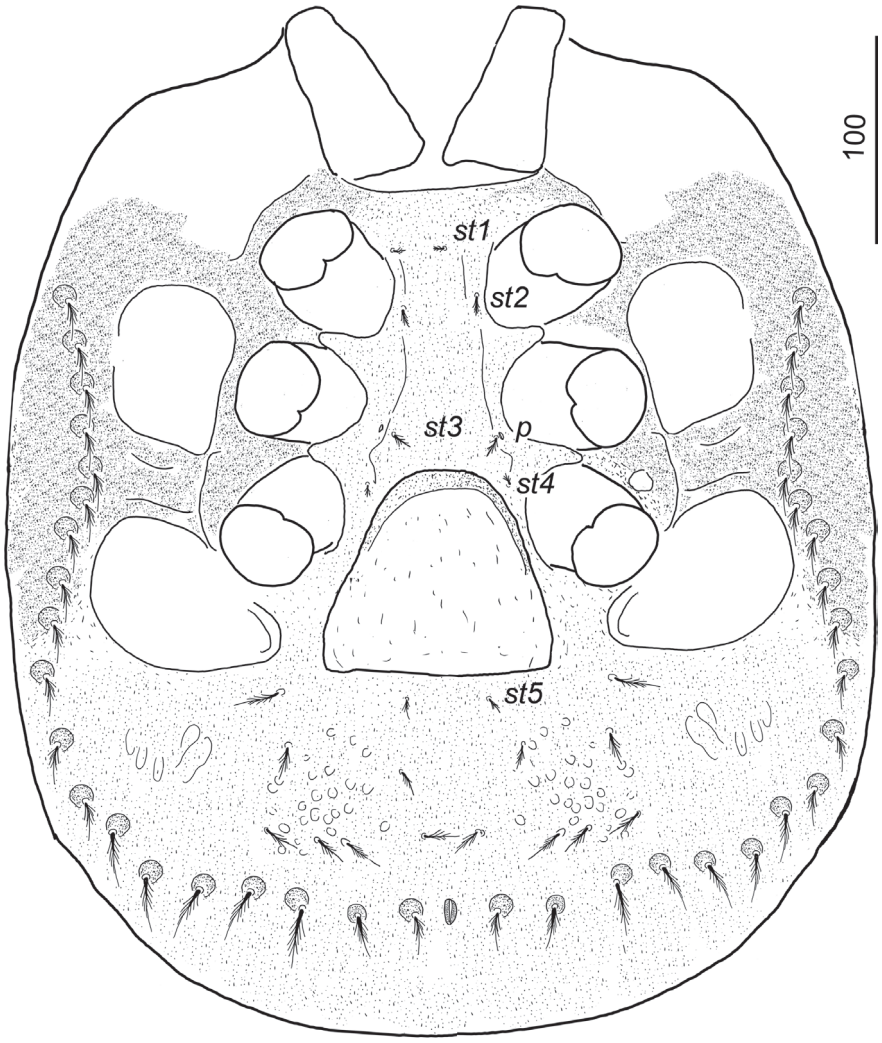

Figure 2. *Ivoria alourouai* sp. nov., female, holotype, ventral view.

Ventral idiosoma (Figs 2, 4c, d). Five pairs of sternal setae pilose, *st1* and *st4* shorter (ca 7–8), *st2*, *st3* and *st5* longer (ca 10–12). Setae *st1* inserted at level of anterior margin of coxae II, *st2* at level of central region of coxae II, *st3* at level of posterior margin of coxae III, *st4* at level of central area of coxae III, *st5* close to basal margin of genital shield. Sternal shield without sculptured pattern, one pair of poroid situated close to *st3*. 7–8 pairs of short (ca 21–25), marginally pilose ventral setae situated posterior to genital shield, surface around these setae covered by oval pits. 20–21 pairs of long (ca 34–36), marginally pilose setae placed on small protuberance situated on L-shaped longitudinal row from peritremes to anal opening. Ventral surface bears reticulate sculptural pattern posterior to pedofossae IV. Anal opening oval ca

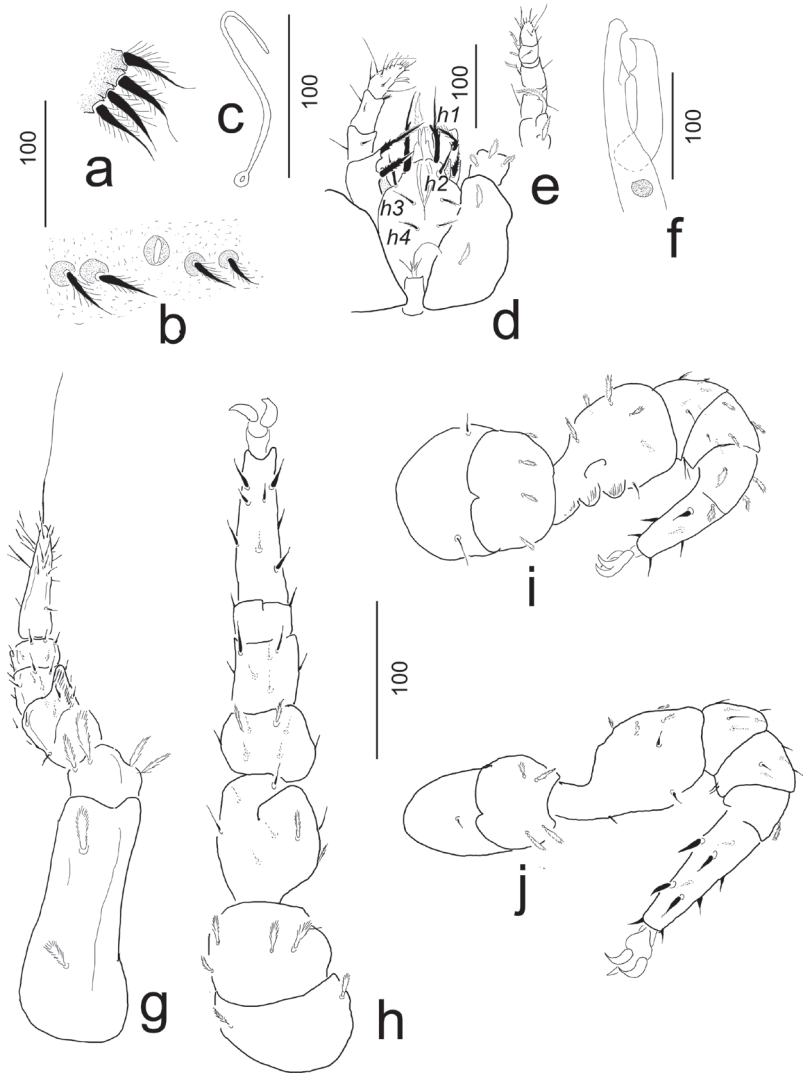

Figure 3. *Ivoria alourouai* sp. nov., female, holotype. **a** setae on vertex **b** setae around anal opening **c** peritreme **d** ventral view of gnathosoma, coxae I and palp **e** lateral view of palp **f** lateral view of chelicera **g** ventral view of leg I **h** ventral view of leg II **i** lateral view of leg III **j** lateral view of leg IV.

10–12 long and ca 4–6 wide, anal valves narrow and with smooth surface (Fig. 3b). Genital shield triangular, length 100–105, width at basal level 105–115, situated between coxae IV and pedofossae IV; surface without sculptural pattern. Peritremes hook-shaped (Fig. 3c). Pedofossae deep, their surface smooth, separate furrow for tarsi IV absent. Tritosternum (Fig. 3d) with vase-like base, apically with one pair of spines, its laciniae subdivided into two pairs of short lateral branches and one pair of long central branches.

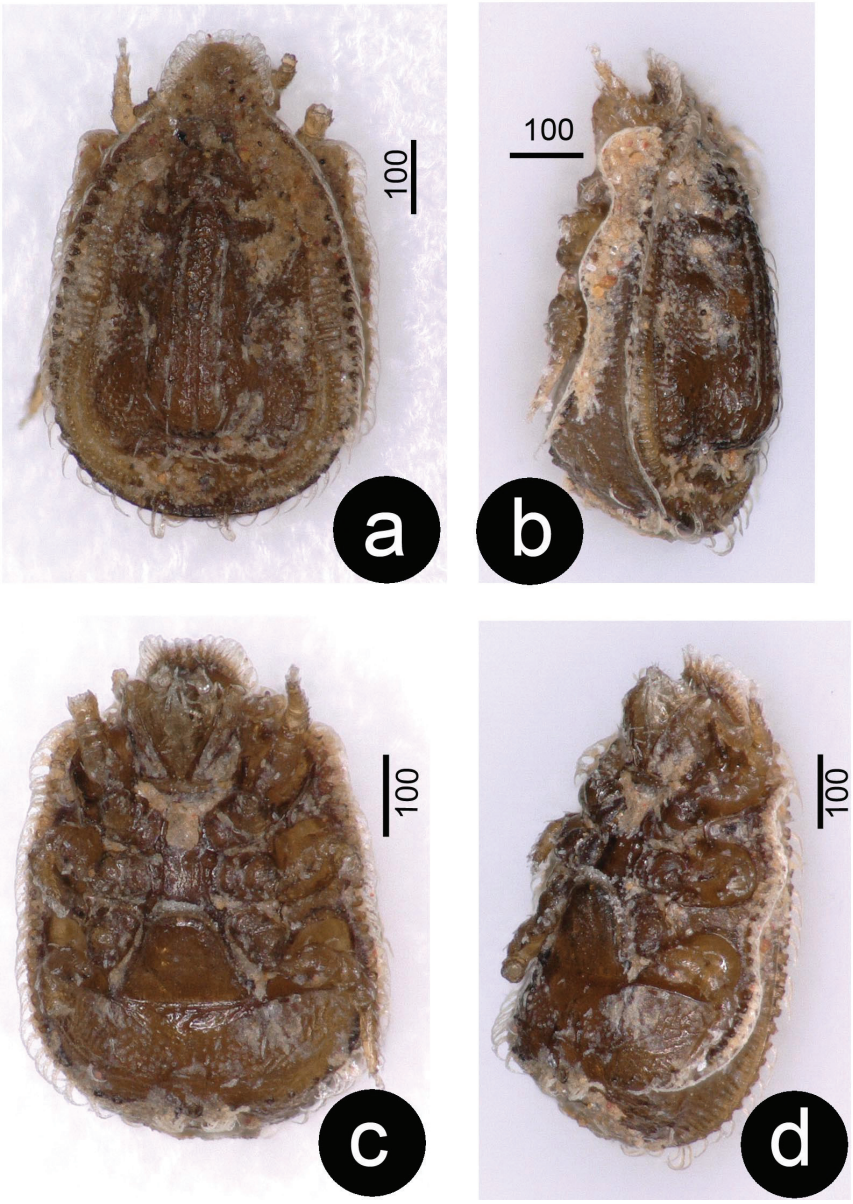

Figure 4. Photos about *Ivoria alourouai* sp. nov., female, holotype. **a** dorsal view **b** latero-dorsal view **c** ventral view **d** latero-ventral view.

Gnathosoma (Fig. 3d-f). Corniculi small, smooth and horn-like, situated posterior to *h2*; internal malae smooth with a short lateral branch, two times longer than corniculi. Hypostomal setae *h1* long (ca 90–95), robust and with a short lateral branch and with numerous lateral teeth. Setae *h2* (ca 35–37), *h3* and *h4* (ca 20–24)

Table 1. Distinguishing characteristics separating the two known *Ivoria* species.

	I. taiensis	*I. alourouai*
Dorsal setae around elevated area	leaf-like with serrate margins	marginally pilose
Centro-caudal part of marginal shield	with two incisions and without separated part	with a separated quadrangular part
Sternal setae	smooth	pilose
Needle-like ventral setae	present	absent
Oval pits on ventral shield	absent	present
Anterior margin of female genital shield	between coxae II	between coxae IV
Shape of anterior margin of female genital shield	peaked	rounded
Peritremes	L-shaped	hook-shaped

marginally serrate. Deutosternal region without teeth or denticulate rows. Chelicerae large and robust with internal sclerotized nodes (Fig. 3f). Fixed digit of chelicerae longer (ca 146–150) than movable digit (ca 119–120); both digits of chelicerae bearing a large central tooth. Palp trochanter setae *v1* robust and serrate (ca 49–52), *v2* long (ca 90–92), basally serrate and apically pilose and situated on a small protuberance. Other setae on palp segments smooth (Fig. 3d, e). Palp apotele bifurcated. Epistome marginally serrate.

Legs (Fig. 3g–j). Length of legs (from base of coxae to apex of tarsus): I 340–350, II 380–385, III 330–340, IV 345–355. Leg I without ambulacral claws, majority of setae on all legs pilose, some setae on tarsi and the ventral area smooth.

Etymology. The name of the new species is dedicated to Alouroua the mythical creator of the Akan (Baoule) people who are the major cultural group of the Ivory Coast.

Remarks. Until now, only one species had been described from this poorly-known genus. The differences between of the two species are summarized in Table 1.

Discussion

The genus *Ivoria* seems to be a rare, endemic genus in the West African region. The two known species occur only in Ivory Coast. The Uropodina fauna and the distribution of the known species are very poorly investigated in this region, therefore discovery of numerous additional species might be expected. A similar situation exists for the East African Uropodina genus *Bloszykiella* (Kontschán and Ermilov 2020).

Acknowledgements

We are very grateful to Dr Peter Schwendinger (MHNG) for his kind hospitality during the first author's stay in Geneva. We would like to thank Dr Jason Dunlop for his linguistic correction of the manuscript. This study was also supported by the Hungarian-Russian TÉT Grant (2019-2.1.11-TÉT-2019-00027).

References

Berlese A (1917) Intorno agli Uropodidae. Redia 13: 7–16.

Hiramatsu N (1983) Gangsystematik der Parasitiformes Teil 444. Die Gattung *Wernerhirschmannia* nov. gen. Hiramatsu 1983. Stadium einer neuen *Wernerhirschmannia*-Art aus Bolivien (Uropodidae). Acarologie. Schriftenreihe für Vergleichende Milbenkunde 30: 159–161.

Hirschmann W (1973) Gangsystematik der Parasitiformes Teil 161. Die Gattungen *Baloghjkaszabia* und *Kaszabjbaloghia* nova genera (Uropodini, Uropodinae). Acarologie. Schriftenreihe für Vergleichende Milbenkunde 19: 103–105.

Kontschán J (2009) *Rotundabaloghia browni* spec. nov., a new uropodine mite from Ivory Coast (Acari, Mesostigmata, Uropodina, Uropodidae). Spixiana 32(1): 35–38.

Kontschán J (2010) *Bloszykiella africana* gen. nov., sp. nov., a new mite genus from East Africa. Zootaxa 2525: 63–68. https://doi.org/10.11646/zootaxa.2525.1.4

Kontschán J (2011) Uropodina mites with unusual chelicerae from Thailand (Acari: Mesostigmata). Zootaxa 2984: 54–66. https://doi.org/10.11646/zootaxa.2984.1.2

Kontschán J, Starý J (2012) New Uropodina (Acari: Mesostigmata) from California, USA. Zootaxa 3210: 26–38. https://doi.org/10.11646/zootaxa.3210.1.2

Kontschán J (2019) *Ivoria taiensis* gen. nov., sp. nov., a remarkable new mite genus from West Africa (Acari: Mesostigmata: Urodinychidae). Systematic & Applied Acarolog 24(6): 1063–1070. http://doi.org/10.11158/saa.24.6.9

Kontschán J (2020a) A second species of the family Eutrachytidae (Acari: Uropodina) in Africa: *Mahnertellina paradoxa* gen. nov., sp. nov. from the Ivory Coast. Revue suisse de Zoologie 127(1): 75–81. https://doi.org/10.35929/RSZ.0007

Kontschán J (2020b) Out of the Neotropical region: first record of the genus *Origmatrachys* Hirschmann, 1979 (Trachyuropodidae) in Africa with the description of *O. mahnerti* sp. nov. (Acari: Uropodina) from Ivory Coast. Systematic & Applied Acarology 25(3): 420–428. https://doi.org/10.11158/saa.25.3.4

Kontschán J, Ermilov SG (2020) Two new species of the genus *Bloszykiella* (Acari: Uropodidae) from the Afrotropical region. Systematic & Applied Acarology 25(10): 1915–1923. https://doi.org/10.11158/saa.25.10.14

Kramer P (1881) Ueber die Prinzipien der Classification bei den Gamasiden. Zeitschrift für die Gesamte Naturwissenschaften Halle 54: 638–642.

Lindquist EE, Krantz GW, Walter DE (2009) Order Mesostigmata. In: Krantz GW, Walter DE (Eds). A Manual of Acarology. 3rd Edition. Texas Tech University Press, Lubbock, Texas, 124–232.

Wiśniewski J (1993) Gangsystematik der Parasitiformes Teil 549. Die Uropodiden der Erde nach Zoogeographischen Regionen und Subregionen geordnet (Mit Angabe der Lande). Acarologie. Schriftenreihe für Vergleichende Milbenkunde 40: 221–291.

Wiśniewski J, Hirschmann W (1991) *Multidenturopoda* nov. gen. *camerunis* nov. spec. (Acarina, Uropodina) aus Kamerun. Acarologia 32: 303–309

ZooKeys 1082: 73–85 (2022)
doi: 10.3897/zookeys.1082.71859
https://zookeys.pensoft.net

CHECKLIST

A peer-reviewed open-access journal
ZooKeys
Launched to accelerate biodiversity research

First data on the Hirudinea fauna of lotic ecosystems of the Khanty-Mansi Autonomous Area (Russia)

Lyudmila I. Fedorova[1], Irina A. Kaygorodova[2]

1 *Surgut State University, 1 Lenin Ave., Surgut 628412, Russia* **2** *Limnological Institute, Siberian Branch of Russian Academy of Sciences, 3 Ulan-Batorskaya St., Irkutsk 664033, Russia*

Corresponding author: Irina A. Kaygorodova (irina@lin.irk.ru)

Academic editor: Fredric Govedich | Received 20 July 2021 | Accepted 20 December 2021 | Published 19 January 2022

http://zoobank.org/94FC6758-B2E3-4920-80D1-BF19FBD6DEF6

Citation: Fedorova LI, Kaygorodova IA (2022) First data on the Hirudinea fauna of lotic ecosystems of the Khanty-Mansi Autonomous Area (Russia). ZooKeys 1082: 73–85. https://doi.org/10.3897/zookeys.1082.71859

Abstract

Hirudinea, a small and ecologically important group of aquatic organisms, is poorly studied in northern Eurasia. In this study, we demyth the idea of the faunistic poverty of this region and present the first findings of rheophilic leeches from the Khanty-Mansi Autonomous Area, Russia. Investigation of 25 rivers (Severnaya Sosva, Ob, Konda-Irtysh, and Bolshoi Yugan river basins) resulted in finding 10 leech species with parasitic and non-parasitic life strategies. These species belong to two orders (Rhynchobdellida and Arhynchobdellida), three families (Glossiphoniidae, Piscicolidae, and Erpobdellidae) and six genera (*Alboglossiphonia*, *Glossiphonia*, *Helobdella*, *Hemiclepsis*, *Piscicola*, and *Erpobdella*). Five species, *A. hyalina*, *G. verrucata*, *E. monostriata*, *E. vilnensis*, and potentially new morphological species of piscine leeches *Piscicola* sp., have been discovered for the first time in Western Siberia. Data on species diversity of rheophilic leeches include the exact systematic position for all leech taxa. Each species from the list is supplemented with information about its geographical distribution.

Keywords

Hirudinea, new records, north of Western Siberia rivers, species distribution, species diversity

Introduction

Khanty-Mansi Autonomous Area is located in the central part of the West Siberian Plain, stretching for almost 1400 km from the Ural ridge in the west to the Ob-Yenisei watershed in the east, and extending about 800 km from north to south (https://www.geografia.ru). The region has an extensive system of watercourses of various types, of which the Ob and Irtysh rivers are among the largest in Russia. The total length of the hydraulic network is about 100,000 km (Dobrinskii and Plotnikov 1997). The taiga rivers in the region are characterized by wide floodplains and valleys, small slopes, and low flow rates (Frolov and Sazonov 2004). The extended spring-summer flood, freshets in the warm season, and backwater phenomena contribute to a strong watering of watersheds with the formation of lars (floodplain swamps) and sors (seasonal lakes formed in flooded low-lying areas).

Many rivers of the Khanty-Mansi Autonomous Area are undergoing anthropogenic transformations mainly associated with large-scale oil production. Greater damage to ecosystems is caused not only by oil pollution *per se* (Picunov and Bortnikova 2005; Uslamin et al. 2019) but also by salinization of aquatic ecosystems due to the outflow of sodium chloride water to the surface during oil recovery (Moskovchenko et al. 2017). Local emergencies at the sites of production, processing, and transportation of hydrocarbon, often raw, lead to ingress of an oily liquid into the catchments of small watercourses with its subsequent migration to larger water systems (Zakharov et al. 2011). At the same time, the reduced ability of northern rivers for biological self-purification aggravates the vulnerability of aquatic biocenoses (Yakovlev 2005).

Leeches are an integral component of any aquatic biocenoses. Their role is especially significant in freshwater benthic communities of coastal zones where they are the most abundant (Adamiak-Brud et al. 2016). Ecosystem relationships between leeches and other organisms are highly diverse. Non-parasitic representatives of this group are a source of nutrient-valuable substances, and are, therefore, attractive to predatory mammals, semi-aquatic birds, fishes, and amphibians (Lukin 1976). In addition to their role in the food web, leeches are of interest as accumulators of toxicants (Lapkina and Flerov 1980; Romanova and Klimina 2009) and as bioindicators of water pollution (Bezmaternykh 2007; Martins et al. 2008; Fedorova 2020). The ecological role of parasitic forms is not limited to regulating the number of host species by weakening and creating conditions for the development of infections. Leeches are directly related to the transmission of bacterial and viral infections (Ahne 1985; Mulcahy et al. 1990; Faisal and Schulz 2009), as well as hematozoa, including trematodes, cestodes, nematodes (Demshin 1975), and parasitic flagellates (Khan 1976; Khamnueva and Pronin 2004; Burreson 2007), which are considered to be pathogenic organisms for aquatic animals.

To date, no object-orientated studies on the leech fauna of the Khanty-Mansi Area have been performed. The only study reports on three species of Hirudinea from the Khanty-Mansi lakes (Uslamin et al. 2019): the widespread Palaearctic leech, *Helobdella stagnalis* (Linnaeus, 1758), the medicinal leech, *Hirudo medicinalis* (Linnaeus, 1758), which is

unexpected in this region, and the easily recognizable stagnophilic *Erpobdella nigricollis* (Brandes, 1900). The lack of information on the hirudofauna and only a few studies on other groups of rheophilic hydrofauna (Stepanova 2008; Semyonova and Aleksyuk 2010; Sharapova and Babushkin 2013) can be explained by the difficulties in accessing lotic ecosystems due to the peculiarities of their hydrological regime in this region.

This paper presents the first purposeful study of the leech fauna from the watercourses in the Khanty-Mansi Autonomous Area, debunking the myth the aquatic invertebrate fauna in the north of Western Siberia is impoverished.

Materials and methods

Leech sampling was carried out from 6 June to 20 September 2020 at 44 locations along 25 large and small watercourses belonging to the Bolshoi Yugan, Severnaya Sosva, Konda-Irtysh, and Ob watershed basins (Fig. 1).

Figure 1. Schematic map of geographic location of the Khanty-Mansi Autonomous Area and studied lotic systems. River basins: I = Severnaya Sosva, II = Konda-Irtysh, III = Ob, and IV = Bolshoi Yugan.

The use of conventional hydrobiological equipment (sweep net, dredge, scraper, bottom grab, etc.) is less effective in catching leeches than for many other aquatic invertebrates; therefore, the collection of leeches was done manually. To do this, we examined aquatic plants and potential host animals to detect parasitic and predatory leeches, as well as various underwater objects (rotten tree, driftwood, stones, etc.) to which leeches can attach. Collected individuals were fixed after preliminary anesthesia in a low-concentration alcohol solution and kept in 80% ethanol. Morphological analysis was conducted using a stereomicroscope MSP-2 var. 2 (LOMO). Species affiliation was determined using existing systematic keys (Lukin 1976; Nesemann and Neubert 1999). The external morphology of identified leeches was in agreement with the relevant species description. All taxonomic names were given according to the current classification of the group. The collection of leech species with voucher specimens was deposited at Surgut State University, Russia.

Results

An object-oriented hydrobiological survey carried out in the warm season of 2020 resulted in finding leeches in 20 of 25 examined watercourses of the Khanty-Mansi Autonomous Area. This indicates a high frequency of their occurrence in nature. Leeches inhabit at least 88% of the region's rivers. However, not all surveyed water bodies turned out to be suitable for leeches. In particular, we could not find them in some watercourses, namely, in the Shaitanka rivers, Bezymyannyi Creek (Severnaya Sosva river basin), in two nameless brooks (Ob river basin), and the Pach-peu River (Bolshoi Yugan river basin). Very cold water, fast current, and, hence, biotic poverty of streams, creeks, and brooks make these habitats less suitable for leeches. There were no leeches in the navigable sections of the Irtysh. In the Pach-peu River, leeches were absent probably due to poor water quality.

In this first faunistic leech species list, 10 species were documented. The species diversity includes leeches from two orders (Rhynchobdellida and Arhynchobdellida), three families (Glossiphoniidae, Piscicolidae, and Erpobdellidae), and six genera (*Alboglossiphonia*, *Helobdella*, *Hemiclepsis*, *Glossiphonia*, *Piscicola*, and *Erpobdella*). Species composition includes both free-living and parasitic freshwater leeches. Parasitic leeches form the majority of the region's hirudofauna and are represented by seven species, including representatives of five genera: *Alboglossiphonia hyalina* (Müller, 1774), *Helobdella stagnalis* (Linnaeus, 1758), *Hemiclepsis marginata* (Müller, 1774), *Glossiphonia complanata* (Linnaeus, 1758), *Glossiphonia concolor* (Aphathy, 1888), *Glossiphonia verrucata* (F. Müller, 1844), and *Piscicola* sp. Among free-living macrophagous leeches, there were only three *Erpobdella* species: *E. monostriata* (Lindenfeld & Pietruszynski, 1890), *E. octoculata* (Linnaeus, 1758), and *E. vilnensis* (Liskiewicz, 1925).

Our study did not confirm the information provided in the literature about findings of *Hirudo medicinalis* Linnaeus, 1758 and *Erpobdella nigricollis* (Brandes, 1900) (Uslamin et al. 2019) within the Khanty-Mansi Autonomous Area. According to Nesemann and Neubert (1999), *E. nigricollis* belongs to the potamic fauna, with a preference for large rivers; in contrast, Lukin (1976) ranked this species as being typical of small lakes and naturally stagnant water bodies located in the floodplains of rivers.

Most Russian researchers (e.g., Baturina et al. 2020) tend to agree with Lukin's opinion. If the presence/absence of *E. nigricollis* in the watercourses of the Khanty-Mansi Area is discussable, the presence of *H. medicinalis* in the north of Western Siberia is much more questionable and needs additional verification. The range of this medicinal leech species corresponds to areas initially covered by deciduous tree forests and does not extend beyond Central and Northern Europe (Utevsky et al. 2010).

The checklist includes both widespread Palaearctic species (*G. complanata*, *H. marginata*, and *E. octoculata*) and widespread Holarctic species (*H. stagnalis*). Five species, *A. hyalina*, *G. verrucata*, *E. monostriata*, *E. vilnensis*, and *Piscicola* sp. were discovered for the first time in Western Siberia. In this paper, a single specimen of *Piscicola* sp. is cautiously referred to as an unidentified species because its morphology differs from all currently described species. It is highly probable that this unidentified species is potentially new to science. Clarification of its attribution and its description will require additional biological material and in-depth analysis.

The species composition of the Khanty-Mansi hirudofauna has an uneven distribution (Table 1). The greatest species diversity was observed in the Ob basin: nine of 10 species from the regional list (except *A. hyalina*) inhabit its watercourses. This is probably due to the flat nature of the ramified water network, numerous tributaries carrying nutrients from a vast territory, and a high level of self-purification of rivers.

Within the Severnaya Sosva river network, the Hirudinea fauna was the least diverse (Table 1). Due to natural inaccessibility, sampling in this area was carried out less intensively than in other examined basins. However, the four species found here represented every possible variety of life strategies of leeches: the parasitic *G. concolor*, the small predator *H. stagnalis*, and the free-living macrophagous *E. octoculata* and *E. monostriata*. These leeches were found in the Yatria and Schekurya rivers.

Leeches from the Konda-Irtysh and Bolshoi Yugan watershed basins were represented by seven species: *H. marginata*, *G. complanata*, *G. concolor*, *H. stagnalis*, *E. octoculata*, *E. monostriata*, and *A. hyalina* or *E. vilnensis* depending on the basin (Table 1). Among watercourses of the Konda-Irtysh system, the highest diversity was observed in the main riverbed of the Irtysh. The leech populations of the Bolshoi Yugan basin were sparse, and individuals were not numerous.

Table 1. Species composition of the Hirudinea fauna in lotic ecosystems of the Khanty-Mansi Area, with an estimate of occurrence frequency (rather rare +, common ++, everywhere +++).

Taxa	River basins			
	Ob	Konda-Irtysh	Severnaya Sosva	Bolshoi Yugan
Alboglossiphonia hyalina	–	+	–	–
Helobdella stagnalis	++	+++	+	++
Hemiclepsis marginata	++	++	–	+
Glossiphonia complanata	+	++	–	+
Glossiphonia concolor	++	+	+	+
Glossiphonia verrucata	+	–	–	–
Piscicola sp.	+	–	–	–
Erpobdella octoculata	++	++	++	+
Erpobdella monostriata	++	+	+	+
Erpobdella vilnensis	+	–	–	+

Species *H. stagnalis*, *G. concolor*, *E. octoculata*, and *E. monostriata* are widespread in the rivers of the Khanty-Mansi Area, whereas *G. verrucata* and *E. vilnensis* are rare for the eastern Palaearctic obviously prefer the southern areas of the region (Table 1).

Listed below is the information about the species composition of Hirudinea fauna of the the Khanty-Mansi Autonomous Area, with systematic position, geographical distribution, and habitat coordinates for each species.

Systematics

Phylum Annelida Lamarck, 1809
Class Clitellata Michaelsen, 1919
Subclass Hirudinea Lamarck, 1818 (synonym Hirudinida)
Order Rhynchobdellida Blanchard, 1894
Family Glossiphoniidae Vaillant, 1890
Genus *Alboglossiphonia* Lukin, 1976

***Alboglossiphonia hyalina* (Müller, 1774)**

Hirudo hyalina Müller 1774
Clepsine hyalina Moqun-Tandon 1826
Glossobdella hyalina De Blainville1827
Glossiphonia heteroclita f. *hyalina* Pawlowski 1936

Geographical distribution. Palaearctic region. This species is rare in Europe (Nesemann and Neubert 1999) but abundant in Eastern Siberia (Kaygorodova et al. 2013).

Location. Not an abundant species. Point occurrence in floodplain water bodies of the Irtysh River (61°0'58"N, 69°9'26"E).

Genus *Glossiphonia* Johnson, 1816

***Glossiphonia complanata* (Linnaeus, 1758)**

Hirudo complanata Linnaeus, 1758
Glossiphonia tuberculate Johnson, 1816
Glossiphonia complanata Blanchard, 1894

Geographical distribution. Palaearctic region. Previously mentioned as Holarctic. However, recent molecular studies confuted its findings in North America (Williams et al. 2013; Kaygorodova et al. 2020).

Locations. Ob River (61°5'38"N, 69°27'38.6"E; 60°57'56"N, 68°46'38"E), Kabaniy stream (60°54'4"N, 68°42'55"E), Okhotnichiy stream (60°56'9"N, 68°41'52"E), Irtysh River (61°0'58"N, 69°9'26"E; 61°0'14"N, 68°59'10"E; 60°59'57"N, 68°59'19"E; 60°59'37"N, 68°59'22"E), Wachem-peu River (60°16'34.0"N, 73°55'18.0"E), Lungunigyi River (60°11'43.0"N, 74°12'20.0"E), Ugutka River (60°29'26.0"N, 74°03'45.0"E).

Glossiphonia concolor (Aphathy, 1888)

Clepsine concolor Apathy, 1888
Glossiphonia concolor Livanow, 1903

Geographical distribution. Palaearctic region. Distributed in northern, central, and eastern Europe (Nesemann and Neubert 1999). There is information about its occurrence in Iran (Darabi-Darestani et al. 2016) and occasionally in Eastern Siberia (Kaygorodova and Pronin 2013).

Locations. Schekurya River (64°15'52.35"N, 60°54'23.98"E), Yatria River (64°15'50"N, 60°52'39"E), Ob River (61°5'38.0"N, 69°27'38.6"E; 61°5'47"N, 69°27'46"E; 60°57'13"N, 68°39'27"E), Saima River (61°14'41.1"N, 73°25'09.5"E; 61°14'32.6"N, 73°24'53.1"E), Shaitanskaya River (61°4'50.4"N, 69°28'51.9"E), Zhivoy stream (60°53'22"N, 68°41'40"E), Irtysh River (61°1'21"N, 69°8'20"E; 61°0'58"N, 69°9'26"E), Bolshoi Yugan River (60°17'38.0"N, 73°53'32.0"E), Malyi Yugan River (60°31'22.3"N, 74°28'01.9"E), and Wachem-peu River (60°16'17.0"N, 73°55'22.1"E).

Glossiphonia verrucata (F. Müller, 1844)

Clepsine verrucata Müller, 1844
Glossiphonia verrucata Johansson, 1909
Batracobdella verrucata Pawlowski, 1936
Boreobdella verrucata Lukin, 1956

Geographical distribution. Palaearctic region. Although *G. verrucata* is a rare species, it nevertheless has an extensive distribution within the Palaearctic. The boreal species inhabits northern Eurasia (Lukin 1976). There are recent findings from the Kharbey lake system, Russian North (Baturina et al. 2020) and the basins of the Lena River and Lake Baikal, Eastern Siberia (Kaygorodova et al. 2020).

Locations. Not an abundant species. Point occurrence in Shaitanskaya River (61°4'50.4"N, 69°28'51.9"E) and Kabaniy stream (60°54'4"N, 68°42'55"E).

Genus *Helobdella* Blanchard, 1896

***Helobdella stagnalis* (Linnaeus, 1758)**

Hirudo stagnalis Linnaeus, 1758
Glossiphonia stagnalis Blanchard, 1894
Glossiphonia (*Helobdella*) *stagnalis* Moore, 1922
Bakedebdella gibbosa Sciacchitiano, 1939

Geographical distribution. Transpalaearctic species. This is one of the most common leech species inhabiting freshwater ecosystems in Eurasia.

Locations. Yatria River (64°15'50"N, 60°52'39"E), Ob River (61°5'38.0"N, 69°27'38.6"E; 60°57'13"N, 68°39'27"E), Saima River (61°14'41.1"N, 73°25'09.5"E), Shaitanskaya River (61°4'50.4"N, 69°28'51.9"E), Zhivoy stream (60°53'22"N, 68°41'40"E), Kabaniy stream (60°54'4"N, 68°42'55"E), Okhotnichiy stream (60°56'9"N, 68°41'52"E), Sredniy stream (60°55'24"N, 68°42'46"E), Irtysh River (61°1'21"N, 69°8'20"E; 61°0'58"N, 69°9'26"E; 61°0'14"N, 68°59'10"E; 60°59'57"N, 68°59'19"E; 60°59'37"N, 68°59'22"E), Mamontovyi creek (60°57'18"N, 68°32'27"E), Malyi Yugan River (60°31'22.3"N, 74°28'01.9"E), Bolshoi Yugan River (60°17'38.0"N, 73°53'32.0"E; 60°17'33.0"N, 73°53'38.0"E), Lungunigyi River (60°11'43.0"N, 74°12'20.0"E), Ugutka River (60°29'17.0"N, 74°03'41.0"E).

Genus *Hemiclepsis* Vejdovsky, 1884

***Hemiclepsis marginata* (Müller, 1774)**

Hirudo marginata O. F. Müller, 1774
Piscicola marginata Moquin-Tandon, 1827
Clepsine marginata F. Müller, 1844
Hemiclepsis marginata Harding, 1910

Geographical distribution. Palaearctic region. Species has wide but uneven distribution. In Europe, this species is common in countries with temperate climates. Rarely found in North Africa. It has a nonuniform distribution in the Caucasus, Central Asia, Western and Eastern Siberia, the Far East, China, and Japan (Lukin 1976).

Locations. Ob River (61°5'38.04"N, 69°27'38.66"E; 60°57'56"N, 68°46'38"E), Shaitanskaya River (61°4'50.4"N, 69°28'51.9"E), Zhivoy stream (60°53'22"N, 68°41'40"E), Mukhrinka River (60°53'42"N, 68°42'51"E), Kabaniy stream (60°54'4"N, 68°42'55"E), Okhotnichiy stream (60°56'9"N, 68°41'52"E), Sredniy stream (60°55'24"N, 68°42'46"E), Irtysh River (61°0'58"N, 69°9'26"E; 61°0'14"N, 68°59'10"E; 60°59'57"N, 68°59'19"E; 60°59'37"N, 68°59'22"E), Mamontovyi creek (60°57'18"N, 68°32'27"E), Bolshoi Yugan River (60°17'33.0"N, 73°53'38.0"E).

Family Piscicolidae Johnston, 1865 (synonym Ichthyiobdellidae Leuckart, 1863)
Genus *Piscicola* Blanville, 1818

***Piscicola* sp.**

New species records. A single specimen from the Chumpas River (61°16'24"N, 74°42'32"E).

Morphological characteristics. Piscine leech has middle size, its body length is 22 mm and diameter is 3.5 mm. Sucker size is commensurate with the width of the body. Dorsal pigmentation is absent, unlike the widespread *P. geometra* or other known species.

Family Erpobdellidae Blanchard, 1894
Genus *Erpobdella* Blainville, 1918

***Erpobdella octoculata* (Linnaeus, 1758)**

Hirudo octoculata Linnaeus, 1758
Herpobdella octoculata Johansson, 1910
Herpobdella octomaculata Pawlowski, 1935

Geographical distribution. Widespread in the Palaearctic region.

Locations. Yatria River (64°15'50"N, 60°52'39"E), Ob River (61° 5'38.0"N, 69°27'38.6"E; 60°57'13"N, 68°39'27"E), Saima River (61°14'32.6"N, 73°24'53.1"E), Shaitanskaya River (61°4'50.4"N, 69°28'51.9"E), Mukhrinka River (60°53'42"N, 68°42'51"E), Zhivoy stream (60°53'22"N, 68°41'40"E), Kabaniy stream (60°54'4"N, 68°42'55"E), Okhotnichiy stream (60°56'9"N, 68°41'52"E), Sredniy stream (60°55'24"N, 68°42'46"E), Irtysh River (61°1'21"N, 69°8'20"E; 61°0'58"N, 69°9'26"E), Mamontovyi creek (60°57'18"N, 68°32'27"E), Malyi Yugan River (60°31'22.3"N, 74°28'01.9"E), Bolshoi Yugan River (60°17'38.0"N, 73°53'32.0"E), Negus-yah River (60°11'55.0"N, 74°12'54.0"E; 60°11'19.0"N, 74°14'34.0"E), Ugutka River (60°29'17.0"N, 74°03'41.0"E; 60°29'26.0"N, 74°03'45.0"E).

Species: *Erpobdella monostriata* (Lindenfeld et Pietruszynski, 1890)

Nephelis octoculata var. *monostriata* Lindenfeld & Pietruszynski, 1890
Erpobdella vilnensis (Liskiewitz, 1925) in part

Geographical distribution. Palaearctic region. This species occurs in Europe from the Netherlands (Haaren et al. 2004) in the west to the Voronezh region of Russia in the east (Utevsky et al. 2015). It has been recently reported in East Kazakhstan (Kaygorodova & Fedorova, 2016). This study reports the first finding in the north of Western Siberia.

Locations. Schekurya River (64°15'52.35"N, 60°54'23.98"E), Ob River (61°15'27.4"N, 73°20'56.9"E), Saima River (61°14'41.1"N, 73°25'09.5"E), Shaitanskaya River (61°4'50.4"N, 69°28'51.9"E), Mukhrinka River (60°53'42"N, 68°42'51"E), Zhivoy stream (60°53'22"N, 68°41'40"E), Kabaniy stream (60°54'4"N, 68°42'55"E), Okhotnichiy stream (60°56'9"N, 68°41'52"E), Sredniy stream (60°55'24"N, 68°42'46"E), Irtysh River (61°1'21"N, 69°8'20"E; 61°0'58"N, 69°9'26"E), Bolshoi Yugan River (60°17'33.0"N, 73°53'38.0"E), Wachem-peu River (60°16'17.0"N, 73°55'22.1"E).

***Erpobdella vilnensis* (Liskiewicz, 1925)**

Nephelis testacea f. *nigricollis* Brandes, 1900
Herpobdella testacea var. *nigricollis* Johansson, 1929

Geographical distribution. Palaearctic region. *Erpobdella vilnensis* is rather a common leech species that occurs in Central, Eastern, and Southeastern Europe (Nesemann and Neubert 1999). The easternmost distribution records were from Kyrgyzstan (Jueg et al. 2013) and eastern Kazakhstan (Kaygorodova and Fedorova 2016).

Locations. Ob River (60°57'56"N, 68°46'38"E; 61°15'27.4"N, 73°20'56.9"E), Shaitanskaya River (61°4'50.4"N, 69°28'51.9"E), Negus-yah River (60°11'55.0"N, 74°12'54.0"E), Lungunigyi River (60°11'43.0"N, 74°12'20.0"E).

Acknowledgements

We are grateful to E.A. Zvyagina (Lomonosov Moscow State University) and N.V. Filippova (Ugra State University) for help in organizing the expedition.

This study was carried out within the framework of research program of the Department of Education and Youth Policy of the Khanty-Mansiysk Autonomous Okrug, Russia (no. 121052800096–4) and basic research programs of the Ministry of Education and Science, Russia, no. 0279–2021–0011 (121032300198–2).

References

Adamiak-Brud Ż, Bielecki A, Kobak J, Jabłońska-Barna I (2016) Rate of short-term colonization and distribution of leeches (Clitellata: Hirudinia) on artificial substrates. Journal of Zoology 299: 191–201. https://doi.org/10.1111/jzo.12341

Ahne W (1985) *Argulus foliaceus* L. and *Piscicola geometra* L. as mechanical vectors of spring viraemia of carp virus (SVCV). Journal of Fish Diseases 8: 241–242. https://doi.org/10.1111/j.1365-2761.1985.tb01220.x

Baturina MA, Kaygorodova IA, Loskutova OA (2020) New data on species diversity of Annelida (Oligochaeta, Huridinea) in the Kharbey lakes system, Bolchezemelskaya tundra (Russia). ZooKeys 910: 43–78. https://doi.org/10.3897/zookeys.910.48486

Bezmaternykh DM (2007) Zoobenthos as an indicator of ecological state of aquatic ecosystems in Western Siberia: an analytical review. Ekologiya 85: 1–86.

Burreson EM (2007) Hemoflagellates of Oregon marine fishes with the description of new species of *Trypanosoma* and *Trypanoplasma*. Journal of Parasitology 93(6): 1442–1451. https://doi.org/10.1645/GE-1220.1

Darabi-Darestani K, Sari A, Sarafrazi A (2016) Five new records and annotated checklist of the leeches (Annelida: Hirudinida) of Iran. Zootaxa 4170(1): 041–070. https://doi.org/10.11646/zootaxa.4170.1.2

Demshin NI (1975) Oligochaeta and Hirudinea as Intermediate Hosts of Helminthes. Nauka, Novosibirsk, 190 pp.

Dobrinskii LN, Plotnikov VV (1997) Ecology of the Khanty-Mansi Autonomous Okrug. Tyumen': SoftDizayn, 288 pp.

Faisal M, Schulz CA (2009) Detection of viral hemorrhagic septicemia virus (VHSV) from the leech *Myzobdella lugubris* Leidy, 1851. Parasites & Vectors 282(1): e45. https://doi.org/10.1186/1756-3305-2-45

Fedorova LI (2020) Environmental factors influence on leeches distribution in the middle reaches of the Irtysh River. Samara Journal of Science 9(4): 159–164. https://doi.org/10.17816/snv202094124

Frolov RD, Sazonov AA (2004) Prospects of development internal waterways XMAO. Vestnik of Volga State University of Water Transport 8: 94–101.

Haaren T, Hop H, Soes M, Tempelman D (2004) The freshwater leeches (Hirudinea) of the Netherlands. Lauterbornia 52: 113–131.

Jueg U, Grosser C, Pešić V (2013) Bemerkungen zur Egelfauna (Hirudinea) von Kirgistan. Lauterbornia 76: 103–109.

Kaygorodova IA, Fedorova LI (2016) The first data on species diversity of leeches (Hirudinea) in the Irtysh River Basin, East Kazakhstan. Zootaxa 4144(2): 287–290. https://doi.org/10.11646/zootaxa.4144.2.10

Kaygorodova IA, Pronin NM (2013) New records of Lake Baikal leech fauna: species diversity and spatial distribution in Chivyrkuy Gulf. The Scientific World Journal 2013: 1–10. http://dx.doi.org/10.1155/2013/206590

Kaygorodova IA, Bolbat NB, Bolbat AV (2020) Species delimitation through DNA barcoding of freshwater leeches of the *Glossiphonia* genus (Hirudinea: Glossiphoniidae) from Eastern Siberia, Russia. Journal of Zoological Systematics and Evolutionary Research 58: 1437–1446. https://doi.org/10.1111/jzs.12385

Kaygorodova IA, Dzyuba EV, Sorokovikova NV (2013) First records of potamic leech fauna of Eastern Siberia, Russia. Dataset Papers in Biology 2013: 1–6. https://doi.org/10.7167/2013/362683

Khamnueva TR, Pronin NM (2004) New kinetoplastid species (Kinetoplastida: Kinetoplastidea). In: Timoshkin OA (Ed.) Index of Animal Species in Inhabiting Lake Baikal and its Area. 1, Book 2. Nauka, Novosibirsk, 1255–1260.

Khan RA (1976) The life cycle of *Trypanosoma murmanensis* Nikitin. Canadian Journal of Zoology 54(11): 1840–1849. https://doi.org/10.1139/z76-214

Lapkina LN, Flerov BA (1980) Using leeches to identify pesticides in water. Hydrobiological Journal 3: 113–118.

Lukin EI (1976) The Leech Fauna of the Soviet Union: Leeches in Fresh and Brackish Water Bodies. Nauka, Leningrad, 284 pp.

Martins RT, Stephan NNC, Alves RG (2008) Tubificidae (Annelida: Oligochaeta) as an indicator of water quality in an urban stream in southeast Brazil. Acta Limnologica Brasiliensia 20(3): 221–226.

Moskovchenko DV, Babushkin AG, Ubaidulaev AA (2017) Salt pollution of surface water in oil fields of Khanty-Mansi Autonomous Area-Yugra. Water Resources 44(1): 91–102. https://doi.org/10.7868/S0321059617010102

Mulcahy D, Klaybor D, Batts WN (1990) Isolation of infectious hematopoietic necrosis virus from a leech (*Piscicola salmositica*) and a copepod (*Salminocola* sp.), ectoparasites of sockeye salmon *Oncorhynchus nerka*. Diseases of Aquatic Organisms 8: 29–34. https://doi.org/10.3354/dao008029

Nesemann H, Neubert E (1999) Clitellata, Branchiobdellada, Acanthobdellada, Hirudinea. Spectrum Akademischer Verlag, Berlin, 6(2): 1–178.

Picunov SV, Bortnikova SB (2005) Dynamics of pollution of small rivers in oil productions regions (by the example of the Lyukkolekegan and Chernaya rivers, Nizhnevartovsky district, KHMAO). Geology. Geophysics and Development of Oil and Gas Fields 12: 27–33.

Romanova EM, Klimina OM (2009) The role of leeches in the biological mechanism of accumulation of toxicants. Vestnik of Ulyanovsk State Agricultural Academy 1(9): 85–88.

Semyonova LA, Aleksyuk VA (2010) Zooplankton of the Lower Ob' River. Bulletin of Ecology, Forestry and Landscape Science 10: 156–169

Sharapova TA, Babushkin ES (2013) Comparison of zoobenthos and zooperiphyton of large and medium rivers. Contemporary Problems of Ecology 6(6): 622–627. https://doi.org/10.1134/S1995425513060097

Stepanova VB (2008) Macrozoobenthos of the lower Ob'. Bulletin of Ecology, Forestry and Landscape Science 9: 155–162.

Uslamin DV, Aleshina OA, Gashev SN, Gradova AV (2019) Characteristics of the species composition and structure of macrozoobenthos in taiga lakes in oil-producing regions in western Siberia. Inland Water Biology 12: 306–316. https://doi.org/10.1134/S1995082919030179

Utevsky S, Dubov PG, Prokin AA (2015) First Russian record of *Erpobdella monostriata*: DNA barcoding and geographical distribution. Spitaxa 38(2): 161–168.

Utevsky S, Zagmajster M, Atemasov A, Zinenko O, Utevska O, Utevsky A, Trontelj P (2010) Distribution and status of medicinal leeches (genus *Hirudo*) in the Western Palaearctic: anthropogenic, ecological, or historical effects? Aquatic Conservation: Marine and Freshwater Ecosystems 20: 198–210. https://doi.org/10.1002/aqc.1071

Williams B, Gelder S, Proctor H, Coltman D (2013) Molecular phylogeny of North American Branchiobdellida (Annelida: Clitellata). Molecular Phylogenetics and Evolution 66(1): 30–42. https://doi.org/10.1016/j.ympev.2012.09.002

Yakovlev VA (2005) Freshwater Zoobenthos of Northern Fennoscandia (Diversity, Structure and Anthropogenic Dynamics) Apatity. Part 1. Kola Scientific Center of the Russian Academy of Sciences, Syktyvkar, 161 pp.

Zakharov AB, Loskutova OA, Fefilova EB, Khokhlova LG, Shubin YP (2011) Communities of Hydrobionts in Oil-polluted Water Areas of the Pechora River Basin. Kola Scientific Center of the Russian Academy of Sciences, Syktyvkar, 268 pp.

ZooKeys 1082: 87–102 (2022)
doi: 10.3897/zookeys.1082.73019
https://zookeys.pensoft.net

RESEARCH ARTICLE

A peer-reviewed open-access journal
ZooKeys
Launched to accelerate biodiversity research

Corynoneura Winnertz species from Hunan Province, Oriental China, delineated with morphological and 16S rDNA data (Diptera, Chironomidae)

Yue Fu[1], Xiang-Liang Fang[1], Xin-Hua Wang[2], Mi Shen[1], Yun-Li Xiao[1]

1 *Hubei Key Laboratory of Economic Forest Germplasm Improvement and Resources Comprehensive Utilization, Hubei Collaborative Innovation Center for the Characteristic Resources Exploitation of Dabie Mountains, Hubei Zhongke Research Institute of Industrial Technology, Huanggang Normal University, Huanggang City, Hubei, 438000, China* **2** *College of Life Sciences, Nankai University, Tianjin 300071, China*

Corresponding authors: Yue Fu (fuyue2007915@yahoo.com), Yun-Li Xiao (xiaoyunli0817@126.com)

Academic editor: F. L. da Silva | Received 14 August 2021 | Accepted 16 December 2021 | Published 19 January 2022

http://zoobank.org/A0290B6E-A420-4EB1-B08B-496622662A2C

Citation: Fu Y, Fang X-L, Wang X-H, Shen M, Xiao Y-L (2022) *Corynoneura* Winnertz species from Hunan Province, Oriental China, delineated with morphological and 16S rDNA data (Diptera, Chironomidae). ZooKeys 1082: 87–102. https://doi.org/10.3897/zookeys.1082.73019

Abstract

The genus *Corynoneura* Winnertz, 1846 from Hunan Province in Oriental China is reviewed. Four new species, *C. enormis* Fu **sp. nov.**, *C. gibbera* Fu **sp. nov.**, *C. incuria* Fu **sp. nov.**, and *C. longshanensis* Fu **sp. nov.** are described and illustrated based on adult males. Sequence data from the 16S rDNA gene were used to infer relationships between these species and complement morphological delineation. Sequences from the mitochondrial large ribosomal subunit (16S rDNA) from these species are uploaded to the National Center for Biotechnology Information (NCBI). Relationships were inferred using the Neighbor-Joining method based on 16S rDNA.

Keywords

Mitochondrial gene, morphology, non-biting midge, taxonomy

Introduction

Corynoneura was erected by Winnertz (1846) with *Corynoneura scutellata* Winnertz, 1846 as the type species. Fu et al. (2009) and Fu and Sæther (2012) reviewed the East Asia and Nearctic members of this genus. In addition, the different life stages of species

of the genus from different geographical areas were studied by a number of authors (Schlee 1968; Wiedenbrug and Trivinho-Strixino 2011; Wiedenbrug et al. 2012; Moubayed-Breil 2015; Makarchenko et al. 2019).

Prior to this study, there were 107 valid species in the world, including 47 species from the Palearctic Region, 19 species from the Nearctic Region, 25 species from the Neotropical Region, 27 species from the Oriental Region, four species from the Afrotropical Region, and five species from the Australasian Region (Ashe and O'Connor 2012; Fu and Sæther 2012; Fu et al. 2018, 2019, 2020; Makarchenko et al. 2019).

Previously, only one species, namely *Corynoneura prominens* Fu, Sæther & Wang, 2009 was recorded in Hunan Province. In this study, four new species are described and illustrated based on the new material from Hunan Province: *Corynoneura enormis* sp. nov., *Corynoneura gibbera* sp. nov., *Corynoneura incuria* sp. nov. and *Corynoneura longshanensis* sp. nov.. The female of *C. incuria* sp. nov., associated with the male by 16S rDNA, is described and illustrated.

Materials and methods

Adults were mainly collected in the habitats of small streams and lakes next to mountain forests. Adults were collected by light traps near the water body or swept from marginal vegetation beside natal aquatic sites. The specimens were preserved in 85% ethanol, and stored in the dark at 4 °C before molecular analyses. Total genomic DNA of specimens was extracted from the thorax and legs using Qiagen DNA Blood & Tissue Kit. The standard protocol of the Qiagen DNeasy Blood & Tissue Kit was used, except that the final elution volume was 100 μL due to the small specimen size. PCR amplification of the mitochondrial 16S ribosomal RNA gene was carried out with the primers and temperature regimes given in Ekrem et al. (2010). After DNA extraction, the clear exoskeleton was washed with 96% ethanol and mounted in Euparal on microscope slides together with the corresponding antennae, head, wings, and legs following the procedure outlined by Sæther (1969). Morphological nomenclature follows Sæther (1980).

Measurements are given as ranges followed by the mean, when three or more specimens were measured. The specimens examined in this study are deposited at the College of Biology and Agricultural Resources, Huanggang Normal University (**HNU**), Huanggang, China.

Abbreviations used in text as follows:

AR antennal ratio = length of ultimate flagellomere/combined lengths of flagellomeres one to penultimate;
VR venarum ratio;
Cu cubitus;
P_1, P_2, P_3 fore, middle, and hind legs, respectively;
fe femur;

ti	tibia;
ta	tarsomere;
LR	leg ratio (ratio of metatarsus to tibia in front leg);
BV	Bein ratio (length of (femur + tibia + ta_1) /length of (ta_2 + ta_3 + ta_4 + ta_5));
SV	Schenkel-Schiene ratio (length of (femur + tibia) / length of ta);
BR	bristle ratio (ratio of longest seta on ta1 to minimum width of ta_1 measured one third from apex);
HR	hypopygium ratio = gonocoxite length / gonostylus length;
HV	hypopygium value =body length / gonostylus length × 10.

Measurements and ratios of hind tibia follow Schlee (1968) as follows:

a	Maximum width;
b	Length of ventral elongation;
c_1	Length of strong broad part, measured from apex;
c_2	Total length of broadening;
d	Width of tibia basally to the apical broadening.

Results

Taxonomic account

***Corynoneura* Winnertz, 1846**

Corynoneura Winnertz, 1846: 12.

***Corynoneura enormis* Fu, sp. nov.**
http://zoobank.org/6D4BD075-EC3F-4BC2-9A53-D86F97A7202D
Figure 1

Type material. *Holotype*, male (HNU: 17091206HJL), China: Hunan Province, Loudi City, Xinhua County, Xihe Town, Cushi Village, 27°51'45"N, 111°31'51"E, 315 m a. s. l., 29.VII.2016, sweep net, leg. Jingli Huang.

Etymology. From Latin, *enormis*, immense, huge, vast, referring to lateral sternapodeme with a large attachment point.

Diagnosis. The male imago is characterized by having an antenna with eight flagellomeres, AR 0.51; anterior margin of cibarial pump distinctly concave; hind tibia with hooked spur; superior volsella small rounded and undeveloped; inferior volsella narrow, with dented edge, along the inner margin of gonocoxite; phallapodeme apically curved, placed in lateral position of sternapodeme; sternapodeme curved into a U-shape, and lateral sternapodeme with large caudal attachment point.

Description. Adult males (*N* = 1). Total length 0.92 mm. Wing length 0.53 mm. Total length/wing length ratio 1.74. Wing length/profemur length ratio 2.69.

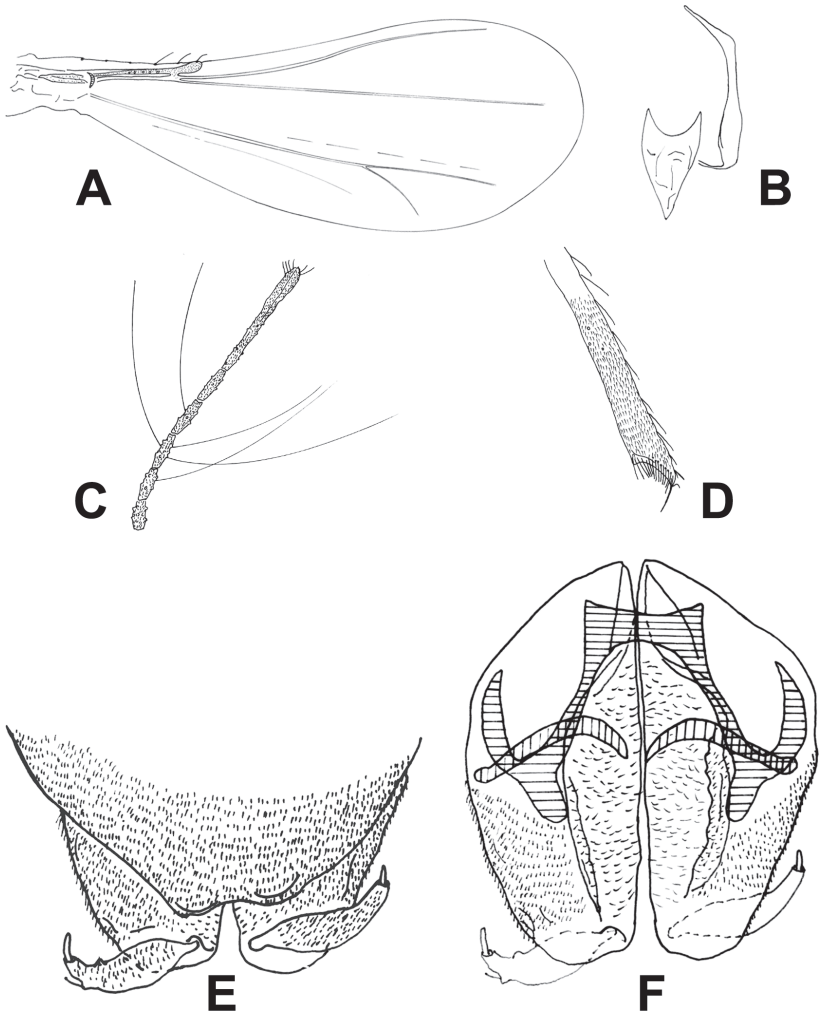

Figure 1. *Corynoneura enormis* sp. nov., male imago. **A** wing **B** tentorium and cibarial pump **C** apex of antenna **D** legs **E** hypopygium, dorsal view **F** hypopygium, ventral view.

Coloration. Head dark brown; thorax dark brown. Legs yellowish. Abdomen brown.

Head. Antenna with eight flagellomeres, AR 0.51, ultimate flagellomere 115 μm long, with many short apical sensilla chaetica (Fig. 1C). Tentorium and cibarial pump as in Figure 1B, tentorium 110 μm long; 12 μm wide; Anterior margin of cibarial pump strongly concave. Clypeus with four setae.

Thorax. Five dorsocentral setae. Scutellum with two setae. One or two prealar setae.

Wing (Fig. 1A). VR 3.0. Cu/wing length ratio 0.54; costa 120 μm long, with five setae; Cu 288 μm long; wing width/wing length ratio 0.45.

Legs. Fore trochanter with dorsal keel. Most of fore- and mid-legs lost. Spurs of hind tibia 25 μm and 10 μm long. Width of hind tibia at apex (a) 29 μm, width

Table 1. Lengths (in μm) and proportions of leg segments of male *Corynoneura enormis* sp. nov. (*N* = 1).

	fe	ti	ta_1	ta_2	ta_3	ta_4	ta_5	LR	BV	SV	BR
P_1	197	240	130	71	42	20	28	0.54	3.52	3.36	1.80
P_2	216	245	145	70	35	16	27	0.59	4.09	3.17	2.00
P_3	216	211	113	67	29	19	29	0.54	3.75	3.78	1.80

of hind tibia $^1/_3$ from apex (d) 18 μm, elongation length (b) 34 μm, length of maximum thickening (c_1) 48 μm, total length of thickening (c_2) 72 μm; hind tibial ratios: a/d 1.61; b/d 1.89; c_1/d 2.61; c_2/d 4.00. Hind tibia expanded with comb of 17 setae and S-shaped spur (Fig. 1D). Lengths and other proportions of legs given in Table 1.

Hypopygium (Fig. 1E, F). Tergite IX medially incurved. Superior volsella small, with rounded margin, anteromedially fused. Inferior volsella along inner margin of gonocoxite with many glandular setae. Phallapodeme scalpel-like, apical curved, 35 μm long, and joint with sternapodeme placed lateral. Transverse sternapodeme 20 μm wide, inverted U-shaped, with small oral projection, lateral sternapodeme with very large attachment point placed and directed caudally. Gonostylus curved tapering, 29 μm long; megaseta 5 μm long. HR 2.31; HV 3.17.

Remarks. This species is similar to *Corynoneura ascensa* Fu & Sæther, 2012 and *Corynoneura sesquipedalis* Fu & Fang, 2018 by having a large attachment point on the lateral sternapodeme. The new species can be separated from *C. ascensa* by having antenna with 8 flagellomeres, narrow and undeveloped inferior volsella; and differs from *C. sesquipedalis* by having a narrow inferior volsella, transverse sternapodeme present and with an oral projection (broad inferior volsella, transverse sternapodeme V-shaped,without transverse part in *C. sesquipedalis*). The sequence of 16S rDNA from this species is highly similar to *Corynoneura tumula* Fu & Fang, 2018, but there are distinct morphological differences between them: in *C. enormis* the antenna has 8 flagellomeres, AR 0.51; inferior volsella narrow, lateral sternapodeme with large caudal attachment point, while *C. tumula* has an antenna with 9 flagellomeres, AR 0.46; inferior volsella relatively broad, lateral sternapodeme with small caudal attachment point.

***Corynoneura gibbera* Fu, sp. nov.**

http://zoobank.org/51E7C7EA-3496-4E7D-A6D4-6009D0B8A94E

Figure 2

Type material. ***Holotype*** male (HNU: 17090801HJL), China: Hunan Province, Huaihua City, Hecheng County, Wushui River, Xiyi Bridge, 27°33'29"N, 109°57'41"E, 259 m a. s. l., 23.VII.2016, light trap, leg. Haixia Shi. 6 males (HNU: 17090902HJL, 17090904HJL, 17091004HJL, 17091003HJL, 17090804HJL, 17090803HJL), 21–23.VII. 2016, as holotype.

Etymology. From Latin, *gibbera*, protuberant, referring to the prominent inferior volsella.

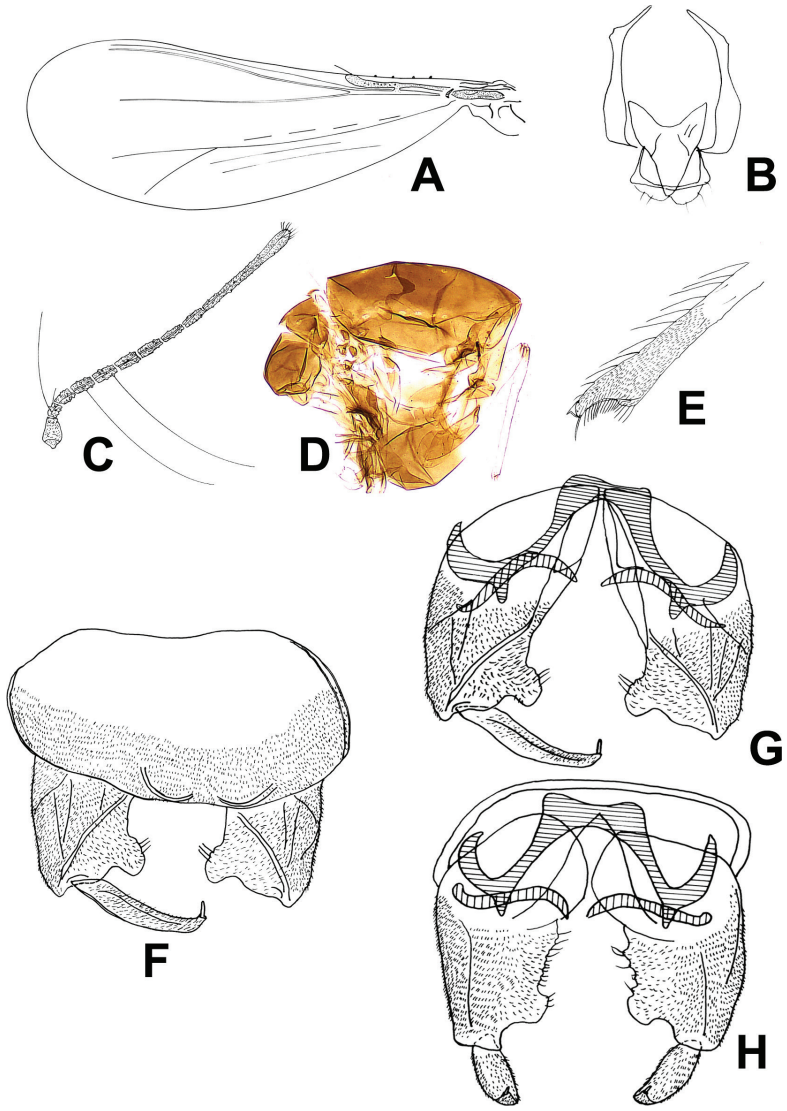

Figure 2. *Corynoneura gibbera* sp. nov., male imago. **A** wing **B** tentorium and cibarial pump **C** antenna **D** thorax **E** hind tibial apex **F** hypopygium, dorsal view **G, H** hypopygium, ventral view.

Diagnostic characters. The male imago is characterized by having an antenna with nine or ten flagellomeres, AR 0.43–0.57, 0.52; superior volsella triangular; inferior volsella prominent, like a small rectangle, and placed caudally of gonocoxite; transverse sternapodeme inverted U-shaped; phallapodeme scalpel-like, in caudal position of sternapodeme.

Description. Adult male (*N* = 7). Total length 0.82–1.10, 0.95 mm. Wing length 0.45–0.66, 0.57 mm. Total length/wing length ratio 1.67–1.82, 1.70. Wing length/profemur length ratio 2.32–3.04, 2.79.

Table 2. Lengths (in μm) and proportions of legs segments of male *Corynoneura gibbera* sp. nov. (*N* = 7).

	fe	ti	ta_1	ta_2	ta_3	ta_4
P_1	194–225, 208	225–255,245	120–146,131	70–82, 73	38–46,42	19–22, 20
P_2	265–323,297	245–284, 265	144–176, 162	65–79, 72	34–36, 35	14–19, 17
P_3	225–265, 243	235–284, 255	120–146, 132	70–77, 75	29–31, 30	17–19, 18
	ta_5	LR	BV	SV	BR	
P_1	26–31, 29	0.51–0.56,0.53	3.35–3.75, 3.55	3.32–3.68, 3.48	1.30–2.20, 1.70	
P_2	26–31, 29	0.59–0.62, 0.61	4.61–4.88, 4.74	3.40–4.16, 3.64	1.50–2.20, 1.80	
P_3	26–31, 29	0.51–0.54, 0.52	3.91–4.46, 4.15	3.56–3.92, 3.76	2.00–2.20, 2.10	

Coloration. Head brown, with dark brown eyes; thorax dark brown; legs yellowish; tergites I-V yellowish, VI-IX brownish.

Head. Antenna with nine or ten flagellomeres, AR 0.43–0.57, 0.52, ultimate flagellomere 98–144, 124 μm long, slightly expanded apically, with many short apical sensilla chaetica (Fig. 2C). Tentorium and cibarial pump as in Figure 2B, tentorium 101–120, 110μm long; 10–26, 15 μm wide; stipes 48–55, 52 μm long, 2–4, 3 μm wide. Anterior margin of cibarial pump strongly concave. Clypeus with 8–10, 9 setae. Length of palpomeres (in μm): 10–12, 11; 12–14, 13; 14–19, 17; 22–26, 24; 32–53, 44. Palpomere 5/3 ratio: 1.71–2.82, 2.14.

Thorax (Fig. 2D). Four or five dorsocentral setae. Scutellum with two setae. One or two prealar setae.

Wing (Fig. 2A). VR 3.0. Cu/wing length ratio 0.44–0.48, 0.46; costa 151–157, 155 μm long, with five or six setae; Cu 255–275, 260 μm long; wing width/wing length ratio 0.38–0.44, 0.42.

Legs. Fore trochanter with dorsal keel. Spurs of fore tibia 17–24, 19 μm long and 7–12, 10 μm long, spurs of mid tibia 7–10, 8 and 10–12, 11 μm long, and spurs of hind tibia 22–29, 24 μm long and 12–14, 13 μm long. Width of fore tibia at apex 17–22, 19 μm, of mid tibia 12–19, 15 μm, of hind tibia (a) 17–24, 22 μm. Width of hind tibia $^1/_3$ from apex (d) 17–22, 20 μm, elongation length (b) 31–43, 36 μm, length of maximum thickening (c_1) 60–72, 66 μm, total length of thickening (c_2) 84–120, 95 μm; hind tibial ratios: a/d 1.41–2.00, 1.60; b/d 1.41–2.39, 2.10; c_1/d 2.73–4.00, 3.75; c_2/d 3.83–6.67, 5.62. Hind tibia expanded, with comb of 15–19, 16 setae, with S-shaped spur (Fig. 2E). Lengths and other proportions of legs as in Table 2.

Hypopygium (Fig. 2F-H). Tergite IX medially slightly incurved. Superior volsella triangular, with rounded margin. Inferior volsella prominent, rectangular, placed caudally. Phallapodeme scalpel-like, apically curved, 31–36, 34 μm long, in caudal position of sternapodeme. Transverse sternapodeme 17–26, 21 μm wide, with oral projection, inverted U-shaped. Gonostylus relatively long and slender, curved tapering, 26–29, 28 μm long; megaseta 4–5 μm long. HR 2.24–2.48, 2.38; HV 3.15–3.79, 3.39.

Remarks. This species is closely related to *Corynoneura macula* Fu & Sæther, 2012 by having similarly shaped inferior volsella and an inverted U-shaped sternapodeme. The new species can be separated from the latter by having AR 0.43–0.57, 0.52, gonostylus relatively long and slender, apically curved, while *C. macula* has a yellowish antenna

with a dark brown apical spot, AR 0.27–0.37, and the gonostylus is relatively short and strongly curved. The new species is also similar to *Corynoneura aurora* Makarchenko & Makarchenko, 2010 by having similar inferior volsella, the same shaped sternapodeme and phallapodeme, but differs from the latter by the antenna having 12 flagellomeres, and the gonostylus being slightly convex on the outer edge in *C. aurora.*

***Corynoneura incuria* Fu, sp. nov.**
http://zoobank.org/D06DACE6-EDDD-4172-90AC-E9589D535DAD
Figures 3, 4

Type material. ***Holotype*** male (HNU: 17090903HJL), China: Hunan Province, Huaihua City, Hecheng County, Wushui River, Xiyi Bridge, 29°33'29"N, 109°57'41"E, 259 m a. s. l., 23.VII.2016, light trap, leg. Jingli Huang. ***Paratype*:** 1 female (HNU:17091205HJL), CHINA: Hunan Province, Loudi City, Xinhua County, Xihe Town, Cushi Village, 27°51'45"N, 111°31'51"E, 315 m a. s. l., 29.VII.2016, sweep net, leg. Jingli Huang.

Etymology. From Latin, *incuria*, neglect, referring to the inferior volsella being absent and fused with the inner margin of gonocoxite.

Diagnostic characters. The male imago is characterized by having antenna with eleven flagellomeres, AR 0.31; anterior margin of cibarial pump strongly concave; superior volsella developed and with right-angled corner; inferior volsella almost absent, fused with the inner margin of gonocoxite; transverse sternapodeme curved into U-shaped; phallapodeme scalpel-like, apical slightly curved, placed caudal position of sternapodeme. The female imago is characterized by coxosternapodeme with a single transparent, well-developed lamella.

Description. Ault male (*N* = 1). Total length 1.08 mm. Wing length 0.63 mm. Total length/wing length ratio 1.70.

Coloration. Head and thorax brown, eyes dark brown. Legs pale yellow. Abdominal tergites I-V yellowish, VI-IX yellow-brown.

Head. Antenna with eleven flagellomeres, AR 0.31, ultimate flagellomere 96 μm long, slightly expanded apically, with many apical sensilla chaetica (Fig. 3C). Tentorium and cibarial pump as in Figure 3B, tentorium 120 μm long; 12 μm wide. Anterior margin of cibarial pump strongly concave. Palpomeres lost.

Thorax (Fig. 3E). Five dorsocentral setae. Scutellum with two setae.

Wing (Fig. 3A). VR 3.2. Cu/wing length ratio 0.52; Costa 175 μm long, with five setae; Cu 245 μm long; wing width/wing length ratio 0.49.

Legs. Fore trochanter with dorsal keel. Spurs of fore tibia 12 μm long and 7 μm long, spurs of mid tibia 7 and 9 μm long, and spurs of hind tibia 31 μm long and 10 μm long. Width of fore tibia at apex 17 μm, of mid tibia 17 μm, of hind tibia (a) 36 μm. Width of hind tibia $^{1}/_{3}$ from apex (d) 19 μm, elongation length (b) 38 μm, length of maximum thickening (c_1) 60 μm, total length of thickening (c_2) 103 μm; hind tibial

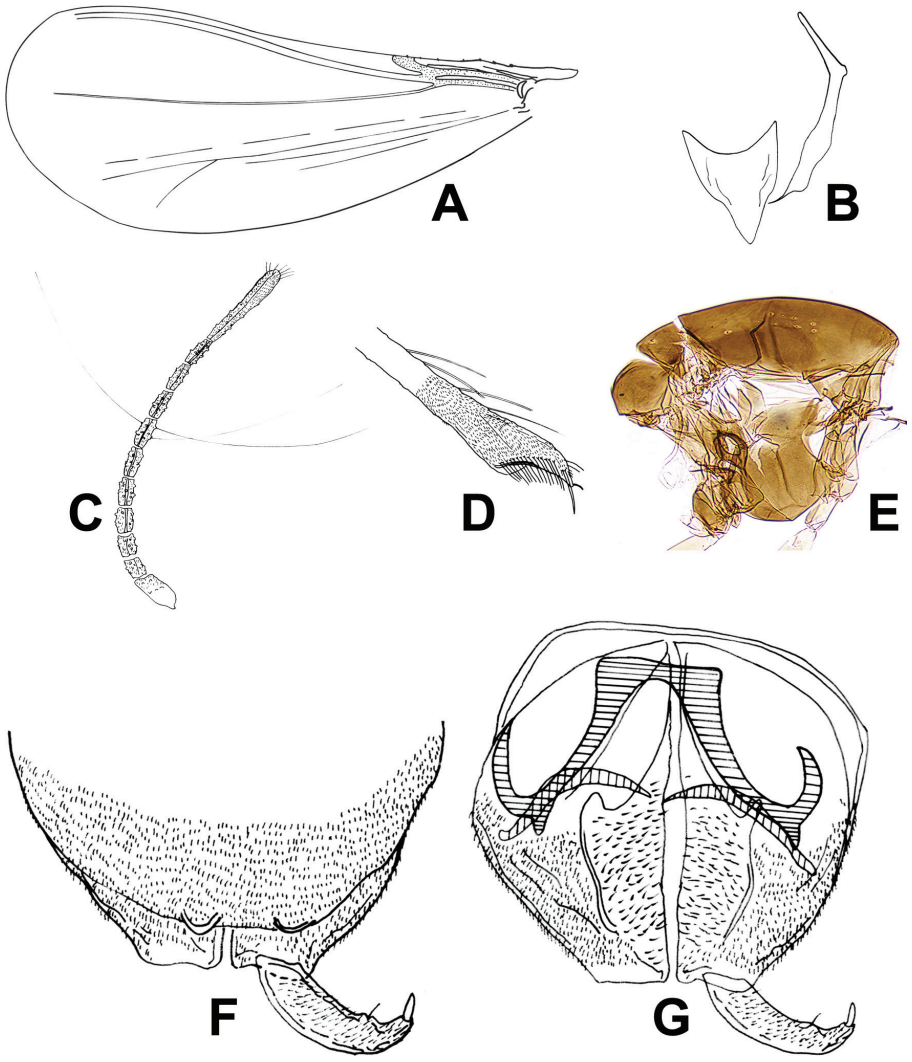

Figure 3. *Corynoneura incuria* sp. nov., male imago. **A** wing **B** tentorium and cibarial pump **C** antenna **D** legs **E** thorax **F** hypopygium, dorsal view **G** hypopygium, ventral view.

ratios: a/d 1.89; b/d 2.00; c_1/d 3.16; c_2/d 5.42. Hind tibia expanded, with comb of 16 setae, with S-shaped spur (Fig. 3D). Lengths and proportions of legs as in Table 3.

Hypopygium (Fig. 3F-G). Tergite IX very developed, almost covering the gonocoxite, medially distinctly incurved. Superior volsella with right-angled corner and triangle, and anteromedially separated. Inferior volsella fused with inner margin of gonocoxite bearing many glandular setae. Phallapodeme scalpel-like, apex slightly curved, 31 μm long, and joined with sternapodeme placed caudally. Transverse sternapodeme 14 μm wide, inverted U-shaped with small oral projection, lateral

Table 3. Lengths (in μm) and proportions of legs segments of male *Corynoneura incuria* sp. nov. (*N* = 1).

	fe	ti	ta_1	ta_2	ta_3	ta_4	ta_5	LR	BV	SV	BR
P_1	228	255	134	72	41	22	26	0.53	3.83	3.60	1.90
P_2	323	265	158	73	34	16	28	0.60	4.96	4.35	2.00
P_3	255	265	134	77	31	17	31	0.51	4.19	3.88	2.00

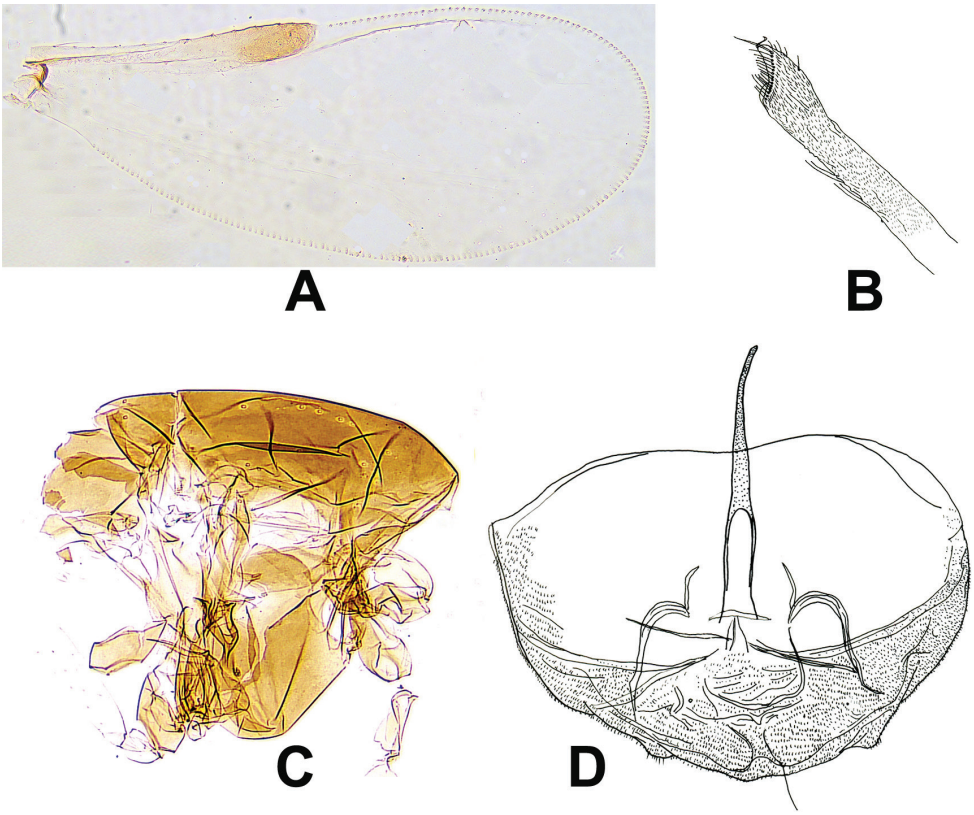

Figure 4. *Corynoneura incuria* sp. nov., female imago. **A** wing **B** hind tibial apex **C** thorax **D** genitalia.

sternapodeme with small attachment point placed and directed caudally. Gonostylus curved, tapering, 23 μm long; megaseta 4 μm long. HR 2.77; HV 4.15.

Adult female (*N* = 1). Total length 0.83 mm. Wing length 0.59 mm. Total length/wing length ratio 1.41. Wing length/profemur length ratio 3.61.

Coloration. Head, eyes, and thorax brown. Legs pale yellow. Abdomen yellowish brown.

Head. Tentorium 72 μm long; 7 μm wide. Clypeus with four setae.

Thorax (Fig. 4C). Five dorsocentral setae. Scutellum with two setae. Two prealar setae.

Wing (Fig. 4A). Wing broader than in male. VR 2.5. Cu 305 μm long; Cu/wing length ratio 0.52; C 265 μm long; C/wing length ratio 0.45; wing width/wing length ratio 0.49. Costa with 13 setae.

Table 4. Lengths (in μm) and proportions of legs segments of female *Corynoneura incuria* sp. nov. (*N* = 1).

	fe	ti	ta_1	ta_2	ta_3	ta_4	ta_5	LR	BV	SV	BR
P_1	183	214	106	65	36	17	26	0.50	3.35	3.56	2.50
P_2	314	230	146	67	31	17	24	0.63	4.96	3.73	1.70
P_3	199	216	113	70	27	17	24	0.52	3.83	3.67	1.80

Legs. Fore trochanter with dorsal keel. Spurs of fore tibia 10 μm long, spurs of mid tibia 7 and 12 μm long, and spurs of hind tibia 22 μm and 12 μm long. Width fore tibia at apex of 17 μm, of mid tibia 14 μm, of hind tibia (a) 29 μm. Width of hind tibia $^1/_3$ from apex (d) 22 μm, elongation length (b) 31 μm, length of maximum thickening (c_1) 60 μm, total length of thickening (c_2) 96 μm; hind tibial ratios: a/d 1.32; b/d 1.41; c_1/d 2.72; c_2/d 4.36. Hind tibia expanded, with comb of 14 setae, with S-shaped spur (Fig. 4B). Lengths and other proportions of legs as in Table 4.

Genitalia (Fig. 4D). Tergite IX without long caudal setae. Cercus 26 μm long, 23 μm wide. Notum length 96 μm. Coxosternapodeme with a single transparent well-developed lamella. Seminal capsule 40 μm long, neck 8 μm long, 6 μm wide.

Remarks. This species is closely related to *Corynoneura tokarapequea* Sasa & Suzuki, 1995 by having antenna with eleven flagellomeres, the same shaped sternapodeme and phallapodeme, and a similar gonostylus. The new species can be separated from the latter by having AR 0.31, the inferior volsella almost absent and fused with the inner margin of the gonocoxite, while *C. tokarapequea* has AR 0.62–0.70, the inferior volsella obvious and near rectangular. The new species is also similar to *Corynoneura floridaensis* Fu & Sæther, 2012 by the antenna with eleven flagellomeres, AR 0.36, same shaped sternapodeme and phallapodeme, but differs from the latter by having a thick transverse sternapodeme, and the gonostylus is strongly curved in *C. floridaensis*.

Corynoneura longshanensis **Fu, sp. nov.**

http://zoobank.org/DAFBB15F-09EE-46EA-B6AC-6DBCDE0C3673

Figure 5

Type material. ***Holotype*** male (HNU: 17091204HJL), China: Hunan Province, Loudi City, Lianyuan County, Longshan National Forest Park, 27°31'20"N, 111°45'23"E, 674 m a. s. l., 26.VII.2016, sweep net, leg. Jingli Huang.

Etymology. Named after the type locality.

Diagnostic characters. The male imago is characterized by having an antenna with seven flagellomeres, AR 0.55; superior volsella undeveloped, and inferior volsella with right-angular corner, fused with the inner margin of gonocoxite; sternapodeme inverted U-shaped; phallapodeme scalpel-like, apical curved, in caudal position of sternapodeme.

Description. Adult male (*N* = 1). Total length 0.92 mm. Wing length 0.45 mm. Total length/wing length 2.04.

Coloration. Head and thorax brown, legs and abdomen yellowish.

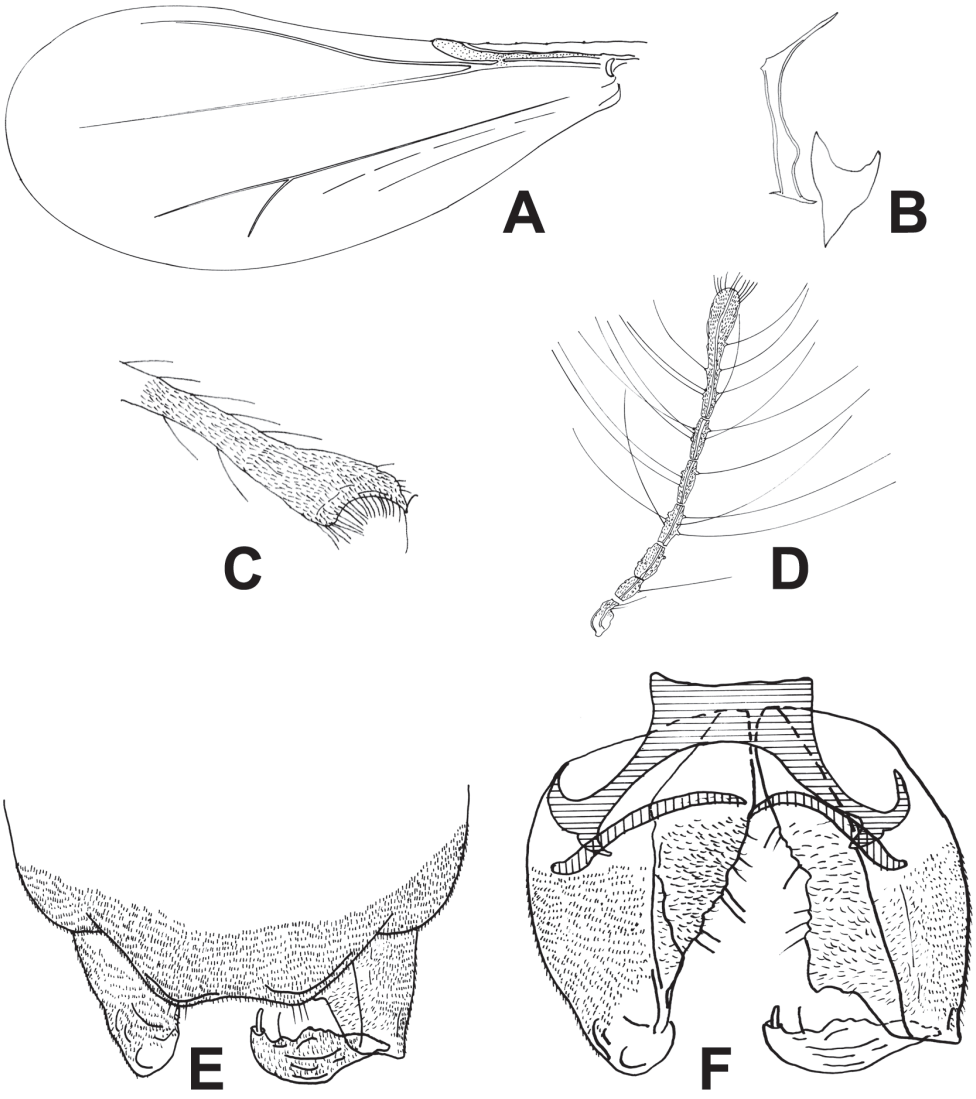

Figure 5. *Corynoneura longshanensis* sp. nov., male imago. **A** wing **B** tentorium and cibarial pump **C** hind tibial apex **D** antenna **E** hypopygium, dorsal view **F** hypopygium, ventral view.

Head. Antenna with seven flagellomeres, AR 0.55, ultimate flagellomere 89 μm long, ultimate flagellomere distinctly expanded apically, with about 10 apical sensilla chaetica (Fig. 5D). Tentorium and cibarial pump as in Figure 5B, tentorium 96 μm long; 10 μm wide. Anterior margin of cibarial pump strongly concave. Length of palpomeres (in μm): 10; 12; 12; 17; 24. Palpomere 5/3 ratio: 2.0.

Thorax. Five dorsocentral setae. Scutellum with two setae.

Wing (Fig. 5A). VR 3.1. Cu/wing length 0.51; Costa 100 μm long, with five setae; Cu 230 μm long; wing width/wing length ratio 0.47.

Table 5. Lengths (in μm) and proportions of legs segments of male *Corynoneura longshanensis* sp. nov. (*N* = 1).

	fe	ti	ta_1	ta_2	ta_3	ta_4	ta_5	LR	BV	SV	BR
P_1	160	180	106	48	26	16	24	0.59	3.91	3.21	1.90
P_2	209	182	110	48	24	14	22	0.60	4.64	3.55	1.70
P_3	175	199	91	50	19	12	24	0.46	3.86	4.11	1.80

Legs. Fore legs lost. Spurs of mid tibia 5 μm and 8 μm long, and spurs of hind tibia 19 μm and 10 μm long. Width of mid tibia at apex 14 μm, of hind tibia (a) 29 μm. Width of hind tibia $^1/_3$ from apex (d) 14 μm, elongation length (b) 36 μm, length of maximum thickening (c_1) 60 μm, total length of thickening (c_2) 79 μm; hind tibial ratios: a/d 2.07; b/d 2.57, 2.10; c_1/d 4.29; c_2/d 5.64. Apex of hind tibia obvious expanded, with comb of 16 setae, with S-shaped spur (Fig. 5C). Lengths and proportions of legs as in Table 5.

Hypopygium (Fig. 5E, F). Tergite IX medially slightly incurved. Superior volsella rounded. Inferior volsella with right-angled corner, fused with inner margin of gonocoxite. Phallapodeme 29 μm long, scalpel-like, apex curved, in caudal position of sternapodeme. Transverse sternapodeme 17 μm wide, with small oral projection, inverted U-shape. Gonostylus medially broadened, curved, tapering, 17 μm long; megaseta 5 μm long. HR 2.82; HV 5.40.

Remarks. This new species is similar to *Corynoneura hortonensis* Fu & Sæther, 2012 by having the same shaped sternapodeme and phallapodeme. The new species can be separated from the latter by the broad and thick transverse sternapodeme, and the median part of the gonostylus expanded with a rugged inner edge.

Notes on 16S rDNA analysis

The primary structure of the mitochondrial large ribosomal subunit (16S rDNA) gene is conservative, while the secondary structure shows spiral differences, which are more suitable for systematic studies of species and genera (Simon et al.1994; Harrison 2004). This gene has been successful in identification of chironomids (Cranston et al. 2002; Ekrem et al. 2010). A neighbor-joining tree (Fig. 6) based on 16S rDNA sequences has been proven effective for quickly delimiting and identifying specimens, and supports differentiation of the new species. This study is the first to use 16S rDNA for auxiliary delimitation and identification of specimens in the genus *Corynoneura*.

Discussion

The four new species referred in this study share the same morphological features: a transverse sternapodeme inverted U-shape, and the attachment point for the phallapodeme is placed in a caudal position of the sternapodeme. According to Fu et al. (2009), these new species belong to the *celeripes* species group. Additionally, short DNA fragments have been shown to play an important role in the definition of

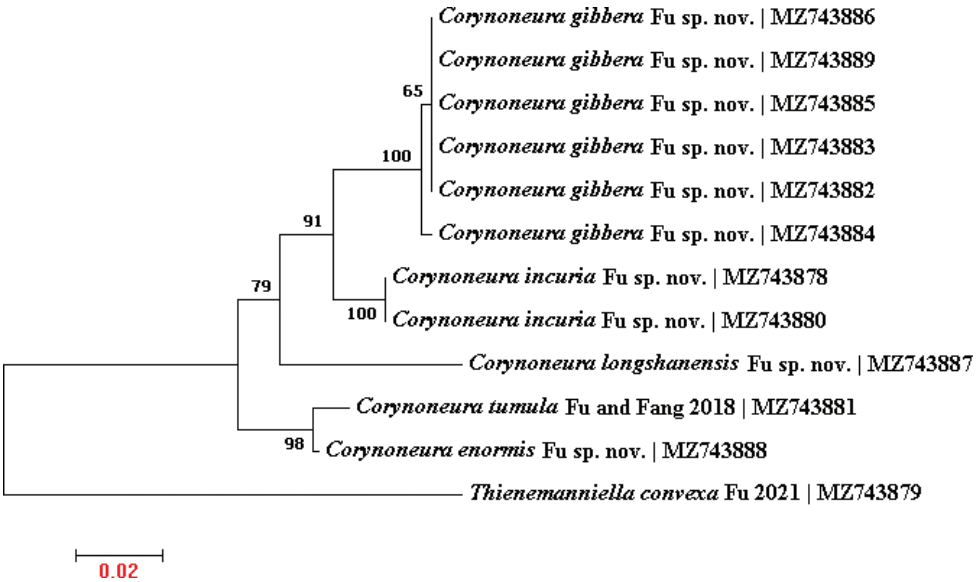

Figure 6. Neighbor-joining Kimura 2 parameter tree based on 16S rDNA of five *Corynoneura* species and *Thienemanniella convexa* Fu in Fang et al. (2021). Numbers on branches refer to the percentage of replicate trees in which the associated taxa clustered together in the bootstrap test (500 replicates). Taxa names include scientific names and GenBank accession numbers of corresponding 16S rDNA.

morphospecies (Hebert et al. 2004; Sharkey et al. 2021). In this study, 16S rDNA was used to match male and female individuals from different collections. A similarity of 100% was considered as the same species: thus, the female of *C. incuria* sp. nov. was successfully matched with the male by 16S rDNA.

Acknowledgements

The project was supported by the National Natural Science Foundation of China (NSFC) (Grant No. 32070483, 31101624, 31460572), Natural Science Foundation of Hubei Province (Grant No. 2020CFB757), Scientific Research Starting Foundation for Ph. D. of Huanggang Normal University (Grant No.2020010), Huanggang Normal University Team Project (4022019006).

References

Ashe P, O'Connor JP (2012) A world catalogue of Chironomidae (Diptera). Part 2. Orthocladiinae. Irish Biogeographical Society, National Museum of Ireland, Dublin, 968 pp.

Cranston P, Edward D, Cook L (2002) New status, species, distribution records and phylogeny for australian mandibulate chironomidae (diptera). Australian Journal of Entomology, 41(4): 357–366. https://doi.org/10.1046/j.1440-6055.2002.00304.x

Ekrem T, Willassen E, Stur E (2010) Phylogenetic utility of five genes for dipteran phylogeny: a test case in the Chironomidae leads to generic synonymies. Molecular Phylogenetics and Evolution 57(2): 561–571. https://doi.org/10.1016/j.ympev.2010.06.006

Fang XL, Wang XH, Xiao YL, Fu Y (2021) *Thienemanniella* convexa (Diptera, Chironomidae), a new species from Hunan Province, China. Annales Zoologici Fennici 59: 29–33. https://doi.org/10.5735/086.059.0103

Fu Y, Sæther OA (2012) *Corynoneura* Winnertz and *Thienemanniella* Kieffer from the Nearctic region (Diptera: Chironomidae: Orthocladiinae). Zootaxa 3536: 1–61. https://doi.org/10.11646/zootaxa.3536.1.1

Fu Y, Fang XL, Wang XH (2019) Taxonomy of *Corynoneura* Winnertz (Diptera: Chironomidae), Science Press & Academic Press, 343 pp. https://doi.org/10.1016/c2017-0-02369-8

Fu Y, Liu T, Fang XL, Wang Q, Wang XH (2018) Three new species of *Corynoneura* Winnertz from Oriental China (Diptera: Chironomidae: Orthocladiinae). Zootaxa 4418(1): 085–092. https://doi.org/10.11646/zootaxa.4418.1.5

Fu Y, Sæther OA, Wang XH (2009) *Corynoneura* Winnertz from East Asia, with a systematic review of the genus (Diptera: Chironomidae: Orthocladiinae). Zootaxa 2287: 1–44. https://doi.org/10.11646/zootaxa.2287.1.1

Fu Y, Wang XH, Fang XL, Xiao YL, Fu J, Lin XL (2020) *Corynoneura* Winnertz (Diptera, Chironomidae, Orthocladiinae) from Zhejiang Province, China. Zootaxa 4890(1): 083–096. https://doi.org/10.11646/zootaxa.4890.1.4

Harrison JS (2004) Evolution, biogeography, and the utility of mitochondrial 16s and COI genes in phylogenetic analysis of the crab genus *Austinixa* (Decapoda: Pinnotheridae). Molecular Phylogenetics and Evolution 30(3): 743–754. https://doi.org/10.1016/S1055-7903(03)00250-1

Hebert PDN, Penton EH, Burns JM, Janzen DH, Halwachs W (2004) Ten species in one: DNA barcoding reveals cryptic species in the neotropical skipper butterfly Astraptes fulgerator. Proceedings of the National Academy of Sciences of the United States of America 101: 14812–14817. https://doi.org/10.1073/pnas.0406166101

Makarchenko EA, Makarchenko MA, Semenchenko AA (2019) Towards the taxonomy of *Corynoneura* Winnertz (Diptera: Chironomidae: Orthocladiinae) from the Russian Far East and Eastern Siberia. Zootaxa 4612(2): 221–236. https://doi.org/10.11646/zootaxa.4612.2.5

Moubayed-Breil J (2015) *Corynoneura* tyrrhena sp. n., a crenophilous species occurring in high mountain streams of Corsica (Diptera, Chironomidae, Orthocladiinae). Ephemera 16(1): 1–12.

Sæther OA (1969) Some Nearctic Podonominae, Diamesinae and Orthocladiinae (Diptera: Chironomidae). Bulletin of the Fisheries Research Board of Canada 170: 1–154.

Sæther OA (1980) Glossary of Chironomid morphology terminology (Diptera: Chironomidae). Entomologica Scandinavica Supplement 14: 1–51.

Schlee D (1968) Vergleichende Merkmalsanalyse zur Morphologie und Phylogenie der *Corynoneura*-Gruppe (Diptera: Chironomidae). Zugleich eine allgemeine Morphologie der Chironomiden-Image (♂). Stuttgarter Beiträge zur Naturkunde 180: 1–150.

Sharkey MJ, Janzen DH, Hallwachs W, Chapman EG, Smith MA, Dapkey T, Brown A, Ratnasingham S, Naik S, Manjunath R, Perez K, Milton M, Hebert P, Shaw S, Kittel R, Solis M, Metz M, Goldstein P, Brown J, Quicke D, Achterberg C, Brown B, Burns JM (2021) Minimalist revision and description of 403 new species in 11 subfamilies of Costa Rican

braconid parasitoid wasps, including host records for 219 species. Zookeys 1013: 1–665. https://doi.org/10.3897/zookeys.1013.55600

Simon C, Frati F, Beckenbach A, Crespi B, Liu H, Flook P (1994) Evolution, weighting, and phylogenetic utility of mitochondrial gene sequences and a compilation of conserved polymerase chain reaction primers. Annals of the Entomological Society of America 87: 651–701. https://doi.org/10.1093/aesa/87.6.651

Wiedenbrug S, Trivinho-Strixino S (2011) New species of the genus *Corynoneura* Winnertz (Diptera, Chironomidae) from Brazil. Zootaxa 2822: 1–40. https://doi.org/10.11646/zootaxa.2822.1.1

Wiedenbrug S, Lamas CE, Trivinho-Strixino S (2012) A review of the genus *Corynoneura* Winnertz (Diptera: Chironomidae) from the Neotropical region. Zootaxa 3574: 1–61. https://doi.org/10.11646/zootaxa.3574.1.1

Winnertz J (1846) Beschreibung einiger neuer Gattungen aus der Ordnung der Zweiflügler. Stettiner entomologische Zeitung 7: 11–20.

ZooKeys 1082: 103–125 (2022)
doi: 10.3897/zookeys.1082.69851
https://zookeys.pensoft.net

RESEARCH ARTICLE

A peer-reviewed open-access journal
ZooKeys
Launched to accelerate biodiversity research

Surprisingly high genetic divergence of the mitochondrial DNA barcode fragment (COI) within Central European woodlice species (Crustacea, Isopoda, Oniscidea)

Michael J. Raupach[1], Björn Rulik[2], Jörg Spelda[3]

1 *Sektion Hemiptera, Bavarian State Collection of Zoology (SNSB – ZSM), Münchhausenstraße 21, 81247 München, Germany* **2** *Department Arthropoda, Zoologisches Forschungsmuseum Alexander Koenig, Adenauerallee 160, 53113 Bonn, Germany* **3** *Bavarian State Collection of Zoology (SNSB – ZSM), Münchhausenstraße 21, 81247 München, Germany*

Corresponding author: Michael J. Raupach (raupach@snsb.de)

Academic editor: Stefano Taiti | Received 8 June 2021 | Accepted 20 December 2021 | Published 20 January 2022

http://zoobank.org/5EF93E90-4AE6-484F-92AD-4D4FE228DC13

Citation: Raupach MJ, Rulik B, Spelda J (2022) Surprisingly high genetic divergence of the mitochondrial DNA barcode fragment (COI) within Central European woodlice species (Crustacea, Isopoda, Oniscidea). ZooKeys 1082: 103–125. https://doi.org/10.3897/zookeys.1082.69851

Abstract

DNA barcoding has become the most popular approach for species identification in recent years. As part of the German Barcode of Life project, the first DNA barcode library for terrestrial and freshwater isopods from Germany is presented. The analyzed barcode library included 38 terrestrial (78% of the documented species of Germany) and five freshwater (63%) species. A total of 513 new barcodes was generated and 518 DNA barcodes were analyzed. This analysis revealed surprisingly high intraspecific genetic distances for numerous species, with a maximum of 29.4% for *Platyarthrus hoffmannseggii* Brandt, 1833. The number of BINs per species ranged from one (32 species, 68%) to a maximum of six for *Trachelipus rathkii* (Brandt, 1833). In spite of such high intraspecific variability, interspecific distances with values between 12.6% and 29.8% allowed a valid species assignment of all analyzed isopods. The observed high intraspecific distances presumably result from phylogeographic events, *Wolbachia* infections, atypical mitochondrial DNAs, heteroplasmy, or various combinations of these factors. Our study represents the first step in generating an extensive reference library of DNA barcodes for terrestrial and freshwater isopods for future molecular biodiversity assessment studies.

Keywords

Asellota, cytochrome *c* oxidase subunit I (COI), freshwater, German Barcode of Life (GBoL), mitochondrial DNA, molecular specimen identification, *Platyarthrus hoffmannseggii*

Introduction

Isopods are a highly diverse group of invertebrates, with more than 10,300 species described to date (Boyko et al. 2008; Poore 2012). Most of these peracarid crustaceans are free-living, but a number of marine species represent bizarre ectoparasites that infest crustacean and fish species (e.g., Raupach and Thatje 2006; Williams and Boyko 2012; Hadfield et al. 2014; Smit et al. 2014). Isopods range in body length from 0.5 mm (members of the family Microcerberidae) up to 500 mm (species of the famous giant deep-sea isopod genus *Bathynomus* Milne-Edwards, 1879) (McClain et al. 2015). With more than 4,500 known marine species to date, isopods can be found from all shorelines of the world down to the abyssal depths of the oceans where asellote isopods have undergone a massive radiation and represent the dominant taxon (e.g., Wilson and Hessler 1987; Wägele 1989; Raupach et al. 2004, 2009). Approximately 900 isopod species colonized freshwater habitats including lakes, rivers, underground waters, and even thermal springs (e.g., Verovnik et al. 2005; Wilson 2008).

Isopods are, however, not restricted to the aquatic realms only. One group, the Oniscidea or woodlice, are the most successful group of crustaceans that invaded the land by far. Without doubt, these animals represent the most familiar and well-known group of isopods to humans. In contrast to other amphibious crustaceans, e.g., land crabs of the family Geocarcinidae or terrestrial hermit crabs of the genus *Coenobita* Latreille, 1829, no developmental stage (egg, juvenile, etc.) of the Oniscidea requires free water and all biological activities are conducted on land (e.g., Broly et al. 2013). The Oniscidea have evolved a number of unique adaptations, such as the water conducting system, various forms of pleopodal lungs and the cotyledons in the marsupium (e.g., Sfenthourakis and Taiti 2015). Based on the dorsal surface of their exoskeleton, various other morphological traits as well as ecological strategies and behavior, woodlice can be roughly categorized in three main groups (Schmalfuss 1984; Hornung 2011): i) the runners, characterized with an elongate, slightly convex body and long pereopods (e.g., *Philoscia* Latreille, 1804), ii) the clingers, with a flat broad body and short but strong pereopods (e.g., *Platyarthrus* Brandt, 1833), and iii) the rollers, with a highly convex body able to roll up into a ball (pill bugs) (e.g., *Armadillidium* Brandt, 1833) (Fig. 1). Whereas their dispersion ability is rather limited, woodlice are found in almost all biomes of the world except the poles and high mountain ranges (Hornung 2011; Sfenthourakis and Taiti 2015). A hot spot of woodlice diversity is located in the Mediterranean region (Sfendourakis and Taiti 2015), and some species have been introduced to other parts of the world by humans in the past, e.g., to North America (Jass and Klausmeier 2000; Singer et al. 2012; Hornung et al. 2015) and other regions (e.g., Gruner 1966; Slabber and Chown 2002; Karasawa and Nakata 2018). Furthermore, oniscid isopods are amongst the most common and species-rich components of cave-dwelling animal groups with high numbers of troglobitic species (Sfenthourakis and Taiti 2015). In some ecosystems, e.g., European forests, woodlice

Figure 1. Various woodlouse species of Germany **A** *Oniscus asellus* Linnaeus, 1758 **B** *Armadillidium nasatum* Budde-Lund, 1885 **C** *Trachelipus ratzeburgii* (Brandt, 1833) **D** *Mesonicus alpicola* (Heller, 1858) **E** *Philoscia muscorum* (Scopoli, 1763) **F** *Haplophthalmus mariae* Strouhal, 1953 **G** *Armadillidium opacum* (C. Koch, 1841) **H** *Platyarthrus hoffmannseggii* Brandt, 1833. Scale bar: 1 mm. Photograph credits: **A–G** Jörg Spelda **H** Armin Rose.

perform a central role in the decomposition, being largely phytosaprophagous and often occur in very high population densities (e.g., Dias and Hassall 2005; Gongalsky et al. 2005; Hättenschwiler et al. 2005; David 2014; Špaldoňová and Frouz 2014), but also act as important prey for a broad range of predatory arthropods (Raupach 2015). Until now, more than 3,700 species of oniscid isopods have been described worldwide (Schmidt 2008; Sfenthourakis and Taiti 2015). For Germany, 49 species of terrestrial and eight species of freshwater isopods are reported so far (Grünwald 2016).

Since its beginning almost 15 years ago, the concept of DNA barcoding for species identification has revolutionized biodiversity research (Valentini et al. 2009; Cristescu 2014). For many groups of animals, an approximate 650 base pair (bp) fragment of the mitochondrial cytochrome *c* oxidase subunit I (COI) gene was selected as marker of choice (Hebert et al. 2003a). The efficiency of DNA barcoding is based on a simple assumption: each species will most likely have similar DNA barcode sequences representing their intraspecific variability whereas the genetic variation between species exceeds the variation within species (Hebert et al. 2003a, 2003b). In this context, the German Barcode of Life initiative (GBoL; www.bolgermany.de) aims at capturing the genetic diversity of animals, fungi, and plants of Germany. Various comprehensive barcode libraries of arthropods, e.g., marine crustaceans (Raupach et al. 2015), spiders (Astrin et al. 2016), and myriapods (Spelda et al. 2011), have been generated in the past. In terms of isopods, most DNA barcoding studies focused on marine species so far (e.g., Khalaji-Pirbalouty and Raupach 2014, 2016; Raupach et al. 2015; ; Brix et al. 2018; Chew et al. 2018; Kakui et al. 2019), whereas for terrestrial and freshwater taxa almost no studies do exist (Asmyhr and Cooper 2012; Zimmermann et al. 2015, 2018a, 2018b). However, no comprehensive DNA barcode reference library has been published for these taxa until now.

In this study we present the first DNA barcode library of terrestrial and freshwater isopods with a focus on Central European species, with a specific emphasis on the Oniscidea. The analyzed barcode library includes 38 terrestrial (78% of the known species of Germany) and five freshwater (63%) species. In summary, 513 new barcodes were generated and a total number of 518 DNA barcodes was analyzed.

Materials and methods

Sampling of specimens

Samples used for this study were collected between 2000 and 2018 by pitfall traps, sieves, or by hand. Specimens were stored in ethanol (96%) and identified by two of the authors (MJR, JS) using a combination of keys provided in Schmölzer (1964), Gruner (1966), Hopkin (1991), and Berg and Wijnhoven (1997). In total, 513 new DNA barcodes of 46 species were generated. For our analysis we also included five DNA barcodes of the sea slater *Ligia oceanica* (Linnaeus, 1767) as part of a previous study (Raupach et al. 2010), generating a total data set of 518 DNA barcodes from 46 species. Five of

the analyzed species, *Armadillidium album* Dollfus, 1887 (*n* = 1, Spain), *Armadillidium granulatum* Brandt, 1833 (*n* = 2, France), *Ligia italica* Fabricius, 1798 (*n* = 2, Italy), *Porcellionides sexfasciatus* (Budde-Lund, 1885) (*n* = 4, Mallorca, Spain), and *Tylos ponticus* Grebnitzky, 1874 (*n* = 1, Spain) are not recorded from Germany so far but were included for comparison. The number of analyzed specimens per species ranged from one (5 species) to a maximum of 57 for *Porcellio scaber* Latreille, 1804. Most isopods were collected in Germany (*n* = 458, 88.3%), whereas some specimens from other countries were included: Austria (3, 0.6%), Denmark (4, 0.8%), France (3, 0.6%), Italy (3, 0.6%), Luxembourg (38, 7.3%), Spain (6, 1.2%), and Switzerland (3, 0.6%).

DNA barcode amplification, sequencing, and data depository

Laboratory operations were carried out either at the Canadian Center for DNA Barcoding (CCDB), University of Guelph, following standardized protocols for COI amplification and sequencing (Ivanova et al. 2006; deWaard et al. 2008), the molecular lab rooms of the German Centre of Marine Biodiversity Research (DZMB), Senckenberg am Meer, in Wilhelmshaven, the working group Systematics and Evolutionary Biology at the Carl von Ossietzky University Oldenburg, or the Zoologisches Forschungsmuseum Alexander Koenig (ZFMK), Bonn, all located in Germany. Photographs were taken for each studied isopod before molecular work was performed. One or two legs of one body side were removed for the subsequent DNA extraction. For some very small isopods with a body length < 3 mm, e.g., specimens of *Haplopthalmus* Schöbl, 1860 or *Jaera* Leach, 1814, partial or complete specimens were used for DNA extraction. In the case of own molecular studies, DNA was extracted using the QIAmp Tissue Kit (Qiagen GmbH, Hilden, Germany) or NucleoSpin Tissue Kit (Macherey-Nagel, Düren, Germany), following the extraction protocol. Detailed information of used primers, PCR amplification and sequencing protocols are given in previous publications (see Raupach et al. 2015; Astrin et al. 2016). All purified PCR products were cycle-sequenced and sequenced in both directions at a contract sequencing facility (GATC, Konstanz, Germany), using the same primers as used in PCR. Double stranded sequences were assembled and checked for putative mitochondrial pseudogenes (numts) by analyzing the presence of stop codons, frameshifts as well as double peaks in chromatograms with the Geneious version 8.1.9 software package (Biomatters, Auckland, New Zealand) (Kearse et al. 2012). For sequence verification, BLAST searches (nBLAST, search set: others, program selection: megablast) were performed to confirm the identity of all new sequences as isopod sequences based on already published sequences (high identity values, very low E-values) (Zhang et al. 2000; Morgulis et al. 2008).

Comprehensive voucher information, taxonomic classifications, photos, DNA barcode sequences, used primer pairs and trace files including their quality are publicly accessible through the public data set "DS-BISCE" (Dataset ID: dx.doi.org/10.5883/DS-BISCE) on the Barcode of Life Data Systems (BOLD; www.boldsystems.org) (Ratnasingham and Hebert 2007). Parallel to this, all new barcode data were deposited in GenBank (accession numbers MN810569–MN810873, MT521085–MT521292).

DNA barcode analysis

Following a standardized approach of DNA barcode analysis, the BOLD workbench was used to calculate the nucleotide composition of the sequences and distributions of Kimura-2-parameter distances (K2P; Kimura 1980) within and between species (align sequences: BOLD aligner; ambiguous base/gap handling: pairwise deletion). All barcodes became subject of the Barcode Index Number (BIN) system as it is implemented in BOLD (2020–06–05). In doing so, DNA barcodes are clustered in order to produce operational taxonomic units that closely correspond to species (Ratnasingham and Hebert 2013). Using the given default settings, a recommended threshold of 2.2% was applied for a rough differentiation of intraspecific and interspecific K2P distances (Ratnasingham and Hebert 2013). It should be noted, however, that the BIN assignments on BOLD may change due to the addition of new sequences. Therefore, individual BINs can be split or merged in the light of new data (Ratnasingham and Hebert 2013).

A neighbor-joining cluster analysis (NJ; Saitou and Nei 1987) was performed for all studied species for a graphical representation of the genetic differences between sequences and clusters of sequences using MEGA 10.0.5 (Kumar et al. 2018). Again, the K2P model was chosen as the model for sequence evolution for comparison purposes with previous studies. For validation, non-parametric bootstrap support values were obtained by resampling and analyzing 1,000 replicates (Felsenstein 1985). All analyses were based on an alignment of all studied barcode sequences that was generated using MUSCLE (Edgar 2004) implemented in MEGA 10.0.5. It should be explicitly noted that this analysis is not intended to be phylogenetic. Instead of this, the shown topology represents a graphical visualization of DNA barcode divergences/distances and putative species cluster.

Results

We analyzed 518 DNA barcode sequences of 46 isopod species. A list of species is presented in the supporting information (Suppl. material 1). Fragment lengths of the analyzed DNA barcodes ranged from 407 to 658 bp. As previously shown for arthropods, the DNA barcode region was characterized by a high AT-content: average sequence compositions were A = 24.6%, C = 18.1%, G = 21.5%, and T = 35.8%. Fourteen (30.4%) species had intraspecific distances > 2.2%, with a maximum of 29.4% for *Platyarthrus hoffmannseggii* Brandt, 1833. Interspecific distances within the analyzed taxa had values between 12.6% (*Armadillidium granulatum* Brandt, 1833; *Armadillidium versicolor* Stein, 1859) and 29.8% (*Jaera sarsi* Valkanov, 1936; *Armadillidium nasatum* Budde-Lund, 1885). In total, 76 BINs were found. The number of BINs per species ranged from one (32 species, 68%) to a maximum of six (*Trachelipus rathkii* (Brandt, 1833)). No BIN sharing between species was observed. The NJ analyses revealed non-overlapping clusters with bootstrap support values > 95% for 39 species (95%) with more than one studied specimen (Fig. 2). A more detailed topology of all analyzed specimens is presented in the supporting information (Suppl. material 2).

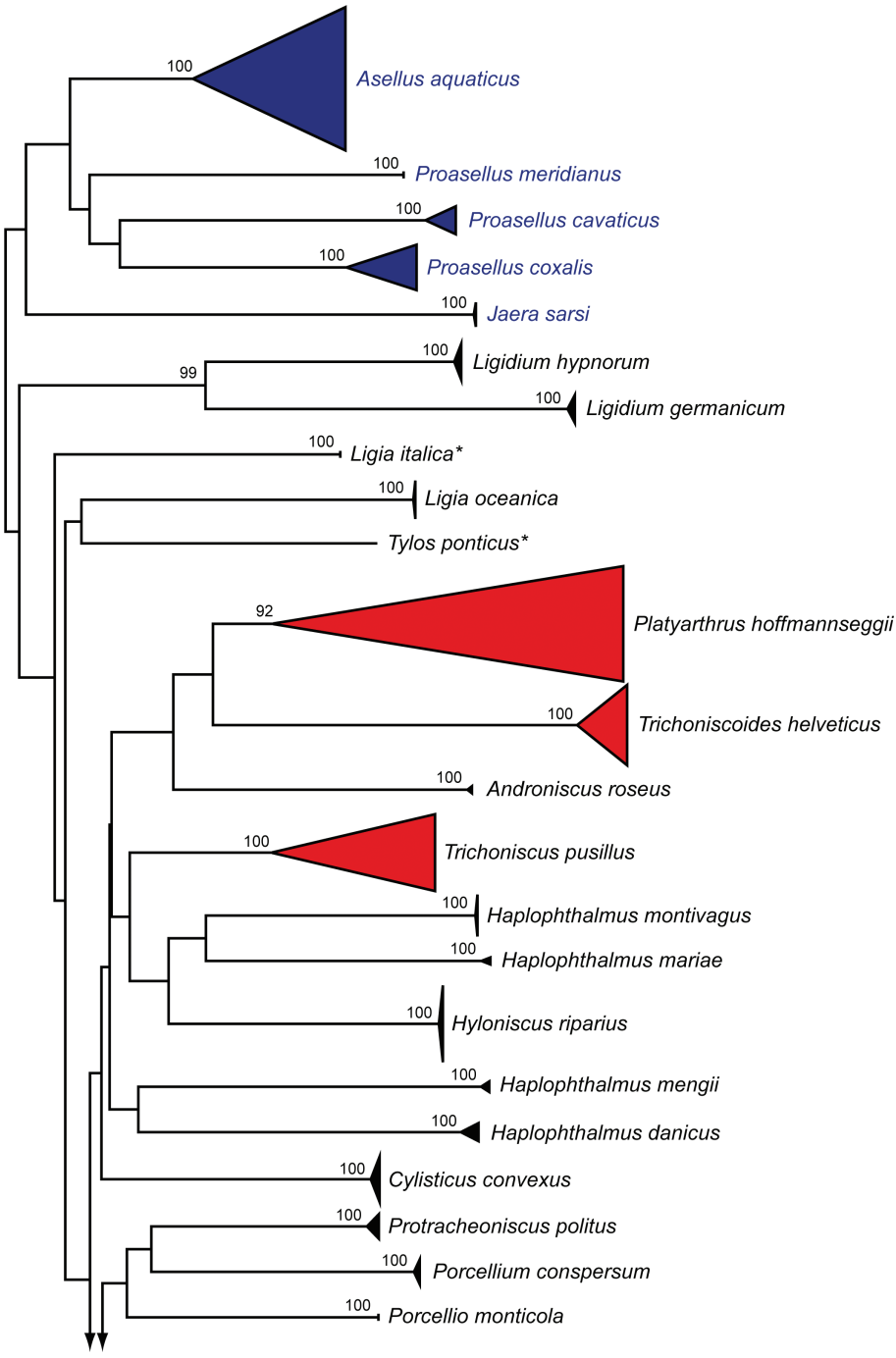

Figure 2. Neighbor-joining (NJ) topology of the analyzed isopod species based on Kimura 2-parameter distances. Triangles show the relative number of individual's sampled (height) and sequence divergence (width). Red triangles highlight terrestrial species with intraspecific maximum pairwise distances > 2.2%, whereas dark blue triangles indicate freshwater species with such distances. Numbers next to nodes represent non-parametric bootstrap values > 90% (1,000 replicates). Asterisks indicate species not recorded in Germany.

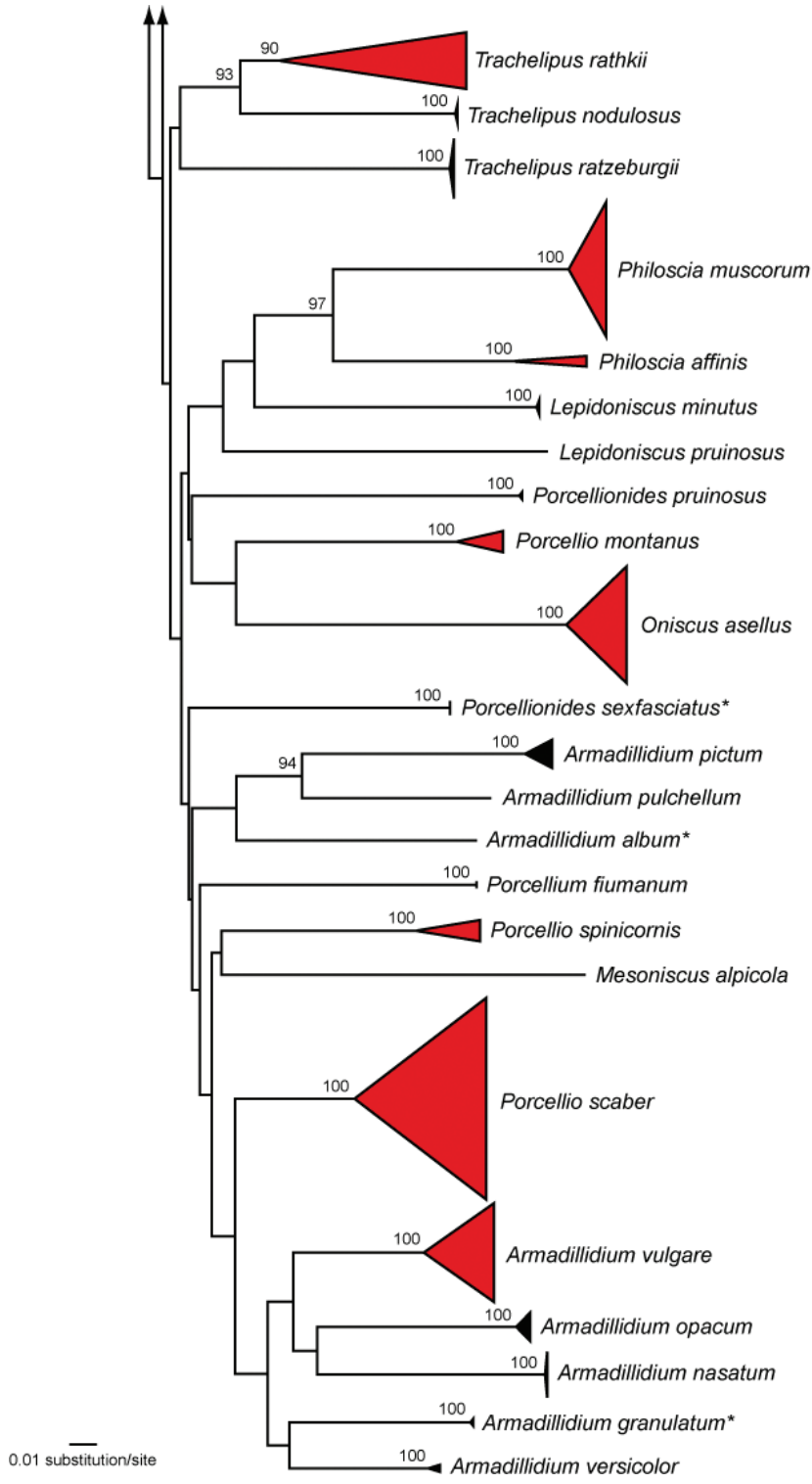

Figure 2. Continued.

Discussion

Our study revealed very high intraspecific distances for numerous woodlice species (Tab. 1), including abundant and well-known species as *Porcellio scaber* Latreille, 1804 (maximum intraspecific distances (ISD): 12.16) or *Trachelipus rathkii* (Brandt, 1833) (max ISD: 13.47). Intraspecific distance values higher than 2.2% were also shown for three of the five analyzed freshwater species (Tab. 1). The observed high variability can be caused by a number of different factors and will be discussed in the following.

First, phylogeographic events may generate different haplotypes and distinct mitochondrial lineages. In the case of European woodlice species, numerous studies showed complex phylogeographic patterns correlated with high variability of the studied mitochondrial markers including COI, e.g., for species of the genus *Alpioniscus* Racovitza, 1908 (Bedek et al. 2019), the common sea slater *Ligia oceanica* (Linneaus, 1767) (Raupach et al. 2014), *Ligidium* spp. (Klossa-Kilia et al. 2005), the common woodlouse *Oniscus asellus* Linnaeus, 1758 (Bilton et al. 1999), *Orthometopon* spp. (Poulakakis and Sfenthourakis 2008), *Helleria brevicornis* Ebner, 1868 (Gentile et al. 2010), or two species of the genus *Trachelipus* Budde-Lund, 1908 (Parmakelis et al. 2008). Similar results have been also demonstrated for freshwater isopods of the genus *Asellus* Geoffroy, 1762 (Verovnik et al. 2004; Verovnik et al. 2005; Sworobowicz et al. 2015; Pérez-Moreno et al. 2017) and *Proasellus* Dudich, 1925 (Ketmaier 2002; Eme et al. 2013; Kilikowska et al. 2013). Our data set revealed extremely high intraspecific distance values for the myrmecophilous isopod *Platyarthrus hoffmannseggii* Brandt, 1833 (n = 33), with a maximum value of 29.4% (Tab. 1). It is a small, white, and blind oniscid isopod that is widely-distributed in Europe and strictly associated with various ant species (e.g., Mathes and Strouhal 1954; Gruner 1966; Parmentier et al. 2017). A few other species are found in the Mediterranean region, e.g., *Platyarthrus schoebli* Budde-Lund, 1879 (Garci and Cruz 1986), which can be easily differentiated from *Platyarthrus hoffmannseggii*. The NJ topology revealed three distinct lineages associated with three BINs (Fig. 3), but no clear correlation of the analyzed specimens to specific sampling regions. Furthermore, we found no ant-host-specific correlation of the observed lineages. For some other species distinct lineages were also detected, but no conspicuous substructures were revealed (see Suppl. material 3).

Second, the presence of the inherited alpha-proteobacteria *Wolbachia* Hertig, 1936 can affect the mitochondrial variability in arthropods (e.g., Hurst and Jiggins 2005; Werren et al. 2008; Correa and Ballard 2016). These endosymbionts are transmitted vertically through host eggs and alter the biology of their host in various ways, including the induction of reproductive manipulations, such as feminization, parthenogenesis, male killing and sperm-egg incompatibility (Werren et al. 2008). If a population is infected by *Wolbachia*, patterns of mitochondrial polymorphisms will be altered by natural selection that acts on these symbionts, either increasing or decreasing the frequency distribution of haplotypes within a population (Hurst and Jiggins 2005). Previous studies documented high infection rates of *Wolbachia* within many terrestrial as well as freshwater isopod species (e.g., Bouchon et al. 1998; Rigaud et al. 1999; Cordaux et al. 2012), including numerous species that have been analyzed in this study, e.g., *Platyarthrus hoffmannseggii*, *Porcellio scaber*, and *Trachelipus rathkii*. However, it is

Table 1. Molecular distances based on the Kimura 2-parameter model of the analyzed specimens of the analyzed isopod species with intraspecific distances > 2.2% using the BOLD work bench. ISD = intraspecific distance. BINs are based on the barcode analysis from 05–06–2020. See methods for explanation of basis.

Species	*n*	BINs	Mean ISD	Max ISD
Armadillidium vulgare (Latreille, 1804)	28	AAE6611, AAH4108, AAH4111, AAU1529	3.76	6.44
Asellus aquaticus (Linnaeus, 1758)	41	ACF1266, AEC4774, AAA1970	4.25	13.37
Oniscus asellus (Linnaeus, 1758)	33	ADM8743, ADM8116, ADK9123	2.12	5.63
Philoscia affinis Verhoeff, 1908	3	ADM8125, AAY1058	3.63	5.44
Philoscia muscorum (Scopoli, 1763)	38	AAH4103, AAH4104	0.3	2.98
Platyarthrus hoffmannseggii Brandt, 1833	33	AAV8050, AAV8051, ADK9658	9.4	29.35
Porcellio montanus Budde-Lund, 1885	6	ADR0694, ADM7742	1.26	3.81
Porcellio scaber Latreille, 1804	57	AAC3755, AAZ0248, ABA5892, ADK8850, ADM8147	2.58	12.16
Porcellio spinicornis Say, 1818	6	ADF7011, ADI3596	3.01	5.13
Proasellus cavaticus (Leydig, 1871)	8	ADX3790, ADW6988, ADX4659	1.61	2.95
Proasellus coxalis (Dollfus, 1892)	13	ACI1746, ACH7545	2.81	5.78
Trachelipus rathkii (Brandt, 1833)	16	AAH4102, ADK8699, ADK8533, ADM8087, ADM8088, ADF6188	6.89	16.59
Trichoniscoides helveticus (Carl, 1908)	23	ADM7247, ADM7248, ADM7249	1.07	5.46
Trichoniscus pusillus Brandt, 1833	22	AAN7523, AAZ1993	6.8	13.47

very difficult to distinguish demographic variation from symbiont-induced effects of mitochondrial variability (see Hurst and Jiggins 2005).

Third, the amplification and sequencing of nuclear mitochondrial pseudogenes (numts) can obscure the true mitochondrial variability within a species (Bensasson et al. 2001). Numts are nonfunctional copies of mitochondrial DNA in the nuclear genome. As consequence of reduced selection pressure, nucleotide substitutions and insertions as well as deletions may introduce stop codons and shifts in the reading frame of these inactive copies (Buhay 2009; Schizas 2012). Various studies documented such numts for a number of different crustacean taxa (e.g., Buhay 2009; Baeza and Fuentes 2013; Kim et al. 2013). For isopods, however, numts have not been reported so far, and a careful inspection of our COI sequences revealed no double peaks and translation without stop codons.

Fourth, many oniscid species, e.g., *Armadillidium vulgare* (Latreille, 1804), *Cylisticus convexus* (De Geer, 1778), or *Philoscia muscorum* (Scopoli, 1763), are characterized by atypical mitochondrial DNA structures that are composed of linear monomers and circular dimers, generating different mitochondrial lineages (Doublet et al. 2012, 2013). There is also a possible link between such atypical mitochondrial DNAs and heteroplasmy (i.e., the mixture of mtDNA genotypes within an organism) which has been documented for various woodlice in the past (Doublet et al. 2008, 2012). However, only a few studies are available until now, and most details still remain unclear.

Finally, distinct mitochondrial lineages that correlate with high genetic distances can give evidence for the existence of currently overseen cryptic species. Considering the previous discussed aspects, however, additional morphological and/or nuclear DNA sequence data are essential for a verification of truly distinct lineages. For freshwater and terrestrial isopods, a few studies demonstrated such integrative taxonomic approaches (McGaughran et al. 2005; Santamaria et al. 2017; Santamaria 2019). In terms of the analyzed taxa, no previous studies discussed the existence of cryptic species, and all specimens were checked and determined carefully before molecular works started.

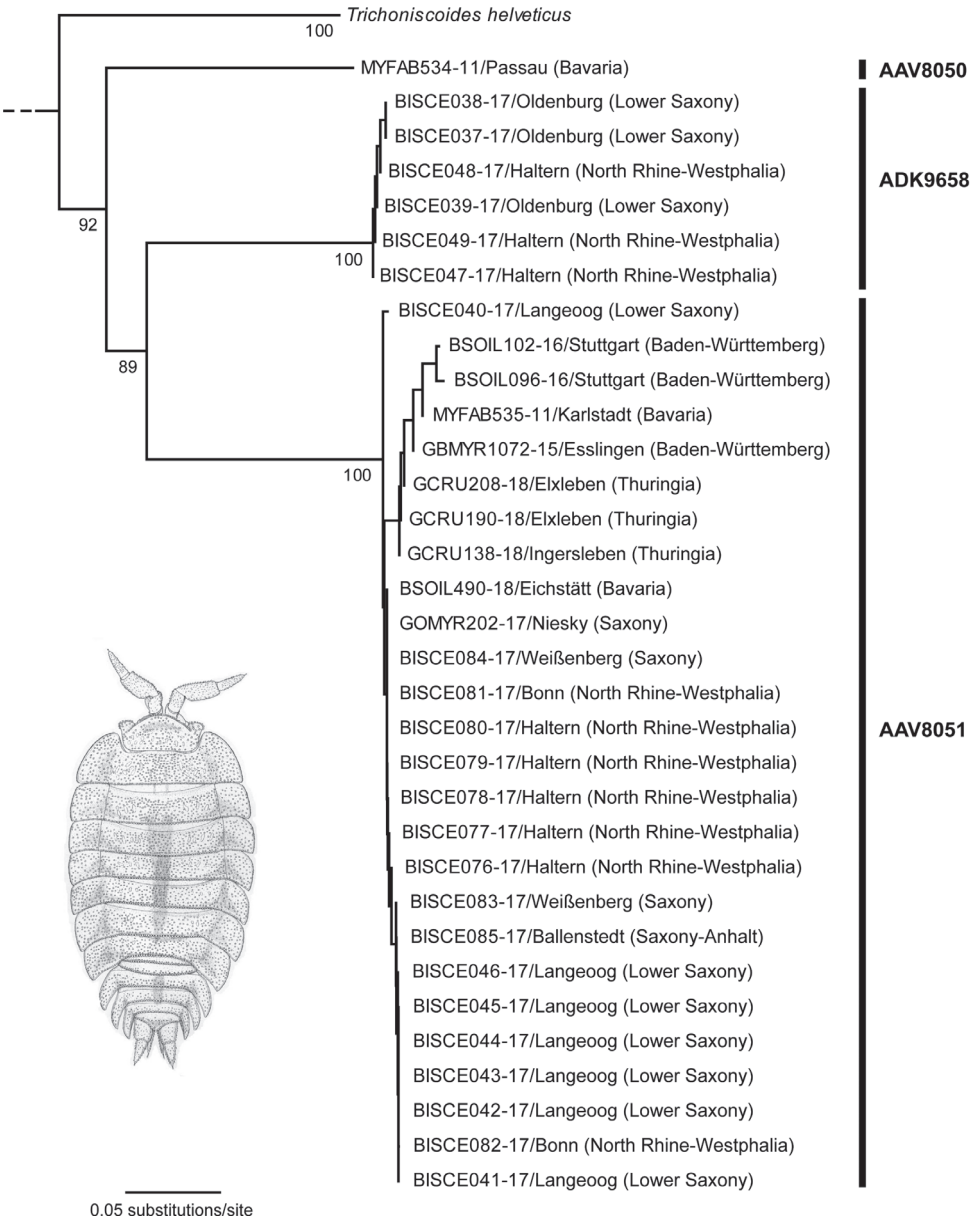

Figure 3. Subtree of the Neighbor-joining topology based on Kimura 2-parameter distances of all analyzed specimens of *Platyarthrus hoffmannseggii* Brandt, 1833 and nearest neighbor. Branches with specimen ID-number from BOLD and sample localities. Numbers next to internal nodes are non-parametric bootstrap values (in %) with values higher than 80. BIN values are based on the barcode analysis from 05-06-2020. The isopod drawing by Christian Schmidt was obtained from Raupach (2005).

Based on the given data we are currently unable to clarify the reasons of the observed high intraspecific variability within some of the analyzed species in detail. We suggest, however, that the detected high distances result from i) phylogeographic

effects, ii) *Wolbachia* infections, iii) atypical mitochondrial DNAs and/or heteroplasmy, or, most likely, iv) various combinations of these phenomena in many cases. More specimens from different geographic regions as well as additional nuclear markers should be analyzed to verify this in detail. Despite these high intraspecific distances and multiple BINs for some species, however, high interspecific distances in combination with monophyletic lineages allow a correct determination of all studied taxa.

Conclusions

The development of new sequencing technologies changed biological science significantly. As a consequence, DNA-based approaches have become more and more popular for the assessment of biodiversity and identification of specimens. Parallel analysis of thousands of specimens, bulk samples (metabarcoding) or environmental DNA (eDNA) will become routinely used techniques in modern species diversity assessment studies (e.g., Shokralla et al. 2012; Moriniere et al. 2016; Brauckmann et al. 2019; Hardulak et al. 2020). Whereas hypervariable regions of nuclear rRNA genes or other mitochondrial gene fragments may represent useful markers for such studies (e.g., Mohrbeck et al. 2015; Gillet et al. 2018; Lopez-Escardo et al. 2018), COI has become the most popular and efficient marker of choice (e.g., Andujar et al. 2018; Curry et al. 2018; Brauckmann et al. 2019; Hausmann et al. 2020). All these approaches, however, rely highly on comprehensive on-line reference libraries of correctly identified specimens (e.g., Brandon-Mong et al. 2015; Creer et al. 2016; Staats et al. 2016). Ideally, such libraries include sequence data of a species` complete distribution range that can provide additional information of phylogeographic substructures that are well-known for many species (e.g., Gentile et al. 2010; Raupach et al. 2014; Paill et al. 2021).

The necessity of DNA barcode reference libraries is also important for the modern molecular-based analysis of soil biodiversity (Taberlet et al. 2012; Orgiazzi et al. 2014; Rota et al. 2020). Reference libraries have been already published for a variety of typical soil-inhabiting taxa, e.g., earthworms (Porco et al. 2013; Pansu et al. 2015; Sun et al. 2018), mites (Young et al. 2012; Young et al. 2019), springtails (Hogg and Hebert 2004; Porco et al. 2013), spiders (Astrin et al. 2016), myriapods (Spelda et al. 2011) and ground beetles (Raupach et al. 2016; Raupach et al. 2018). In our present study we lay the foundations for a comprehensive DNA barcode data set for terrestrial and freshwater isopods of Central Europe.

Acknowledgements

We would like to thank Laura von der Mark, Jana Thormann (both ZFMK, Bonn) and Jana Deppermann (DZMB, Wilhelmshaven) for their laboratory assistance. Furthermore, we are very grateful to numerous persons that provided and/or identified specimens, including Jürgen Becker, Ernst-Gerhard Burmeister, Moritz Fahldiek, Guido

Haas, Günter Hansbauer, Dietrich von Knorre, Martin Lemke, Andrea Männl, Dirk Mattern, Ole Stan Møeller, Ioanna Salvarina, Christian Schmidt, Sabine Schmidt-Halewicz, Wolfgang Pankow, Wolfgang Scharl, Christoph Schubart, Karl-Heinz Schwamberger, Bernhard Seifert, Bärbel Vogel, Dieter Weber, Alexander Weigand, Thomas Wesener, Tobias Windmaisser, Stefan Zaenker, and others. Further, not yet used material was provided by Christian Owen (Wales), Karen Wilkinson, Roy Anderson, David Bilton, and Steve Gregory as well as Peter Hofmann and Andreas Wolf. We are also grateful to Armin Rose for giving his permission to use his photo of *Platyarthrus hoffmannseggii*. This publication was partially financed by German Federal Ministry for Education and Research (FKZ01LI1101A, FKZ01LI1101B, FKZ03F0664A), the Land Niedersachsen and the German Science Foundation (INST427/1–1), as well as by grants from the Bavarian State Government (BFB) and the German Federal Ministry of Education and Research (GBOL2, GBOL3: 01LI1901B). We are grateful to the team of Paul Hebert in Guelph (Ontario, Canada) for great support and assistance, and in particularly to Sujeevan Ratnasingham for developing the BOLD database infrastructure and the BIN management tools. Sequencing work was partly supported by funding from the Government of Canada to Genome Canada through the Ontario Genomics Institute, whereas the Ontario Ministry of Research and Innovation and NSERC supported development of the BOLD informatics platform. Finally, the authors would like to express their gratitude to Lanna Cheng for useful comments on improving language and style.

References

Andujar C, Arribas P, Yu DW, Vogler AP, Emerson BC (2018) Why the COI barcode should be the community DNA metabarcode for the Metazoa. Molecular Ecology 27: 3968–3975. https://doi.org/10.1111/mec.14844

Asmyhr MG, Cooper SJB (2012) Difficulties barcoding in the dark: the case of crustacean stygofauna from eastern Australia. Invertebrate Systematics 26: 583–591. https://doi.org/10.1071/IS12032

Astrin JJ, Höfer H, Spelda J, Holstein J, Bayer S, Hendrich L, Huber BA, Kielhorn K-H, Krammer H-J, Lemke M, Monje JC, Morinière J, Rulik B, Petersen M, Janssen H, Muster C (2016) Towards a DNA barcode reference database for spiders and harvestmen of Germany. PLoS ONE 11: e0162624. https://doi.org/10.1371/journal.pone.0162624

Baeza JA, Fuentes MS (2013) Exploring phylogenetic informativeness and nuclear copies of mitochondrial DNA (numts) in three commonly used mitochondrial genes: mitochondrial phylogeny of peppermint, cleaner, and semi-terrestrial shrimps (Caridea: *Lysmata*, *Exhippolysmata*, and *Merguia*). Zoological Journal of the Linnean Society 168: 699–722. https://doi.org/10.1111/zoj.12044

Bedek J, Taiti S, Bilhandžija H, Ristori E, Baratti M (2019) Molecular and taxonomic analyses in troglobiotic *Alpioniscus* (*Illyrionethes*) species from the Dinaric Karst (Isopoda: Trichoniscidae). Zoological Journal of the Linnean Society 187: 539–584. https://doi.org/10.1093/zoolinnean/zlz056

Bensasson D, Zhang D-X, Hartl DL, Hewitt GM (2001) Mitochondrial pseudogenes: evolution`s misplaced witnesses. Trends in Ecology and Evolution 16: 314–321. https://doi.org/10.1016/S0169-5347(01)02151-6

Berg MP, Wijnhoven H (1997) Landpissebedden. Een tabel voor de landpissebedden (Crustacea; Oniscidea) van Nederland en België. Wetenschappelijke Mededelingen van de KNNV 221: 1–80. [In Dutch]

Bilton DT, Goode D, Mallet J (1999) Genetic differentiation and natural hybridization between two morphological forms of the common woodlouse, *Oniscus asellus* Linnaeus 1758. Heredity 82: 462–469. https://doi.org/10.1038/sj.hdy.6885170

Bouchon D, Rigaud T, Juchault P (1998) Evidence for widespread *Wolbachia* infection in isopod crustaceans: molecular identification and host feminization. Proceedings of the Royal Society Series B: Biological Sciences 265: 1081–1090. https://doi.org/10.1098/rspb.1998.0402

Boyko CB, Bruce NL, Hadfield KA, Merrin KL, Ota Y, Poore GCB, Taiti S, Schotte M, Wilson GDF (2008 onwards) World marine, freshwater and terrestrial isopod crustaceans database. http://www.marinespecies.org/isopoda [Accessed 2020–06–05]

Brandon-Mong GJ, Gan HM, Sing KW, Lee PS, Lim PE, Wilson JJ (2015) DNA metabarcoding of insects and allies: an evaluation of primers and pipelines. Bulletin of Entomological Research 105: 717–727. https://doi.org/10.1017/S0007485315000681

Brauckmann TWA, Ivanova NV, Prosser SWJ, Elbrecht V, Steinke D, Ratnasingham S, deWaard JR, Sones JE, Zakharov EV, Hebert PDN (2019) Metabarcoding a diverse arthropod mock community. Molecular Ecology Resources 19: 711–727. https://doi.org/10.1111/1755-0998.13008

Brix S, Bober S, Tschesche C, Kihara T-C, Driskell A, Jennings RM (2018) Molecular species delimitation and its implications for species descriptions using desmosomatid and nannoniscid isopods from the VEMA fracture zone as example taxa. Deep Sea Research Part II: Topical Studies in Oceanography 148: 180–207. https://doi.org/10.1016/j.dsr2.2018.02.004

Broly P, Deville P, Maillet S (2013) The origin of terrestrial isopods (Crustacea: Isopoda: Oniscidea). Evolution and Ecology 27: 461–476. https://doi.org/10.1007/s10682-012-9625-8

Buhay JE (2009) "COI-like" Sequences are becoming problematic in molecular systematic and DNA Barcoding studies. Journal of Crustacean Biology 29: 96–110. https://doi.org/10.1651/08-3020.1

Chew M, Rahim AbA, binti Mohd Yusof NY (2018) A new species of *Eisothistos* (Isopoda, Cymothoida) and first molecular data on six species of Anthuroidea from the Penninsular Malaysia. Zoosystematics and Evolution 94: 73–81. https://doi.org/10.3897/zse.94.23000

Cordaux R, Pichon S, Hatira HBA, Doublet V, Grève P, Marcadé I, Braquart-Varnier C, Souty-Grosset C, Charfi-Cheikhrouha F, Bouchon D (2012) Widespread *Wolbachia* infection in terrestrial isopods and other crustaceans. In: Štrus J, Taiti S, Sfenthourakis S (Eds) Advances in Terrestrial Isopod Biology. ZooKeys 176: 123–131. https://doi.org/10.3897/zookeys.176.2284

Correa CC, Ballard JWO (2016) *Wolbachia* associations with insects: winning or losing against a master manipulator. Frontiers in Ecology and Evolution 3: e153. https://doi.org/10.3389/fevo.2015.00153

Creer S, Deiner K, Frey S, Porazinska D, Taberlet P, Thomas WK, Potter C, Bik HM (2016) The ecologist`s filed guide to sequence-based identification of biodiversity. Methods in Ecology and Evolution 7: 1008–1018. https://doi.org/10.1111/2041-210X.12574

Cristescu ME (2014) From barcoding single individuals to metabarcoding biological communities: towards an integrative approach to the study of global biodiversity. Trends in Ecology and Evolution 29: 566–571. https://doi.org/10.1016/j.tree.2014.08.001

Curry CJ, Gibson JF, Shokralla S, Hajibabaei M, Baird DJ (2018) Identifying North American freshwater invertebrates using DNA barcodes: Are existing COI sequence libraries fit for purpose? Freshwater Science 37: 178–189. https://doi.org/10.1086/696613

David JF (2014) The role of litter-feeding macroarthropods in decomposition processes: a reappraisal of common views. Soil Biology and Biochemistry 76: 109–118. https://doi.org/10.1016/j.soilbio.2014.05.009

deWaard JR, Ivanova NV, Hajibabaei M, Hebert PDN (2008) Assembling DNA barcodes: analytical protocols. In: Martin C (Ed.) Methods in Molecular Biology: Environmental Genetics. Humana Press, Totowa, 275–293. https://doi.org/10.1007/978-1-59745-548-0_15

Dias N, Hassall M (2005) Food, feeding and growth rates of peracarid macro-decomposers in a Ria Formosa salt marsh, southern Portugal. Journal of Experimental Marine Biology and Ecology 325: 84–94. https://doi.org/10.1016/j.jembe.2005.04.017

Doublet V, Souty-Grosset C, Bouchon D, Cordaux R, Marcadé I (2008) A thirty million year-old inherited heteroplasmy. PLoS ONE 3: e2938. https://doi.org/10.1371/journal.pone.0002938

Doublet V, Raimond R, Grandjean F, Lafitte A, Souty-Grosset C, Marcadé I (2012) Widespread atypical mitochondrial DNA structure in isopods (Crustacea, Peracarida) related to a constitutive heteroplasmy in terrestrial species. Genetics 55: 234–244. https://doi.org/10.1139/G2012-008

Doublet V, Helleu Q, Raimond R, Souty-Grosset C, Marcadé I (2013) Inverted repeats and genome architecture conversions of terrestrial isopods mitochondrial DNA. Journal of Molecular Evolution 77: 107–118. https://doi.org/10.1007/s00239-013-9587-7

Edgar RC (2004) MUSCLE: a multiple sequence alignment method with reduced time and space complexity. BMC Bioinformatics 5: e113. https://doi.org/10.1186/1471-2105-5-113

Eme D, Malard F, Konecny-Dupré L, Lefébure T, Douady CJ (2013) Bayesian phylogeographic inferences reveal contrasting colonization dynamics among European groundwater isopods. Molecular Ecology 22: 5685–5699. https://doi.org/10.1111/mec.12520

Felsenstein J (1985) Confidence limits on phylogenies: an approach using the bootstrap. Evolution 39: 783–791. https://doi.org/10.2307/2408678

Garcia L, Cruz A (1986) Els isopodes terrestres (Crustacea: Isopoda: Oniscidea) de les illes Balears: catalog d`especies. Boletin de la Sociedad de Historia Natural de Baleares 39: 77–99.

Gentile G, Campanaro A, Carosi M, Sbordoni V, Argano R (2010) Phylogeography of *Helleria brevicornis* Ebner 1868 (Crustacea, Oniscidea): Old and recent differentiations of an ancient lineage. Molecular Phylogenetics and Evolution 54: 640–646. https://doi.org/10.1016/j.ympev.2009.10.005

Gillet B, Cottet M, Destanque T, Kue K, Descioux S, Chanudet V, Hughes S (2018) Direct fishing and eDNA metabarcoding for biomonitoring during a 3-year survey significantly improves number of fish detected around a South East Asian reservoir. PLoS ONE 13: e0208592. https://doi.org/10.1371/journal.pone.0208592.

Gongalsky KB, Savin FA, Pokarzhevskii AD, Filimonova ZV (2005) Spatial distribution of isopods in an oak-beech forest. European Journal of Soil Biology 41: 117–122. https://doi.org/10.1016/j.ejsobi.2005.09.012

Gruner HE (1966) 53. Teil: Krebstiere oder Crustacea V. Isopoda 2. Lieferung. In: Die Tierwelt Deutschlands und der angrenzenden Meeresteile, begründet von Professor Dr. Friedrich Dahl. VEB Gustav Fischer Verlag Jena, 1–380. [In German]

Grünwald M (2016) Rote Liste und Gesamtartenliste der Landasseln und Wasserasseln (Isopoda: Oniscidea et Asellota) Deutschlands, 1. Fassung, Stand November 2011. In: Bundesamt für Naturschutz (BfN) (Hrsg.): Rote Liste gefährdeter Tiere, Pflanzen und Pilze Deutschlands; Band 4: Wirbellose Tiere (Teil 2). Naturschutz und Biologische Vielfalt 70(4): 349–363. [In German]

Hadfield KA, Sikkel PC, Smit NJ (2014) New records of fish parasitic isopods of the gill-attaching genus *Mothocya* Costa, in Hope 1851 from the Virgin Islands, Carribean, with description of a new species. ZooKeys 439: 109–125. https://doi.org/10.3897/zookeys.439.8093

Hardulak LA, Moriniere J, Hausmann A, Hendrich L, Schmidt S, Doczkal D, Müller J, Hebert PDN, Haszprunar G (2020) DNA metabarcoding for biodiversity monitoring in a national park: Screening for invasive and pest species. Molecular Ecology Resources 20: 1542–1557. https://doi.org/10.1111/1755-0998.13212

Hättenschwiler S, Tiunov AV, Scheu S (2005) Biodiversity and litter decomposition in terrestrial ecosystems. Annual Review of Ecology, Evolution, and Systematics 36: 191–218. https://doi.org/10.1146/annurev.ecolsys.36.112904.151932

Hausmann A, Segerer A, Greifenstein T, Knubben J, Moriniere J, Bozicevic V, Doczkal D, Günther A, Ulrich W, Habel JC (2020) Towards a standardized quantitative and qualitative insect monitoring scheme. Ecology and Evolution 10: 4009–4020. https://doi.org/10.1002/ece3.6166

Hebert PDN, Cywinska A, Ball SL, deWaard JR (2003a) Biological identifications through DNA barcodes. Proceedings of the Royal Society of London Series B: Biological Sciences 270: 313–321. https://doi.org/10.1098/rspb.2002.2218

Hebert PDN, Ratnasingham S, deWaard JR (2003b) Barcoding animal life: cytochrome *c* oxidase subunit 1 divergences among closely related species. Proceedings of the Royal Society of London Series B: Biological Sciences 270: S96–S99. https://doi.org/10.1098/rsbl.2003.0025

Hogg ID, Hebert PDN (2004) Biological identification of springtails (Hexapoda: Collembola) from the Canadian Arctic, using mitochondrial DNA barcodes. Canadian Journal of Zoology 82: 749–754. https://doi.org/10.1139/z04-041

Hopkin S (1991) A key to the woodlice of Britain and Ireland. Field Studies 7: 599–650.

Hornung E (2011) Evolutionary adaptation of oniscidean isopods to terrestrial life: structure, physiology and behavior. Terrestrial Arthropod Reviews 4: 95–130. https://doi.org/10.1163/187498311X576262

Hornung E, Szlavecz K, Dombos M (2015) Demography of some non-native isopods (Crustacea, Isopoda, Oniscidea) in a Mid-Atlantic forest, USA. In: Taiti S, Hornung E, Štrus J, Bouchon D (Eds) Trends in Terrestrial Isopod Biology. ZooKeys 515: 127–143. https://doi.org/10.3897/zookeys.515.9403

Hurst GDD, Jiggins FM (2005) Problems with mitochondrial DNA as a marker in population, phylogeographic and phylogenetic studies: the effects of inherited symbionts. Proceedings

of the Royal Society Series B: Biological Sciences 272: 1525–1534. https://doi.org/10.1098/rspb.2005.3056

Ivanova NV, deWaard JR, Hebert PDN (2006) An inexpensive, automation-friendly protocol for recovering high-quality DNA. Molecular Ecology Notes 6: 998–1002. https://doi.org/10.1111/j.1471-8286.2006.01428.x

Jass J, Klausmeier B (2000) Endemics and immigrants: North American terrestrial isopods (Isopoda, Oniscidea) North of Mexico. Crustaceana 73: 771–799. https://doi.org/10.1163/156854000504804

Kakui K, Shimomura M, Kimura S, Kimura T (2019) Topotype-based DNA barcode of the parasitic *Pseudione nephropsi* (Bopyridae), with a supplementary morphological description. Species Diversity 24: 103–108. https://doi.org/10.12782/specdiv.24.103

Kamilari M, Klossa-Kilia E, Kilias G, Sfenthourakis S (2014) Old Aegean palaeoevents driving the diversification of an endemic isopod species (Oniscidea, Trachelipodidae). Zoologica Scripta 43: 379–392. https://doi.org/10.1111/zsc.12060

Karasawa S, Nakata K (2018) Invasion stages and potential distributions of seven exotic terrestrial isopods in Japan. BioRisk 13: 53–76. https://doi.org/10.3897/biorisk.13.23514

Kearse M, Moir R, Wilson A, Sone-Havas S, Cheung M, Sturrock S, Buxton S, Cooper A, Markowitz S, Duran C, Thierer T, Ashton B, Meintjes P, Drummond A (2012) Geneious Basic: an integrated and extendable desktop software platform for the organization and analysis of sequence data. Bioinformatics 15: 1647–1649. https://doi.org/10.1093/bioinformatics/bts199

Ketmaier V (2002) Isolation by distance, gene flow and phylogeography in the *Proasellus coxalis*-group (Crustacea, Isopoda) in Central Italy: allozyme data. Aquatic Sciences 64: 66–75. https://doi.org/10.1007/s00027-002-8055-z

Khalaji-Pirbalouty V, Raupach MJ (2014) A new species of *Cymodoce* Leach, 1814 (Crustacea: Isopoda: Sphaeromatidae) from the Persian Gulf based on morphological and molecular characteristics, with a redescription of *Cymodoce tribullis* from Queensland. Zootaxa 3826: 230–254. https://doi.org/10.11646/zootaxa.3826.1.7

Khalaji-Pirbalouty V, Raupach MJ (2016) DNA barcoding and morphological studies confirm the occurrence of three *Atarbolana* (Crustacea: Isopoda: Cirolanidae) species along the coastal zone of the Persian Gulf and Gulf of Oman. Zootaxa 4200: 153–173. https://doi.org/10.11646/zootaxa.4200.1.7

Kilikowska A, Wysocka A, Burzyński A, Kostoski G, Rychlińska J, Sell J (2013) Patterns of genetic differentiation and population history of endemic isopods (Asellidae) from ancient Lake Ohrid: combining allozyme and mtDNA data. Central European Journal of Biology 8: 854–875. https://doi.org/10.2478/s11535-013-0204-y

Kim S-J, Lee KY, Ju S-J (2013) Nuclear mitochondrial pseudogenes in *Austinograea alayseae* hydrothermal vent crabs (Crustacea: Bythograeidae): effects on DNA barcoding. Molecular Ecology Resources 13: 781–787. https://doi.org/10.1111/1755-0998.12119

Kimura M (1980) A simple method for estimating evolutionary rates of base substitutions through comparative studies of nucleotide sequences. Journal of Molecular Evolution 16: 111–120. https://doi.org/10.1007/BF01731581

Klossa-Kilia E, Kilias G, Sfenthourakis S (2005) Increased genetic diversity in Greek populations of the genus *Ligidium* (Crustacea: Isopoda: Oniscidea) revealed by RFLP analysis of mtDNA segments. Contributions to Zoology 74: 255–264. https://doi.org/10.1163/18759866-0740304003

Kumar S, Stecher G, Li M, Knyaz C, Tamura K (2018) MEGA X: Molecular Evolutionary Genetics Analysis across computing platforms. Molecular Biology and Evolution 35: 1547–1549. https://doi.org/10.1093/molbev/msy096

Linsenmair KE (1984) Comparative studies on the social behavior of the desert isopod *Hemilepistus reaumuri* and of a *Porcellio* species. Symposia of the Zoological Society of London 53: 423–453.

Lopez-Escardo D, Paps J, de Vargas C, Massana R, Ruiz-Trillo I, del Campo J (2018) Metabarcoding analysis on European coastal samples reveals new molecular metazoan diversity. Scientific Reports 8: e9106. https://doi.org/10.1038/s41598-018-27509-8

Mathes I, Strouhal H (1954) Zur Ökologie and Biologie der Ameisenassel *Platyarthrus hoffmannseggii* Brandt. Zeitschrift für Morphologie und Ökologie der Tiere 43: 82–93. https://doi.org/10.1007/BF00446232 [In German]

McClain CR, Balk MA, Benfield MC, Branch TA, Chen C, Cosgrove J, Dove ADM, Gaskins LC, Helm RR, Hochberg FG, Lee FB, Marshall A, McMurray SE, Schanche C, Stone SN, Thaler AD (2015) Sizing ocean giants: patterns of intraspecific size variation in marine megafauna. PeerJ 3: e715. https://doi.org/10.7717/peerj.715

McGaughran A, Hogg ID, Stevens MI, Chadderton WL, Winterbourn MJ (2005) Genetic divergence of three freshwater isopod species from southern New Zealand. Journal of Biogeography 33: 23–30. https://doi.org/10.1111/j.1365-2699.2005.01338.x

Mohrbeck I, Raupach MJ, Martinez Arbizu P, Knebelsberger T, Laakmann S (2015) High-throughput sequencing – the key to rapid biodiversity assessment of marine Metazoa? PLoS ONE 10: e0140342. https://doi.org/10.1371/journal.pone.0140342

Morgulis M, Coulouris G, Rayselis Y, Madden TL, Agarwala R, Schäffer AA (2008) Database indexing for production MegaBLAST searches. Bioinformatics 24: 1757–1764. https://doi.org/10.1093/bioinformatics/btn322

Moriniere J, de Arauja BC, Lam AW, Hausmann A, Balke M, Schmidt S, Hendrich L, Doczkal D, Farthmann B, Arvidsson S, Haszprunar G (2016) Species identification in Malaise trap samples by DNA barcoding based on NGS technologies and a scoring matrix. Public Library of Science. PLoS ONE 11: e0155597 https://doi.org/10.1371/journal.pone.0155497

Orgiazzi A, Dunbar MB, Panagos P, de Groot GA, Lemanceau P (2015) Soil biodiversity and DNA barcodes: opportunities and challenges. Soil Biology and Biochemistry 80: 244–250. https://doi.org/10.1016/j.soilbio.2014.10.014

Paill W, Koblmüller S, Friess T, Gereben-Krenn B-A, Mairhuber C, Raupach MJ, Zangl L (2021) Relicts from glacial times: The ground beetle *Pterostichus adstrictus* Eschscholtz, 1823 (Coleoptera: Carabidae) in the Austrian Alps. Insects 12: e84. https://doi.org/10.3390/insects12010084

Pansu J, De Danieli S, Puissant J, Gonzalez J-M, Gielly L, Cordonnier T, Zinger L, Brun J-J, Choler P, Taberlet P, Cécillon L (2015) Landscape-scale distribution patterns of earthworms inferred from soil DNA. Soil Biology and Chemistry 83: 100–105. https://doi.org/10.1016/j.soilbio.2015.01.004

Parmakelis A, Klossa-Kilia E, Kilias G, Triantis KA, Sfenthourakis S (2008) Increased molecular divergence of two endemic *Trachelipus* (Isopoda, Oniscidea) species from Greece reveals patterns not congruent with current taxonomy. Biological Journal of the Linnean Society 95: 361–370. https://doi.org/10.1111/j.1095-8312.2008.01054.x

Parmentier T, Vanderheyden A, Dekoninck W, Wenseleers T (2017) Body size in the ant-associated isopod *Platyarthrus hoffmannseggii* is host-dependent. Biological Journal of the Linnean Society 121: 305–311. https://doi.org/10.1093/biolinnean/blw052

Pérez-Moreno JL, Balázs G, Wilkins B, Herczeg G, Bracken-Grissom HD (2017) The role of isolation on contrasting phylogeographic patterns in two cave crustaceans. BMC Evolutionary Biology 17: e247. https://doi.org/10.1186/s12862-017-1094-9

Porco D, Decaëns T, Derharveng L, James SW, Skarżyński D, Erséus C, Butt KR, Richard B, Hebert PDN (2013) Biological invasions in soil: DNA barcoding as a monitoring tool in a multiple taxa survey targeting European earthworms and springtails in North America. Biological Invasions 15: 899–910. https://doi.org/10.1007/s10530-012-0338-2

Poulakakis N, Sfenthourakis S (2008) Molecular phylogeny and phylogeography of the Greek populations of the genus *Orthometopon* (Isopoda, Oniscidea) based on mitochondrial DNA sequences. Zoological Journal of the Linnean Society 152: 707–715. https://doi.org/10.1111/j.1096-3642.2007.00378.x

Ratnasingham S, Hebert PDN (2007) BOLD: The Barcode of Life Data Systems. Molecular Ecology Notes 7: 355–364. https://doi.org/10.1111/j.1471-8286.2007.01678.x

Ratnasingham S, Hebert PDN (2013) A DNA-based registry for all animal species: the Barcode Index Number (BIN) system. PLoS ONE 8: e66213. https://doi.org/10.1371/journal.pone.0066213

Raupach MJ (2005) Die Bedeutung von Landasseln als Beutetiere für Insekten und andere Arthropoden. Entomologie heute 17: 3–12. [In German]

Raupach MJ, Held C, Wägele JW (2004) Multiple colonization of the deep sea by the Asellota (Crustacea: Peracarida: Isopoda). Deep-Sea Research II – Topical Studies in Oceanography 51: 1787–1795. https://doi.org/10.1016/j.dsr2.2004.06.035

Raupach MJ, Thatje S (2006) New records of the rare shrimp parasite *Zonophryxus quinquedens* Barnard, 1913 (Crustacea, Isopoda, Dajidae): ecological and phylogenetic implications. Polar Biology 29: 439–443. https://doi.org/10.1007/s00300-005-0069-2

Raupach MJ, Mayer C, Malyutina M, Wägele JW (2009) Multiple origins of deep-sea Asellota (Crustacea: Isopoda) from shallow waters revealed by molecular data. Proceedings of the Royal Society of London Series B 276: 799–808. https://doi.org/10.1098/rspb.2008.1063

Raupach MJ, Bininda-Emonds ORP, Knebelsberger T, Laakmann S, Pfaener J, Leese F (2014) Phylogeographic analysis of *Ligia oceanica* (Crustacea: Isopoda) reveals two deeply divergent mitochondrial lineages. Biological Journal of the Linnean Society 112: 16–30. https://doi.org/10.1111/bij.12254

Raupach MJ, Barco A, Steinke D, Beermann J, Laakmann S, Mohrbeck I, Neumann H, Kihara TC, Pointner K, Radulovici A, Segelken-Voigt A, Weese C, Knebelsberger T (2015) The application of DNA barcodes for the identification of marine crustaceans from the North Sea and adjacent regions. PLoS ONE 10: e0139421. https://doi.org/10.1371/journal.pone.0139421

Raupach MJ, Hannig K, Moriniére J, Hendrich L (2016) A DNA barcode library for ground beetles (Insecta: Coleoptera: Carabidae) of Germany: The genus *Bembidion* Latreille, 1802 and allied taxa. ZooKeys 592: 121–141. https://doi.org/10.3897/zookeys.592.8316

Raupach MJ, Hannig K, Moriniére J, Hendrich L (2018) A DNA barcode library for ground beetles of Germany: The genus *Amara* Bonelli, 1810 (Insecta: Coleoptera: Carabidae). ZooKeys 759: 57–80. https://doi.org/10.3897/zookeys.759.24129

Rigaud T, Moreau J, Juchault P (1999) *Wolbachia* infection in the terrestrial isopod *Oniscus asellus*: sex ratio distortion and effect on fecundity. Heredity 83: 469–475. https://doi.org/10.1038/sj.hdy.6885990

Rota N, Canedoli C, Ferre C, Ficetola GF, Guerrieri A, Padoa-Schioppa E (2020) Evaluation of soil biodiversity in Alpine habitats through eDNA metabarcoding and relationships with environmental features. Forests 11: e738. https://10.3390/f11070738

Saitou N, Nei M (1987) The neighbor-joining method: a new method for reconstructing phylogenetic trees. Molecular Biology and Evolution 4: 406–425.

Santamaria CA, Bluemel JK, Bunbury N, Curran M (2017) Cryptic biodiversity and phylogeographic patterns of Seychellois *Ligia* isopods. PeerJ 5: e3894. https://doi.org/10.7717/peerj.3894

Santamaria CA (2019) Molecular taxonomy of endemic coastal *Ligia* isopods from the Hawaiian Islands: re-description of *L. hawaiensis* and description of seven novel cryptic species. PeerJ 7: e7531. https://doi.org/10.7717/peerj.7531

Schizas NV (2012) Misconceptions regarding nuclear mitochondrial pseudogenes (numts) may obscure detection of mitochondrial novelties. Aquatic Biology 17: 91–96. https://doi.org/10.3354/ab00478

Schmalfuss H (1984) Eco-morphological strategies in terrestrial isopods. Symposia of the Zoological Society of London 53: 49–63.

Schmidt C (2008) Phylogeny of the terrestrial Isopoda (Oniscidea): a review. Arthropod Systematics & Phylogeny 66: 191–226.

Schmölzer K (1964) Ordnung Isopoda (Landasseln). In: Franz H (Ed.) Bestimmungsbücher zur Bodenfauna Europas, Lieferung 4/5. Akademie-Verlag, Berlin, 1–486. [In German]

Sfenthourakis S, Taiti S (2015) Patterns of taxonomic diversity among terrestrial isopods. In: Taiti S, Hornung E, Štrus J, Bouchon D (Eds) Trends in Terrestrial Isopod Biology. ZooKeys 515: 13–25. https://doi.org/10.3897/zookeys.515.9332

Shokralla S, Spall JL, Gibson JF, Hajibabaei M (2012) Next-generation sequencing technologies for environmental DNA research. Molecular Ecology 21: 1794–1805. https://doi.org/10.1111/j.1365-294X.2012.05538.x

Singer C, Bello NM, Snyder BA (2012) Characterizing prevalence and ecological impact of non-native terrestrial isopods (Isopoda, Oniscidea) in tallgrass prairie. Crustaceana 85: 1499–1511. https://doi.org/10.1163/15685403-00003126

Slabber S, Chwon SL (2002) The first record of a terrestrial crustacean, *Porcellio scaber* (Isopoda, Porcellionidae), from sub-Antarctic Marion Island. Polar Biology 25: 855–858. https://doi.org/10.1007/s00300-002-0420-9

Smit NJ, Bruce NL, Hadfield KA (2014) Global diversity of fish parasitic isopod crustaceans of the family Cymothoidae. International Journal for Parasitology: Parasites and Wildlife 3: 188–197. https://doi.org/10.1016/j.ijppaw.2014.03.004

Špaldoňová A, Frouz J (2014) The role of *Armadillidium vulgare* (Isopoda: Oniscidea) in litter decomposition and soil organic matter stabilization. Applied Soil Ecology 83: 186–192. https://doi.org/10.1016/j.apsoil.2014.04.012

Spelda J, Reip HS, Oliveira-Biener U, Melzer RR (2011) Barcoding Fauna Bavarica: Myriapoda – a new contribution to DNA-based identifications of centipedes and millipedes. In: Mesibov R, Short M (Eds) Proceedings of the 15th International Congress of Myriapodology, 18–22 July 2011, Brisbane, Australia. ZooKeys 156: 123–139. https://doi.org/10.3897/zookeys.156.2176

Staats M, Arulandhu AJ, Gravendeel B, Horst-Jensen A, Scholtens I, Peelen T, Prins TW, Kok E (2016) Advances in DNA metabarcoding for food and wildlife forensic species identification. Analytical and Bioanalytical Chemistry 408: 4615–4630. https://doi.org/10.1007/s00216-016-9595-8

Sun X, Bedos A, Deharveng L (2018) Unusually low genetic divergence at COI barcode locus between two species of intertidal *Thalassaphorura* (Collembola: Onychiuridae). PeerJ 6: e5021. https://doi.org/10.7717/peerj.5021

Sworobowicz L, Grabowski M, Mamos T, Burzyński A, Kilikowska A, Sell J, Wysocka A (2015) Revisiting the phylogeography of *Asellus aquaticus* in Europe: insights into cryptic diversity and spatiotemporal diversification. Freshwater Biology 60: 1824–1840. https://doi.org/10.1111/fwb.12613

Taberlet P, Coissac E, Pompanon F, Brochmann C, Willerslev E (2012) Towards next-generation biodiversity assessment using DNA metabarcoding. Molecular Ecology 21: 2045–2050. https://doi.org/10.1111/j.1365-294X.2012.05470.x

Valentini A, Pompanon F, Taberlet P (2009) DNA barcoding for ecologists. Trends in Ecology and Evolution 24: 110–117. https://doi.org/10.1016/j.tree.2008.09.011

Verovnik R, Sket B, Trontelj P (2004) Phylogeography of subterranean and surface populations of water lice *Asellus aquaticus* (Crustacea: Isopoda). Molecular Ecology 13: 1519–1532. https://doi.org/10.1111/j.1365-294X.2004.02171.x

Verovnik R, Sket B, Trontelj P (2005) The colonization of Europe by the freshwater crustacean *Asellus aquaticus* (Crustacea; Isopoda) proceeded from ancient refugia and was directed by habitat connectivity. Molecular Ecology 14: 4355–4369. https://doi.org/10.1111/j.1365-294X.2005.02745.x

Wägele JW (1989) Evolution und phylogenetisches System der Isopoda: Stand der Forschung und neue Erkenntnisse. Zoologica 140: 1–262. [In German]

Werren JH, Baldo L, Clark ME (2008) *Wolbachia*: master manipulators of invertebrate biology. Nature Reviews 6: 741–751. https://doi.org/10.1038/nrmicro1969

Williams JD, Boyko CB (2012) The global diversity of parasitic isopods associated with crustacean hosts (Isopoda: Bopyroidea and Cryptoniscoidea). PLoS ONE 7: e35350. https://doi.org/10.1371/journal.pone.0035350

Wilson GDF, Hessler RR (1987) Speciation in the deep sea. Annual Review of Ecology and Systematics 18: 185–207. https://doi.org/10.1146/annurev.es.18.110187.001153

Wilson GDF (2008) Global diversity of isopod crustaceans (Crustacea; Isopoda) in freshwater. Hydrobiologia 595: 231–240. https://doi.org/0.1007/s10750-007-9019-z

Young MR, Behan-Pelletier VM, Hebert PDN (2012) Revealing the hyperdiverse mite fauna of subarctic Canada through DNA Barcoding. PLoS ONE 7: e48755. https://doi.org/10.1371/journal.pone.0048755

Young MR, Moraza ML, Ueckermann E, Heylen D, Baardsen LF, Lima-Barbero JF, Gal S, Gavish-Regev, Gottlieb Y, Roy L, Recht E, El Adouzi M, Palevsky E (2019) Linking

morphological and molecular taxonomy for the identification of poultry house, soil, and nest dwelling mites in the Western Palearctic. Scientific Reports 9: e5784. https://doi.org/10.1038/s41598-019-41958-9

Zhang Z, Schwartz S, Wagner L, Miller W (2000) A greedy algorithm for aligning DNA sequences. Journal of Computational Biology 7: 203–214. https://doi.org/10.1089/10665270050081478

Zimmermann BL, Campos-Filho IS, Deprá M, Araujo PB (2015) Taxonomy and molecular phylogeny of the Neotropical genus *Atlantoscia* (Oniscidea, Philosciidae): DNA barcoding and description of two new species. Zoological Journal of the Linnean Society 174: 702–717. https://doi.org/10.1111/zoj.12256

Zimmermann BL, Campos-Filho IS, Araujo PB (2018a) Integrative taxonomy reveals a new genus and new species of Philosciidae (Crustacea: Isopoda: Oniscidea) from the Neotropical region. Canadian Journal of Zoology 96: 473–485. https://doi.org/10.1139/cjz-2017-0289

Zimmermann BL, Campos-Filho IS, Cardoso GM, Santos S, Aguiar JO, Araujo PB (2018b) Two new species of *Atlantoscia* Ferrara & Taiti, 1981 (Isopoda: Oniscidea: Philosciidae) from southern Brazil. Zootaxa 4482: 551–565. https://doi.org/10.11646/zootaxa.4482.3.7

Supplementary material 1

Barcode analysis using the BOLD workbench

Authors: Michael J. Raupach, Björn Rulik, Jörg Spelda

Data type: Data table

Explanation note: Molecular distances based on the Kimura 2-parameter model of the analyzed specimens of the analyzed isopod species. Divergence values were calculated for all studied sequences, using the Nearest Neighbor Summary implemented in the Barcode Gap Analysis tool provided by the Barcode of Life Data System (BOLD). Align sequencing option: BOLD aligner (amino acid based HMM), ambiguous base/gap handling: pairwise deletion. ISD = intraspecific distance. BINs are based on the barcode analysis from 05–06–2020. Asterisks indicate species not recorded from Germany. Species pairs with intraspecific distances > 2.2% are marked in bold.

Link: https://doi.org/10.3897/zookeys.1082.69851.suppl1

Supplementary material 2

Neighbor-joining topology

Authors: Michael J. Raupach, Björn Rulik, Jörg Spelda

Data type: Neighbor-joining topology

Explanation note: Neighbor-joining phylogram of all analyzed isopod specimen based on Kimura 2-parameter distances. Individuals are classified using ID numbers from BOLD and species name. Numbers next to nodes represent non-parametric bootstrap values (1,000 replicates, in %).

Link: https://doi.org/10.3897/zookeys.1082.69851.suppl2

Supplementary material 3

Neighbor-joining topology of the BOLD workbench including BIN analysis

Authors: Michael J. Raupach, Björn Rulik, Jörg Spelda

Data type: Neighbor-joining topology

Explanation note: Neighbor-joining phylogram of all analyzed isopod specimen based on Kimura 2-parameter distances using the BOLD workbench from 07–06–2020. Individuals are classified using ID numbers from BOLD and species name. Furthermore, geographic information and BIN numbers are provided for each specimen.

Link: https://doi.org/10.3897/zookeys.1082.69851.suppl3

ZooKeys 1082: 127–134 (2022)
doi: 10.3897/zookeys.1082.75816
https://zookeys.pensoft.net

RESEARCH ARTICLE

A peer-reviewed open-access journal
ZooKeys
Launched to accelerate biodiversity research

A revision of the genus *Cylindroeme* Vives (Coleoptera, Cerambycidae, Cerambycinae)

Yingqi Wang[1,2], Guanglin Xie[1,3], Wenkai Wang[1,3]

1 *Institute of Entomology, College of Agriculture, Yangtze University, Jingzhou, Hubei, 434025, China* **2** *Qingdao Hotincomon Agricultural Materials Marketing Co., Ltd, Jingzhou, China* **3** *Hubei Engineering Research Center for Pest Forewarning and Management, Yangtze University, Jingzhou, Hubei, 434025, China*

Corresponding authors: Guanglin Xie (xieguanglin@yangtzeu.edu.cn), Wenkai Wang (wwk@yangtzeu.edu.cn)

Academic editor: Francesco Vitali | Received 27 September 2021 | Accepted 20 December 2021 | Published 20 January 2022

http://zoobank.org/2812B659-14E2-43CB-8B90-7A876515E62B

Citation: Wang Y, Xie G, Wang W (2022) A revision of the genus *Cylindroeme* Vives (Coleoptera, Cerambycidae, Cerambycinae). ZooKeys 1082: 127–134. https://doi.org/10.3897/zookeys.1082.75816

Abstract

The genus *Cylindroeme* Vives, 2019 is taxonomically revised. The type species, *Cylindroeme vietnamica* Vives, 2019 is redescribed and a second species from Qinghai (China), *Cylindroeme shii* **sp. nov.**, is described and illustrated. The genus is redescribed and a key to the known species is presented. The genus is also recorded from China for the first time.

Keywords

Longhorned beetles, Oemini, new generic record, new species, Qilian Mountains, China

Introduction

The tribe Oemini (圆天牛族) currently includes 96 genera (Tavakilian and Chevillotte 2021). Of them, seven were so far known to occur in China (Chen et al. 2019; Tavakilian and Chevillotte 2021).

The genus *Cylindroeme* was established by Vives in 2019; up to now, only the type species, *Cylindroeme vietnamica* Vives, described and illustrated from Vietnam, was known (Vives 2019).

In the present paper, the genus *Cylindroeme* is reported from China for the first time with description and illustration of a new species under the name *Cylindroeme shii* sp. nov., based on specimens from Qinghai province. The genus is redescribed and a key to the two known species is presented.

Materials and methods

The genitalia were prepared by soaking the whole beetle in boiling water for several minutes, then opening the abdomen from the apex along the dorsopleural margin. The genitalia were then removed with fine forceps and ophthalmic scissors, and later cleared in 10% KOH at 80–100 °C for several minutes.

All habitus photographs were taken with a Canon 5D Mark II digital camera equipped with a Canon EF 100mm f/2.8L IS USM lens and genitalia images were taken with a Leica DFC450 digital camera mounted on a Leica M205A microscope. Images of the genitalia were taken by keeping them in glycerin. All images were edited using Adobe Photoshop 2020.

Taxonomy

Genus *Cylindroeme* Vives, 2019
扁柱胸天牛属

Cylindroeme Vives, 2019: 1. Type species: *Cylindroeme vietnamica* Vives, 2019.

Redescription. Body nearly cylindrical, elongate, equipped with relatively soft integument, clothed with slightly silky pubescence, fringed with sparse hairs on inner side of antennae.

Eyes large, coarsely faceted, deeply emarginate, with large lower lobe. Antennae slender, antennal tubercles feebly prominent and broadly separated, scape thickened apically, remaining segments similar in thickness. Prothorax cylindrical, slightly flat dorsally; pronotum longer than wide, slightly expanded laterally. Scutellum ligulate. Elytra elongate, with subparallel sides; humerus rounded and protruding forward; apex rounded; each elytron with a feeble longitudinal costa on the disc. Prosternal intercoxal process nearly absent, procoxal cavities completely opened posteriorly and strongly angled laterally; mesosternum wide and short, mesosternal intercoxal process rather short and small, triangular, mesocoxal cavities opened posteriorly; metasternum longer than wide, with a longitudinal median sulcus at posterior half; metepisternum rather wide at anterior half and narrowed at posterior half. Abdomen cylindrical, slightly expanded at posterior half, with six (male) or five (female) visible abdomeres. Legs relatively short, femora strongly enlarged, laterally flattened; metatibia about as long as metatarsus, first metatarsomere longer than next two combined.

Male genitalia. Tergite and sternite VIII subrectangular, truncated apically and strongly protruding laterally, with moderately long setae. Tegmen with parameres fused, sparsely clothed with setae apically; ringed part rounded, with lateral arms converged into a long median stem. Median lobe wide and short, slightly arcuate in lateral view, with two long median struts; dorsal apex straight, ventral apex cuspidal. Endophallus thin and long, with two arched basal sclerites.

Distribution. Vietnam, China (new country record).

Cylindroeme vietnamica Vives , 2019

扁柱胸天牛

Figs 1–2, 9, 12

Cylindroeme vietnamica Vives, 2019: 1–2. Type locality: Lung Cu, Ha Giang, Vietnam. Type depository: coll. E. Vives, Spain.

Type material examined. ***Holotype*** (male, Figs 1–2, 9) and one paratype (female, Fig. 12), only examined by photos (provided by Vives).

Redescription. (modified according to the original description and the quality photographs). Male, body length 13 mm, width 2.1 mm (holotype). Body elongate, mostly chestnut-brown, clothed with golden pubescence. Head and pronotum blackish brown, antennae and tarsi brown. Elytra clothed with two types of golden pubescence, one very short and dense, the other relatively long, sparse and arched.

Head parallel-sided behind the eyes; frons trapeziform, with a longitudinal median sulcus; eyes large, strongly emarginate at inner edge; genae rather short. Antennae thin, scape pyriform, strongly punctate, antennomere III clearly longer than antennomere IV, the following segments subequal in length. Pronotum longer than broad, broadest near basal fourth; disc slightly flattened, middle of apical margin equipped with an inverted triangle notch with raised edge, then followed by an inverted V-shaped ridge nearly reaching to posterior edge. Scutellum ligulate, with raised edge. Elytra elongate, about 5.0 times as long as humeral width; humeri rather rounded, protruding forward; sides subparallel, slightly converged towards apex; apex rounded; disc slightly flattened, finely punctate, with a short longitudinal basal rib at the middle of each elytron. Prosternum smooth and shiny on anterior quarter, finely dotted on posterior half; mesosternum transverse, metasternum slightly longer than wide, with a longitudinal median indentation at posterior half, prosternal intercoxal process nearly absent. Abdomen cylindrical, slightly wider at apical half, with six visible ventrites, first ventrite longer than wide, the others shorter and ventrites I–IV with a smooth and shiny posterior border. Legs short, femora strongly widened, laterally flattened, first metatarsomere about 2.0 times as long as next two combined, claws divaricate.

Distribution. Vietnam (Ha Giang province).

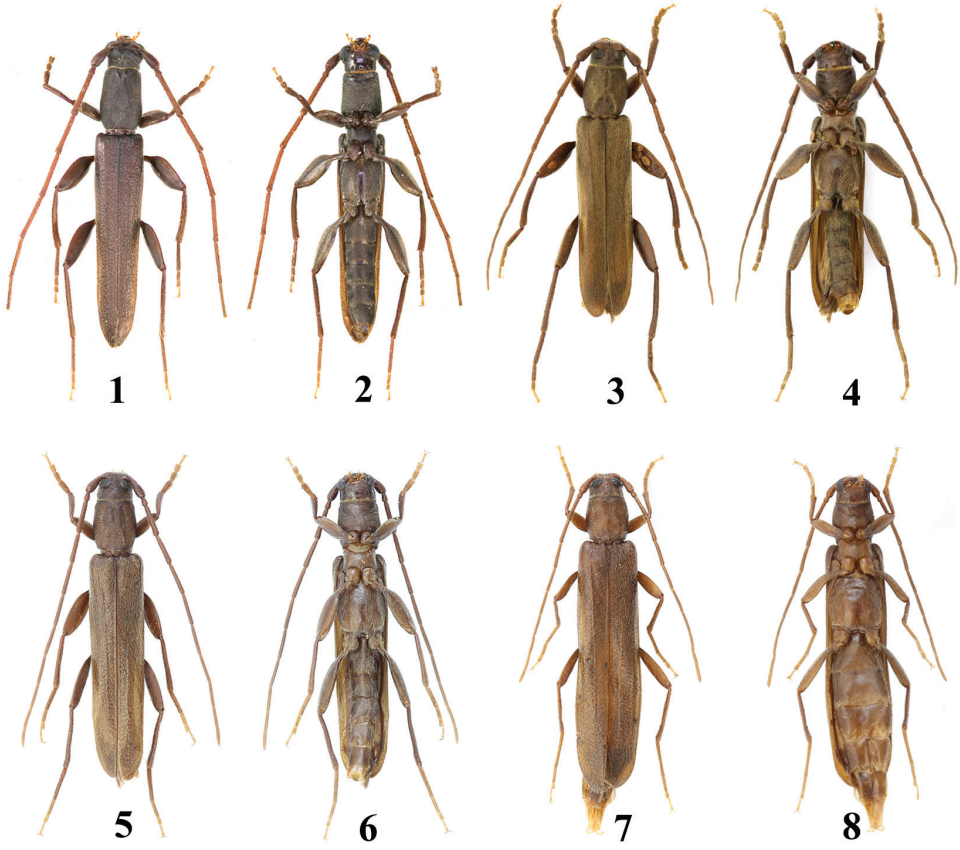

Figures 1–8. Habitus of *Cylindroeme* spp. **1–2** *Cylindroeme vietnamica* Vives **3–8** *Cylindroeme shii* sp. nov. **1–2, 5–6** holotypes **3–4, 7–8** paratypes **1–6** male **7–8** female.

***Cylindroeme shii* sp. nov.**
http://zoobank.org/E01F5371-2002-4860-90EC-CD2F92A67520
石氏扁柱胸天牛
Figures 3–8, 10–11, 13–24

Type material. ***Holotype***: male, China: Qinghai, Qilian County, Babao town (八宝镇), Ice Valley (Bing gou, 冰沟), 3110 m, 38°7'60"N, 100°10'21"E, July 25, 2019, leg. Guanglin Xie. Paratypes: 7 males and 1 female, the same as holotype data; 3 males and 3 females, Qinghai, Qilian County, A'rou Township (阿柔乡), Deerhorn Valley (Lujiao Gou, 鹿角沟), 3020 m, 38°8'20"N, 100°24'15"E, July 20, 2019, leg. Guanglin Xie; 5 males, Qinghai, Qilian County, A'rou Township (阿柔乡), Deerhorn Valley (Lujiao Gou, 鹿角沟), 3020 m, 38°8'20"N, 100°24'15"E, July 22, 2019, leg. Guanglin Xie. All of the type specimens are deposited in the Entomological Museum, Yangtze University, Jingzhou, Hubei, China, except for two male paratypes in the private collection of Chen Mou (Shanghai, China) and one male paratype in the private collection of Tianlong He (Anhui, China).

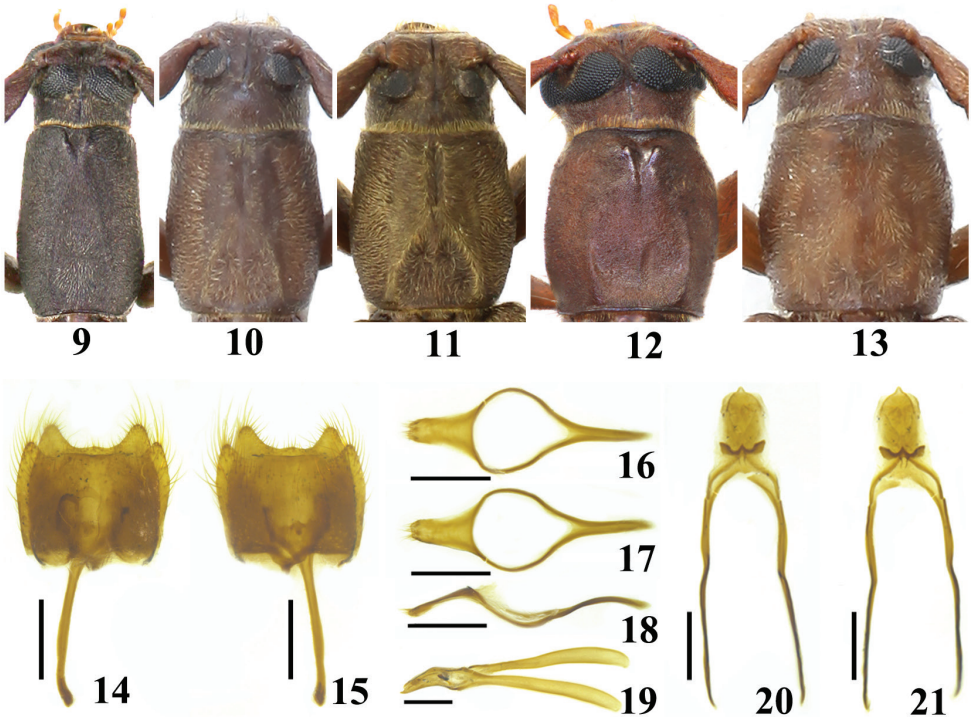

Figures 9–21. Habitus of *Cylindroeme* spp. **9–13** head and pronotum **14–21** male genitalia **9, 12** *Cylindroeme vietnamica* Vives **10–11, 13–21** *Cylindroeme shii* sp. nov. **9–10** holotypes **11–13** paratypes **9–11** male **12–13** female **14–15** abdominal segments VIII–IX **16–18** tegmen **19–21** median lobe **14, 16, 20** dorsal view **15, 17, 21** ventral view **18–19** lateral view Scale: 0.5 mm.

Description. Male, body length 8.0–11.0 mm, humeral width 1.5–2.0 mm. Body mostly yellowish brown to light chestnut-brown, clothed with yellowish silky pubescence. Head slightly darker, mandible black apically, clothed with yellowish hairs on outside; labrum and apex of clypeus pale yellow. Antennae sometimes lighter in colour towards to end, fringed with sparse yellowish hairs on inner side of basal segments, more conspicuous on antennomeres III and IV. Pronotum with pubescence obviously silky, forming a squared area on anterior half that looks distinctly different in appearance due to the different direction of the pubescence. Elytra with semirecumbent pubescence. Abdomen with apical ventrite yellowish. Legs with tarsi wholly or only apically yellowish and claw wholly yellowish.

Head about as broad as pronotum, subparallel-sided behind eyes; frons short, subrectangular, with a longitudinal median sulcus; eyes large, upper lobes widely separated; genae very short. Antennae slightly shorter than body, antennomere III slightly longer than antennomere IV, antennomeres V–XI gradually shortened in length. Pronotum longer than broad, broadest behind middle; disc with three narrow longitudinal indentations at apex, median one relatively short, located before the middle, lateral two relatively long, exceeding the middle backwards; with two oblique fine longitudinal ridges at base, anterior ends connected behind the median indentation, forming an inverted

V-shaped structure, enclosing a quite flat triangular area. Scutellum ligulate, with distinct edge. Elytra elongate, about 4.2 times as long as humeral width; humeri rounded, slightly protruding forward; sides subparallel; apex rounded; disc finely punctate, with an inconspicuous longitudinal rib at the middle of each elytron, not reaching the apex. Prosternum finely transversely wrinkled apically, mesosternum transverse, metasternum longer than wide, with a longitudinal median indentation at posterior half, pro- and mesosternal intercoxal processes nearly absent. Abdomen cylindrical, distinctly narrower than metathorax, first abdomere obviously longer than others. Legs short, femora strongly widened, laterally flattened, metafemur distinctly exceeding ventrite II, first metatarsomere about 1.4 times as long as next two combined, claws divaricate.

Male genitalia. About apical half of tergite and sternite VIII clothed with sparse setae, longer on sides, apical edge of ventrite VIII more broadly transverse-truncate than tergite VIII. Tegmen waved in lateral view, parameres fused, converged towards apex; apex slightly truncate and sparsely setiferous; ringed part quite rounded, with lateral arms converged into a long median stem; relative length ratios of paramere, vertical diameter of ringed part (except median stem) and median stem equal to 4.84:7.22:6.41. Median lobe wide and short, relative length ratios of median lobe and median struts about 1:3, dorsal apex nearly straight, ventral apex mastoid. Endophallus with two arched basal sclerites connected together.

Female. Body length 9.0–10.5 mm, humeral width 1.6–2.0 mm. Similar to male but body colour a little lighter, antennae only reaching behind middle of body, pronotum nearly as long as broad, anterior lateral indentations and posterior longitudinal ridges less obvious than in the male, elytra about 4.3 times as long as humeral width, abdomen with five visible abdomeres, legs slightly shorter, metafemur reaching to about end of second abdomere.

Remarks. The new species can be easily distinguished from the type species, *Cylindroeme vietnamica*, by the wider spacing of the upper eye lobes, shorter antennae, less elongate pronotum and elytra, and different discal structure of pronotum.

In the new species, the distance between the upper eye lobes is about as wide as the transverse diameter of a single upper eye lobe (Figs 10, 11, 13), while the upper eye lobes are almost connected in *C. vietnamica* (Figs 9, 12); the male antennomere VIII about reaches to the apical two fifths of the elytra (Figs 3–6), while it nearly extends to the apical one tenth in *C. vietnamica* (Figs 1, 2); the length-width ratio of male pronotum and elytra is about 1.1 and 4.2, respectively (Figs 3–6), while it is about 1.4 and 5.0 in *C. vietnamica* (Figs 1, 2); the pronotum is without a remarkable V-shaped median depression at apex (Figs 10, 11, 13), while it is equipped with a remarkable, broad and short median depression with a V-shaped raised edge in *C. vietnamica* (Figs 9, 12); the male pronotum is equipped with a distinct narrow longitudinal indentation at the apex, extending backwards to the middle and jointed with an inverted V-shaped ridge with two short lateral arms (Figs 10, 11), while the apical median indentation is rather short, inverted triangular, and both lateral arms of the inverted V-shaped ridge are quite long in *C. vietnamica* (Fig. 9).

Etymology. The new species is named after Professor Dr. Fuming Shi (Hebei University, China), a famous Chinese katydid taxonomist.

Distribution. China (Qinghai).

Biological notes. The adults of *Cylindroeme shii* sp. nov. were found on trunks of *Picea crassifolia* Komarov (Qinghai spruce). They were attracted by half-dead trees

Figures 22–24. Living adults of *Cylindroeme shii* sp. nov. **22–23** male **24** mating pair, lateral view.

whose trunks were bored by xylophagous insects or damaged by other animals. The adults were found crawling and mating on these damaged tree trunks. Based on this, it can be speculated that Qinghai spruce (*Picea crassifolia*) should be its host plant.

The adults were first discovered on July 20, 2019. At the same time, one egg-laying female adult and one free-moving male adult of *Necydalis inermis* Pu, 1992 (Cerambycidae, Necydalinae) and the free-moving adults of *Tetropium castaneum* (Linnaeus, 1758) (Cerambycidae, Spondylidinae) were also found on Qinghai spruce. However, two year later, when the second author visited the same place again on 1–3 August, 2021, no individuals of the new species were found. It indicated that the adults of the new species may be active till the end of July at the latest.

Key to the known species of *Cylindroeme* Vives

1 Upper eye lobes close to each other, almost connected; male with median notch at apex of pronotum rather remarkable, short, inverted triangle shaped, and with inverted V-shaped ridge with lateral arms quite long ..... ***C. vietnamica* Vives**

– Upper eye lobes widely separated; male with median indentation at apex of pronotum quite long and narrow, and with inverted V-shaped ridge with lateral arms short ..... ***C. shii* sp. nov.**

Acknowledgements

We thank Eduard Vives (Natural Science Museum of Barcelona, Spain) for taking the type specimen photographs of *C. vietnamica*, Ping Wang (Yangtze University, China) for helping to deal with the male genitalia, Cunxin Ma (Qilian Mountain National Park, China) for taking the living adult photographs of the new species, Yuxia Yang (Hebei University, China) for giving useful suggestions during the preparation of the manuscript. We wish to express our thanks to Zhenning Chen and Fan Cheng (Qinghai Normal University, China) for their assistance during specimen collection. Also, we are grateful to the reviewers for their helpful suggestions, and especially to Francesco Vitali, subject editor of ZooKeys, for patiently handling the manuscript. This work was supported by the commissioned project of the Qilian Mountain National Park administration of Qinghai Province, P. R. China (QHTX-2021-006) and the National Natural Science Foundation of China (No. 31672327).

References

Vives E (2019) Description of a new Oemini from Vietnam belonging to a new genus (Coleoptera, Cerambycidae). (Cerambycidae new or little known from Vietnam. Pars X). Faunitaxys 7 (10): 1–2.

Chen L, Liu ZP, Li Z (2019) Subfamily Cerambycinae Latreille, 1802. In: Lin MY, Yang XK (Eds) Catalogue of Chinese Coleoptera. Vol. 9. Chrysomeloidea. Vesperidae, Disteniidae, Cerambycidae. Science Press, Beijing, 98–216.

Tavakilian GJ, Chevillotte H (2021) Titan: base de données internationales sur les Cerambycidae ou Longicornes. [online] http://titan.gbif.fr/index.html [Accessed on 12 November 2021]

ZooKeys 1082: 135–151 (2022)
doi: 10.3897/zookeys.1082.73611
https://zookeys.pensoft.net

RESEARCH ARTICLE

A peer-reviewed open-access journal
ZooKeys
Launched to accelerate biodiversity research

New leafhopper species and new records of Typhlocybini (Hemiptera, Cicadellidae, Typhlocybinae) from China

Xian Zhou[1], Yalin Zhang[1], Min Huang[1]

1 *Key Laboratory of Plant Protection Resources and Pest Management of Ministry of Education, Entomological Museum, College of Plant Protection, Northwest A&F University, Yangling, Shaanxi Province, 712100, China*

Corresponding authors: Yalin Zhang (yalinzh@nwsuaf.edu.cn), Min Huang (huangmin@nwsuaf.edu.cn)

Academic editor: Mick Webb | Received 28 August 2021 | Accepted 6 January 2022 | Published 20 January 2022

http://zoobank.org/8C1CFB38-1449-4F0B-8129-F3257AE75A2F

Citation: Zhou X, Zhang Y, Huang M (2022) New leafhopper species and new records of Typhlocybini (Hemiptera, Cicadellidae, Typhlocybinae) from China. ZooKeys 1082: 135–151. https://doi.org/10.3897/zookeys.1082.73611

Abstract

Five genera from China of the leafhopper tribe Typhlocybini are treated. *Linnavuoriana* Dlabola, 1958 and *Shamala* Dworakowska, 1980 and seven known species, *Edwardsiana corylicola* Vilbaste, 1968, *E. praedestina* Dlabola, 1967, *E. singularis* Anufriev, 1975, *Hiratettix distanti* Dworakowska, 1982, *H. malaisei* Dworakowska, 1982, *L. antiqua* Dworakowska, 1982, and *L. malicola* Zachvatkin, 1949 are newly recorded from China. Two new species, *Shamala annulata* and *Paracyba biprocessa* **spp. nov.**, are described and illustrated. Keys to Chinese species of each genus are also provided.

Keywords

Auchenorrhyncha, distribution, morphology, taxonomy, Typhlocybini

Introduction

Typhlocybini (Hemiptera, Cicadellidae, Typhlocybinae) is a moderately large leafhopper tribe with over 924 species in 93 genera worldwide, of which 253 species in 44 genera have been recorded from China (including Zyginellini) (Dmitriev 2003; Yan 2019). Recent studies on Typhlocybinae from China have revealed many new taxa and new re-

cords, especially in the tribe Typhlocybini. Here, we treat nine species belonging to five genera of this tribe, including two new species which are described and illustrated and seven new records. Updated keys to Chinese species of each genus are also provided.

Materials and methods

Figures of the specimens were made using a Leica M205 light microscope with a Leica DFC425 camera. Images were produced using the Leica Application Suite V3.7 and edited using Adobe Photoshop CS6.0 (Adobe Systems). Abdomens were removed from examined specimens and macerated in cold 10% NaOH solution overnight, subsequently rinsed for 30 s with pure water, and stored in glycerin. An Olympus SZX10 microscope was used for dissecting specimens and an Olympus PM-10AD was used for drawing the dissected male genitalia.

Morphological terminology in this work follows Zhang (1990), but wing venation follows Dworakowska (1993).

Type specimens of the new species are deposited in the collections of the Entomological Museum, Northwest A&F University, Yangling, China (**NWAFU**).

Taxonomy

Edwardsiana Zachvatkin

Edwardsiana Zachvatkin, 1929: 439.

Type species. *Cicada rosae* Linnaeus, 1758, by original designation.

Remarks. The genus *Edwardsiana* includes 80 known species worldwide (Dmitriev 2003), with two species having been reported from China. Here we record three more species from China and provide a key to all Chinese species.

Diagnosis. Body cream with variable patches (Figs 1–3). Crown bluntly produced, medial length shorter than distance between eyes; coronal suture distinct. Pronotum slightly wider than head (Figs 6–8). Forewing with apical area short, 1/4–1/3 of total length; RP and MP' petiolate or not. Hind wing with R and M confluent distally.

Male sternal abdominal apodemes well developed, often extending to middle of 6th sternite.

Male genitalia. Pygofer side often with rounded extension at basal angle; ventral part always with depressed areas, dense stout setae on ventral-basal part and row of short rigid setae caudally. Subgenital plate elongate with subapical part twisted outwards; long macroseta basally and row of short rigid setae from middle to subapex. Paramere with distal part long and curved. Connective with central ridge developed. Aedeagus with preatrium and dorsal apodeme developed; aedeagal shaft with paired apical processes; gonopore apical.

Distribution. Palaearctic and Nearctic regions.

Figures 1–20. Typhlocybini of China **1–5** dorsal view **6–10** head and thorax, dorsal view **11–15** lateral view **16–20** face **1, 6, 11, 16** *Edwardsiana corylicola* **2, 7, 12, 17** *E. praedestina* **3, 8, 13, 18** *E. singularis* **4, 9, 14, 19** *Hiratettix distanti* **5, 10, 15, 20** *H. malaisei*. Scale bars: 1.0 mm (**1–5, 11–15**); 0.5 mm (**6–10, 16–20**).

Key to species (males) of the genus *Edwardsiana* from China

1 Aedeagal shaft with two pairs of unbranched apical processes ..... ***E. rosae*** **(Linnaeus)**
– Aedeagal shaft with apical processes branched **2**
2 Aedeagal shaft with both dorsal and ventral processes branched (Figs 41, 42) ..... ***E. singularis*** **Anufriev**
– Aedeagal shaft just with dorsal processes branched **3**
3 Ventral processes of aedeagal shaft short and directed ventrad (Figs 37, 38) .. .. ***E. corylicola*** **Vilbaste**
– Ventral processes of aedeagal shaft long and directed dorsad **4**
4 Aedeagal shaft with dorsal and ventral processes branched near base (Figs 39, 40) ..... ***E. praedestina*** **Dlabola**
– Aedeagal shaft with dorsal and ventral processes branched at middle or near apex ..... ***E. ishidai*** **(Matsumura)**

Edwardsiana corylicola **Vilbaste, rec. nov.**
Figs 1, 6, 11, 16, 37, 38

Edwardsiana corylicola Vilbaste, 1968: 98, Dworakowska 1982: 121, figs 205, 206.

Specimens examined. 2♂♂, 2♀♀, China, Heilongjiang Province, Mishan, 2.ix.2001, coll. Qiang Sun.

Distribution. China (Heilongjiang), Russia, Korea, North Korea.

Edwardsiana ishidai **(Matsumura)**

Typhlocyba ishidai Matsumura, 1932: 98, pl. II, fig. 3a, b.
Typhlocyba lanternae Wagner, 1937: 154.
Edwardsiana ussurica Vilbaste, 1968: 97.
Edwardsiana ishidai (Matsumura): Dworakowska 1982: 112, figs 156–178; Huang and Zhang 2002: 290.

Distribution. China (Jilin), Japan, Mongolia, Russia.

Edwardsiana praedestina **Dlabola, rec. nov.**
Figs 2, 7, 12, 17, 39, 40

Edwardsiana praedestina Dlabola, 1967: 217, figs 12–14.

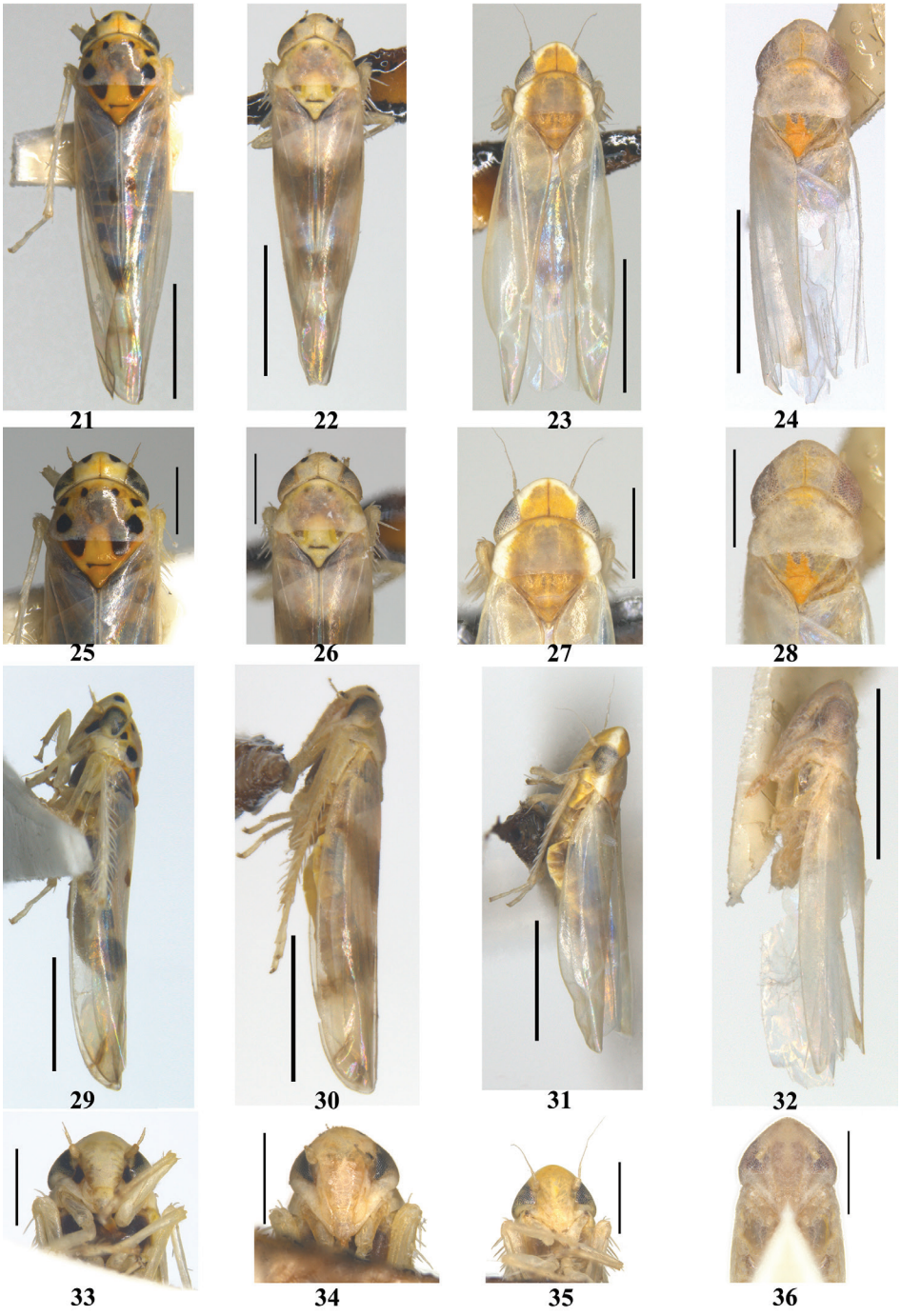

Figures 21–36. Typhlocybini of China **21–24** dorsal view **25–28** head and thorax, dorsal view **29–32** lateral view **33–36** face **21, 25, 29, 33** *Linnavuoriana antiqua* **22, 26, 30, 34** *L. malicola* **23, 27, 31, 35** *Paracyba biprocessa* sp. nov. **24, 28, 32, 36** *Shamala annulata* sp. nov. Scale bars: 1.0 mm (**21–24, 29–32**); 0.5 mm (**25–28, 33–36**).

Specimens examined. 1♂, 19♀♀, China, Shandong Province, Kunyu Mountain, 12.vii.2001, coll. Daozheng Qin and Zhenjiang Liu.

Distribution. China (Shandong), Mongolia.

Edwardsiana rosae (Linnaeus)

Cicada rosae Linnaeus, 1758: 439.
Edwardsiana subrosea Vilbaste, 1980: 41.
Edwardsiana rosae (Linnaeus): Dworakowska 1982: 107, figs 106–117.

Distribution. China (Gansu, Xinjiang), Cyprus, Turkey, Iran, Russia, Kazakhstan, Kirghizstan, Uzbekistan, Tajikistan.

Edwardsiana singularis Anufriev, rec. nov.

Figs 3, 8, 13, 18, 41, 42

Edwardsiana singularis Anufriev, 1975: 531; Dworakowska 1982: 117, figs 216, 217.

Specimens examined. 1♂, China, Heilongjiang Province, Mishan, 2.ix.2001, coll. Qiang Sun.

Distribution. China (Heilongjiang), Russia, Kazakhstan.

Hiratettix Matsumura

Hiratettix Matsumura, 1931: 59 (in key); Matsumura 1932: 102 (full description); Dworakowska 1982: 152.

Type species. *Hiratettix arisanellus* Matsumura, 1932.

Remarks. After Matsumura (1931) described the genus *Hiratettix* (in a key to genera), Dworakowska (1982) added three new species from China (Taiwan), Myanmar, and India, and Sohi et al. (1990) published a new species from Nepal. Here we report two species new to China and provide a key to the Chinese species.

Diagnosis. Body flat and overall black (Figs 4, 5). Face wide and short (Figs 19, 20). Pronotum with minute transverse sculpture (Figs 9, 10). Forewing with 3rd apical cell triangular. Hind wing truncated terminally with two cross veins; apical cells short.

Male genitalia. Genital capsule high and short. Pygofer with several short rigid setae terminally on inner surface and long macrosetae ventrobasally. Subgenital plate broad basally, slightly narrowed distally, with several long macrosetae near middle part, a row of short rigid setae laterally and progressively shorter subbasally to apex. Connective wide with central lobe underdeveloped. Paramere thick with central part longer

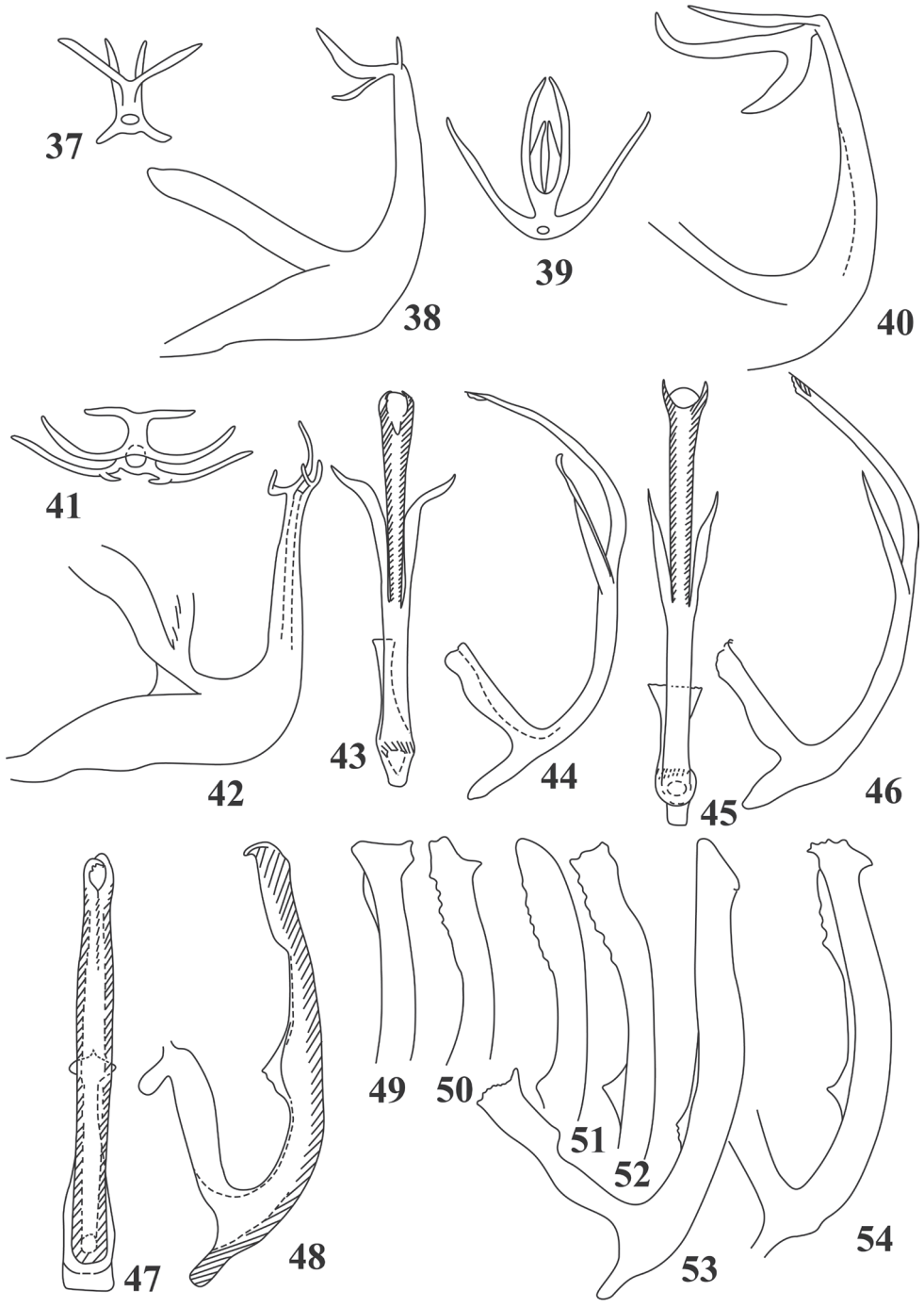

Figures 37–54. Male genitalia of Typhlocybini of China (after Dworakowska 1982) **37, 38** *Edwardsiana corylicola* **39, 40** *E. praedestina* **41, 42** *E. singularis* **43, 44** *Hiratettix distanti* **45, 46** *H. malaisei* **47, 48** *Linnavuoriana antiqua* **49–54** *L. malicola*.

than basal and distal parts together; caudal part with sensorial pits on inner margin. Aedeagal shaft with paired apical and lateral processes; gonopore apical.

Distribution. Oriental Region.

Key to species (males) of the genus *Hiratettix* from China

1 Aedeagal shaft with two long basal processes and two pairs of short apical processes **2**
– Aedeagal shaft with two medium sized lateral processes and one pair of short apical processes **3**
2 Aedeagal shaft with basal processes S-bent and two pairs of apical processes basally closed ..... ***H. arisanellus*** **Matsumura**
– Aedeagal shaft with basal processes arched and two pairs of apical processes detached from each other basally ..... ***H. matsumurai*** **Dworakowska**
3 Aedeagal shaft with median processes curved outwards, apical processes directed to each other distally (Figs 43, 44) ..... ***H. distanti*** **Dworakowska**
– Aedeagal shaft with median processes straight, apical processes widely separated distally (Figs 45, 46) ..... ***H. malaisei*** **Dworakowska**

Hiratettix arisanellus **Matsumura**

Hiratettix arisanellus Matsumura, 1932: 102; Dworakowska 1982:153, figs 635–649.

Distribution. China (Taiwan).

Hiratettix distanti **Dworakowska, rec. nov.**

Figs 4, 9, 14, 19, 43, 44

Hiratettix distanti Dworakowska, 1982: 154, figs 661–666.

Specimens examined. 1♂, China, Yunnan Province, Mengla, Nangong Mountain, 1850 m, 13.xii.1999, coll. Dworakowska.

Distribution. China (Yunnan), India.

Hiratettix malaisei **Dworakowska, rec. nov.**

Figs 5, 10, 15, 20, 45, 46

Hiratettix malaisei Dworakowska, 1982: 153, figs 667–676.

Specimens examined. 1♂, China, Sichuan Province, Emei Mountain, 950 m, 30.x.1999, coll. Dworakowska. 1♂, 2♀♀, China, Guizhou Province, Huaxi, Huaxi

Garden, 1100 m, 25.vii.2001, coll. Qiang Sun, at light. 1♂, 14♀♀, China, Yunnan Province, Shilin, 9.vii.2021, coll. Xian Zhou.

Distribution. China (Sichuan, Guizhou, Yunnan), Myanmar.

Hiratettix matsumurai Dworakowska

Hiratettix matsumurai Dworakowska, 1982: 153, figs 650–660.

Distribution. China (Taiwan).

Linnavuoriana Dlabola, rec. nov.

Linnavuoriana Dlabola 1958: 54; Dworakowska 1971: 647; Dworakowska 1982: 121.

Type species. *Cicada decempunctata* Fallen, 1806.

Remarks. Up to now, there are eight known species in the genus *Linnavuoriana*. In Xinjiang and Yunnan provinces, we collected two known species that are the first records of the genus from China. A key to the Chinese species is given.

Diagnosis. Body cream, light yellow (Figs 21, 22). Crown and pronotum with symmetrical black round patches, and basal triangle black (Figs 25, 26). Forewing semitransparent with light smoky brown or brown patches (Figs 21, 22, 29, 30).

Head bluntly produced, little narrower than width of pronotum, and 1/3 times middle length of pronotum (Figs 25, 26). Forewing slender and obtuse apically with both sides parallel; RP+MP' petiolate at base; 1st apical cell usually smallest; 2nd apical cell biggest. Hind wing with two cross veins far away from each other.

Abdominal apodemes well developed, often extending to 5th abdominal sternite.

Male genitalia. Hind margin of pygofer with inner ridge, several rigid microsetae near posterior-dorsal margin and numerous minute tubercles posteroventrally. Subgenital plate parallel-sided and lack macrosetae at base, narrowing from apical 1/3–1/2 of outer margin, rounded terminally, usually with row of rigid microsetae and some fine microsetae scattered on apex. Paramere rarely curved with subapical tooth; distally with row of microsetae on outer margin and row of sensorial pits on inner margin. Connective small with central ridge underdeveloped. Aedeagal shaft with a pair of triangular protrusions on dorsal surface laterally; gonopore apical.

Distribution. Oriental and Palaearctic regions.

Key to species of *Linnavuoriana* from China (males)

1 Crown and pronotum with large dark patches; aedeagal shaft with apex hook-like (Figs 47, 48) ..... ***L. antiqua* Dworakowska**

– Crown and pronotum with few light patches; aedeagal shaft with apex not hook-like (Figs 49–54) ..... ***L. malicola* (Zachvatkin)**

***Linnavuoriana antiqua* Dworakowska, rec. nov.**
Figs 21, 25, 29, 33, 47, 48

Linnavuoriana antiqua Dworakowska, 1982: 123, figs 326–341.

Specimens examined. 1♂, 1♀, China, Yunnan Province, Lijiang, Xinzhu Botanical Garden, 16.xi.1999, coll. Dworakowska. 1♂, Yunnan Province, Tengchong, 1650 m, 26.iv.1981, coll. Fasheng Li.

Distribution. China (Yunnan), India.

***Linnavuoriana malicola* (Zachvatkin), rec. nov.**
Figs 22, 26, 30, 34, 49–54

Typhlocyba malicola Zachvatkin, 1949: 220.
Linnavuoriana taschkentica Dlabola, 1961: 302, figs 152–156. Synonymized by Mitjaev 1967: 710.
Linnavuoriana apunctata Mitjaev, 1963: 49, nec Dlabola.
Typhlocyba roseipennis Kusnezov, 1932: 232, nec Oshanin (Zachvatkin 1949; Mitjaev 1967).
Linnavuoriana populicola Dubovsky, 1966: 132; Synonymized by Dworakowska 1982: 123, figs 313–325.

Specimens examined. 4♂♂, 3♀♀, China, Xinjiang Province, Xinjiang Agricultural Vocational and Technical College, 16.ix.1986, coll. Yalin Zhang. 13♂♂, 4♀♀, Xinjiang Agricultural University, 16.ix.1986, coll. Yalin Zhang.

Distribution. China (Xinjiang), Kazakhstan, Kirghizstan, Uzbekistan, Tajikistan, Afghanistan.

***Paracyba* Vilbaste**

Paracyba Vilbaste, 1968: 96; Dworakowska 1982: 148, figs 602–621.

Type species. *Zygina akashiensis* Takahashi, 1928.

Remarks. Until now, the genus *Paracyba* included three known species, including two species from China. Here we add a new species from China and give a key to all species of the genus.

Diagnosis. Body slim. Head bluntly produced, middle length equal to or shorter than width between eyes, coronal suture long and distinct. Forewing laterally with apex rounded; RP and MP' petiolate at base; 1st apical cell nearly equal in size to 4th apical cell; 2nd apical cell biggest. Hind wing with two cross veins.

Male sternal abdominal apodemes extending to distal margin of 4th sternite.

Male genitalia. Pygofer side tall and divided into two or three small lobes caudally, upper lobe and central lobe with short rigid setae terminally, lower lobe deeply con-

tracted, usually with long macrosetae. Subgenital plate elongate, triangular with a row of short fine setae subbasally to apex, with indistinct peg-like setae at apex. Paramere with basal part slim and central part broad, thereafter gradually tapered to apex, with a row of microsetae on outer margin. Connective trapezoidal. Aedeagus with short preatrium; dorsal apodeme well developed bifurcate apically; aedeagal shaft usually short with long and asymmetrical processes apically; gonopore apical.

Distribution. Oriental and Palaearctic regions.

Key to species (males) of the genus *Paracyba*

1 Aedeagal shaft with two distal processes (Figs 60–62) ..... ***P. biprocessa* sp. nov.**

– Aedeagal shaft with three distal processes **2**

2 Aedeagus with lateral process arising from mid-length of shaft; two other processes slightly arched, longest process bent to right ..... ***P. akashiensis* (Takahashi)**

– Aedeagus with lateral process arising near apex; other two processes relatively straight, longest process bent to left **3**

3 Two apical processes of aedeagus twice as long as subapical process..... ***P. soosi* Dworakowska**

– Two apical processes of aedeagus nearly equal in length to subapical process. ..... ***P. nopporensis* Matsumura**

Paracyba akashiensis (Takahashi)

Zygina akashiensis Takahashi, 1928: 442; Dworakowska 1982: 148, figs 602–614.

Distribution. China (Taiwan), Japan, Russia.

Paracyba soosi Dworakowska

Paracyba soosi Dworakowska, 1977: 41, figs 253–259.

Distribution. China (Hunan), Vietnam.

Paracyba nopporensis (Matsumura)

Typhlocyba nopporensis Matsumura, 1932: 100; Dworakowska 1982: 150, figs 615–621.

Distribution. Japan, Russia.

***Paracyba biprocessa* sp. nov.**
http://zoobank.org/NomenclaturalActs/7504C225-8537-4115-9196-9783F7F4A8D4
Figs 23, 27, 31, 35, 55–62

Note. Head with coronal suture extended to anterior margin (Fig. 23). Face yellow, eyes dark brown, thorax light brown (Figs 27, 35). Crown with anterior margin white; pronotum with lateral margin white, remainder covered with a continuous large ocher patch extending to distal end of clavus of forewing (Figs 23, 27); scutellum with apex orange (Fig. 27). Forewing light ocher with few light smoky patches in apical half, remaining part transparent except for white brochosome field.

Male sternal abdominal apodemes extending to middle of 5th sternite (Fig. 55).

Pygofer side tall and bilobate caudally, upper lobe with short setae terminally, lower lobe with several fine moderately long setae (Fig. 56). Subgenital plate elongate, triangular with single macroseta near base, a row of short rigid setae adjacent row of fine setae laterally and two indistinct peg-like setae apically (Fig. 58). Paramere with row of microsetae on outer margin and row of sensorial pits on inner margin (Fig. 59). Connective trapezoidal, with central ridge (Fig. 57). Aedeagal shaft with two apical processes, in ventral view left process slim, S-shaped, right process short and straight (Figs 60–62).

Specimens examined. ***Holotype***: ♂, China, Shaanxi Province, Yangling, ix.1983, coll. Yalin Zhang. ***Paratypes***: 10♂♂, 4♀♀, same data as holotype.

Measurement. Male, 3.1–3.3 mm (including wing).

Etymology. This new species is named for the two aedeagal processes, rather than three in other species.

Remarks. This new species resembles *Paracyba soosi* Dworakowska, 1977 in coloration and male genitalia, but it differs from the latter in aedeagal shaft having two rather than three distal processes and processes of very different length.

***Shamala* Dworakowska, rec. nov.**

Shamala Dworakowska, 1980: 169, figs 174–187.

Type species. *Shamala mikra* Dworakowska, 1980.

Remarks. The genus *Shamala* was erected by Dworakowska (1980); thereafter she described four additional species from India and Nepal (1981), Sikkim (1994), and India (1982). In this paper, a new species, *S. annulata* sp. nov., from Yunnan, China, is described and illustrated which increases the number of valid species in this genus to six.

Diagnosis. Body slim and cream with occasional light brown patches. Head slightly wider than pronotum with length along midline slightly shorter than distance between eyes. Forewing parallel-sided, rounded terminally; RP and MP' petiolate at base. Hind wing gradually narrowing from base to apex and rounded terminally with two cross veins.

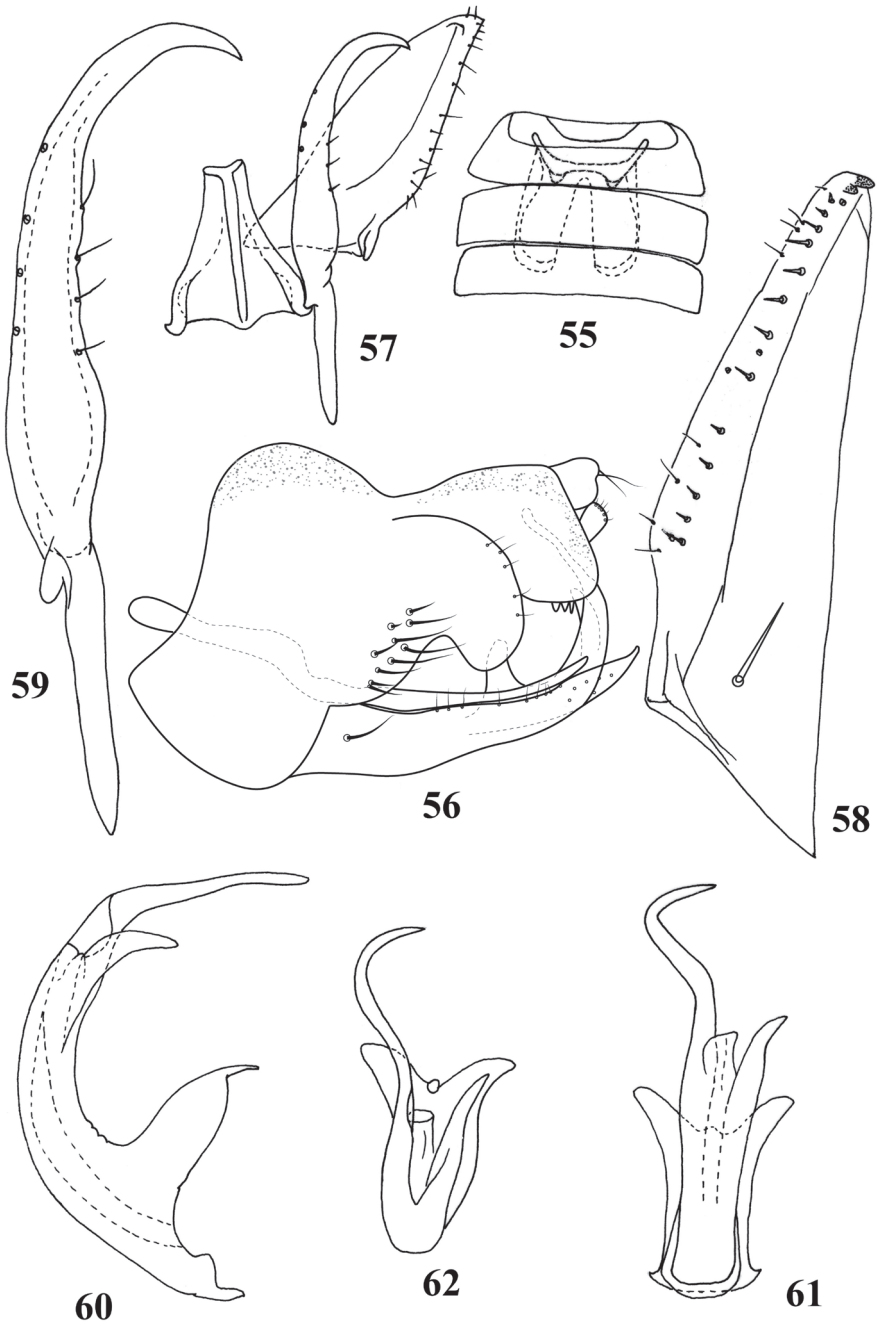

Figures 55–62. Male genitalia and sternal abdominal apodemes of *Paracyba biprocessa* sp. nov. **55** sternal abdominal apodemes **56** genitalia capsule, lateral view **57** paramere, connective and subgenital plate, dorsal view **58** subgenital plate **59** paramere **60** aedeagus, lateral view **61** aedeagus, posterior view **62** apical part of aedeagus, dorsal view.

Male sternal abdominal apodemes extending to 4th or 5th sternite.

Male genitalia. Genital capsule short; pygofer side with a weekly sclerotized area near middle of hind margin; several rigid setae at caudo-ventral angle and macrosetae on middle part. Subgenital plate gradually narrowing towards apex with a macroseta at base and row of short peg-like setae from middle to apex of outer margin; two rigid setae apically and few fine setae on inner margin subapically. Connective laminate, with stem well developed. Paramere with caudad part long, with several setae on outer margin. Aedeagal shaft with distal asymmetrical processes; with long membranous terminal part.

Distribution. Oriental Region.

***Shamala annulata* sp. nov.**

http://zoobank.org/3853DE59-4325-4DFB-A39B-F3364B8B0CC4

Figs 24, 28, 32, 36, 63–71

Note. Body cream (Fig. 24). Scutellum orange with basal triangles yellowish green (Fig. 28). Forewing bluish white with brownish patch on CuA".

Abdominal apodemes extending to distal margin of 4th sternite.

Male genitalia. Pygofer side with several macrosetae ventrally and rigid short setae terminally (Figs 63, 64). Subgenital plate long and narrow with row of short peg-like setae from middle part to apex on outer margin (Fig. 66). Connective slender with short central lobe, stem relatively long (Fig. 68). Aedeagal shaft with four asymmetrical processes apically, of which two dorsal processes are longer and curved inward forming a ring-like shape, two ventral processes straight and slightly divergent (Figs 69–71).

Specimens examined. ***Holotype***: ♂, China, Yunnan Province, Sanchahe, 7.vi.1991, coll. Rungang Tian. ***Paratypes***: 3♂♂, same data as holotype.

Measurement. Male, 2.94 mm (including wing).

Etymology. The name of this species is derived from the Latin word "annulus", referring to the two dorsal processes of the aedeagal shaft forming a ring-like shape.

Remarks. This new species resembles *Shamala ricasta* Dworakowska, 1981 in the structure of the male genitalia, but it differs from the latter by the two longer apical processes of aedeagal shaft forming a ring-like shape.

Acknowledgements

We are very grateful to Dr I. Dworakowska for her contribution to the knowledge of Chinese Typhlocybinae. We give sincere thanks to students in the Entomological Museum of Northwest A&F University for their great help in obtaining specimens. We also thank Prof. John Richard Schrock (Emporia State University, USA) for proofreading of the manuscript and giving us valuable advice before submission. We extend our heartfelt gratitude to Mick Webb and Valérie Lemaître (The Natural History Museum,

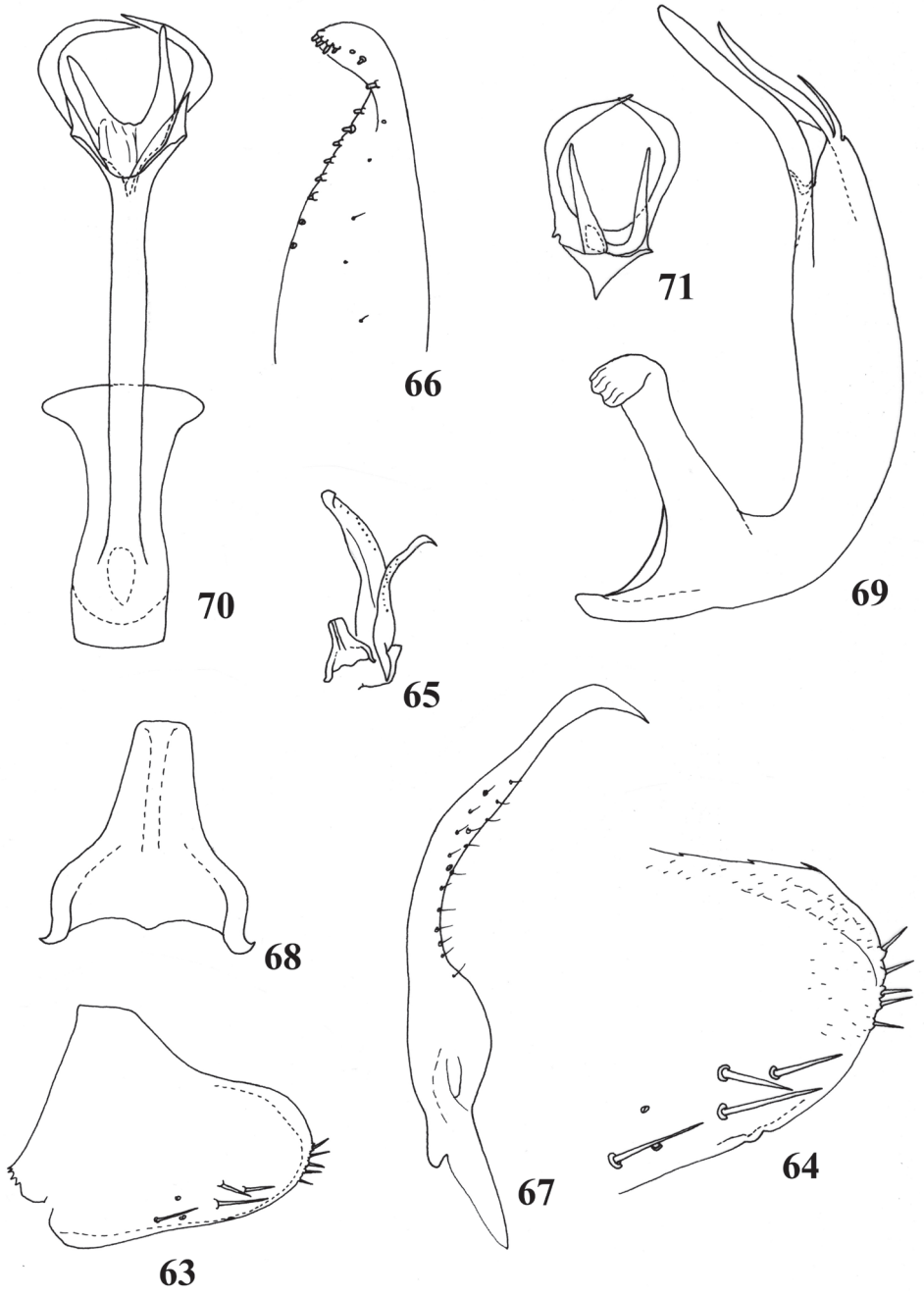

Figures 63–71. Male genitalia of *Shamala annulata* sp. nov. **63, 64** pygofer side, lateral view **65** paramere, connective and subgenital plate, dorsal view **66** subgenital plate **67** paramere **68** connective **69** aedeagus, lateral view **70** aedeagus, posterior view **71** apical part of aedeagus, ventral view.

London, UK) and anonymous reviewers for their earnest reviews. This study is supported by the National Natural Science Foundation of China (32070478, 31372233, 31420103911) and The Ministry of Science and Technology of the People's Republic of China (2006FY120100, 2015FY210300).

References

Anufriev GA (1975) Notes on the genus *Edwardsiana* Zachv. and *Pithyotettix* Rib. (Homoptera: Cicadellidae) with descriptions of two new species. Bulletin de l'Academie Polanaise des Sciences (Série des Sciences Biologiques) 23: 531–536.

Dlabola J (1958) A reclassification of Palaearctic Typhlocybinae (Homopt., Auchenorrh). Časopis Československé Společnosti Entomologické 55: 44–57.

Dlabola J (1961) Die Zikaden von Zentralasien, Dagestan und Transkaukasien (Homopt. Auchenorrhyncha). Acta Entomologica Musei Nationalis Pragae 34: 241–358.

Dlabola J (1967) Ergebnisse der 2. Mongolisch-tschechoslowakischen entomologisch-botanischen Expedition in der Mongolei. Nr. 12: Reisebericht, Lokalitateniibersicht und Bearbeitung der gesammelten Zikaden (Homopt., Auchenorrh.). Acta Faunistica Entomologica Musei Nationalis Pragae 12: 207–230.

Dmitriev DA (2003) 3i interactive keys and taxonomic databases. http://dmitriev.speciesfile.org/ [Accessed on: 2022-1-7]

Dubovsky GK (1966) Cicadina (Auchenorrhyncha) of the Fergana Valley. Uzbekistan SSR, Tashkent, 256 pp. [In Russian]

Dworakowska I (1971) *Opamata* gen. n. from Viet-Nam and some other Typhlocybini (Auchenorrhyncha, Cicadellidae, Typhlocybinae). Bulletin de l'Academie Polonaise des Sciences (Série des Sciences Biologiques) 19: 647–657.

Dworakowska I (1977) On some Typhlocybinae from Vietnam (Homoptera: Cicadellidae). Folia Entomologica Hungarica 30: 9–47.

Dworakowska I (1980) On some Typhlocybinae from India (Homoptera, Auchenorrhyncha, Cicadellidae). Entomologische Abhandlungen und Berichte aus dem Staatlichen Museum fur Tierkunde in Dresden 43: 151–201.

Dworakowska I (1981) On some Typhlocybini from India and Nepal (Auchenorrhyncha, Cicadellidae, Typhlocybinae). Bulletin de l'Academie Polonaise des Sciences (Série des Sciences Biologiques) 28: 593–602.

Dworakowska I (1982) Typhlocybini of Asia (Homoptera, Auchenorrhyncha, Cicadellidae). Entomologische Abhandlungen und Berichte aus dem Staatlichen Museum fur Tierkunde in Dresden 45: 99–181.

Dworakowska I (1993) Remarks on *Alebra* Fieb. and Eastern Hemisphere Alebrini (Auchenorrhyncha: Cicadellidae: Typhlocybinae). Entomotaxonomia 15(2): 91–121.

Huang M, Zhang YL (2002) A taxonomic study of the genus *Thampoa* Mahmood from China (Homoptera: Cicadellidae: Typhlocybinae). Entomotaxonomia 27: 290–303.

Kusnezov V (1932) Spisok: vrediteli selskogo hozjnjstva, podotrjad cikadovye. In: Vrednye nasekomye SSSR i sopredel'nyh stran, I. Trudy po Zashchite Rastenii Ser. I, Entomologiia.

Linnaeus C (1758) II. Hemiptera. Systema Naturae: per regna tria naturae, secundum classes, ordines, genera, species cum characteribus, differentiis, synonymis, locis. Editio decima, reformata. L. Salvii, Stockholmiae, 1: 1–824. https://doi.org/10.5962/bhl.title.542

Matsumura S (1931) A revision of the Palaearctic and Oriental typhlocybid genera with descriptions of new species and new genera. Insecta Matsumurana 6: 55–91.

Matsumura S (1932) A revision of the Palaearctic and Oriental typhlocybid genera with descriptions of new species and new genera. Insecta Matsumurana 6: 93–120.

Mitjaev ID (1963) Data on the fauna and biology of Typhlocybinae (Homoptera; Auchenorrhyncha) of Kazakhstan. Trudy Instituta Zoologii Akademii Nauk Kazakhskoi SSR 21: 49–73. [In Russian]

Mitjaev ID (1967) On systematics and ecology of cicades [sic!] of the genus *Linnavuoriana* Dlab., 1958 (Homoptera, Typhlocybinae) of south-eastern Kazakhstan. Zoologicheskii Zhurnal 46: 710–714. [In Russian]

Sohi AS, Mann JS, Thapa VK (1990) A new species of *Hiratettix* Matsumura (Cicadellidae: Typhlocybinae) from Nepal. Journal of Insect Science 3: 115–117.

Takahashi S (1928) Treatise on Vegetable Insects. Sosai Gaichu Kakuron, 442 pp.

Vilbaste J (1968) Über die Zikadenfauna des Primorje Gebietes. Valgus, Tallinn, 178 pp. [In Russian]

Vilbaste J (1980) Homoptera Cicadinea of Tuva. Valgus, Tallinn, 217 pp. [In Russian]

Wagner W (1937) Am licht gefangene Typhlocybiden. Verhandlungen des Vereins für Naturwissenschaftliche Heimatforschung zu Hamburg 26: 154–155.

Yan B (2019) Study on Taxonomy and Molecular Systematics of Typhlocybini from China (Hemiptera: Cicadellidae: Typhlocybinae). Guizhou University, Guiyang, Guizhou, 1–3. [in Chinese]

Zachvatkin AA (1929) Description d'une nouvelle espèce du genre *Edwardsiana* Jaz. 1929 (Homoptera, Eupterygidae) des environs de Moscou. Revue Russe d'Entomologie 23: 262–265.

Zachvatkin AA (1949) II Vrediteli plodovo-jagodnyh kultur. Podotrjad (Cicadoidea) cikadovye. In: Vrednye zivotnye Srednej Azii. Moskva/Leningrad, 220–222.

Zhang YL (1990) A Taxonomic Study of Chinese Cicadellidae (Homoptera). Tianze Eldonejo, Yangling, Shaanxi, 218 pp. [in Chinese]

ZooKeys 1082: 153–178 (2022)
doi: 10.3897/zookeys.1082.75400
https://zookeys.pensoft.net

RESEARCH ARTICLE

A peer-reviewed open-access journal
ZooKeys
Launched to accelerate biodiversity research

Meotipa species (Araneae, Theridiidae) from China

Zhongwei Deng[1,2,3], Ingi Agnarsson[3,4], Zhanqi Chen[1], Jie Liu[2,3,5]

1 *CAS Key Laboratory of Tropical Forest Ecology, Xishuangbanna Tropical Botanical Garden, Chinese Academy of Sciences, Mengla, Yunnan 666303, China* **2** *Hubei Key Laboratory of Regional Development and Environmental Response, Faculty of Resources and Environmental Science, Hubei University, Wuhan 430062, China* **3** *The State Key Laboratory of Biocatalysis and Enzyme Engineering of China, College of Life Sciences, Hubei University, Wuhan 430062, Hubei, China* **4** *University of Vermont, Department of Biology, 109 Carrigan Drive, Burlington, VT 05405–0086, USA* **5** *School of Nuclear Technology and Chemistry and Biology, Hubei University of Science and Technology, Xianning 437100, Hubei, China*

Corresponding authors: Zhanqi Chen (chenzhanqi@xtbg.ac.cn), Jie Liu (sparassidae@aliyun.com)

Academic editor: Gergin Blagoev | Received 17 September 2021 | Accepted 7 December 2021 | Published 20 January 2022

http://zoobank.org/2D3FA191-A984-4F5A-99D5-C34473D5DC93

Citation: Deng Z, Agnarsson I, Chen Z, Liu J (2022) *Meotipa* species (Araneae, Theridiidae) from China. ZooKeys 1082: 153–178. https://doi.org/10.3897/zookeys.1082.75400

Abstract

In an ongoing effort to expand knowledge of the Chinese cobweb spider fauna (Theridiidae), the genus *Meotipa* Simon, 1894 is reviewed. Two new species are described, *Meotipa pseudopicturata* **sp. nov.**, *Meotipa striata* **sp. nov.**, and five known species are redescribed: *Meotipa argyrodiformis* (Yaginuma, 1952), *Meotipa pulcherrima* (Mello-Leitão, 1917), *Meotipa picturata* Simon, 1895, *Meotipa spiniventris* (O. Pickard-Cambridge, 1869), and *Meotipa vesiculosa* Simon, 1895.

Keywords

Cobweb spider, comb-footed spider, flattened black spines, long-legged theridiid spiders, new species, taxonomy

Introduction

Meotipa Simon, 1895 is an enigmatic and taxonomically poorly understood theridiid genus, in part because it was synonymized with the much larger and more widespread genus *Chrysso* by Levi (1962) until being resurrected by Deeleman-Reinhold (2009). *Meotipa* are long-legged theridiid spiders bearing a conspicuous synapomorphic feature: flattened black spines on the abdomen and/or legs (Deeleman-Reinhold 2009). However,

some *Chrysso* species also have obvious spines on the abdomen which are often sharp or needle-like (Kulkarni et al. 2017), such as *Chrysso lingchuanensis* Zhu & Zhang, 1992 known from China. Their relationship needs further research based on more evidence, such as molecular data. *Meotipa* contains 18 known species (World Spider Catalog 2021) that are quite common in gardens and secondary forests across the tropics in Asia (Deeleman-Reinhold 2009; Kulkarni et al. 2017). Nine *Meotipa* species are known from China: *M. argyrodiformis* (Yaginuma, 1952), *Meotipa capacifaba* Li, Liu, Xu & Yin, 2020, *Meotipa luoqiae* Lin & Li, 2021, *Meotipa menglun* Lin & Li, 2021, *M. picturata* Simon, 1895, *M. pulcherrima* (Mello-Leitão, 1917), *M. spiniventris* (O. Pickard-Cambridge, 1869), *M. vesiculosa* Simon, 1895, and *Meotipa zhengguoi* Lin & Li, 2021.

In the past two years, a series of surveys for Chinese theridiid spiders were conducted by the colleagues of Hubei University in China and yielded numerous new species. This is our second paper on Chinese cobweb spiders with the aim to review the Chinese *Meotipa* spiders and includes two new species, one new record for Hunan, and four known species (Li et al. 2021).

Materials and methods

In the field, we collected cobweb spiders by using visual searching and beating vegetation. We attempted to take photographs of every species, alive, in the field, and webs of all species encountered in web were photographed. All specimens were preserved in 99% ethanol and examined with an Olympus SZX16 stereomicroscope; details were further investigated with an Olympus BX51 compound microscope. Male palps and female genitalia were examined and their photographs taken after dissection from the spider bodies. The epigynum was cleared with Proteinase K. Habitus and photographs were obtained using a Leica 205C digital microscope. We added some key marginal lines for genitalia photographs using the Apple pencil (2nd generation) and edited the photographs in Adobe Photoshop 2020. Leg measurements are shown as: total length (femur, patella, tibia, metatarsus, tarsus). The terminology used in text and figure legends, and palpal homologies follow Agnarsson (2004a) and Agnarsson et al. (2007a). Geographical co-ordinates were recorded in decimal degrees. All measurements are given in millimeters. All specimens are deposited in the Centre for Behavioural Ecology and Evolution, College of Life Sciences, Hubei University, Wuhan, China (**CBEE**). The abbreviations used in this paper are as follows:

ALE anterior lateral eyes;
AME anterior median eyes;
C conductor;
CD copulatory duct;
CO copulatory opening;
E embolus;
FD fertilization duct;
MA median apophysis;
PE posterior eyes;
PLE posterior lateral eyes;
PME posterior median eyes;
S spermathecae;
SE stuck emboli.
ST subtegulum;
T tegulum;

Taxonomic account

Family Theridiidae Sundevall, 1833
Subfamily Theridiinae Sundevall, 1833

Genus *Meotipa* Simon, 1895
Table 1

Diagnosis. Female of *Meotipa* differs from all other theridiids by the conspicuous flattened black spines on the abdomen and/or legs. Therefore, they are often referred to as spiny theridiids. *Meotipa* males are significantly smaller than females. The male palp of *Meotipa* can be distinguished from other theridiids by the spoon-shaped conductor and embolus being thin and short, with the straight base, completely surrounded by the spoon-shaped conductor or the tip of embolus, which is opposite to the conductor (except *Meotipa bituberculata*, see Deeleman-Reinhold 2009: 419, figs 20–37). The species included in *Meotipa* are given below, with their distributions.

Table 1. The distributions of known *Meotipa* species in the world.

Meotipa andamanensis (Tikader, 1977) (♀)	India (Andaman Is.)
Meotipa argyrodiformis (Yaginuma, 1952) (♂♀)	China, Japan, Philippines, India
Meotipa bituberculata Deeleman-Reinhold, 2009 (♂♀)	Indonesia
Meotipa capacifaba Li, Liu, Xu & Yin, 2020 (♂♀)	China
Meotipa impatiens Deeleman-Reinhold, 2009 (♂♀)	Malaysia, Indonesia
Meotipa luoqiae Lin & Li, 2021 (♂)	China
Meotipa makiling (Barrion-Dupo & Barrion, 2015) (♀)	Philippines
Meotipa menglun Lin & Li, 2021 (♂)	China
Meotipa multuma Murthappa, Malamel, Prajapati, Sebastian & Venkateshwarlu, 2017 (♂♀)	India
Meotipa pallida Deeleman-Reinhold, 2009 (♀)	Indonesia
Meotipa picturata Simon, 1895 (♂♀)	India, Thailand, Laos, Indonesia
Meotipa pulcherrima (Mello-Leitão, 1917) (♂♀)	tropical Africa, introduced to the Americas, Papua New Guinea, China, Korea, Japan, and Pacific Islands
Meotipa sahyadri Kulkarni, Vartak, Deshpande & Halali, 2017 (♂♀)	India
Meotipa spiniventris (O. Pickard-Cambridge, 1869) (♂♀)	Sri Lanka to Taiwan, China, Japan, introduced to the Netherlands
Meotipa thalerorum Deeleman-Reinhold, 2009 (♂♀)	Malaysia and Indonesia
Meotipa ultapani Basumatary & Brahma, 2019 (♀)	India
Meotipa vesiculosa Simon, 1895 (♂♀)	China, Vietnam to Japan, Philippines, Indonesia
Meotipa zhengguoi Lin & Li, 2021 (♂)	China

Meotipa argyrodiformis (Yaginuma, 1952)
Figures 1A–H, 10

Ariamnes argyrodiformis Yaginuma, 1952: 14, figs 1–6 (description of female).
Topo argyrodiformis Yaginuma, 1955: 16 (transferred from *Ariamnes*, at the time in synonymy with *Argyrodes*).

Chrysso argyrodiformis Yaginuma, 1965: 35 (transferred from *Topo*, at the time in synonymy with *Thwaitesia*); Yaginuma 1986: 45, fig. 24.3 (female, description of male); Chikuni 1989: 32, fig. 14 (male and female); Chen and Gao 1990: 93, fig. 116 (female); Barrion and Litsinger 1995: 419, figs 248a–i, 249a, b (male and female); Yoshida 2003: 128, figs 338, 343–345, 584 (male and female); Yin et al. 2012: 293, figs 106a–d (female); Sen et al. 2015: 85, figs 493–498, pl. 19 (female).
Meotipa argyrodiformis Yoshida, 2009: 378, figs 208–210 (transferred from *Chrysso*).

Material examined (holotype not examined). Hunan Province: 9♀, Changsha City, Yuelu Mountain Scenic Area (28.19°N, 112.94°E, 210 m), 12 August 2018, Z.C. Li & Z.W. Deng leg. (CBEE).

Diagnosis. *Meotipa argyrodiformis* is similar to *M. pulcherrima* (Fig. 2A–H) in: having the abdomen pointed to a tubercle posteriorly (Fig. 1B), lacking obvious copulatory openings, and having a spoon-shaped conductor in the male palp. However, it can be distinguished from the latter by the following combination of characters: (1) the abdomen extends beyond spinnerets ~ 3/4 of total abdomen length in *M. argyrodiformis* (Fig. 1A), but less than half in *M. pulcherrima* (Fig. 2A); (2) the epigynum does not have a tongue-shaped apophysis posteriorly and medially in *M. argyrodiformis* (Fig. 1D), but has in *M. pulcherrima* (Fig. 2D); (3) the copulatory ducts are tube-shaped in *M. argyrodiformis* (Fig. 1F), but spherical in *M. pulcherrima* (Fig. 2F); (4) the cymbium is long and nearly ovoid in *M. argyrodiformis* (see Yoshida 2003: fig. 345), but shorter and nearly spherical in *M. pulcherrima* (see Yoshida 2003: fig. 342); (5) the embolus is long with a twisted tip, extending beyond conductor in *M. argyrodiformis* (see Yoshida 2003: fig. 345), but short and straight, completely surrounded by conductor in *M. pulcherrima* (see Yoshida 2003: fig. 342).

Description. Female. Total length 5.20; Prosoma length 1.20, width (at middle) 0.81, height (at middle) 0.88; Opisthosoma length 4.05, width (at middle) 1.97, height (at middle) 2.46; Eye diameters: ALE 0.07, AME 0.07, PLE 0.07, PME 0.07; Eye interdistances: AME–AME 0.05, ALE–ALE 0.15, PLE–ALE contiguous, PLE–PLE 0.22, PME–PME 0.07, PME–PLE 0.07, AME–ALE 0.05; Clypeus height (at middle) 0.38, width (at middle) 0.16; Measurements of legs: Leg I (right) 11.18 [4.93, 0.84, 2.36, 2.34, 0.71], II (right) 6.72 [1.85, 0.49, 1.50, 2.17, 0.71], III (right) 4.61 [1.44, 0.38, 0.85, 1.42, 0.52], IV (right) 9.27 [2.80, 0.59, 2.69, 2.43, 0.76]. Carapace rather ovate with V-shaped longitudinal fovea, cephalic area short and narrow, thoracic area widest between coxae II and III (Fig. 1A). Eyes in two rows with black or pale brown ring, strongly recurved (Fig. 1B); anterior eye row curved, shorter than the straight posterior eye row. Sternum yellow, longer than wide, lateral margins slightly indented. Labium contiguous to the sternum, yellow with a brown, rounded to slightly triangular, apical margin (Fig. 1C). Chelicerae vertical, yellow with pale brown fang. Yellow legs long and slender with or without gray bands and bearing a few dark brown short spines, tibiae with two dorsal spines in legs I, II and IV, and one in leg III, tarsus three-clawed with 5–7 teeth in the superior claws. Leg formula 1423. Pedipalp yellow and length ~ 2/3 carapace, single-clawed, with many short hairs; tibia laterally with

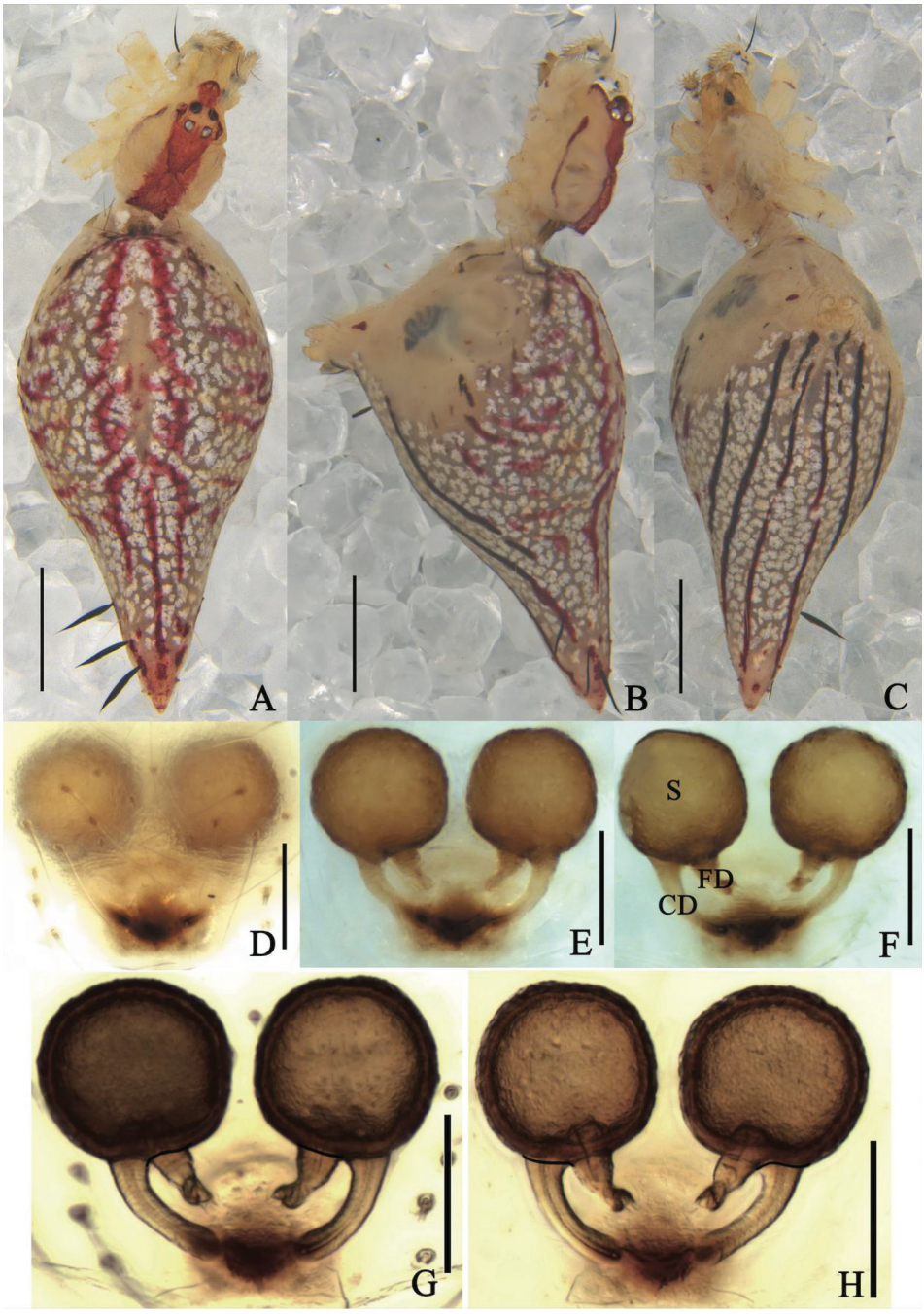

Figure 1. *Meotipa argyrodiformis* (Yaginuma, 1952) **A–C** female habitus (some flattened black spines on the abdomen and legs were broken off during photography) (**A** dorsal **B** prolateral **C** ventral). **D–H** epigynum (**D** ventral, on the body **E, F** in alcohol **E** ventral **F** dorsal **G, H** in gum arabic **G** ventral **H** dorsal). Scale bars: 1 mm **(A–C)**; 0.1 mm **(D–H)**. Abbreviations: CD = copulatory duct, FD = fertilization duct, S = spermathecae.

a lanceolate spine. Abdomen pale yellowish, anterior portion overhangs the carapace, approximately triangular in lateral view, dorsum with red cardiac marking and several transverse reddish brown bands laterally. Posterior area of ventral abdomen with deep red stripes, pointed posteriorly, with six black and medially broad setae with sharp ends, and ventrally projected spinnerets (Fig. 1B). Epigynum forming a triangular atrium, without obvious copulatory openings (Fig. 1D); two round spermathecae can be clearly seen in ventral view (Fig. 1E); copulatory ducts long, narrow, almost straight; fertilization ducts short, close to copulatory ducts, and both of them are located at the directly below spermathecae (Fig. 1F); spermathecae round, slightly separate from each other (Fig. 1H).

Male. Not collected.

Distribution. China (Anhui, Fujian, Hunan, Liaoning, Shaanxi, Sichuan, Taiwan, Zhejiang), Japan, Philippines, India.

Meotipa pulcherrima (Mello-Leitão, 1917)

Figures 2A–H, 9, 10

Argyrodes pulcherrimus Mello-Leitão, 1917: 86, figs 7, 8 (description of female).
Meotipa clementinae Petrunkevitch, 1930: 212, figs 61, 62 (description of female); Schmidt 1956a: 30, fig. 6 (description of male); Schmidt, 1956b: 240, fig. 1 (female).
Argyrodes elevatus Exline and Levi, 1962: 135 (synonymy, rejected by Levi 1967a).
Chrysso clementinae Levi, 1962: 231, figs 71–75 (male and female); Müller 1992: 99, figs 5, 6 (female).
Chrysso pulcherrima Levi, 1967a: 26 (removed female from synonymy of *Argyrodes elevatus*, synonymy of male); Levi 1967b: 182, figs 28–31 (male and female); Zhu and Zhang 1992: 23, fig. 3A–D (male and female); Yoshida 1993: 30, figs 10–12, 20 (male and female); Zhu 1998: 54, fig. 28A–D (male and female); Song et al. 1999: 103, fig. 50A, B, J (male and female); Yoshida 2003: 126, figs 337, 341, 342 (male and female, synonymy); Seo 2005: 123, fig. 2A, B (male).
Chrysso mussau Chrysanthus, 1975: 48, figs 174–177 (descriptions of male and female).
Meotipa pulcherrima Yoshida, 2009: 378, figs 211–213 (transferred from *Chrysso*).

Note. The taxonomy of *M. pulcherrima*, presumed to be widely introduced, including to its type locality in Brazil, requires further scrutiny. Our specimens are not identical to the given type illustrations, and further variation appears globally evident. However, solving the global taxonomy of *M. pulcherrima* is outside the scope of this manuscript and required dedicated research.

Material examined (holotype not examined). Hunan Province: 7♀, Zhangjiajie City, Sangzhi County, Quanyushan Leisure Park (29.48°N, 110.16°E, 370 m), 5 May 2018, F.X. Liu & Z.C. Li leg. (CBEE).

Diagnosis. *Meotipa pulcherrima* is similar to *M. capacifaba* Li, Liu, Xu & Yin, 2020 (see Li et al. 2020: figs 1A–J, 2A–E, 3A–E) by shared characters such as raised

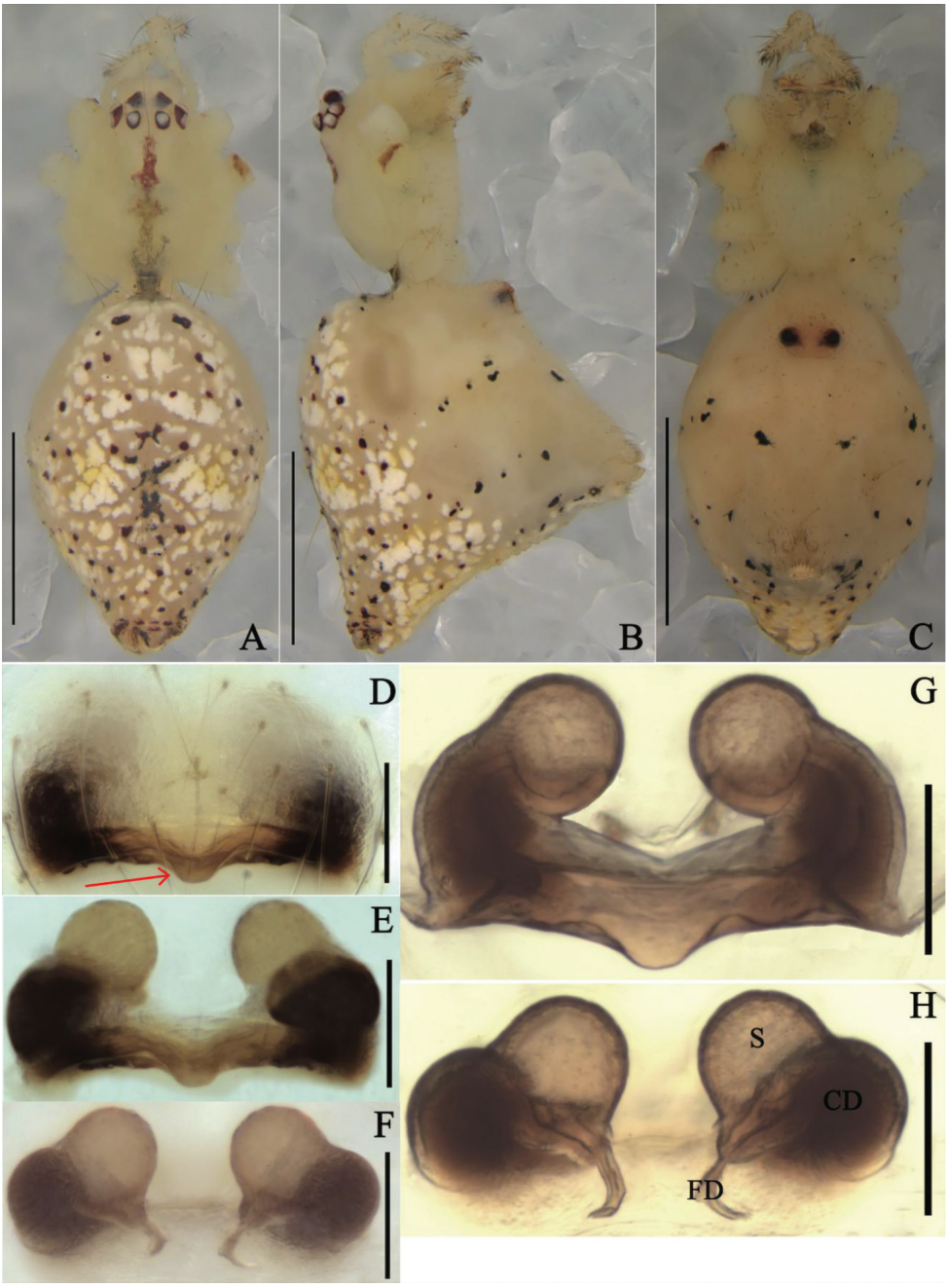

Figure 2. *Meotipa pulcherrima* (Mello-Leitão, 1917) **A–C** female habitus (flattened black spines on the abdomen and legs were broken off during photography) (**A** dorsal **B** prolateral **C** ventral). **D–H** epigynum (**D** ventral, on the body, and the arrow points to tongue-shaped apophysis **E, F** in alcohol **E** ventral **F** dorsal **G, H** in gum arabic **G** ventral **H** dorsal). Scale bars: 1 mm (**A–C**); 0.1 mm (**D–H**). Abbreviations: CD = copulatory duct, FD = fertilization duct, S = spermathecae.

eyes, raised carapace posteriorly, and spherical copulatory ducts (Fig. 2G), but it can be distinguished from the latter by the following characters: (1) the copulatory openings are inconspicuous in *M. pulcherrima* (Fig. 2D), but obvious in *M. capacifaba* (see Li et al. 2020: fig. 2A); (2) the posterior margin of atrium has a tongue-shaped protrusion medially in *M. pulcherrima* (Fig. 2E), but not in *M. capacifaba* (see Li et al. 2020: fig. 2A); (3) the conductor is broad with a sharp point in *M. pulcherrima* (see Levi 1962: figs 74, 75), but relatively narrow with a blunt point in *M. capacifaba* (see Li et al. 2020: figs 2D, 3D).

Description. Female. Total length 3.03; Prosoma length 0.96, width (at middle) 0.90, height (at middle) 0.61; Opisthosoma length 2.07, width (at middle) 1.27, height (at middle) 1.89; Eye diameters: ALE 0.07, AME 0.09, PLE 0.08, PME 0.09; Eye interdistances: AME–AME 0.09, ALE–ALE 0.55, PLE–ALE contiguous, PLE–PLE 0.30, PME–PME 0.08, PME–PLE 0.11, AME–ALE 0.02; Clypeus height (at middle) 0.21, width (at middle) 0.60; Measurements of legs: Leg I (right) 8.3 [2.59, 0.42, 2.34, 2.16, 0.79], II (right) 5.42 [2.03, 0.40, 1.04, 1.43, 0.52], III (right) 3.73 [1.49, 0.24, 0.85, 0.73, 0.42], IV (right) 6.33 [2.40, 0.39, 0.90, 2.00, 0.64]. Carapace with a central reddish brown longitudinal band; cephalic area relatively long and narrow; clypeus bulged outward (Fig. 2A). Median furrow is round, deep, and the radial furrow is not obvious (Fig. 2A). Eyes strongly recurved. AME separation is greater than AME-ALE, and PME separation is also greater than PLE-PME; ALE-PLE contiguous. All eyes nearly uniform in size with brown rings surrounding (Fig. 2A, B). Sternum yellow, heart-shaped. Labium clearly distinguish from the sternum, yellow with brown markings, approximately triangular in shape. Chelicera yellow with pale red fang (Fig. 2C). Yellow legs long and slender with dark brown spots; the ends of tibiae and the bases and ends of metatarsus of each leg have dark brown rings. Leg formula 1423. Pedipalp yellow with many short hairs distally (Fig. 2A, B). Abdomen triangular in lateral view, with caudal region extending upwardly beyond spinnerets. There are 14 feather-like spines on the top of the protuberance and before the protuberance reaches the spinnerets, which break easily (Fig. 2A–C). Dorsum of abdomen yellow with dark red spots. The venter of the abdomen has central black spots on each side (Fig. 2B). Epigynum with a big atrium and inconspicuous copulatory openings (Fig. 2D); copulatory ducts swelling distally, sphere-shaped (Fig. 2E, F); spermathecae smaller than distal end of copulatory ducts, sphere-shaped (Fig. 2H); fertilization ducts are located at the intersection of copulatory ducts and spermathecae (Fig. 2H).

Male. Not collected.

Distribution. China (Fujian; Guangxi; Hainan; Hunan, newly recorded; Taiwan; Zhejiang), Japan, Korea, Pacific Is., Papua New Guinea; also tropical Africa and widespread across the Americas (after Levi 1962).

Remarks. Although we did not examine the female holotype of *M. pulcherrima*, the triangular abdomen with caudal region extending upwardly beyond spinnerets, the short and swollen copulatory ducts, and the sphere-shaped spermathecae all indicate our specimens belong to *M. pulcherrima* according to the original, albeit simple illustrations by Mello-Leitão (1917: 86, figs 7, 8) and detailed illustrations

by Zhu et al. (1992: 23, fig. 3A–D) and Yoshida (2003: 126, figs 337, 341, 342).We also note some slight differences in our specimens against the original illustrations of Brazilian specimens by Mello-Leitão (1917). The specimens we collected only has half of the abdomen extending beyond the spinnerets (Fig. 2B), but the specimens from Brazil have 2/3 of abdomen extending beyond them (see Mello-Leitão 1917: 86, fig. 7). Meanwhile, the shadow of the copulatory ducts and the fertilization ducts can be seen from the ventral view of epigynum, and the shadows on both sides look like two tadpoles in atrium, with fertilization ducts resembling their tails and copulatory ducts resembling their heads. The shadows of the specimen from Brazil in 1917 resemble two tadpoles swimming towards the middle of the atrium (see Mello-Leitão 1917: 86, fig. 8), but the shadows of our specimen resemble two tadpoles swimming to the sides of the atrium (Fig. 2C). However, the tails of tadpoles in the Brazilian specimens may be the spermathecae instead of the fertilization ducts according to the original illustrations. In addition, the posterior margin of atrium has a tongue-shaped protrusion medially in our individuals, but not in the Brazilian specimens.

Meotipa picturata Simon, 1895

Figures 3A–H, 9, 10

Meotipa picturata Simon, 1894: 519 (nomen nudum); Simon, 1895: 133 (description of female); Levi and Levi 1962: 47, figs 112–113 (female); Deeleman-Reinhold, 2009: 410, figs 1–3 (female); Kulkarni et al. 2017: 515, figs 39–44 (female); Murthappa et al. 2017: 590, figs 1A–J, 2A–F, 4A–D (description of male, female).

Material examined (holotype not examined). Yunnan Province: 1♀, Mengla County, Menlun Town, Xishuangbanna Tropical Botanical Garden, Chinese Academy of Sciences (21.92°N, 101.26°E, 550 m), 22 November 2019, J. Chen, J. Liu, Z.C. Li & B. Liang leg. (CBEE).

Diagnosis. *Meotipa picturata* is similar to *M. sahyadri* (Kulkarni et al. 2017: figs 1–38) in having a deep round atrium, the presence of rod-shaped projection with distinct oval openings distally in the median of the atrium (Fig. 3D). It can be distinguished from the latter by the following combination of characters: (1) the rod-shaped projection with three openings in this species (Fig. 3D), but two openings in *M. sahyadri* (see Kulkarni et al. 2017: figs 19, 22); (2) the distal shape of rod-shaped projection is flat, quadrangular in *M. picturata* (Fig. 3E), but triangular in *M. sahyadri* (see Kulkarni et al. 2017: figs 19, 21); (3) the copulatory ducts curve outward in *M. picturata* (Fig. 3F), but curve inward in *M. sahyadri* (see Kulkarni et al. 2017: fig. 18); (4) the end of copulatory ducts enter into the spermathecae ventrally in *M. picturata* (Fig. 3E), but laterally in *M. sahyadri* (see Kulkarni et al. 2017: fig. 18).

Description. Female. Total length 3.78; Prosoma length 1.31, width (at middle) 0.94, height (at middle) 0.47; Opisthosoma length 2.48, width (at middle) 1.17, height (at middle) 1.94; Eye diameters: ALE 0.08, AME 0.08, PLE 0.08, PME 0.08;

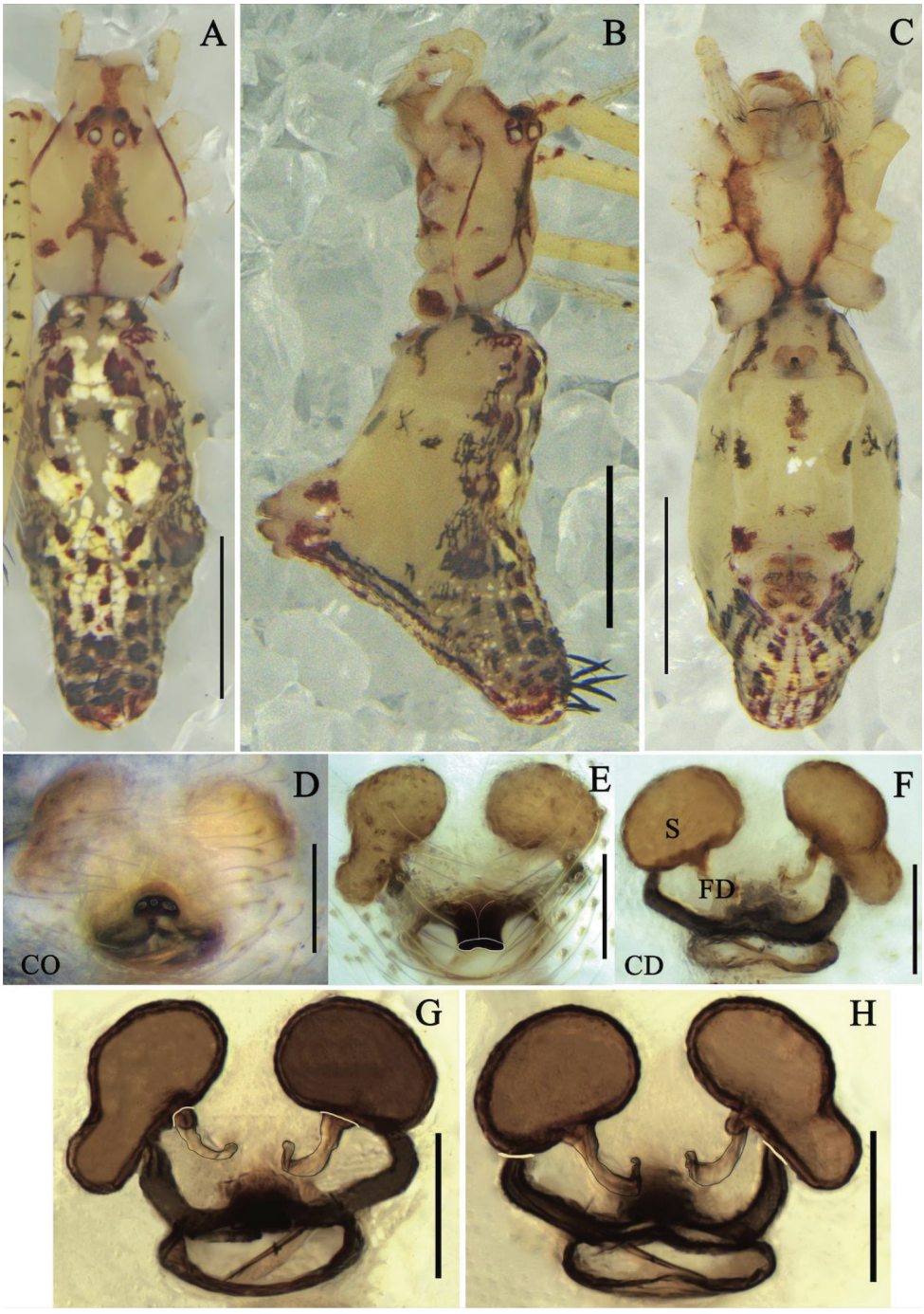

Figure 3. *Meotipa picturata* Simon, 1895 **A–C** female habitus (**A** dorsal **B** prolateral **C** ventral). **D–H** epigynum (**D** ventral, on the body **E, F** in the alcohol **E** ventral **F** dorsal **G, H** in gum arabic **G** ventral **H** dorsal). Scale bars: 1 mm (**A–C**); 0.1 mm (**D–H**). Abbreviations: CD = copulatory duct, FD = fertilization duct, S = spermathecae.

Eye interdistances: AME–AME 0.06, ALE–ALE 0.15, PLE–ALE contiguous, PLE–PLE 0.19, PME–PME 0.09, PME–PLE 0.05, AME–ALE 0.04; Clypeus height (at middle) 0.31, width (at middle) 0.20; Measurements of legs: Leg I (right) 13.96 [4.74, 0.49, 3.02, 4.71, 1.00], II (right) 8.88 [3.02, 0.51, 1.69, 2.86, 0.80], III (right) 7.87 [2.28, 0.26, 0.94, 1.53, 2.86], IV (right) 12.19 [4.14, 0.32, 2.96, 3.96, 0.81]. Prosoma glabrous; clypeus narrow. Carapace with a central arrowed-shaped marking forward; fovea broad, smooth with distinct depression (Fig. 3A). All eyes nearly uniform in size. Sternum triangular, yellow medially, lateral margins deep red and indented. Labium contiguous to the sternum, short with small hairs. Chelicera slanting, yellow with red fang (Fig. 3A–C). Yellow legs long and slender with short hairs. Tibia with lanceolate spines and black ring distally; femur with black spots dorsally and red spots distally. Leg formula 1423. Pedipalp yellow with small hairs; tibia distally with red semicircle ventrally; tarsus with a single claw. Opisthosoma triangular laterally, very broad in lateral view, its dorsum provided with alternate red and yellow spots, posterior region knobbed extending upwardly, provided with lanceolate spines. Venter transparent, some small red, yellow, and white patches posteriorly (Fig. 3B). Atrium broad, with a rod-shaped projection apically (Fig. 3D); copulatory openings depressed, contiguous, located on the end of rod-shaped projection (Fig. 3E); copulatory ducts broad, short, tube extensively curved entering into the base of spermathecae (Fig. 3F); spermathecae asymmetrical in shape, left spermatheca gourd-shaped, right spermatheca oval; fertilization duct long, originating from the medial of basal spermathecae (Fig. 3H).

Male. Not collected.

Distribution. China (Yunnan). New country and province record (Fig. 10).

***Meotipa spiniventris* (O. Pickard-Cambridge, 1869)**
Figures 4A–H, 5A–H, 9, 10

Theridion spiniventre O. Pickard-Cambridge, 1869: 384, pl. 12, figs 52–56 (description of male); Hammen 1949: 76, figs 1–3 (male and female); Yoshida 1977: 9, figs 1–4 (male and female); Song 1987: 128, fig. 89 (male and female).

Theridion buitenzorgi Strand, 1907: 412 (female).

Chrysso spiniventre Yaginuma, 1986: 46, fig. 24–5 (transferred from *Theridion*); Zhu 1998: 66, fig. 38A–D (male and female); Song et al. 1999: 107, fig. 50E–L (male and female); Yoshida 2003: 130, figs 346–350 (male and female).

Meotipa spiniventris Yoshida, 2009: 378, figs 214–216 (transferred from *Chrysso*).

Material examined (holotype not examined). Yunnan Province: 1♀, Mengla County, Menlun Town, Xishuangbanna Botanical Garden, Chinese Academy of Sciences (21.93°N, 101.25°E, 570 m), 22 March 2018, F.X. Liu & Z.C. Li leg. (CBEE); **Hainan Province:** 1♂, 5♀, Wuzhishan City, Shuiman Township, Wuzhishan (18.88°N, 109.66°E, 140 m), 15 April 2018, F.X. Liu & Z.C. Li leg. (CBEE); 3 ♀, Wuzhishan City (18.78°N, 109.52°E, 350 m), 15 April 2018, F.X. Liu & Z.C. Li

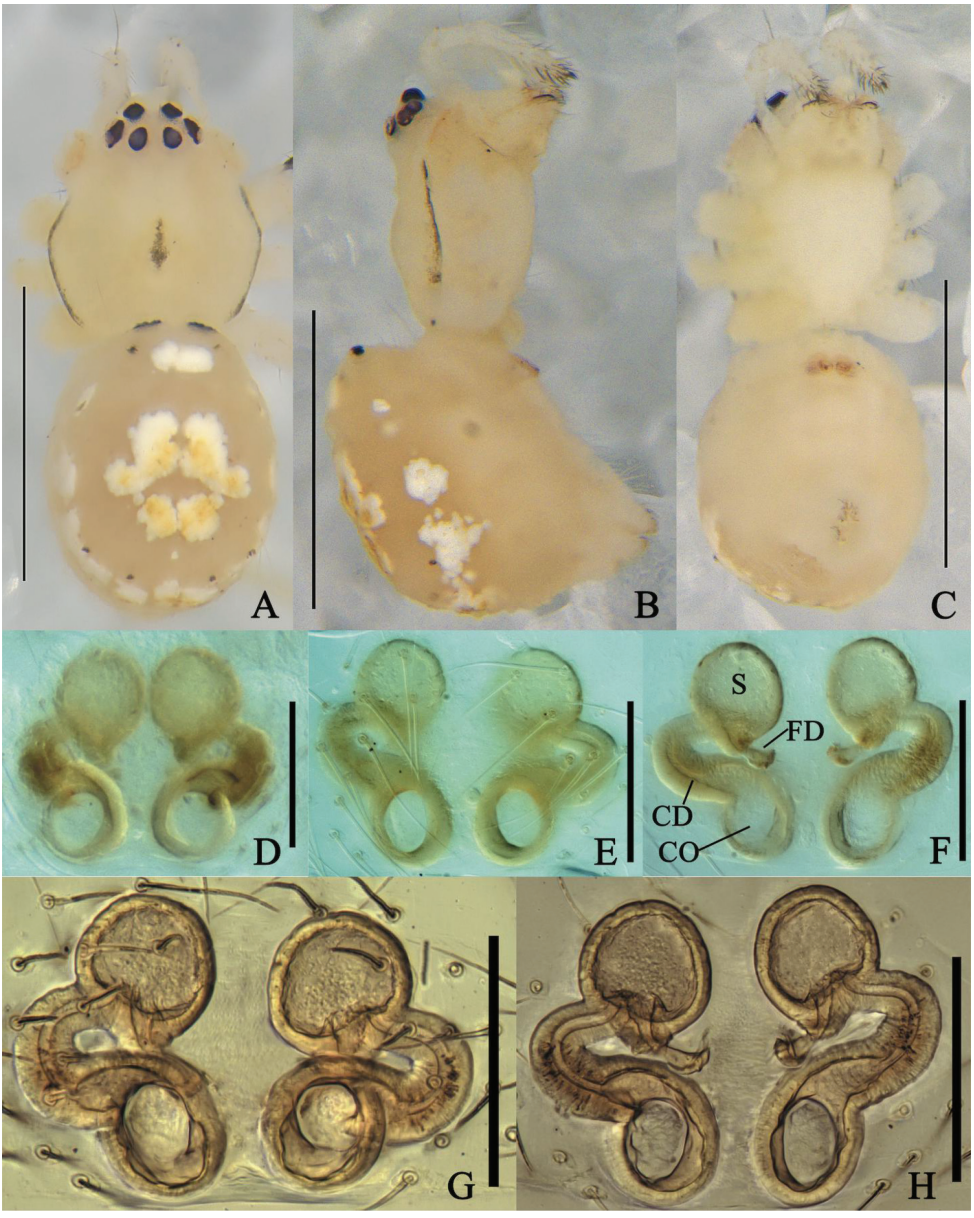

Figure 4. *Meotipa spiniventris* (O. Pickard-Cambridge, 1869) **A–C** female habitus (flattened black spines on the abdomen and legs were broken off during taking photographs) (**A** dorsal **B** Prolateral **C** ventral). **D–H** epigynum (**D** ventral, on the body **E, F** in the alcohol **E** ventral **F** dorsal **G, H** in gum arabic **G** ventral **H** dorsal). Scale bars: 1 mm (**A–C**); 0.1 mm (**D–H**). Abbreviations: CO = copulatory opening, CD = copulatory duct, FD = fertilization duct, S = spermathecae.

leg. (CBEE); 2 ♀, Wuzhishan City, Diaoluo Mountain (18.78°N, 109.52°E, 136 m), 17 April 2018, F.X. Liu & Z.C. Li leg. (CBEE); **Sichuan Province:** 1♀, Ya'an City, Lushan County, Longmen Town (30.25°N, 103.02°E, 810 m), 28 September 2018,

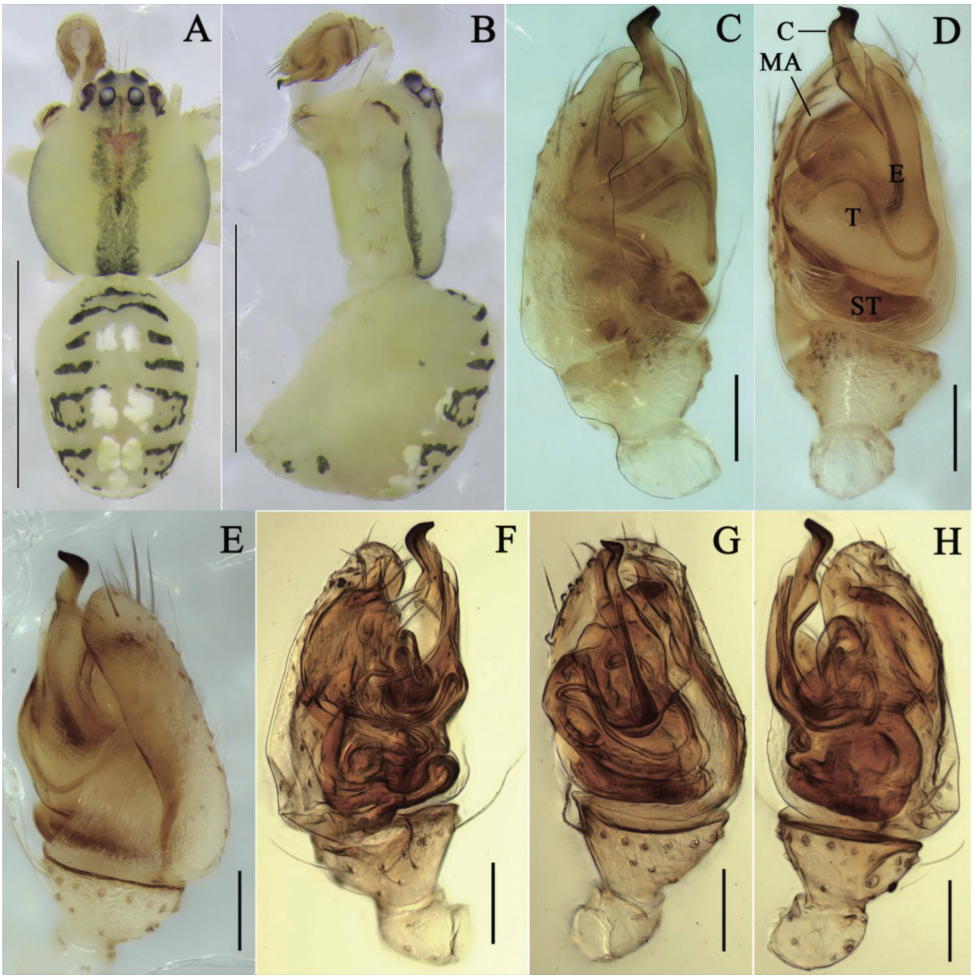

Figure 5. *Meotipa spiniventris* (O. Pickard-Cambridge, 1869) **A–B** male habitus (flattened black spines on the abdomen were absolutly absent) (**A** dorsal **B** prolateral). **C–H** pedipalp (**C–E** in the alcohol **C** prolateral **D** ventral **E** retrolateral **F–H** in gum arabic **F** prolateral **G** ventral **H** retrolateral). Scale bars: 1 mm (**A–C**); 0.1 mm (**D–I**). Abbreviations: E = embolus, MA = median apophysis, ST = subtegulum, T = tegulum.

F.X. Liu, Z.C. Li & Z.W. Deng leg. (CBEE); 1♀, Chengdu City, Qinglong Lake Park (30.65°N, 104.20°E, 490 m), 30 September 2018, F.X. Liu, Z.C. Li & Z.W. Deng leg. (CBEE); 1♀, Chengdu City, Tazishan Park (30.64°N, 104.12°E, 490 m), 30 September 2018, F.X. Liu, Z.C. Li & Z.C. Deng leg. (CBEE); **Hubei Province:** 1♀, Jianshi Country, Chaoyang Temple (30.60°N, 109.71°E, 490 m), 7 October 2018, F.X. Liu, Z.C. Li & Z.W. Deng leg. (CBEE).

Diagnosis. *Meotipa spiniventris* is similar to *M. multuma* Murthappa et al., 2017 (see Murthappa et al. 2017: figs 3A–E, 4E, F) in shared characters such as raised eyes, forward slanting clypeus and two separated copulatory openings. Females of *M. spiniventris* can be distinguished from *M. multuma* by the following combination

of characters: (1) the carapace has a central black band, opisthosoma with four median yellow and white patches, and four or five lanceolate spines posteriorly in *M. spiniventris* (Fig. 4A), but carapace without any marking, opisthosoma with a median black patch and 12–15 lanceolate spines posteriorly in *M. multuma* (see Murthappa et al. 2017: fig. 3A–C); (2) copulatory ducts short, extending to the lateral part of spermathecae (Fig. 4E) and fertilization ducts short in *M. spiniventris* (Fig. 4F, H), but the copulatory ducts are long and convoluted around spermathecae and fertilization ducts longer, twisted in *M. multuma* (see Murthappa et al. 2017: figs 3D, E, 4E, F); (3) the tip of the conductor is uniquely strongly sclerotized and twisted in *M. spiniventris* (Fig. 5C).

Description. Female. Total length 2.23; Prosoma length 1.03, width (at middle) 0.71, height (at middle) 0.51; Opisthosoma length 1.20, width (at middle) 0.81, height (at middle) 1.05; Eye diameters: ALE 0.06, AME 0.07, PLE 0.06, PME 0.07; Eye interdistances: AME–AME 0.06, ALE–ALE 0.11, PLE–ALE contiguous, PLE–PLE 0.17, PME–PME 0.07, PME–PLE 0.05, AME–ALE 0.02; Clypeus height (at middle) 0.15, width (at middle) 0.13; Measurements of legs: Leg I (right) 9.19 [2.95, 0.47, 2.09, 2.93, 0.75], II (right) 4.83 [1.77, 0.36, 1.09, 1.16, 0.45], III (right) 2.98 [1.20, 0.22, 0.50, 0.72, 0.34], IV (right) 6.57 [2.21, 0.37, 1.21, 1.29, 1.49]. Carapace rhomboid with narrow and bar-shaped longitudinal fovea, glabrous; cephalic area relatively long and broad; clypeus slightly elevated. Eye field raised, all eyes in two rows and nearly uniform in size (Fig. 4A). Sternum white, subtly heart-shaped. Labium contiguous with the sternum, white with brown, approximately triangular in shape. Chelicera slanting, white with black fang. Yellow legs long and slender with several black lanceolate spines and the top of tarsus, metatarsus and tibia have black ring in leg I. Leg formula 1423. Yellow pedipalp with short hairs (Fig. 4A–C). Opisthosoma oval higher than long. Abdomen with four black and medially broad setae, dorsum provided with yellow and white (Figs 4B, C). Venter transparent, without any marking (Fig. 4C). Two copulatory openings not juxtaposed (Fig. 4D); copulatory ducts short, inward curving almost 180° and extending to lateral sides of spermathecae (Fig. 4F); spermathecae oval-shaped; fertilization ducts located on the base of spermathecae (Fig. 4H).

Male. Total length 1.82; Prosoma length 0.80, width (at middle) 0.70, height (at middle) 0.54; Opisthosoma length 1.02, width (at middle) 0.93, height (at middle) 0.83; Eye diameters: ALE 0.06, AME 0.08, PLE 0.07, PME 0.07; Eye interdistances: AME–AME 0.08, ALE–ALE 0.15, PLE–ALE contiguous, PLE–PLE 0.19, PME–PME 0.07, PME–PLE 0.06, AME–ALE 0.04; Clypeus height (at middle) 0.19, width (at middle) 0.15; Measurements of legs: Leg I (right) 11.08 [3.36, 0.44, 2.83, 3.52, 0.93], II (right) 6.1 [1.62, 0.36, 1.54, 1.87, 0.71], III (right) 3.55 [1.24, 0.21, 0.74, 0.97, 0.39], IV (right) 7.87 [2.92, 0.38, 2.08, 1.88, 0.61]. Like the female, except by the following. Dwarf in size compared to female (4/5 size of female), without characteristic lanceolate spines. Prosoma with distinct black streaks medially, and a wide red streak in the front of the black streaks; clypeus slightly bulged; eye field wide, elevated, with two long hairs in the middle of AME, white appearance except bulged out black anterior medians (Fig. 5A). Sternum heart shaped; maxillae, labium with dense tuft of hairs; Leg formula 1423 (Fig. 5B). Opisthosoma with alternate deep green and white patches, slightly high, without humps (Fig. 5A). Tegulum spherical, with

median apophyses (Fig. 5D); conductor transparent, spirals upward beyond cymbium, with distal end strongly sclerotized (Fig. 5F); embolus long, narrow, with a sharp tip, almost completely covered by conductor (Fig. 5H).

Distribution. China (Jiangxi; Hainan, newly recorded; Hubei, newly recorded; Sichuan, newly recorded; Yunnan, newly recorded; Taiwan), Japan, Netherlands, Sri Lanka.

Meotipa vesiculosa Simon, 1895

Figures 6A–H, 10

Meotipa vesiculosa Simon, 1894: 514, figs 522, 527 (nomen nudum); Simon 1895: 134 (description of female); Deeleman-Reinhold 2009: 415, figs 13–19 (transferred from *Chrysso*); Yoshida 2009: 378, figs 205–207 (male and female).

Chrysso vesiculosa Levi, 1962: 232, figs 80, 81 (female); Yaginuma 1986: 45, fig. 24–1 (female); Chikuni 1989: 32, fig. 15 (female); Zhu 1998: 51, fig. 25A–C (female); Song et al. 1999: 107, fig. 51E, F (female); Yoshida 2003: 125, figs 336, 339–340, 583 (female); Yoshida 2006: 23, figs 1–7 (female); Yin et al. 2012: 305, fig. 115a–f (male and female).

Chrysso jianglensis Zhu & Song, in Song et al. 1993: 857, fig. 9A–C (description of male); Zhu 1998: 68, fig. 39A–C (male); Song et al. 1999: 103, fig. 49K, L (male).

Material examined (holotype not examined). Yunnan Province: 4♀, Mengla County, Menlun Town, Xishuangbanna Botanical Garden, Chinese Academy of Sciences (21.93°N, 101.25°E, 570 m), 22 March 2018, F.X. Liu & Z.C. Li leg. (CBEE); **Hunan Province:** 4♀, Changsha City, Yuelu Mountain Scenic Area (28.19°N, 112.94°E, 210 m), 12 August 2018, Z.C. Li & Z.W. Deng leg. (CBEE); 1♀, Hengyang City, Hengshan Mountain Scenic Area (27.27°N, 112.71°E, 1300 m), 17 August 2018, Z.C. Li & Z.W. Deng leg. (CBEE).

Diagnosis. This species can be distinguished from other *Meotipa* species by the combination of following characters: (1) atrium large, with shallow heart-shaped depression (Fig. 6D); (2) lateral edges of spermathecae aligned with copulatory ducts (Fig. 6H); (3) conductor expanding laterally converting to ring-shape distally (see Yoshida 2009: fig. 207); (4) embolus incurved and long, knife shaped distally (see Yin et al. 2012: fig. 115e, f).

Description. Female. Cephalothorax pale yellow with a red-brown central stripe; cephalic area relatively long and broad; clypeus narrow, bulged out. Eyes in two rows and nearly uniform in size, strongly recurved; AME separation is greater than AME-ALE, and PE are arranged at almost equal distances; AME black, PME eyes pearly white (Fig. 6A). Sternum deep yellow, triangular, lateral margins slightly indented. Labium contiguous with the sternum, brown, triangular. Chelicera vertical, deep yellow with red fang (Fig. 6B). Legs yellowish white with small hairs and bearing a few dark short spines, the end of tibiae with a black ring in each legs and femur of all legs have small black spots. Leg formula 1423. Pedipalp yellowish white, single-clawed, with many short hairs; tibia with a black ring on the extreme and bearing a lanceolate spine

Figure 6. *Meotipa vesiculosa* Simon, 1895 **A–C** female habitus (**A** dorsal **B** prolateral **C** ventral). **D–H** epigynum (**D** ventral, on the body **E, F** in the alcohol **E** ventral **F** dorsal **G, H** in gum arabic **G** ventral **H** dorsal). Scale bars: 1 mm (**A–C**); 0.1 mm (**D–H**). Abbreviations: CO = copulatory opening, CD = copulatory duct, FD = fertilization duct, S = spermathecae.

laterally (Fig. 6A, B). Opisthosoma approximately triangular laterally, dorsally provided with numerous white and black spots, posterior region extending downwardly towards spinnerets. Two pairs of dorsolateral abdominal humps, black distally (Fig. 6A–C). Atrium large, with a clear herringbone structure medially (Fig. 6D). Copulatory ducts and fertilization ducts short and both of them extending into spermathecae at the same position (Fig. 6H). Spermathecae large, oval-shaped (Fig. 6G).

Male. Not collected.

Distribution. China (Fujian; Guangxi; Hunan; Taiwan; Yunnan, newly recorded), Vietnam to Japan, Philippines, Indonesia.

***Meotipa pseudopicturata* sp. nov.**

http://zoobank.org/E6771BF5-0A42-44A0-B57D-19008459EB38

Figures 7A–H, 10

Type material. ***Holotype*** female (CBEE). **Yunnan Province:** Mengla County, Menlun Town, Xishuangbanna Botanical Garden, Chinese Academy of Sciences (21.93°N, 101.25°E, 570 m), 22 March 2018, F.X. Liu & Z.C. Li leg. ***Paratypes***. **Yunnan Province:** 7♀, same data as holotype.

Etymology. The species epithet refers to its similarity to *Meotipa picturata* Simon, 1895.

Diagnosis. *Meotipa pseudopicturata* sp. nov. is similar to *M. picturata* (see Murthappa et al. 2017: figs 1A–J, 2A–F, 4A–D) and *M. sahyadri* (see Kulkarni et al. 2017: figs 1–38) in having a deep round atrium, and having the copulatory ducts openings in the atrium (Fig. 7E). It can be distinguished from the latter two by the following combination of characters: (1) The tip of rod-shaped projection is narrower than its basal part in this new species, but wide in *M. picturata* (see Murthappa et al. 2017: fig. 4C) and *M. sahyadri* (see Kulkarni et al. 2017: fig. 21) ; (2) the ends of the copulatory ducts are curved and enter the spermathecae ventrally in *M. pseudopicturata* sp. nov. (Fig. 7F), and laterally in *M. picturata* (see Murthappa et al. 2017: figs 1J, 4D) and *M. sahyadri* (see Kulkarni et al. 2017: fig. 18); (3) fertilization ducts relatively short, proximal part confronting without curve in *M. pseudopicturata* sp. nov. (Fig. 7H), but relatively long, proximal part confronting with an apical curve in *M. picturata* (see Murthappa et al. 2017: fig. 4D) and *M. sahyadri* (see Kulkarni et al. 2017: fig. 18). In addition, *M. pseudopicturata* sp. nov. can be distinguished from other *Meotipa* species by the long and triangular opisthosoma which extends beyond spinnerets ~ 3/4 of total abdomen length, with blunt end curved ventrally.

Description. Female (holotype). Total length 3.31; Prosoma length 1.08, width (at middle) 1.11, height (at middle) 0.69; Opisthosoma length 2.26, width (at middle) 0.91, height (at middle) 1.83; Eye diameters: ALE 0.07, AME 0.08, PLE 0.08, PME 0.07; Eye interdistances: AME–AME 0.05, ALE–ALE 0.10, PLE–ALE contiguous, PLE–PLE 0.26, PME–PME 0.10, PME–PLE 0.08, AME–ALE 0.03; Clypeus height (at middle) 0.43, width (at middle) 0.15; Measurements of legs: Leg I (right) 12.44

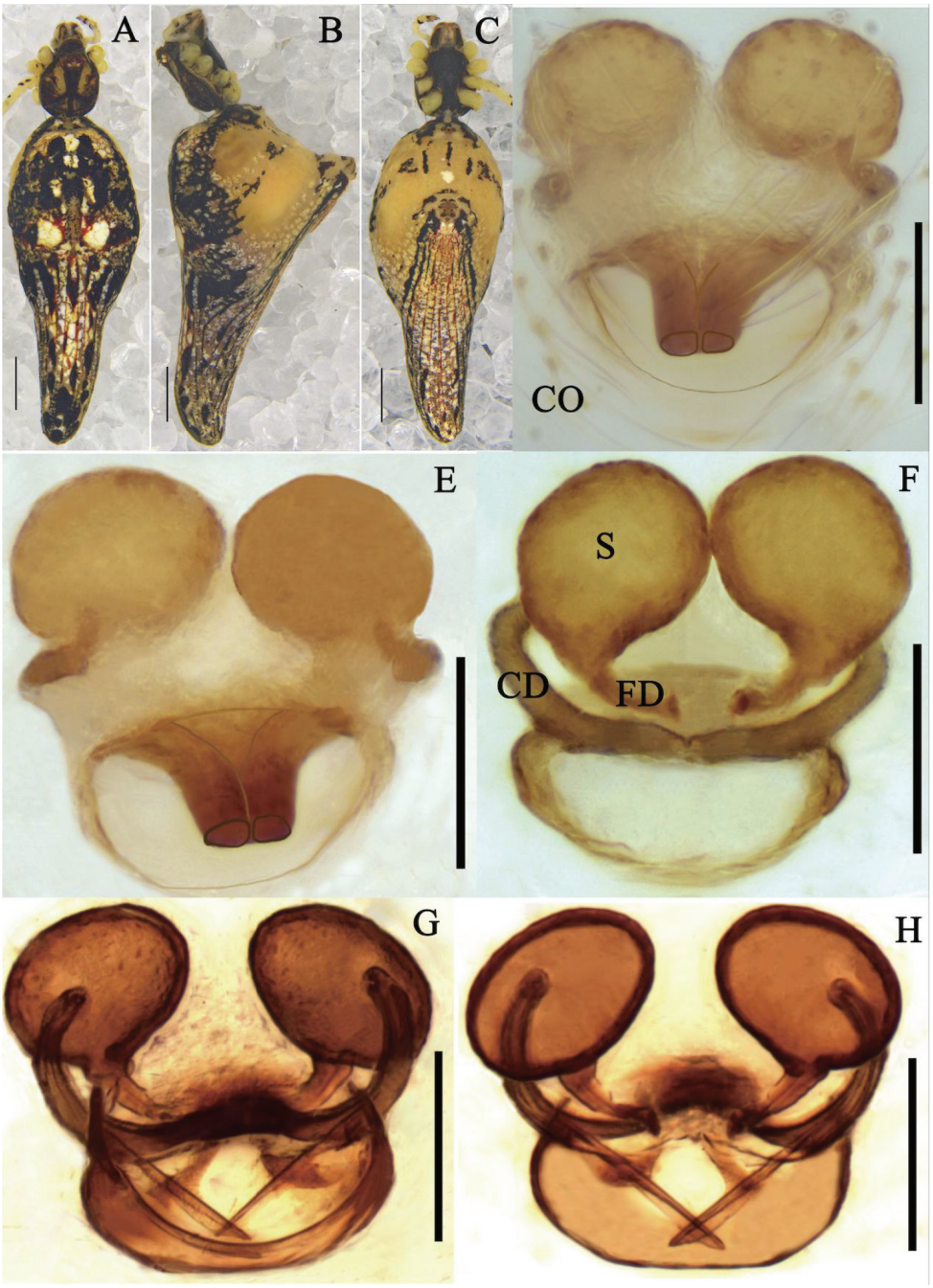

Figure 7. *Meotipa pseudopicturata* sp. nov. **A–C** female habitus (flattened black spines on the abdomen and legs were broken off during taking photographs) (**A** dorsal **B** prolateral **C** ventral). **D–H** epigynum (**D** ventral, on the body **E, F** in the alcohol **E** ventral **F** dorsal **G, H** in gum arabic **G** ventral **H** dorsal). Scale bars: 1 mm (**A–C**); 0.1 mm (**D–H**). Abbreviations: CO = copulatory opening, CD = copulatory duct, FD = fertilization duct, S = spermathecae.

[4.23, 0.54, 2.58, 4.20, 0,89], II (right) 8.11 [2.73, 0.44, 1.65, 2.55, 0.74], III (right) 4.7 [1.68, 0.31, 0.99, 1.28, 0.44], IV (right) 10.91 [4.06, 0.38, 2.42, 3.44, 0.61]. Prosoma anteriorly and posteriorly truncated, medially flat, glabrous; cephalic area elevated. Carapace with black stripes, medially radiating streaks; fovea broad, smooth with distinct depression and irregular ridges (Fig. 7A). All eyes nearly uniform in size. Sternum black, heart shaped (Fig. 7C). Labium contiguous with the sternum, short with small hairs. Chelicerae vertical, black with red fangs (Fig. 7A–C). Femur, patella, and tibia with lanceolate spines distally; tibia with reddish black spot distally; leg segments except tibia with short, fine, dense hairs; femur IV with a row of lanceolate spines distoventrally; metatarsus I blackish distally. Leg formula 1423. Pedipalp short relative to its body size; tibia dorsally with lanceolate spines, long proximally, distally small with swelling. Opisthosoma triangular, very broad in lateral view, its dorsum provided with long alternate red and black stripes and white spots, caudal region knobbed extending downwardly towards spinnerets, provided with lanceolate spines. Venter transparent, some small black and white patches posteriorly (Fig. 7C). Atrium broad, with a rod-shaped projection apically (Fig. 7D); copulatory openings depressed, contiguous, located on the end of rod-shaped projection (Fig. 7E); copulatory ducts moderately long, tube curved extremely entering into ventral view of spermatheca (Fig. 7F); spermathecae oval-shaped, separated; fertilization duct thick, originating from basal spermathecae (Fig. 7H).

Male. Unknown.

Distribution. China (Yunnan) (Fig. 10).

***Meotipa striata* sp. nov.**

http://zoobank.org/1FA8D560-A36E-4A56-80F8-F7662B2BF3CB

Figures 8A–H, 10

Type material. ***Holotype*** female (CBEE). **Yunnan Province:** Mengla County, Wangtianshu Scenic Area (21.62°N, 101.58°E, 680 m), 15 November 2019, J. Chen, J. Liu, Z.C. Li & B. Liang leg.

Etymology. The species epithet refers to the black and yellow stripes on the abdomen of the specimen.

Diagnosis. The new species is similar to *M. spiniventris* (Figs 4A–H, 5A–H) and *M. capacifaba* (see Li et al. 2020: figs 1A–J, 2A–E, 3A–E) in sharing characters such as the raised eyes, a marking in the middle of carapace, and two conspicuous copulatory openings. It can be distinguished from the two species by the following characters: (1) the atrium is divided into two circular openings by the epigynal septum in *M. capacifaba* (see Li et al. 2020: figs 2A, B) and *M. spiniventris* (Fig. 4D–H), but not in *M. striata* sp. nov.; (2) the copulatory ducts gradually narrow from copulatory openings to spermathecae in *M. striata* sp. nov. (Fig. 8F) and *M. spiniventris* (Fig. 3F), but swell into sphere-shaped in *M. capacifaba* (see Li et al. 2020: figs 2A, B).

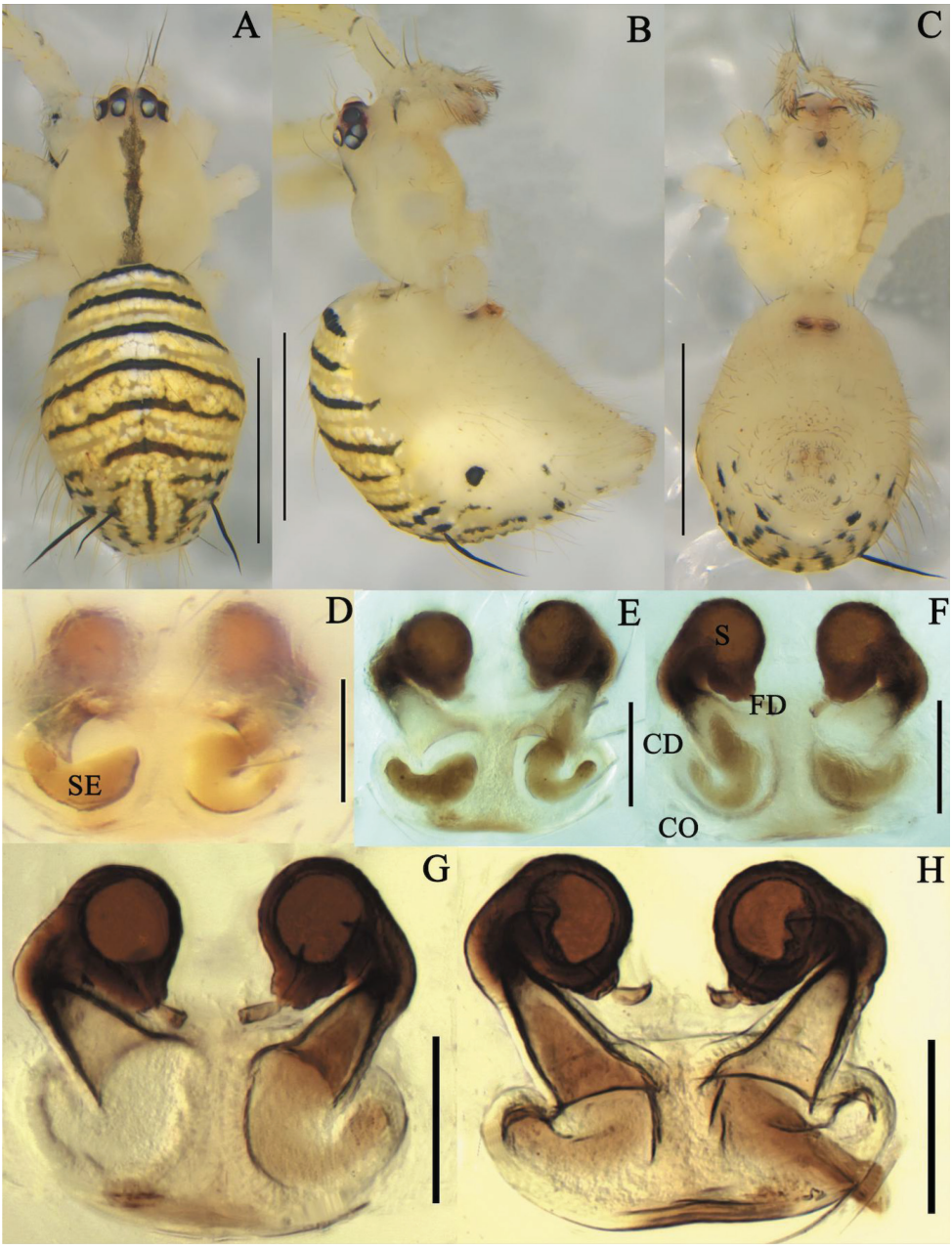

Figure 8. *Meotipa striata* sp. nov. **A–C** female habitus (some flattened black spines on the abdomen and legs were broken off during taking photographs) (**A** dorsal **B** prolateral **C** ventral). **D–H** epigynum (**D** ventral, on the body **E, F** in the alcohol **E** ventral **F** dorsal **G, H** in gum arabic **G** ventral **H** dorsal). Scale bars: 1 mm (**A–C**); 0.1 mm (**D–H**). Abbreviations: CO = copulatory opening, CD = copulatory duct, FD = fertilization duct, S = spermathecae, SE = stuck emboli.

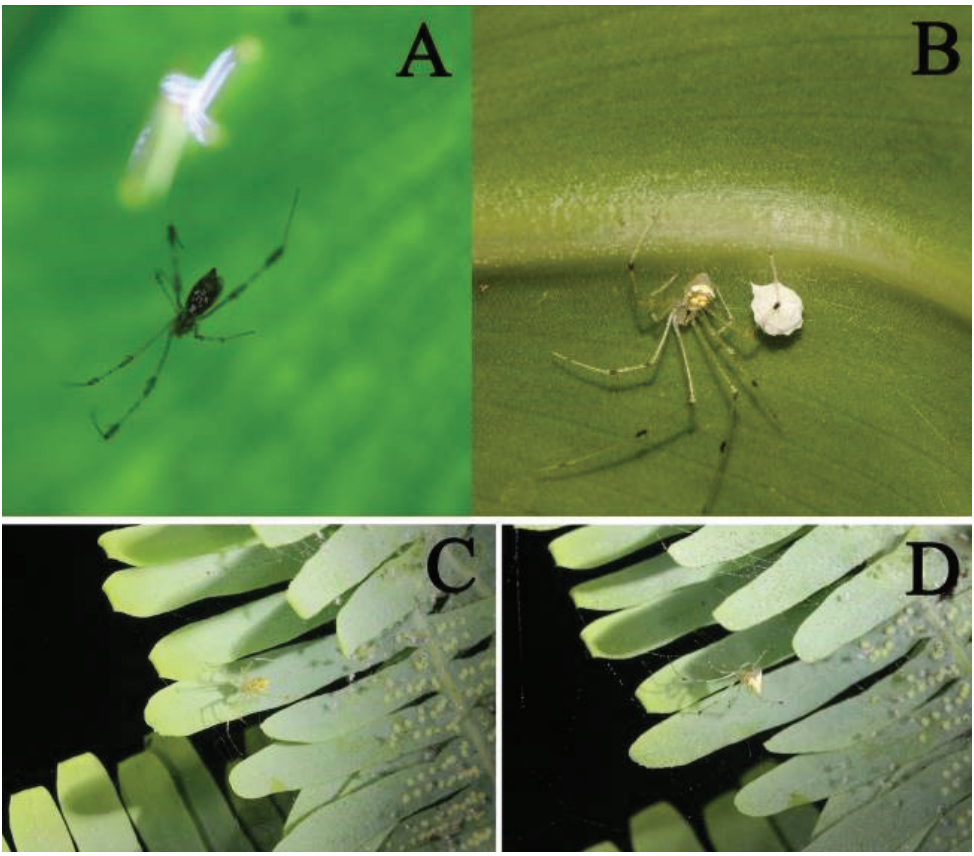

Figure 9. Field photographs **A** *M. picturata* female on its web **B** *M. spiniventris* female with egg sac **C, D** *M. pulcherrima* female with its spiderlings. Photographs by Zhongwei Deng in Yunnan Province.

Description. Female (holotype). Total length 2.41; Prosoma length 0.96, width (at middle) 0.83, height (at middle) 0.61; Opisthosoma length 1.4, width (at middle) 1.10, height (at middle) 1.50; Eye diameters: ALE 0.07, AME 0.08, PLE 0.08, PME 0.08; Eye interdistances: AME–AME 0.03, ALE–ALE 0.23, PLE–ALE contiguous, PLE–PLE 0.28, PME–PME 0.08, PME–PLE 0.06, AME–ALE 0.03; Clypeus height (at middle) 0.26, width (at middle) 0,14; Measurements of legs: Leg I (right) 9.30 [2.80, 0.45, 2.12, 3.01, 0.92], II (right) 5.85 [1.96, 0.36, 1.21, 1.51, 0.81], III (right) 4.85 [1.40, 0.22, 0.80, 1.39, 0.50], IV (right) 6.86 [2.50, 0.40, 1.42, 1.87, 0.67]. Carapace rather ovate with bar-shaped longitudinal narrow fovea; cephalic area relatively short and narrow. All eyes uniform in size, strongly recurved; dark AME surrounded by red-brown rings; PME pearly white surrounded by black rings (Fig. 8A). Sternum yellow, subtle heart-shaped, lateral margins slightly indented (Fig. 8C). Labium contiguous with the sternum, white, approximately triangular in shape. Chelicera vertical, white

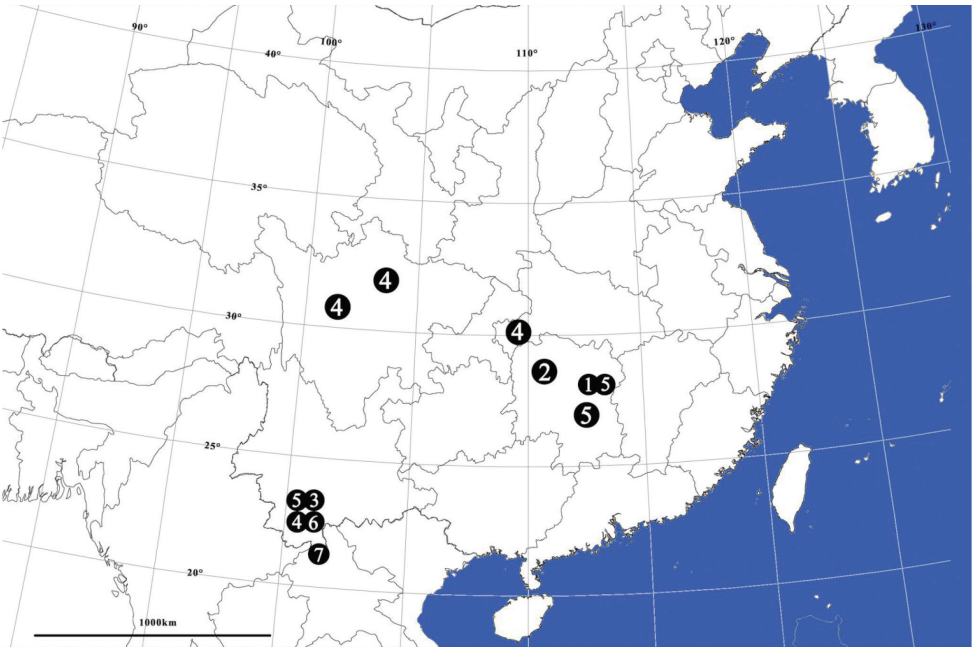

Figure 10. Map with sampling localities for *Meotipa* species from China: 1 *M. argyrodiformis* 2 *M. pulcherrima* 3 *M. picturata* 4 *M. spiniventris* 5 *M. vesiculosa* 6 *M. pseudopicturata* sp. nov. 7 *M. striata* sp. nov..

with black fang (Fig. 8B). Legs yellowish white with small hairs and bearing a few dark short spines; coxae and femora white with pale black spots; the ends of metatarsi with pale brown band (Fig. 8B). Leg formula 1423. Pedipalp white, short, single-clawed, with many short hairs. Opisthosoma oval, provided with yellowish setae. Abdomen with black patch and snowy white patches medially, dorsally with four lanceolate spines; spinnerets oriented downwards (Fig. 8A). Copulatory openings large, separated from each other, with mating plugs (Fig. 8D); copulatory ducts gradually narrow from copulatory opening to spermathecae and bend, vertical at lateral sides of spermathecae (Fig. 8F); spermathecae spherical (Fig. 8G); fertilization ducts located on the basal of spermathecae, facing each other (Fig. 8H).

Male. Unknown.

Distribution. China (Yunnan) (Fig. 10).

Discussion

Meotipa Simon, 1895 is a relatively small genus of the family Theridiidae, totaling 20 species globally including two new species reported here. Most species are distributed in East Asia (eleven species in China, three species in Japan and Korea), Southeast Asia (eight species in Brunei, Indonesia, Laos, Malaysia, Myanmar, Thailand, and Vietnam), and South Asia (five species in India). Only *M. pulcherrima* is found outside Asia: it is widely distributed in tropical Africa and is presumed to have been

introduced to Papua New Guinea, China, Korea, Japan, and the Pacific islands, and the Americas, including its type locality in Brazil (see Note under *M. pulcherrima*). *Meotipa* spiders prefer to inhabit the underside of leaves typically decorated by lichens and fungi. Against this background, the black, white, and red patterns on the body and the brushes of black scale-like spines on legs and abdomen blur their outline and enhance their disguise (Deeleman-Reinhold 2009). Therefore, these long-legged spiny theridiids are difficult to find and collect in the wild. Given the broad distribution of *Meotipa* in Asia spanning many poorly sampled areas where taxonomic expertise is lacking, it is likely that many species await discovery and thus further taxonomical work focused on this genus is needed.

It is difficult to speculate on *Meotipa* interrelationships without a phylogeny, but some morphological observation may serve to indicate certain relationships: 1. Abdomen bearing two pairs of humps on dorso-lateral sides is only present in *M. impatiens*, *M. ultapani*, and *M. vesiculosa*; 2. A rod-shaped projection in the epigynum is found in *M. picturata M. sahyadri*, and *M. pseudopicturata* sp. nov.; 3. The copulatory ducts are spherical in *M. capacifaba* and *M. pulcherrima*, but distinctly curved in *M. capacifaba* and *M. pulcherrima*; 4. The conductor is spoon-shaped in *M. argyrodiformis*, *M. menglun*, *M. picturata*, *M. sahyadri*, and *M. vesiculosa*. These characters have minimum overlap (*M. vesiculosa* may belong to two of the groups) and might suggest the following species groups and relationships: (*M. impatiens*, *M. ultapani*, and *M. vesiculosa*),((*M. picturata*, *M. sahyadri*, and *M. pseudopicturata*) *M. argyrodiformis*)), (*M. capacifaba* and *M. pulcherrima*). However, whether these characters actually reflect relationships remains to be seen upon the systematic collection of phylogenetic data. In addition, we must consider that the two new species (only female) covered in the current paper were collected from same region (Mengla County, Xishuangbanna Dai Autonomous Prefecture) with three known species (only males of *M. luoqiae*, *M. menglun*, *M. zhengguoi*) recently reported (Lin et al. 2021), but we are sure that they do not match with each other based on the following reasons: 1. the habitus of our new species (*M. pseudopicturata* sp. nov. and *M. striata* sp. nov.) are significantly different from the males of the three known species (Figs 7A–C, 8A–C); 2. the male of *M. pseudopicturata* sp. nov. should be similar to *M. picturata* and *M. sahyadri* according to our above hypothesis about *Meotipa* interrelationships, but none of these three species is similar; 3. the female of *M. striata* sp. nov. is similar to *M. spiniventris* (Figs 4A–H, 5A–H) and *M. capacifaba* (see Li et al. 2020: figs 1A–J, 2A–E, 3A–E) in having two conspicuous copulatory openings; therefore, we speculate that its male should be similar to *M. spiniventris* (Figs 4A–H, 5A–H) and *M. capacifaba* in having a straight embolus covered completely by conductor, but the embolus is not covered by the conductor in these three species (*M. luoqiae*, *M. menglun*, and *M. zhengguoi*; see Lin et al. 2021: figs 47–52).

Meotipa clearly belongs to the subfamily Theridiinae based both on molecular phylogenetic data (Liu et al. 2016), and clear morphological synapomorphies, in particular the complete absence of the colulus and the hooded paracymbium (Agnarsson 2004a). The exact position of *Meotipa* within Theridiinae is less certain: Deeleman-Reinhold (2009) resurrected *Meotipa* from *Chrysso* mainly based on the

presence of flattened black spines on the abdomen and/or legs, and the cutinized conductor in the male palp. However, the genus *Chrysso* seems to be polyphyletic (Liu et al. 2016). Deeleman-Reinhold (2009) speculated that the *Chrysso* species distributed in Southeast Asia are more closely related to *Theridion* and *Achaearanea* than they are to the type species *Chrysso albomaculata* from the Americas (Deeleman-Reinhold, 2009). We do not see any evidence of the close relationship between *Theridion* and *Meotipa* (but note that Agnarsson et al. (2007b) included an undetermined *Meotipa* species from Malaysia but its placement as sister to *Theridion* was poorly supported). However, the type of *Achaearanea*, *A. trapezoidalis*, shares certain characteristics such as abdomen shape with many species of *Chrysso*. The study of Liu et al. (2016) included one unnamed *Meotipa* species, placing it on a long branch as sister to two *Yunohamella* species: *Y. lyricus* (Walckenaer, 1841) and *Y. palmgreni* (Marusik & Tsellarius, 1986) according to recent research (Marusik and Logunov, 2017). We infer that *Meotipa* may instead belong to the "*Chrysso* clade" of Arnedo et al. (2007), given the similarities between *Meotipa* and *Chrysso*. Such speculations need to be tested through innovative phylogenetic analyses aimed to anchor *Meotipa* to the theridiid tree of life.

Acknowledgements

The manuscript benefited from comments by Gergin Blagoev (Centre for Biodiversity Genomics, University of Guelph, Canada), Nathalie Yonow (Swansea University, Wales), and two anonymous reviewers. This study was financially supported by CAS Key Laboratory of Tropical Forest Ecology, Xishuangbanna Tropical Botanical Garden, Chinese Academy of Sciences (19CAS-TFE-3), the National Natural Sciences Foundation of China (NSFC-31573236/31273268/31772420) and National Science and Technology Fundamental Resources Investigation Program of China (Grant No. 2019FY101800).

References

Agnarsson I (2004a) Morphological phylogeny of cobweb spiders and their relatives (Araneae, Araneoidea, Theridiidae). Zoological Journal of the Linnean Society 141(4): 447–626. https://doi.org/10.1111/j.1096-3642.2004.00120.x

Agnarsson I, Coddington JA, Knoflach B (2007a) Morphology and evolution of cobweb spider male genitalia (Araneae: Theridiidae). Journal of Arachnology 35: 334–395. https://doi.org/10.1636/SH-06-36.1

Agnarsson I, Maddison WP, and Leticia Avilés (2007b) The phylogeny of the social *Anelosimus* spiders (Araneae: Theridiidae) inferred from six molecular loci and morphology. Molecular Phylogenetics & Evolution 43(3): 833–851. https://doi.org/10.1016/j.ympev.2006.09.011

Arnedo MA, Agnarsson I, Gillespie RG (2007) Molecular insights into the phylogenetic structure of the spider genus Theridion (Araneae, Theridiidae) and the origin of the

Hawaiian Theridion-like fauna. Zoologica Scripta 36: 337–352. https://doi.org/10.1111/j.1463-6409.2007.00280.x

Barrion AT, Litsinger JA (1995) Riceland spiders of South and Southeast Asia. CAB International Wallingford, UK, 700 pp.

Deeleman-Reinhold CL (2009) Spiny theridiids in the Asian tropics. Systematics, notes on behaviour and species richness (Araneae: Theridiidae: *Chrysso*, *Meotipa*). Contributions to Natural History 12: 403–436.

Levi HW (1962) More American spiders of the genus *Chrysso* (Araneae, Theridiidae). Psyche, Cambridge 69(4): 209–237. https://doi.org/10.1155/1962/32404

Li CM, Liu JX, Xu X, Yin HQ (2020) A new species of spider in the genus *Meotipa* Simon, 1895 (Araneae: Theridiidae) from southern China. Pan-Pacific Entomologist 96(3): 177–184. https://doi.org/10.3956/2020-96.3.177

Li ZC, Agnarsson I, Peng Y, Liu J (2021) Eight cobweb spider species from China building detritus-based, bell-shaped retreats (Araneae, Theridiidae). ZooKeys 1055: 95–121. https://doi.org/10.3897/zookeys.1055.67620

Lin YJ, Marusik YM, Gao CX, Xu H, Zhang XQ, Wang ZY, Zhu WH, Li Q (2021) Twenty-three new spider species (Arachnida: Araneae) from Asia. Zoological Systematics 46(2): 91–152.

Liu J, May-Collado LJ, Pekar S, Agnarsson I (2016) A revised and dated phylogeny of cobweb spiders (Araneae, Araneoidea, Theridiidae): a predatory Cretaceous lineage diversifying in the era of the ants (Hymenoptera, Formicidae). Molecular Phylogenetics and Evolution 94: 658–675. https://doi.org/10.1016/j.ympev.2015.09.023

Kulkarni S, Vartak A, Deshpande V, Halali D (2017) The spiny theridiid genus *Meotipa* Simon, 1895 in india, with description of a strange new species with translucent abdomen and a phylogenetic analysis about the genus placement (Araneae, Theridiidae). Zootaxa 4291(3): 504–520. https://doi.org/10.11646/zootaxa.4291.3.4

Malamel JJ, Pradee MS, Sebastian PA (2013) *Fecenia travancoria* Pocock is recognised as a junior synonym of *Fecenia protensa* Thorell (Araneae: Psechridae): a case of intraspecific variation. Zootaxa 3741: 359–368. https://doi.org/10.11646/zootaxa.3741.3.4

Marusik YM, Logunov DV (2017) New faunistic and taxonomic data on spiders (Arachnidae: Aranei) from the Russian Far East. Acta Arachnologica 66(2): 87–96. https://doi.org/10.2476/asjaa.66.87

Mello-Leitão CF de (1917) Notas arachnologicas. 5, Especies novas ou pouco conhecidas do Brasil. Brotéria (Ser. Zool.) 15: 74–102.

Murthappa PS, Malamel JJ, Prajapati DA, Sebastian PA, Venkateshwarlu M (2017) First description of the male of the type species *Meotipa picturata* Simon, 1895 and description of a new *Meotipa* species (Araneae, Theridiidae) from India. Zootaxa 4344(3): 589–596. https://doi.org/10.11646/zootaxa.4344.3.9

Seo BK (2010) New species and two new records of the spider family Theridiidae (Araneae) from Korea. Entomological Research 40(3): 171–176. https://doi.org/10.1111/j.1748-5967.2010.00281.x

Vanderhaegen K, Jocqué R (2017) A new Afromontane species of the ant-eating spider genus *Dusmadiores* and description of the male of *D. deserticola* (Araneae: Zodariidae). Zootaxa 4318(3): 548–560. https://doi.org/10.11646/zootaxa.4318.3.7

World Spider Catalog (2021) World Spider Catalog. Natural History Museum Bern. Version 22.5. https://wsc.nmbe.ch/ [accessed 7 November 2021].

Yin CM, Peng XJ, Yan HM, Bao YH, Xu X, Tang G, Zhou QS, Liu P (2012) Fauna Hunan: Araneae in Hunan, China. Hunan Science and Technology Press, Changsha, 1590 pp.

Yoshida H (2003) The spider family Theridiidae (Arachnida: Araneae) from Japan. Arachnological Society of Japan, Hokkaido, 224 pp.

Yoshida H (2009) Uloboridae, Theridiidae, Ctenidae. In: Ono H (Ed.) The spiders of Japan with keys to the families and genera and illustrations of the species. Tokai University Press, Kanagawa, 142–147, 356–393, 467–468.

Zhu MS (1998) Fauna Sinica: Arachnida: Araneae: Theridiidae. Science Press, Beijing, 436 pp.

Zhu MS, Zhang YQ (1992) Notes of some species of Theridiidae in Guangxi (Arachnida: Araneae). Journal of the Guangxi Agricultural College 11(1): 20–29.